UNIVERSITY OF CALGARY

Structural and Sedimentological Analysis of the Cardium Formation within Blind Frontal Duplex Structures west of the Pembina Oil Field, Alberta

by

Markus Josef Ebner

A THESIS

SUBMITTED TO THE FACULTY OF GRADUATE STUDIES

IN PARTIAL FULFILLMENT OF THE REQUIREMENTS FOR THE

DEGREE OF MASTER OF SCIENCE

DEPARTMENT OF GEOLOGY AND GEOPHYSICS

CALGARY, ALBERTA

August, 2007

UNIVERSITY OF
CALGARY

ABSTRACT

Five lithofacies were identified from 17 cores and 367 wireline logs between Townships 46-48 and Ranges 14-17W5, Alberta. Sedimentary bedforms and ichnofossils assemblages indicate that the Cardium Formation in the study area is of a shallow marine, storm dominated origin. Seismic investigation reveals blind duplexes developed between two foreland detachments, approximately 50 km east of the outcropping foreland edge of deformation. Analysis of 2D seismic data yields 3D duplex geometry with two horses in the foreland, formed on a lower detachment that progressively loses displacement from northwest to southeast, due to an underlying lateral ramp. In the hinterland, a large, single-horse duplex is formed between the upper and lower detachment surfaces. The upper detachment of the structure is folded due to the development of a “sticking point”. This study shows that blind frontal structures show variation along strike, much like frontal Foothill structures have also been observed to do.

Acknowledgements

Many people deserve recognition for making this thesis what it has become over the past couple of years. I would like to thank my supervisors, Drs. Deborah Spratt and Federico Krause, for their support, providing freedom to work at this project how I wished, helpful discussions and patience. Additionally, their critical reviews of this manuscript are greatly appreciated.

The sponsors of the Fold Fault Research Project and the University of Calgary are gratefully acknowledged for their financial contribution for this thesis. Shell Canada Limited is thanked for allowing me to use their resources.

Wayne Rydman, Toonie Fink and Nathan Leonard of ConocoPhilips Canada are thanked for their donation of seismic data used in this study and for helpful discussions of data issues. Dr. Helen Isaac is thanked for the hours she spent on depth converting the seismic data from time. Without her assistance I probably still would be trying to figure out the finer details of geophysics. Dr. John Peirce of GEDCO is thanked for providing the High Resolution Aero-Magnetic Data in the study area. Midland Valley is thanked for their donation of *2DMove*® and *3DMove*® to the FRP at the University of Calgary. Wellsight Systems Inc. is thanked for their donation of a software key that enabled me to create the digital core logs. David '¿Quién es? Ramos' Repol is thanked for providing me with a crash course on *2D*- and *3DMove*®, many 'structured' discussions about 'the beach' and constant encouragement. Kris Vickerman is thanked for his critical review of many previous drafts of this manuscript which greatly improved it and for thoughtful geological discussions over beers. Mark Kirtland and Leslie Desreux of the FRP are thanked for their assistance with computer and administrative support respectively. IHS Energy is thanked for providing licenses of *AccuMap*® to the University of Calgary's Geology and Geophysics department.

The ‘Ladies of the Library’ (Claudette Cloutier, Sandy Blazina and Patricia Johnson) are thanked for assisting in searches, rounding up some obscure requests, and extending due dates. The ‘Ladies of the Front Office’ (Cathy Hubbell, Laurie Vaughan and Faye Nicholson are thanked for helping me find my way through the pile of never ending forms, good entertainment and a constant candy supply.

Lastly, I thank my family and friends for enduring and assisting me on my journey during the past two-and-a-half years. Most specifically, to my parents, for their unending support and ‘wise in retrospect’ input over all these years – If it were not for them, I would be nowhere close to where I am today. Thank you.

To Annelies and Erwin

TABLE OF CONTENTS

LIST OF TABLES

LIST OF FIGURES

All things are difficult before they are easy.

-Dr. Thomas Fuller, *Gnomologia,* 1732.

Chapter One: Introduction

1.1 Area of Study

The study area (1106 km^2) is located approximately 150 km southwest of Edmonton, Alberta (Figure 1-1) and lies directly west of the giant Pembina oil field and east of the surficial expression of the edge of the deformed belt. This study focuses particularly on the structure and sedimentology of the subsurface Cardium Formation. Little work in the area has documented the sedimentology or the subsurface deformation that exists northeastward of the Triangle Zone, apart from works by Skuce *et al.* (1992) and Skuce (1996). Comparatively, there has been a significant amount of work published on the depositional origin and lithological variation of the Cardium Formation in Alberta since the discovery of the Pembina oil field in 1953 (Krause *et al*., 1987a and Krause *et al*., 1994)

1.2 Purpose

The purpose of this thesis is two-fold:

1. Delineate the subsurface 3D structural geometry in the study area based on the interpretation of 2D seismic and well data;
2. Determine the lithofacies and depositional environment of the Cardium Formation within the study area.

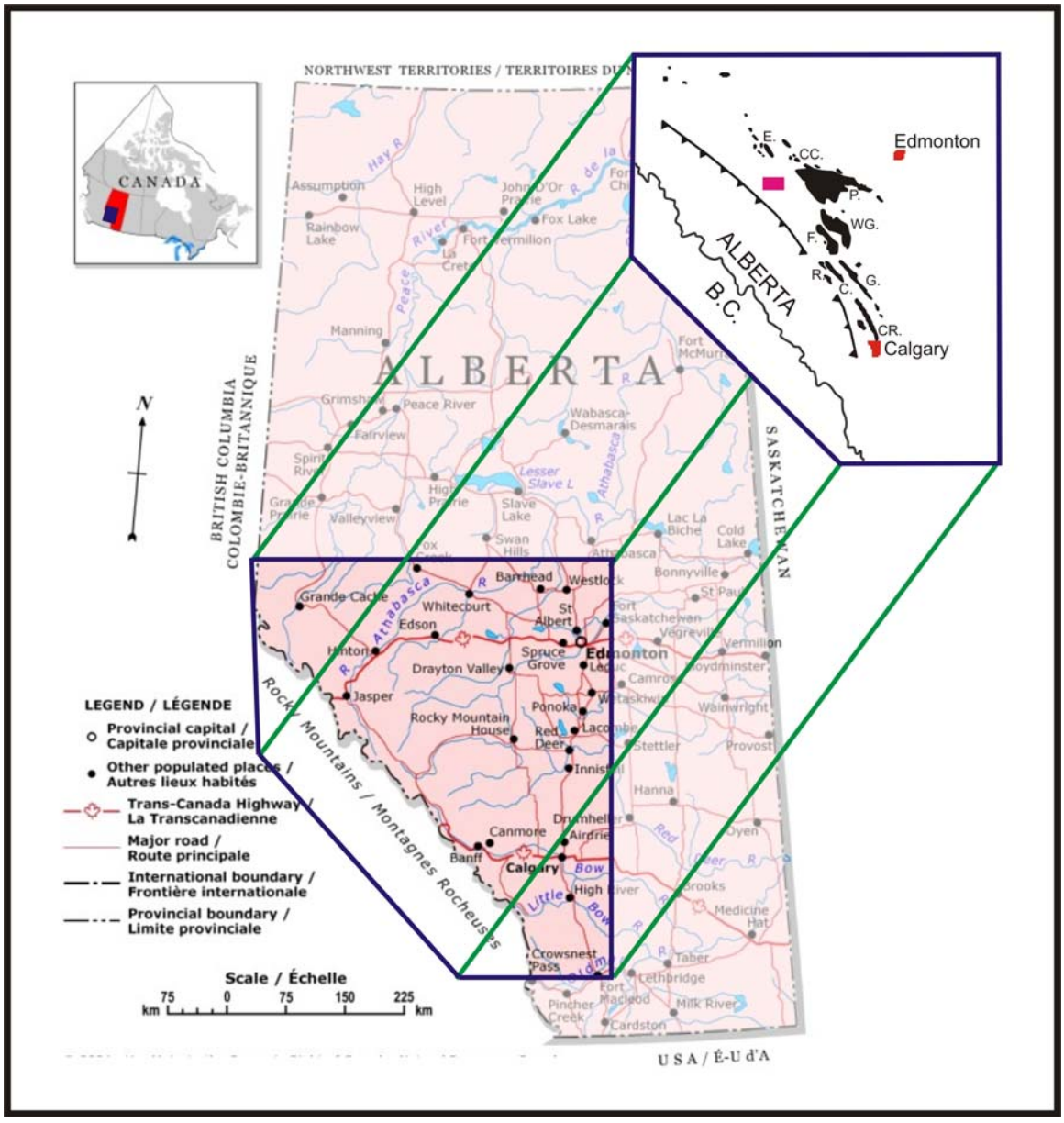

Figure 1-1: The study area is located approximately 150 km southwest of Edmonton, Alberta. It is noted on the inset map as a pink rectangle and lies directly west of the giant Pembina oil field and east of the surficial expression of the edge of the deformed belt. Cardium Formation hydrocarbon fields are shown on the inset map: Edson (E), Carrot Creek (CC), Pembina (P), Ferrier (F), Willisden Green (WG), Ricinus (R), Caroline (C), Garrington (G), and Crossfield (CR). Modified from Krause and Nelson (1984) and http://atlas.gc.ca/site/english/maps/reference/provincesterritories/alberta.

In addition to this, an investigation into a potential correlation between the lithological variation of lithofacies types and zones of deformation is discussed. Accomplishing these goals involved the interpretation of 2D seismic data and construction of a 3D model.

1.3 Data and Software

A processed seismic data set was received from ConocoPhillips covering a large majority of the study area. Because of various vintages of seismic data that ranged from the 1970's to the early 1990's, great variation was noted in the quality of the processed images. Five seismic lines were chosen for the 2D interpretation. 3D models were subsequently developed from the 2D interpretations. Aeromagnetic data were acquired from GEDCO and tied to the 2D seismic data to offer additional confidence in the interpretations made.

The lithofacies scheme developed for the Cardium Formation in this study was accomplished by examination of 17 cores taken through the appropriate stratigraphic intervals within the study area. All of the electric wireline logs from the wells in the regional study area were examined by the author to pick the tops of the Blackstone Formation, Cardium Formation and Cardium Zone Member. Isopach and structure maps were generated after all of the wells were examined for consistency of formational tops based on correlations of electric wireline responses. A total of eight electric wireline log cross sections were created to show the geometry of the Cardium Formation sandstone.

Numerous software applications were utilized in this thesis to accomplish the goals previously stated.

- ***AccuMap*®** was used for well data manipulation and construction of structure and isopach maps.
- ***Promax*®** was used to convert the seismic sections from time to depth.
- ***2DMove*®** was used to perform the seismic interpretation as well as the seismic and line palinspastic restorations.
- ***3DMove*®** was used to generate a three dimensional model from the five 2D seismic lines received.
- ***4DVista*®** is a software suite that accompanies *2DMove*® and *3DMove*® and enables preliminary visualisation and manipulation of 2D data in 3D. The software also confirms the correct tying of formational tops between interpreted seismic sections before commencing construction of 3D models.

1.4 Approach to the Study

The thesis is divided into chapters that address the two major themes of research listed above. Chapter Two addresses the stratigraphy and depositional environment of the Cardium Formation within the study area and attempts to draw analogies from the Cardium Formation in adjacent fields. The chapter describes the lithofacies scheme developed from core examination as well as examines the distribution of the sandstone across the study region. The

geometry of the sandstone is assessed with the interpretation of the lithofacies, three regional well log-cross sections, and isopach and structure contour maps. Variations in thickness of the Cardium Formation are also investigated using the isopach and structure contour maps.

Chapter Three presents the 2D structural interpretations and the 3D model. The chapter closely investigates the 3D geometry of the structures and discusses the variation along strike in this frontal Foreland position. Magnetic data are also used to add additional confidence to the seismic interpretation and are useful in outlining the geometry of the near surface geology more clearly. The chapter concludes by investigating a potential relationship between the defined lithofacies of the study area discussed in Chapter Two and the structural deformation identified.

Chapter Four summarizes the conclusions of each of the primary chapters, provides suggestions for potential future work and lists some practical applications of this research to the exploration for hydrocarbons in the Western Canada Sedimentary Basin.

Chapter Two: Sedimentology and Depositional Environment

2.1 Introduction

The Upper Cretaceous (Turonian-Coniacian) Cardium Formation has received much attention and geological study since the discovery of the Pembina oil field in 1953 (Krause *et al*., 1994; Hall *et al*., 1995). Although many studies have been conducted on the Cardium Formation, no common consensus has been arrived at regarding the depositional processes that emplaced it. This study investigates the depositional environment and lithofacies associations of the sandstone and conglomerate units within the Cardium Formation west of the Pembina field in west-central Alberta.

A detailed study of the Cardium Formation has not been well documented in the literature within the study area, whereas many sedimentological studies have been conducted on the Cardium Formation fields to the north, east and south of this study area, including: Carrot Creek (Swagor, 1975; Bergman and Walker, 1986; Arnott, 2003); Pembina (Beach, 1955; Nielsen, 1957; Michaelis, 1957; Krause and Nelson, 1984; Krause *et al*., 1987; Vosselar and Pemberton, 1989) Ferrier and Willesden Green (Griffith, 1981; Keith, 1991); Ricinus (Walker, 1983b); Caroline and Garrington (Berven, 1966; Walker, 1983b,c); and Crossfield (Krause and Nelson, 1991). The locations of these fields relative to this study area can be noted in Figure 1-1.

Achieving the goals of the study was accomplished by dissecting the lithofacies structure from core analysis and systematically using it to define a

series of processes responsible for the deposition of the Cardium Formation within the study area. This was accomplished by:

1. Defining and describing the lithofacies present and documenting the internal stratigraphy of the study area;
2. Investigating the geometry of the Cardium Formation in strike and dip section cross sections and constructing isopach and structure maps; and
3. Proposing interpretations of the depositional processes and suggesting a potential sequential development scheme for the Cardium Formation in the study area.

The Cardium Formation in Alberta is of significant scientific importance because of the economic implications associated with the enormous volume of hydrocarbons that have been produced from it and still remain within it.

2.2 Study Area

The study targets an area approximately 150 kilometers southwest of Edmonton, Alberta (Figure 1-1), between Townships 45 to 48 and Ranges 14 to 17 west of the Fifth Meridian. (Figure 2-1). The study area encompasses four exploration fields, the western edge of Brazeau River, Columbia, Hanlan and Peco fields (Figure 2-1).

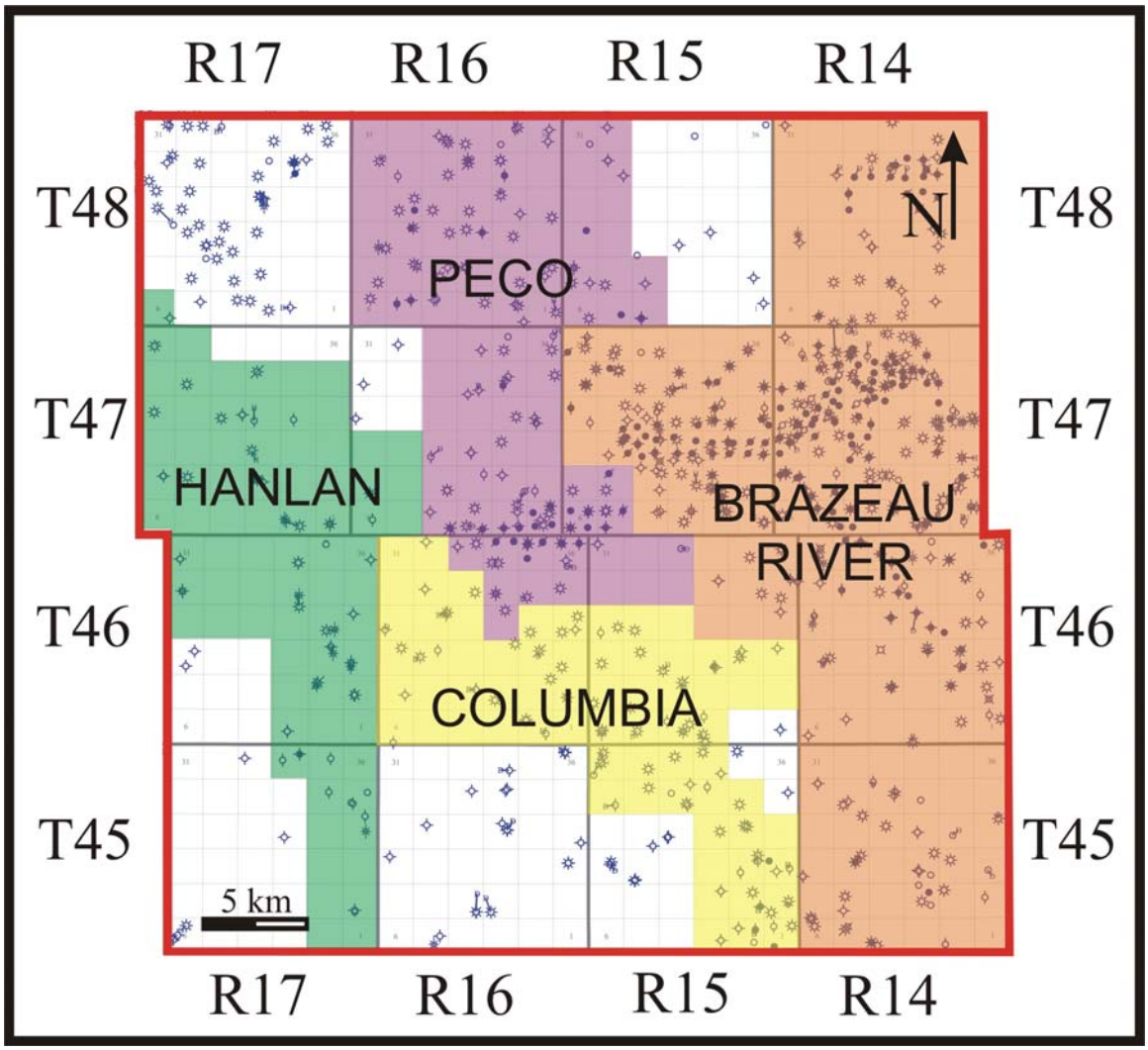

Figure 2-1: Four primary exploration fields lie within the boundary of the study area and include the western edge of Brazeau River, Columbia, Hanlan and Peco fields. Location of field data from *AccuMap*® and AEUB.

2.3 Methods

All of the 367 wireline logs in the study area were examined. Formation tops for the Cardium Zone, Cardium and Blackstone formations were chosen from these logs. The formation tops were picked based on the signatures of the gamma ray, induction and spontaneous potential logs. Raster log images from *AccuMap*® software were used to correlate the tops between individual wells. A total of 35 dip sections and nine strike sections were constructed to effectively correlate the Cardium Formation across the study area; eight of them are presented later in the chapter. The construction of these sections provides a more accurate interpretation than a well by well interpretation because variation can more easily be noted and correlated within the Cardium Formation across the cross sections. The dip sections were constructed approximately orthogonal to the paleo-shoreline to give a proper representation of the geometry of the Cardium Formation. The strike sections lie approximately parallel to the paleo-shoreline and help to properly tie the Cardium Formation across the dip sections. Isopach and structural top maps were created using the kriging contouring feature within *AccuMap*®. This assisted in describing the three dimensional geometry of the Cardium Formation sandstone within the study area.

Seventeen cores were examined across the regional study area to generate graphical core logs to systematically describe and define the lithofacies present. The core logs were drafted using Wellsight Systems *Striplog*® *v*.6.0b. A limited amount of core that intersects the Cardium Formation is present in the study area, which limited the possible correlations in areas between them due to

their spacing. The cores selected for investigation are based on the signature from electric wireline logs that showed a well-developed sandstone signature with intervals being two meters or greater in length. Intervals less than two meters in length provided very limited and unpredictable core recovery as well as limited insight into the depositional environment. The lithofacies identified from the core study, based on similar electrical response signature characteristics, were matched to electrical logs from adjacent wells where no core exists.

2.4 Stratigraphy

Krause *et al*. (1994) state that the Cardium Formation is commonly exposed at the surface in the Foothills within east-verging thrust sheets in packages up to 150 meters thick, thinning eastward to less than 50 meters in the subsurface of the Plains. Figure 2-2 displays a generalised stratigraphic column of the west-central Alberta Plains where the study is focused. Deposition of the Cardium Formation occurred during the Late Cretaceous (Turonian and Coniacian) in an arc-shaped clastic wedge consisting of two lobes that extend from northern British Columbia near Dawson Creek southward to the Canada/U.S.A. border (Figure 2-3). Thrust sheet loading during the Late Cretaceous Cordilleran Orogeny caused the Cardium Formation to become structurally deformed in the Foothills and subsurface of the Plains while developing a regional dip to the southwest.

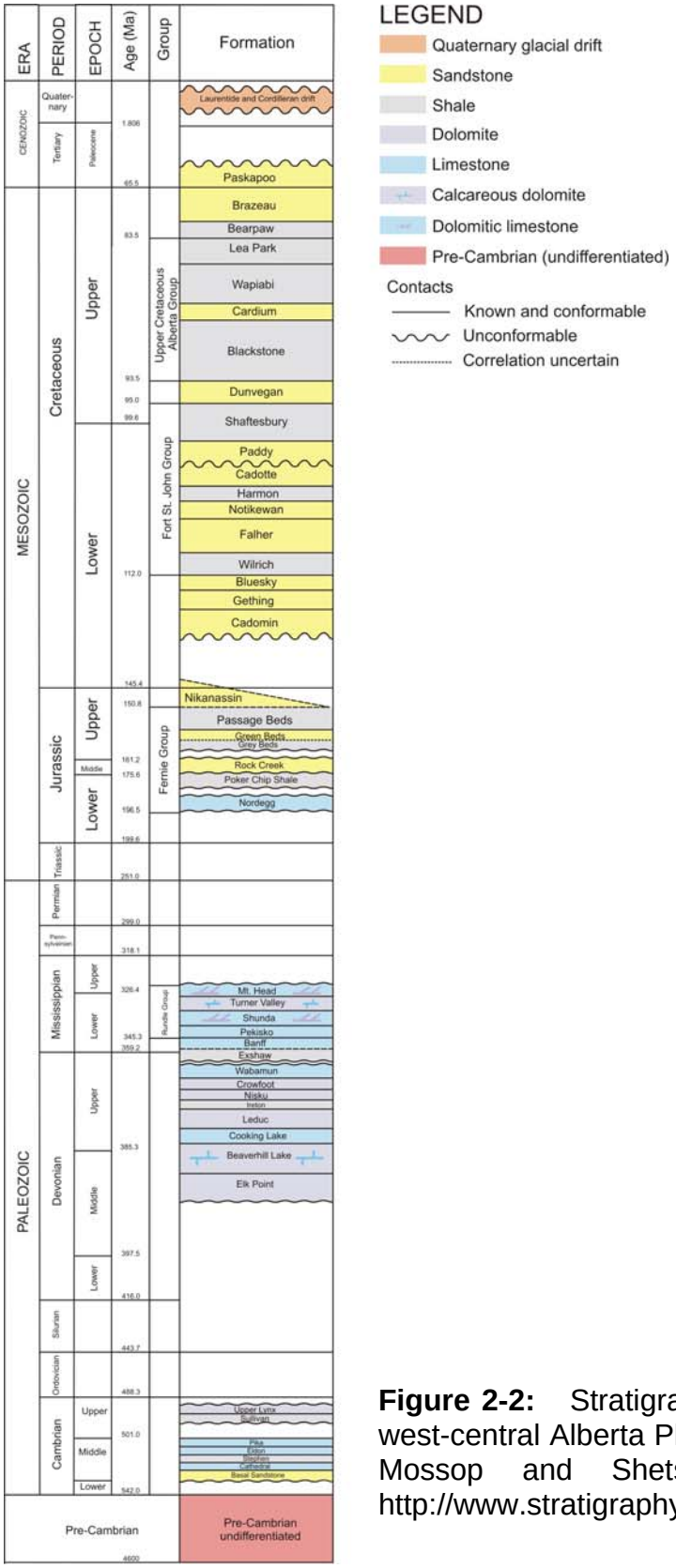

Figure 2-2: Stratigraphic column of the west-central Alberta Plains. Modified from Mossop and Shetson (1994) and http://www.stratigraphy.org/cheu.pdf.

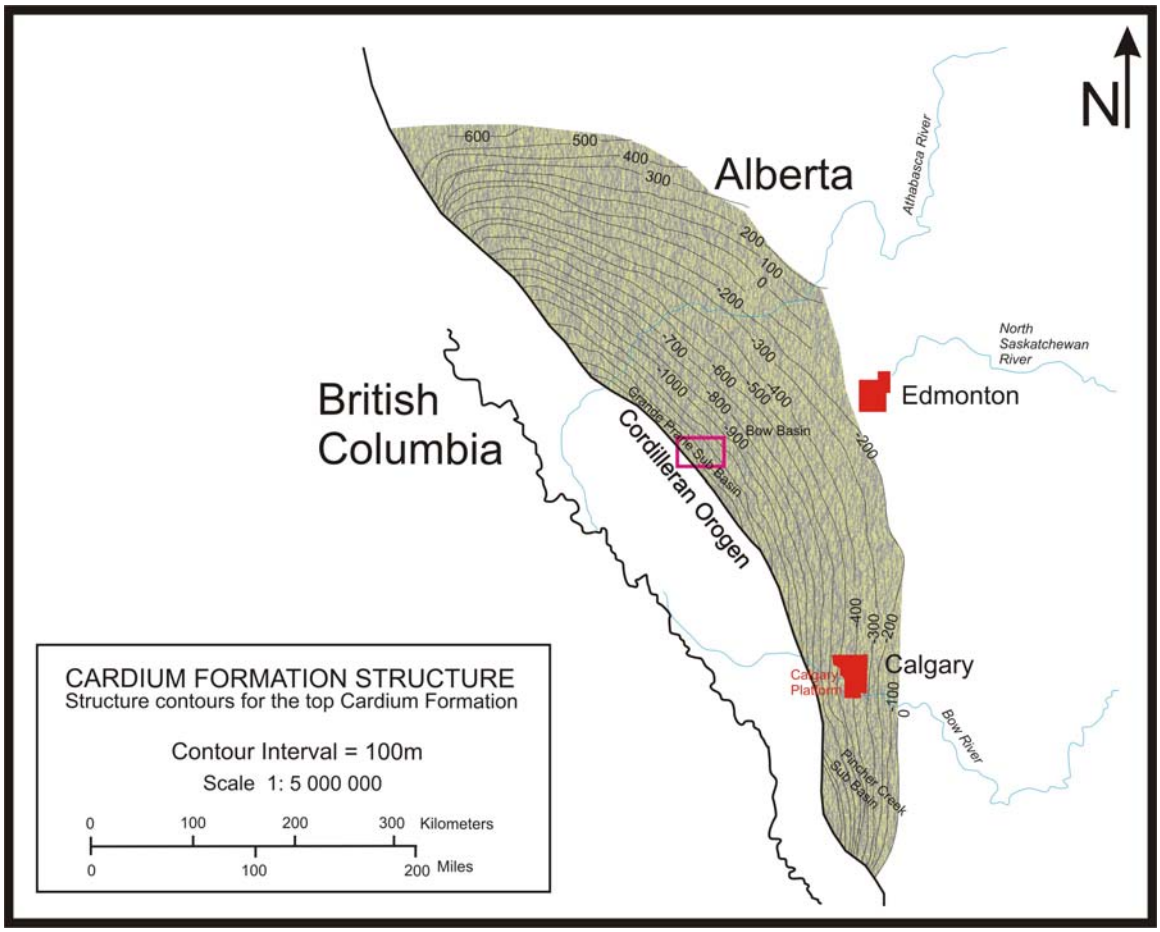

Figure 2-3: Structure contour map of the Cardium Formation showing the arcuate nature of the formation and a general regional dip to the southwest. The regional dip was predominantly developed by thrust sheet loading from the Cordilleran Orogen that occurred to the southwest during the Late Cretaceous and Early Paleogene. The location of the study area is outlined by the pink rectangle. Modified from Krause *et al*. (1994).

Stratigraphically, the Cardium Formation overlies the dark shales of the Blackstone Formation. The black shales of the Wapiabi Formation overlie the Cardium Formation. These formations are all contained within the Upper Cretaceous Alberta Group. The initial age assignment is based on work from Stott (1963), detailing ammonite fauna in the Wapiabi and Blackstone formation shales and limited macrofossils identified directly within the Cardium by Stelck (1955). Stott's (1963) memoir describes the type section of the Cardium along Wapiabi Creek subdividing the formation into six distinctive members, from oldest to youngest: the Ram, Moosehound, Kiska, Cardinal, Leyland and Sturrock members. The Ram, Cardinal and Sturrock members are fine grained marine sandstones that are separated by the marine shales of the Kiska and Leyland members. The Moosehound Member is characterized by non-marine shales, siltstones, sandstones and coals. More recently, Hall *et al*. (1995) collected ammonites from two sections of the Cardium Formation near Seebe, Alberta and from cores from the Pembina field, precisely determining the age of the Cardium Formation to be between upper Turonian and lower Coniacian.

Within the study area the Cardium Formation sandstone is observed to coarsen upward from shales into sandstones. Krause and Nelson (1984) have referred to this coarsening upward sequence as the Pembina River Member while Keith (1985) refers to it as the Cardium 'A' sandstone sequence. This study also refers to the coarsening upward sequence from shales into sandstones as the Cardium 'A' sandstone. It is called the 'A' sandstone because it is the uppermost Cardium sandstone encountered, but it may not be equivalent in age

to the Cardium ‘A’ sandstone in the Pembina field. Nielsen (1957), Michaelis (1957), Griffith (1981), Keith (1985), Plint *et al*. (1986), Krause *et al*. (1987), Krause and Nelson (1991) and Krause *et al.* (1994) among others have noted that the top of the sandstone sequence is truncated by a regional erosion surface. Typically chert pebble conglomerates are observed to overlie the unconformable surface in both core and in outcrops. The marine shales of the Cardium Zone Member regionally overlie the Cardium ‘A’ sandstone sequence sandstones and conglomerates (Krause and Nelson, 1991). The Cardium Zone Member is regionally overlain by the Wapiabi shales. Figure 2-4 outlines the stratigraphic column for the immediate study area and equivalents from Keith (1985, 1991) and Krause and Nelson (1984) in the neighbouring fields of Willesden Green and Pembina, respectively.

On wireline logs, the Cardium ‘A’ sandstone unit is commonly recorded as a series of coarsening upward sequences. Figure 2-5 shows a typical log in the study area that displays the coarsening upward sequence within the Cardium ‘A’ sandstone. The Cardium ‘A’ sandstone sequence is shaly at the base and grades upward into interbedded sandstones, siltstones and minor shales. The Cardium ‘A’ sandstone is commonly capped by coarser conglomerates. The wireline signature for the Cardium ‘A’ sandstone is easily recognizable, as the API reading on the gamma ray log decreases in value from 30 to 45 in the cleanest sandstone and corresponds to an abrupt increase in induction log readings through the coarser clastic sections. The spontaneous potential log shows a negative deflection through the cleaner sandstone interval. The transition from

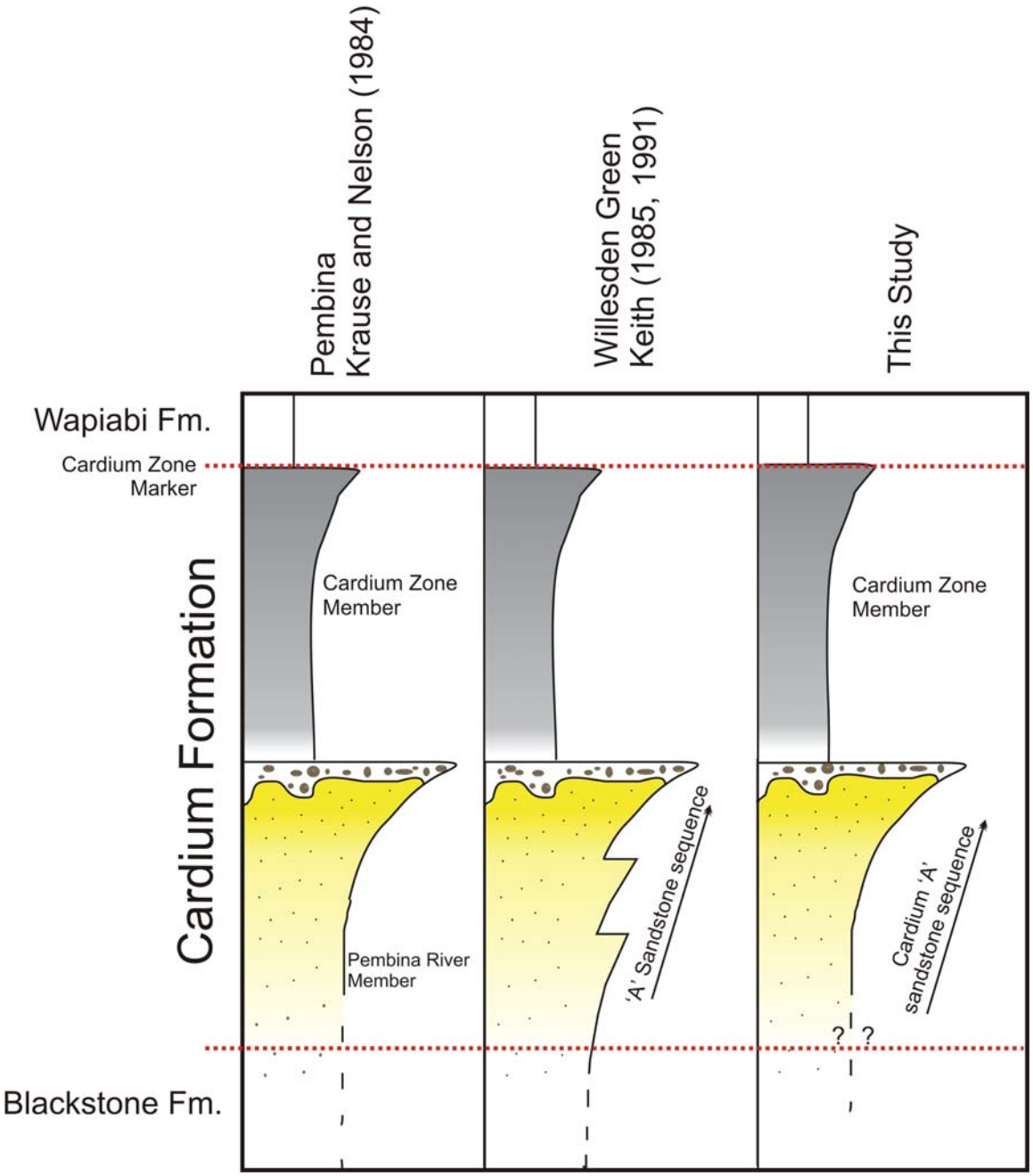

Figure 2-4: Stratigraphy of the study area and neighbouring fields. Coarsening upward trend of the Cardium 'A' sandstone is noted by the inclination of the arrow line toward the right. Modified from Keith (1985, 1991). Figure not to scale.

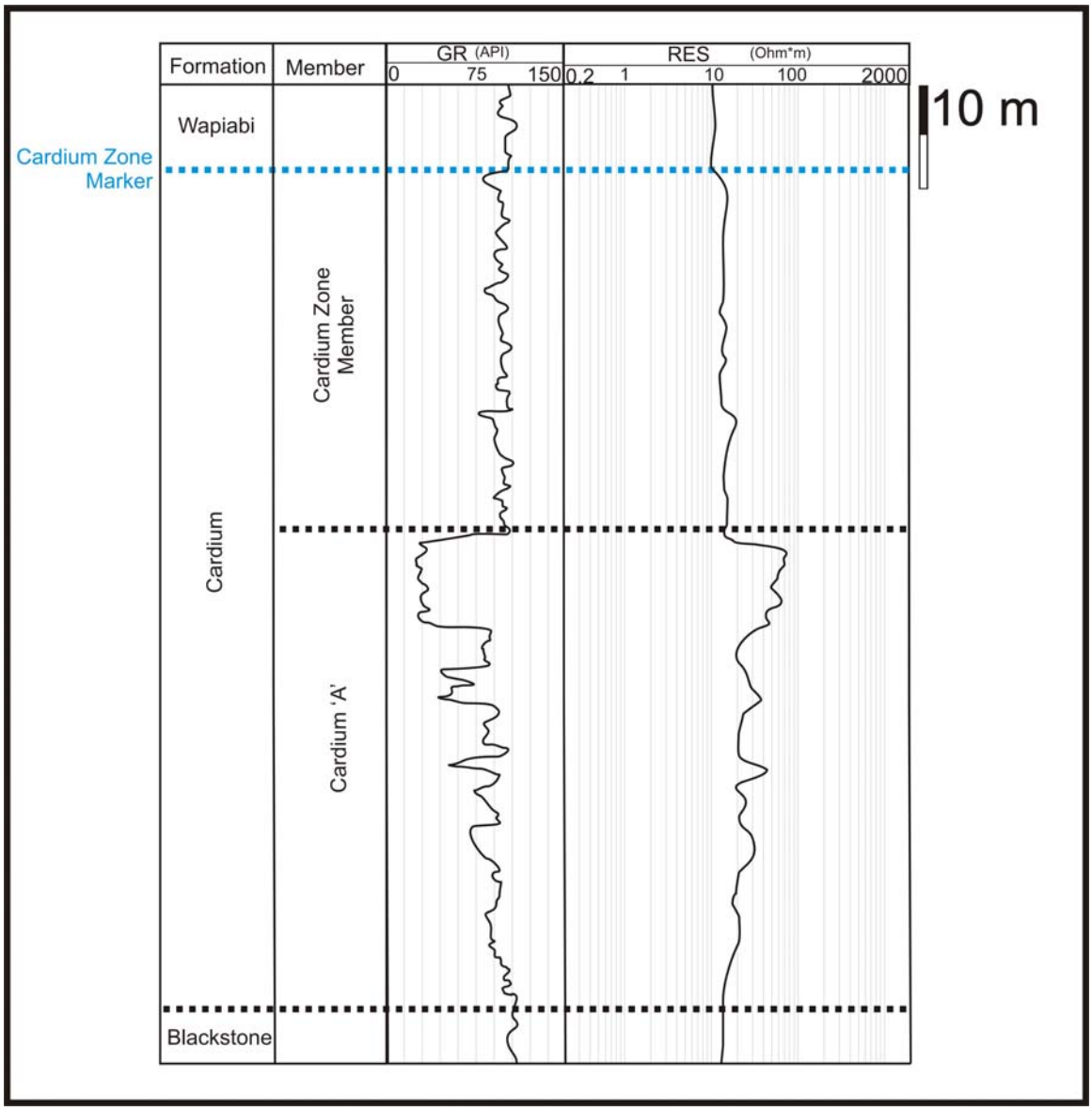

Figure 2-5: Log 9-20-46-16W5 showing the typical Cardium Formation response in the study area. The Cardium 'A' sandstone is noted to coarsen upward, which is evidenced by a decrease in the gamma ray and an increase in the induction log signatures toward the upper contact. The Cardium Zone Member coarsens upward as well, but not as abruptly as the Cardium 'A' sandstone.

the sandstone or conglomerate capping the Cardium ‘A’ sandstone upwards into the Cardium Zone Member shale is always marked by a sharp increase in the gamma ray reading, increasing to 80 API units or greater. A decrease in the induction log response within the Cardium Zone Member to values near 10 Ohm*m is noted, similar to the induction readings in the lower, shalier parts of the Cardium Formation and underlying Blackstone Formation. The Cardium Zone Member gamma ray reading increases to approximately 120 API units and induction readings increase toward the top of the zone from 10 Ohm*m to the 15-20 Ohm*m range. The top of the Cardium Zone Member is identified by a slight decrease in the resistivity where readings usually drop below 10 Ohm*m. and maintain a background level of approximately 8-9 Ohm*m.

2.5 Previous Interpretations

Many previous interpretations have been advanced to explain the depositional setting of the Cardium Formation following the discovery of the Pembina field in 1953. These interpretations have attempted to describe the processes that emplaced sandstones and conglomerates of the Cardium Formation within the bounding marine shales. Beach (1955) was the first to study the Cardium Formation in the subsurface in detail and suggested a turbidity current origin for the emplacement of the sandstones and conglomerates, but in the years following, DeWeil (1956) and Neilsen (1957) had major objections to Beach’s model. DeWeil (1956) suggested that the slope angles of the Cretaceous seas would not have been great enough to feasibly transport the

amount of coarse clastic sediment by turbid flow compared to angles measured from modern day slopes. Parsons (1955 a, b), Michaelis (1957) and Nielsen (1957) wrote that the Cardium Formation was deposited in a deltaic setting below wave-base in the interior Cretaceous seaway. They stated that the origin of the conglomerates was derived from the west from the uprising Foothills. Nielsen (1957) argued that the Cardium Formation at Pembina was a shallow marine-offshore sandstone body, stating that the suggestion of a turbidite was not likely based of the stratigraphic sequence preserved. Mountjoy (1957) suggested that the deposition of the Cardium Formation was caused by storms and offshore currents. He also disagreed with the previous turbidite interpretation due to the lack of significant evidence of bedforms associated with such deposits. After a number of investigations, consensus for one depositional origin was still missing and all studies remained inconclusive.

Switching depositional paradigms to a nearshore, shallow water interpretation, Michaelis (1957) noted an upward shoaling sequence. He described a marginal delta deposit close to a distributary mouth bar grading into tidal lagoonal rocks that were all overlain by beach deposits. Michaelis (1957) wrote that the sequence was deposited on a subaerially exposed, broad coastal plain. Later, conglomerate that had been transported from the Foothills to the subaerial plain was reworked into conglomeratic pods farther out on the coastal plain during a transgression. Off (1963) stated that conglomerate deposition was caused by tidal ridge processes, comparing what he observed in Cardium Formation cores to tidal bars observed in the North Sea. Michaelis and Dixon

(1969) suggested that the Cardium was deposited in a shallow sea on a shelf in terrace bars that were later remolded by storms. They further concluded that data from Foothills wells showed fining upwards sequences in the Cardium Formation and suggested a possible fluvial origin. Swagor (1975) and Swagor *et al.* (1976) argued that the conglomerates of the Cardium Formation in the Carrot Creek field, north of Pembina, were emplaced and molded above and within storm-weather wave-base by storm cycles on a stable shelf. The conglomerates were focused at a break in slope, called the terrace bar, on the northeastern flanks of northeastward-clinoforming sand bars. Storms transported the clastic material to the final depositional site and the clastics were subsequently reworked and aligned at that location. Basin subsidence began to exceed sedimentation, at which point there was a relative rise in sea level and muds were deposited over the coarser clastic material. The outcrop work of Wright and Walker (1981), ichnology studies of Pemberton and Frey (1984) and Williams and Stelck's (1975) paleogeographic reconstruction of Late Cretaceous time has seemingly narrowed the debate to a potential nearshore, shallow water interpretation.

Wright and Walker (1981) describe the Cardium as a storm-controlled deposit based on outcrop investigation near Seebe, Alberta. The idea of storms controlling depositional trends was later transferred to subsurface investigations. In separate papers, two years later, Walker (1983a) describes the Cardium as being deposited by means of turbidites and Walker (1983b, c) describes it as being a "ragged blanket" storm deposit. Shifting ideas again, Bergman and Walker (1987) describe the deposition of the Cardium at Carrot Creek as

occurring in a beach setting that experienced a transgression followed by deposition of the conglomerates during a sea level drop. They invoke large changes in sea level to account for each depositional package. The beach interpretation leads to interpretational problems based on a certain lack of lithological evidence observed. Bergman and Walker (1987) state that, during sea level drop, increased fluvial activity supplied coarse clastic material to the shoreface. Bergman and Walker (1987) have not documented any evidence of channels cutting into the shoreface based on core and electric wireline examination or any sort of paleosol preservation to substantiate the beach interpretation.

In a number of papers published by Krause and others (Krause, 1982; 1983; Krause and Nelson, 1984; Krause *et al*., 1987; Krause *et al*.,1994; and Krause and Nelson, 1991) predominantly describe the Cardium Formation as a storm dominated muddy shelf. Keith (1985, 1991) described the Cardium developing as a series of offlapping depositional units representing prograding offshore strandplains during a period of slow sea level lowering. The geometry of the Cardium Formation was determined to be dispersive and not deposited in a planar, layer-cake fashion (Keith, 1985, 1991; Joiner, 1991). Moreover, the conglomerate distribution across the Pembina field was determined to be irregular and patchy (Krause *et al.,* 1987). Walker and Eyles (1988) and Leggitt *et al.* (1990) contest Keith's (1985) interpretation and suggest that the conglomerate accumulation and distribution is attributed to the geometry of the E5 erosion surface and complex tectonic tilting invoked during deposition.

Most recently, Arnott (2003) describes the Cardium in the Cyn-Pem/Carrot Creek area as being deposited on a steeper delta front via gravity driven sediment flows. Although the Cardium Formation has been extensively studied in the last 50 years, the depositional processes that emplaced it are still not completely understood and an all-encompassing model still eludes geoscientists. Table 2-1 summarizes the authors, Cardium Formation study location and the depositional model and processes invoked in significant works published regarding the Cardium Formation.

2.6 Lithofacies Descriptions

A lithofacies is a body of rock or sediment with specified characteristics that include the following: bedding, colour, composition, grain size, fossils, mineralogy, sedimentary structure (physical and biological) and sorting. The lithofacies identified from the seventeen cores examined for this study closely follow the classification scheme from Krause and Nelson's (1984) study of the adjacent Pembina Field, with only minor modifications. The modifications were necessary to specifically tailor the lithofacies types to minor differences noted within the study area. The bedding classification scheme used for this study was taken from Ingram (1954). The lithofacies generated from core investigation have been divided into five groups, which have been further subdivided within their respective groups into subfacies. The primary lithofacies identified in this study are: 1) Dark grey to black shales with minor bioturbation; 2) Bioturbated, thinly

Table 2-1: Table details author, Cardium Formation study location and the depositional model and processes invoked in significant works published regarding the Cardium Formation in the last 50 years.

AUTHOR	YEAR	STUDY LOCATION	DEPOSITIONAL MODEL and PROCESSES
			TURBIDITY CURRENTS
Beach	1955	Pembina	Turbidites
DeWeil	1956	Pembina	Refutes Beach's turbidite idea
Walker	1983b	Garrington; Caroline; Ricinus	Ragged blanket - storm sedimentation/turbidites
Arnott	2003	Carrot Creek and Pembina	Sediment gravity flow/turbidite
			DELTA
Parsons	1955a,b	Pembina	Delta deposit
Nielsen	1957	Pembina	Delta deposit/shallow marine
Thomas	1996	Cyn-Pem	Delta deposit
			SHELF with other influences
Michaelis	1957	Pembina	Shallow shoal/storm influence
Off	1963	Worldwide analagous outcrops	Shelf with tidal bars
Berven	1966	Garrington	Shelf - offshore bars
Swagor *et al.*	1976	Carrot Creek	Shelf with storm influence
Krause and Nelson	1984	Pembina	Shelf with storm influence
Deutsch and Krause	1991	Kakwa	Shelf/muddy coastline
Krause *et al.*	1987	Pembina	Storm sedimentation/muddy coastline
Keith	1985, 1991	Willisden Green	Shelf sedimentation
			STORM INFLUENCE
Michaelis and Dixon	1969	Pembina	Storm sedimentation
Wright and Walker	1981	Seebe	Storm sedimentation
Krause	1982	Pembina	Storm sedimentation
Krause	1983	Pembina	Storm sedimentation
Walker	1983a,b,c	Garrington; Caroline; Ricinus	Ragged blanket - storm sedimentation/turbidites
Pemberton and Frey	1984	Seebe	Storm sedimentation
Krause *et al.*	1987	Pembina	Storm sedimentation/muddy coastline
Vossler and Pemberton	1989	Carrot Creek and Pembina	Storm sedimentation
			BEACH and SHOREFACE to NONMARINE
Stott	1963	Outcrop work	Marine and non marine (coastal plain)
Bergman and Walker	1987	Carrot Creek	Beach/upper shoreface
Plint and Walker	1987	Kakwa	Shoreface/coastal plain
Walker and Eyles	1988	Willisden Green	Shallow marine/allocyclic sedimentation
Hart and Plint	1989	Encompasses the Cardium Fm.	Shoreface/shelf
Krause *et al.*	1994	Encompasses the Cardium Fm.	Shoreface/shelf

interbedded shales and siltstones with very fine sandstone stringers 3) Bioturbated, thinly bedded sandstone and siltstone with minor to common interbedded shale stringers; 4) Thickly bedded, very fine to medium grained sandstone with rare shaly partings; and 5) Chert conglomerates. Each lithofacies and respective subfacies is addressed in the following individual subsections.

2.6.1 Lithofacies One (F1): Dark Grey to Black Shales

Description: Lithofacies One (F1) is characterized by dark grey to black shales. Interbedded siltstone laminae are rarely observed and, where present, are sometimes disrupted by bioturbation with no identifiable traces. Only minor bioturbation is noted in F1, at less than 30% in all of the cores examined. Figure 2-6 shows the typical F1 lithology identified in core.

***Interpretation*:** The limited amount of identifiable bioturbation and the lack of any significant bedding structure within this lithofacies make an accurate interpretation difficult. Joiner (1991) notes the presence of *Helminthopsis sp.* in his equivalently assigned lithofacies. Seilacher (1967) notes that *Helminthopsis sp.* is contained within the deeper water *Nereites* ichnofacies. Based on the identification of the *Helminthopsis sp.* from core and the somewhat structureless fine sediment, the lithofacies is interpreted to have been deposited in a quiet, deeper water, marine setting. The shale of F1 is typically massive, which suggests sedimentation occurred below fair-weather wave-base and likely below much of the storm-weather wave-base. The basal contact of F1 with Lithofacies Five (F5) is gradational and commonly has interbedded clastic material suspend-

Figure 2-6: **A)** Lithofacies One (F1) (6-21-47-15W5; 2486m): Shale of F1 in core with minor unspecified bioturbation evident through the silty interbedded sections. **B)** F1 (10-28-45-16W5; 2793m): Shale beds of F1. “Rilled” appearance is caused by the core bit during cutting.

ed as thin lag-stringer layers or isolated pebbles up to 30 centimeters above the contact surface. Typically within F1, thin horizons of fine pebble conglomerates up to two cm thick are noted above the primary F5 conglomerate horizon, encased in unbioturbated shales. These are interpreted to be deposited in a series of waning storm surges that provided the last influx of finer conglomeratic material into this deeper marine environment. As sea level deepened, coarser clastic material could no longer be transported to these depths, at which point only black marine shales are present.

2.6.2 Lithofacies Two (F2): Bioturbated, Thinly Interbedded Shale and Siltstone with Minor Sandstone Stringers

Description: Lithofacies Two (F2) is characterized by dark shales with rare to common interbedded laminae of siltstone and sandstone. Typically, the laminae range between 1.0 mm to 1.5 cm. Siderite rich horizons and nodules are commonly observed in this lithofacies, which are up to 5 cm thick and may span the entire core diameter. The siderite horizons are often associated with slickensided surfaces. Limited pyrite nodules up to 3 cm in diameter are also noted. Ripple cross laminations and wavy bedding that have not been disrupted by bioturbation are sometimes observed within the sandstone and siltstone interbeds. The level of biotubation present within this lithofacies is the basis for subdivision into two separate subfacies; 2A and 2B.

Subfacies 2A (F2A) is classified by bioturbation levels that are greater than 40%, whereas *Subfacies 2B* (F2B) is classified by bioturbation levels that

are less than 40%. Ichnofossils observed in core include: *Chondrites sp.*, *Paleophycus sp.*, *Rhyzocorallium sp.*, *Skolithos sp.*, *Teichicnus sp.*, *Terebellina sp.* and *Zoophycos sp.*. Figure 2-7 shows typical examples of F2 and the associated ichnofossils. The varying amount of bioturbation within this lithofacies often gives it a 'mottled' appearance.

***Interpretation*:** F2 represents sediments that have been heavily reworked by benthic organisms. The majority of bioturbation within F2 would have occurred during periods of lower energy and water agitation. The observed ichnofossil assemblage is representative of the *Cruziana* / *Zoophycos* ichnofacies (Seilacher, 1967). Frey and Pemberton (1985) indicate that these ichnofacies represent a sublittoral to outer shelf-bathyal, marine environment. Deposition predominantly would have occurred below daily fair-weather base and, at times, possibly below storm-weather wave-base. At these depths, the influence of currents on the sediments would be minimized, allowing prolific bioturbation to occur. Howard and Reineck (1981) note that long periods of relative quiescence, slow rates of sedimentation and only brief storm events typify an environment that is dominated by biogenic processes.

Occasional punctuation of shale horizons exists with very thin siltstone and fine sandstone beds, indicating that coarser sediment was episodically reaching water at deeper depths. Low current velocities may have been periodically active during the deposition, allowing minor bedding structures to form in the thin sandstone and siltstone lenses. The coarser siltstone and sandstone material may have been transported to the site via seasonal river

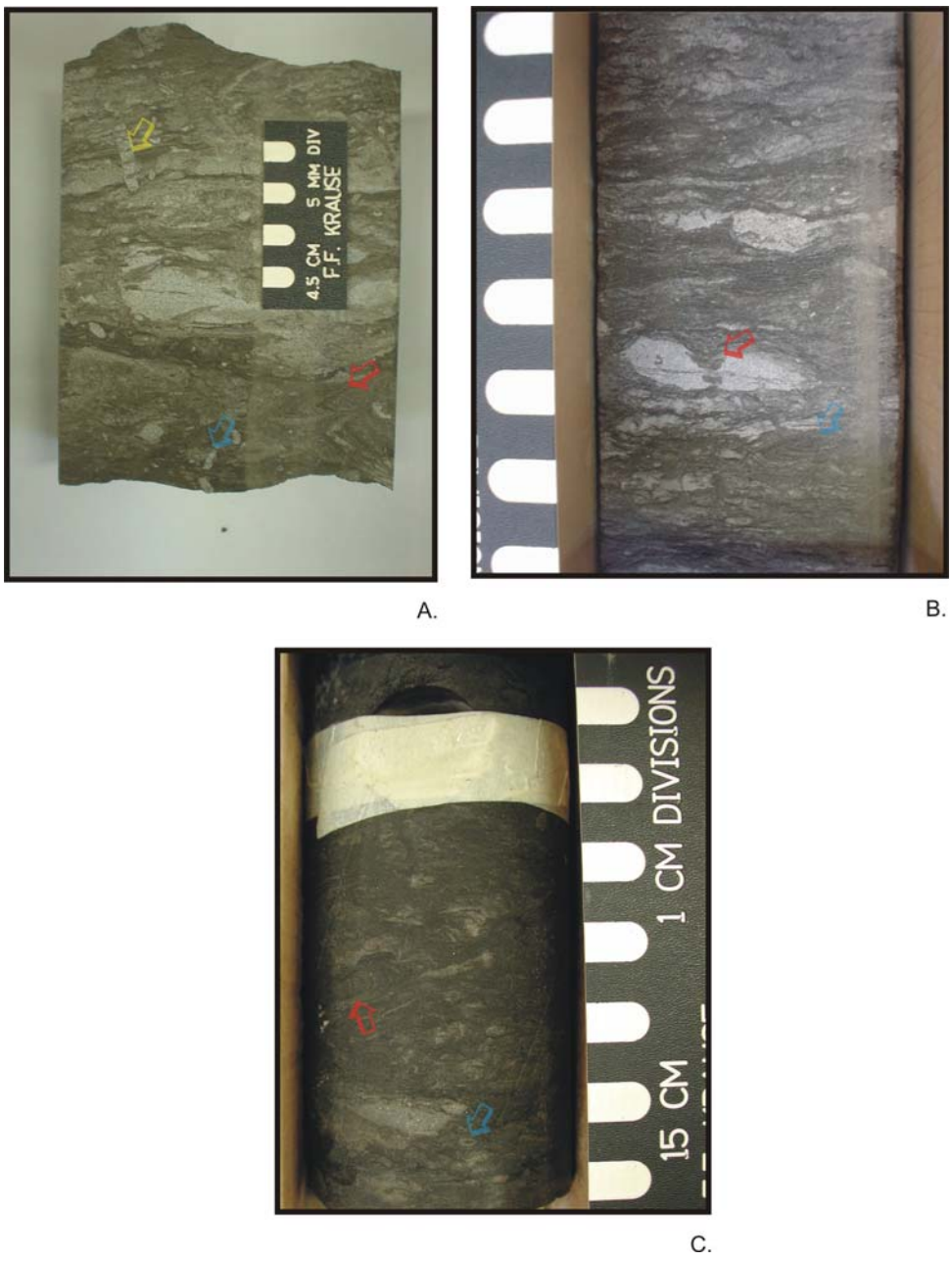

Figure 2-7: **A)** Subfacies 2A (F2A) (10-5-49-11W5; 1789m): *Skolithos sp.* traces with later overprinting of *Zoophycos sp.* and *Phycosiphon sp.* marked by yellow, red and blue arrows respectively. **B)** F2A (14-3-47-14W5; 2477m): Abundant bioturbation within the fine siltstone and sandstone that completely mixes the two lithologies. *Gyrolithes sp.* and *Rhyzocorallium sp.* marked by red and blue arrows respectively. **C)** F2A (6-15-48-9W5; 1620m): *Zoophycos sp.* and *Terebellina sp.* marked by red and blue arrows respectively. Facies is completely churned by abundant bioturbation.

floods causing hyperpycnal flows to assist transport of the sediment to the outer shelf. Conversely, the coarser sediment may have been transported to the offshore location by storm currents.

A higher energy regime temporarily existed during deposition of the coarser sands and silts, which created a disruption of the biogenic activity in the sediment. Minor to moderate levels of bioturbation noted within the sandstone and siltstone horizons are believed to represent biogenic reactivation after a return to the primary shale sedimentation of this lithofacies. Burrows are noted in core to breach the contacts of the bedding structures in the sandstone and siltstone from the shales that sandwich them. Combinations of F3 and F4 are observed to overlie F2. F3 and F4 are characterized by more sandstone and siltstone content and less shale compared to that of F2. F3 and F4 represent a shift to higher energy regimes relative to what is recorded within F2.

2.6.3 Lithofacies Three (F3): Bioturbated, Thinly Bedded Siltstone and Fine to Coarse Grained Sandstone with Interbedded Shale Stringers

Description: Lithofacies Three (F3) consists of interbedded sandstones and siltstones. The shale content of this lithofacies is significantly decreased from that of F2. Sedimentary structures in this lithofacies include current ripple cross lamination, parallel laminations, scour and fill structures, lenticular, wavy and graded bedding. Sideritic horizons up to 5 cm thick are observed interbedded with shale. Flat, platy shale chips ranging in size from millimeters to a couple of

centimeters are often observed within sandstone packages, predominantly located at or near the lower contact of the lithofacies. F3 is subdivided into two subfacies based on common bedding structures noted through the intervals. F3 is most often interbedded with either F4 or F2 in the cores examined across the study area.

Subfacies 3R (F3R) (Ripple cross-laminated), is characterized by thinly interbedded very fine and fine grained sandstones and shales. The sandstones show common ripple cross lamination structure and typically have a lower contact surface that is scoured and has gutter cast infills. Interbedded rippled sandstones range in thickness from 1 to 5 cm. F3R shows minor to moderate bioturbation, up to 30%, commonly disrupting the bedding structure.

Subfacies 3G (F3G) (Graded), is characterized by graded beds that fine upward from fine grained sandstones to shales/siltstones. The shales typically have upper contacts that are somewhat scoured and mark the base of the overlying gradational sequence. The packages of graded sandstone and shale have average thicknesses of 2 to 6 cm. *Chondrites sp.* is the most commonly observed ichnofossil present, whereas less commonly *Palaeophycus sp.*, *Skolithos sp.* and rare *Rosselia sp.* have also been identified. F3G only has rare to minor levels of bioturbation, promoting the preservation of the graded bedding structure quite well. Figure 2-8 shows typical examples of F3 in core.

***Interpretation*:** The ichnofossil assemblage that characterizes F3 is similar to that of F2, and is classified as belonging to the *Cruziana* ichnofacies (Seilacher, 1967). This lithofacies is likely to have been deposited below the daily

Figure 2-8: A) Subfacies 3R (F3R) (10-5-49-11W5; 1787m): Sandstone interlaminated with shale. *Chondrites sp.* is noted in the shale at the bottom of the sample and a Skolithos *sp.* is seen vertically cutting the entire section of core. **B)** F3R (16-29-47-10W5; 1802.5m): *Chondrites sp.* and *Teichichnus sp.* noted in the bioturbated, shaly horizons. Sandstone is relatively undisturbed and shows minor wavy and lenticular bedding as well as parallel and ripple cross laminations. **C)** F3G (1-23-48-16W5; 2418m): Graded bedding from fine sandstone to shale.

fair-weather wave-base, but not below the storm-weather wave-base as indicated by the trace fossil fauna identified in core (Frey and Pemberton, 1985). F3 is interpreted to represent a contrast in energy regimes compared to F2 due to the larger volume of coarser sediment which is observed within core. A series of higher energy events would have been necessary to provide the larger volume of sand and silt to the depositional environment.

The coarser grained sediments of F3 may have been transported to the shore and shelf via large seasonal riverine floods and associated hyperpycnal flows, punctuated by shorter periods of shale deposition. Krause and Nelson (1984) suggest that coarser grained sediments within the Pembina area may have been supplied to the shoreline during a change in sea level stand, which could have been re-molded or re-sedimented by later change in sea level stand. Invoking changes in sea level stand within this study area may explain the increase in the supply of coarser sediments. The increased clastic content of F3 could also be attributable to a change in clastic provenance that coincided with a change in sea level stand. Bedding structures within F3 include ripple cross lamination, parallel laminations, scour and fill structures, and lenticular and wavy beds. These bedding structures likely were emplaced by a combination of storm generated currents, waning flow and some fair-weather oscillatory flows. Swift *et al*. (1983) have noted that these types of bedding structures may be caused by combined and/or oscillatory flows.

A decreased level of bioturbation is noted in F3. Commonly, *Chondrites sp.* is the dominant bioturbation trace present, with a lack of any other significant

trace makers visible. Krause and Nelson (1991) attribute this in their similarly assigned lithofacies to reduced salinities, higher concentrations of suspended muds or possible anoxic conditions. Based on the interpretation from this study, it may also be suggested that the energetic emplacement of higher volumes of sand and silt was likely occurring at more frequent intervals compared to those of F2. There were fewer periods of quiescence during which shale sedimentation could occur and favourable conditions for benthonic colonization could reoccur.

In this study a number of shale clast and chip horizons are noted within F3 and are generally focused at the lower contact of the lithofacies. Krause and Nelson (1991) have also noted such horizons and attributed them to erosive bottom-hugging currents. The currents may have been generated after the sand was deposited, reworking the sand and also redistributing the ‘rip-ups’ from the top of the underlying F2 within it. Conversely, the currents emplacing the sands may have syn-depositionally ripped up underlying, semi-lithified fragments of F2. This would focus the major shale chip horizon at the base of F3. Any other shale chip layers observed within F3 were likely emplaced above substantially less thick shale beds because of shorter depositional hiatuses occurring between sand depositional events. This would have limited the amount of shale material available to be reworked and redistributed within the sandstone or siltstone horizons during successive erosive flow events.

F3R may have been subjected to the influence of more storm generated flows, or combined flows at a shallower water depth, as a greater variety of wave ripple forms have been observed within it. Emplacement of the F3G likely

occurred rapidly, because the shale contact below it is scoured and the sands above grade into shales. This interpretation is consistent with graded bedforms that have been noted to form by storm generated currents (Hayes, 1967) and also potential influences from post-storm physical reworking of the sediment.

2.6.4 Lithofacies Four (F4): Thickly bedded, Very Fine to Medium Grained Sandstone

Description: Lithofacies Four (F4) is primarily composed of very fine to fine grained (125-250 microns) sandstone that is typically bedded on the centimeter to decimeter scale. The light grey sandstone is predominantly composed of quartz sands, darker lithic grains, sideritic cements and unidentified matrix clays. The most commonly observed sedimentary features are low angle-inclined stratification (LIS, as described by Krause and Nelson, 1984), planar lamination, climbing ripples and wave ripple cross lamination. Thin interbeds of shale up to 5 cm in thickness are sometimes present and divide the thicker packages of sandstone. Ichnofossils identified include the traces of *Palaeophycus sp.*, *Rosselia sp.*, *Rhyzocorallium sp.*, *Zoophycos sp.* and sometimes *Chondrites sp.* in the shale horizons. The lithofacies is divided into two subfacies based on the level of bioturbation present.

Subfacies 4A (F4A) represents a subfacies with greater than 30% bioturbation whereas *Subfacies 4B* represents a subfacies with less than 30% bioturbation. F4 is interbedded with F2 or F3 and always noted to underlie Lithofacies Five (F5). Figure 2-9 shows common examples of F4 in core.

A.

B.

C.

Figure 2-9: **A)** Subfacies 4A (F4A) (10-17-49-12W5; 1899.5m): This sandstone appears structureless (likely due to being unslabbed) and shows a range of rounded siditerized clasts within it. **B)** F4A (10-17-49-12W5; 1903.25m): Sandstone showing low angle inclined parallel stratification (LIS) with a truncation surface located in the middle of the interval. **C)** F4B (10-5-49-11W5; 1777.5m – 1779m): Sandstone of F4B with low angle inclined and parallel laminations. Bioturbation is essentially non-existent in this interval.

***Interpretation*:** Trace fossils identified in core indicate that F4 represents a marine environment, ranging between sublittoral to bathyal settings (Crimes, 1975; Frey and Pemberton, 1985). The most common dune scale sedimentary structure observed in core is identified as low angle inclined stratification (LIS). Low angle inclined stratification is inferred to be equivalent to hummocky cross stratification (HCS) in outcrop (Krause and Nelson, 1991). Harms *et al.* (1975) indicated that HCS is a bedform with large scale convex and concave cross-stratification and of storm origin in which divergent laminae exist at very low angles (typically <15 degrees). Swift *et al.* (1983) state that HCS may form by combined-flow currents, accompanied by steady geostrophic or coastal flows. More recently, Dumas and Arnott (2006) conducted a number of wave-tunnel experiments where HCS bedforms were generated by long wave periods, moderate to high oscillatory velocities (50-90 cm/s) and very weak to no unidirectional flow (< 10 cm/s). They continue, stating that formation of HCS optimally occurs at or near storm-weather wave-base where aggradation rates during storms are high enough to preserve hummocks but unidirectional current speeds are sufficiently low to generate low-angle cross-stratification. Hummocky cross stratification has been interpreted in core investigation by Krause and Nelson (1984, 1991) and Keith (1991). Hummocky cross stratification within the Cardium Formation in outcrop has been observed by numerous authors including Wright and Walker (1981); Krause and Nelson (1984), among others. The LIS sedimentary structure observed in core in this study is consistent with what has been recorded by other authors in adjacent Cardium Formation fields. Although a

large scale bedform such as HCS is difficult to identify in core, it is logical to assume that such a bedform observed in outcrop may also be present in the subsurface in an equivalently identified lithofacies, as has been already been shown by Krause and Nelson (1984).

The LIS sedimentary structure noted in core indicate that sediments from F4 were accumulated and reworked in a high energy environment. The sandstones of F4 are interpreted to have been transported to the shelf by frequent storm events, associated longshore drift and geostrophic currents. Hyperpycnal riverine inflow may have also assisted in delivery of the initial sand volumes to the shelf. Storms not only assisted in transport of the sands to the shelf position, but also caused the common hydrodynamic overprinting such as LIS.

F4 is characterized as containing the thickest packages of sandstone and shows very limited bioturbation. Bioturbation is located within discrete horizons within the sandstones. When present, the bioturbation appears to be focused near contacts showing a lithological change at the upper boundary of the lithofacies. It is inferred that these horizons may have existed during a temporary depositional hiatus or quiescent period, allowing colonization, followed by bioturbation. *Palaeophycus sp.*, *Rosselia sp.*, *Rhyzocorallium sp.* and *Zoophycos sp.* are the most common traces noted in F4 and Ekdale *et al*. (1984) indicate that the assemblage is typical within hummocky cross stratified sand layers and bounding mudstones.

2.6.5 Lithofacies Five (F5): Chert Conglomerate

Description: The Lithofacies Five (F5) conglomerates are predominantly composed of chert. A small proportion of the conglomeratic material is quartzose and lithic sandstones. Grain size of the conglomerate is variable and ranges from 1 mm to 32 mm in the studied cores. Minor imbrication of grains within some layers is observed in some places. The conglomerate is typically poorly- to very well sorted, and in some instances the sorting is bimodal. Siderite is observed in the form of an alteration horizon in shales and as isolated clasts or infilling pore spaces in sandy matrices. F5 ranges in thickness from approximately one centimeter to several meters in the investigated cores and has similar or greater thicknesses in other Cardium Formation fields as recorded by Krause (1984), Joiner (1989, 1991) and Keith (1991), among others. Thin layers of F5 are commonly observed to be interbedded with intervals of F3 or F4. Conglomerate distribution within the study area is limited, but when present, is always observed capping the Cardium Formation sandstone. Typically the upper contact of F5 is observed to be gradational where individual pebbles and lags extend into the overlying F1. The lower contact of the lithofacies is generally observed to be sharp and unconformable with the underlying lithofacies, often leaving large scour surfaces. Bioturbation within F5 is rare and is typically confined to *Subfacies 5C*; identified only as *Chondrites sp.*.

F5 has been subdivided into three subfacies based on matrix and conglomerate support materials, modified slightly from Joiner (1991). The subfacies are *Subfacies 5A* (F5A): Sandstone matrix supported conglomerate;

Subfacies 5B (F5B): Clast supported conglomerate with matrix material; and *Subfacies 5C* (F5C): Shale supported conglomerate. Figure 2-10 shows common examples of F5 in the cores studied.

Subfacies 5A **(F5A): Sandstone Matrix Supported Conglomerate**

Description: This subfacies is identified by abundant sandstone matrix supporting the conglomerate. The sandstone is predominantly composed of quartz grains and lithic material. Matrix sandstones are often partially or completely siditerized. The sandstones are most commonly observed to be randomly distributed within the conglomerate, but can also be planarly laminated between conglomeratic layers. The grain size ranges from 177 to 500 microns and is usually coarser than that in other lithofacies. The conglomerate clasts typically range from 2-15 mm in diameter in this subfacies.

Subfacies 5B **(F5B): Clast Supported Conglomerate with Matrix Material**

Description: This subfacies is generally the same as F5A apart from being clast supported. The matrix material is predominantly composed of quartzose and lithic sands. Sometimes minor siditizeration is noted in the sandstones, but it is not as common as seen in F5A. The clast supported conglomerates generally have larger clasts up to 3 cm in diameter and sometimes display bimodality with smaller grain sizes composing the matrix.

Figure 2-10: A) Subfacies 5A (F5A) (11-13-47-15W5; 2523.3m): Sand supported conglomerate. Sandstone matrix is partially siditerized. **B)** F5B (6-15-48-9W5; 1603.25m): Clast supported conglomerate; minor sand is present in the matrix of the coarse conglomerate. In the upper part of this sample a 2 cm thick interval of sand supported conglomerate is present in between the clast supported conglomerate. **C)** F5C (10-13-47-15W5; 2523.6m): Shale supported conglomerate. Note the abrupt scour surface marking the basal contact.

***Subfacies 5C* (F5C): Shale Supported Conglomerate**

Description: This subfacies is typically seen near the top of F5 intervals. The grain size of the conglomerate is extremely variable between 2 mm and 10 mm; granule to small pebble sizes. Typically the conglomerate within the shale occurs in two patterns: as single isolated pebbles 'floating' in a shale matrix, or as thin conglomeratic lag layers up to 2 cm thick that have very sharp contacts with the surrounding shale.

***Interpretations*:** F5 is representative of a change in clastic supply due to the presence of chert pebbles, which are not found in the other four lithofacies. The exact provenance of the clastic supply is unknown, but is predominantly composed of chert pebbles and less common quartz and lithic sands.

A very limited amount of bioturbation is noted in F5 and presumed to be caused by the highly energetic and erosive emplacement of conglomeratic beds combined with a limited amount of finer sediment interbeds. When observed, the bioturbation typically is focused in the interbedded shale or sand horizons within F5. Joiner (1991) believes that the formation of the unconformity underlying the conglomerates formed contemporaneously with the deposition, as bioturbation is sometimes noted at the contact to draw individual pebbles into the underlying Lithofacies. This study has observed similar features. If the conglomerates were not emplaced rapidly, then the top of the F4 surface likely would have had a chance to experience much more biogenic activity. A further interpretation and discussion of the conglomerate deposition is reviewed later in this chapter.

2.7 Lithofacies Associations

Examination of the digital core logs in the Appendix and the cross sections appearing later in this chapter show that the lateral and vertical lithofacies relationships in the study area vary from well to well, making it difficult to establish accurate and continuous correlations. Lithofacies between wells do not show consistent thickness or horizontal continuity; therefore, for the study area (16 townships) only a certain number of conclusions may be distilled.

Contacts between lithofacies are either sharp, bioturbated or gradational. Sharp contacts are most common and exist as planar, angular or scoured contacts. The sharp contacts recorded are present typically in F3, F4 and F5. The scour contacts indicate a higher energy environment with high current velocities, emplacing sediment quite rapidly. Sharp contacts between sandstones and shales indicate an abrupt change to an environment with little to no energy, where sediment would generally fall out of suspension. Bioturbated contacts are commonly observed within F2 and at the boundary with any overlying lithofacies. Bioturbation within F2 is typically so intense that distinguishable contacts are often not preserved. Gradational contacts are most often recorded between the F5 conglomerates and the overlying F1 shale. Krause and Nelson (1984) have noted similar contacts in outcrop compared to their core investigation, where their lithofacies assignment closely resembles the one of this study.

Figure 2-11 displays the regional structure contour map of the top of the Cardium Formation sandstone surface. The dip of the surface is quite variable,

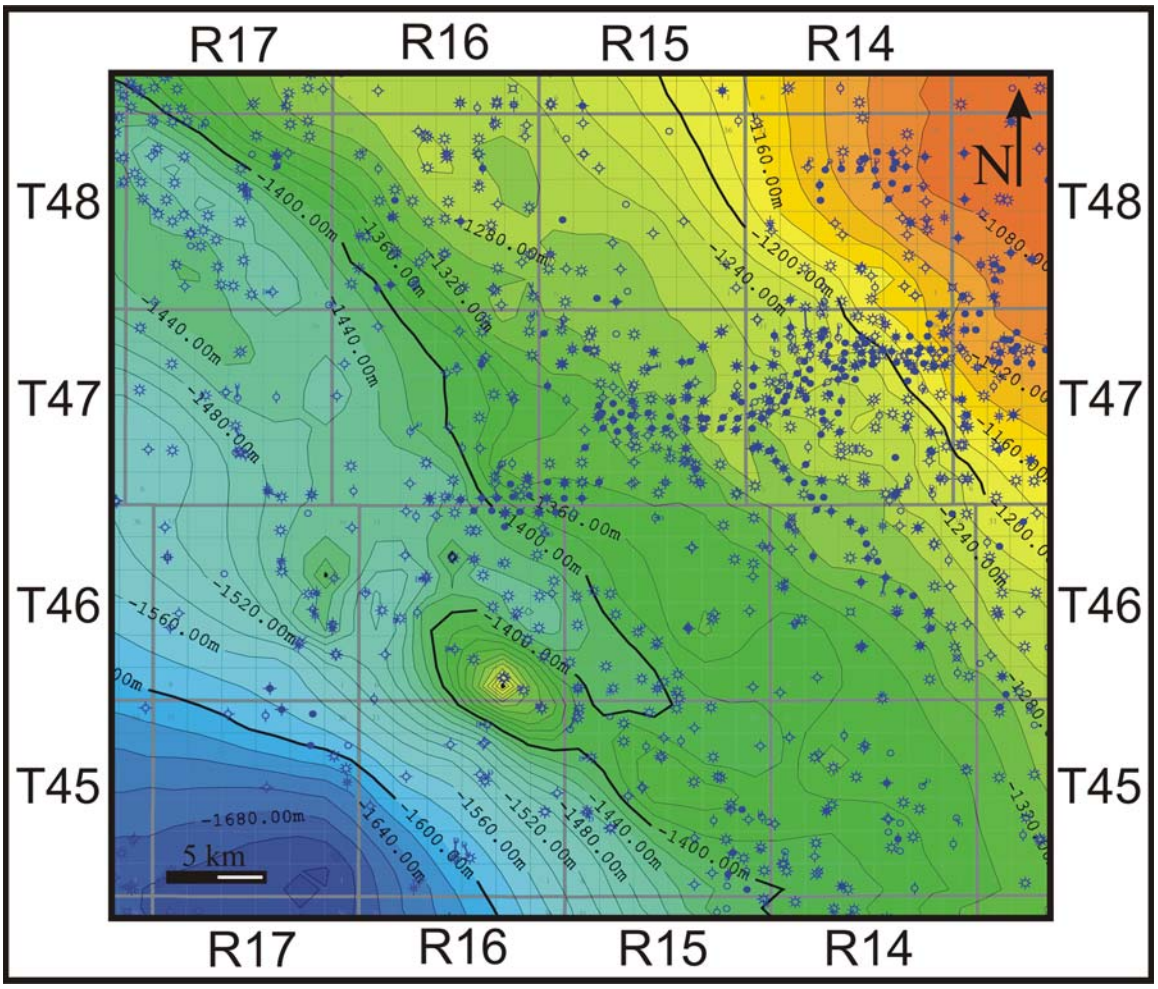

Figure 2-11: Regional structure contour map of the top of the Cardium Formation sandstone surface. The dip of the surface is quite variable but regionally the dip is very shallow and to the southwest. The datum used in the construction of the structural map is sea level. Contour interval is 20 m.

but regionally it dips very shallowly to the west. The datum used in the construction of the structural map is sea level.

2.7.1 Vertical Lithofacies Relationships

In this study the vertical lithofacies relationships from core analysis are all coarsening upward sequences and are not difficult to establish. Commonly within each coarsening upward sequence, individual lithofacies are noted to be repeated on top of one another. F2 is always noted at the bottom of the core intervals where cored deeply enough and it is overlain by either F3, F4 or both. Interbedded packages of F2 sometimes occur between F3 and F4 in some places. F5, where present, unconformably overlies F3 or F4 and marks the top of the main Cardium Formation sandstone sequence. Where F5 is not present, F4 marks the top of the Cardium Formation sandstone sequence. F1 always overlies the top of the Cardium Formation sandstone sequence. The contact of F5 with the overlying F1 is typically gradational and isolated pebbles of F5 are observed to be contained in the shale of F1. Thin conglomeratic stringers up to two cm thick have been noted within the F1 shale. F2 to F5 are all noted to coarsen upward in the cores examined; this correlates well with the electrical logs recorded in the study area. The core logs (Appendix) clearly display the vertical relationships present between the lithofacies. Figure 2-12 shows the typical vertical stacking of the lithofacies in core from the study area. Walker (1983), Keith (1985, 1991) and Krause *et al.* (1987) among other authors have noted similar coarsening upward trends in other Cardium Formation fields.

Figure 2-12: Vertical lithofacies stacking in core 11-13-47-15W5 (2511 – 2529m). See core log in the Appendix for lithofacies assignment and descriptions. Dashed red lines mark contacts between different labelled lithofacies.

2.7.2 Lateral Lithofacies Relationships

Lateral lithofacies relationships are more difficult to determine due to the presence or lack of facies and varying thicknesses of lithofacies between wells. Precise correlation of the lithofacies across the study area with cross sections is difficult due to the discontinuous nature of the identified lithofacies from core analysis. Additionally, the limited number of cores intersecting the appropriate interval which would allow consistent confirmation of the lithofacies across the study area prevents effective continuous correlations. Sequence stratigraphic correlations are very difficult since no micro- or macrofossils were encountered or investigated for. Attempts have been made to correlate the cross sections as accurately as possible across the regional study area by extending the lithofacies interpretations from the logged cores to neighboring wells. This technique is accomplished by examining the electrical responses that correspond to cored intervals and then tying the signatures to similar electrical responses in adjacent wells where core is unavailable. The correlation cannot be considered entirely complete as the precise distance across which to extend the each lithofacies where core is unavailable is interpretational.

The top of the Cardium Zone Member is the marker that the cross sections are hung on to outline the lateral variation across the study area. Nielsen (1957) notes that the Cardium Zone Member is a field-wide marker in Pembina and this observation has also been verified in this study area. The top of the Cardium Zone Member is easy to identify from resistivity logs and shows a

distinct boundary between the lower, silty section and the overlying muddier section, as described earlier in this chapter on page 17.

A total of eight cross sections were constructed from gamma ray and electric wireline logs in the study area. Five dip sections, 1-1', 2-2', 3-3', 4-4' and 5-5' (Figures 2-13, 2-14, 2-15, 2-16 and 2-17) are oriented approximately SW-NE, parallel to the present day regional dip direction and varies around Williams and Stelck's (1975) paleo-shoreline trend (Figure 2-18) of the Cretaceous Interior Seaway in present day southern Alberta. Three strike sections were generated, 6-6', 7-7' and 8-8' (Figures 2-19, 2-20 and 2-21), and are oriented orthogonally to the five dip sections and approximately parallel to the paleo-shoreline trend.

Cross sections 1-1', 2-2', 3-3', 4-4' and 5-5' (Figures 2-13, 2-14, 2-15, 2-16 and 2-17) display a variation in thickening and thinning trends. The westernmost parts of the cross sections show thick sandstones developed; this is also noted in the Cardium Formation sandstone isopach map (Figure 2-22). The sandstone in these sections thins quite rapidly eastward and maintains a consistent thickness in the eastern two thirds of the sections, as readily seen in the isopach map (Figure 2-22). The thick sandstone noted in sections 1-1', 2-2', 3-3', 4-4' and 5-5' (Figures 2-13, 2-14, 2-15, 2-16 and 2-17) trends northwest-southeast, which is approximately parallel to the inferred orientation of the paleo-shoreline trend of Williams and Stelck (1975). Section 6-6' (Figure 2-19) is constructed parallel to the eastern periphery of this thick sandstone and maintains a relatively constant thickness across the section. The lack of any significant geometric variation in vertical displacement in the cross section is because it lies essentially parallel to

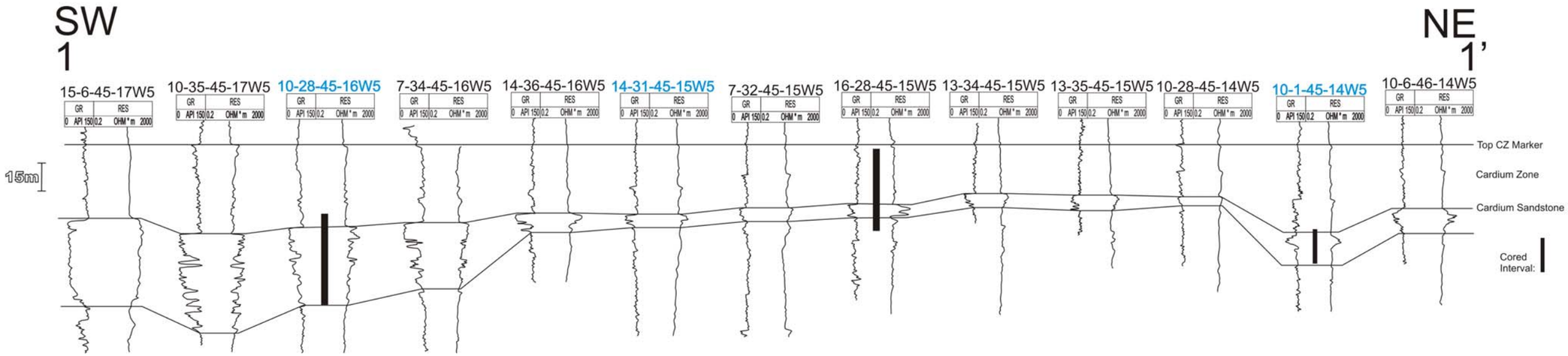

Figure 2-13: Southwest-northeast stratigraphic cross section 1-1'. Section is based on the gamma ray and induction log signatures. This section is oriented approximately in an orthogonal direction to the paleo shoreline trend and generally shows a decrease in thickness in the Cardium Formation toward the northeast. Blue UWI locations in cross section indicate logs that tie to other cross sections. Township and Range map shows the location of cross sections. Red wells with surrounding grey rectangle on the Township and Range index map indicate cored wells from the study area that were examined.

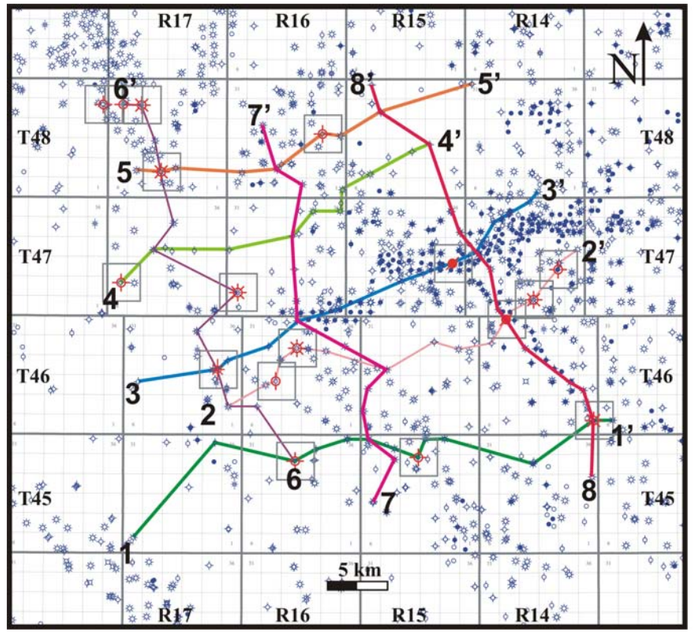

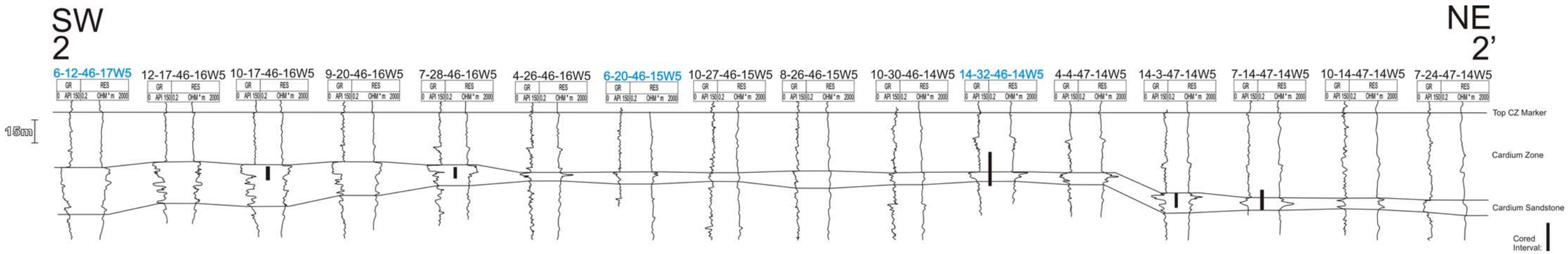

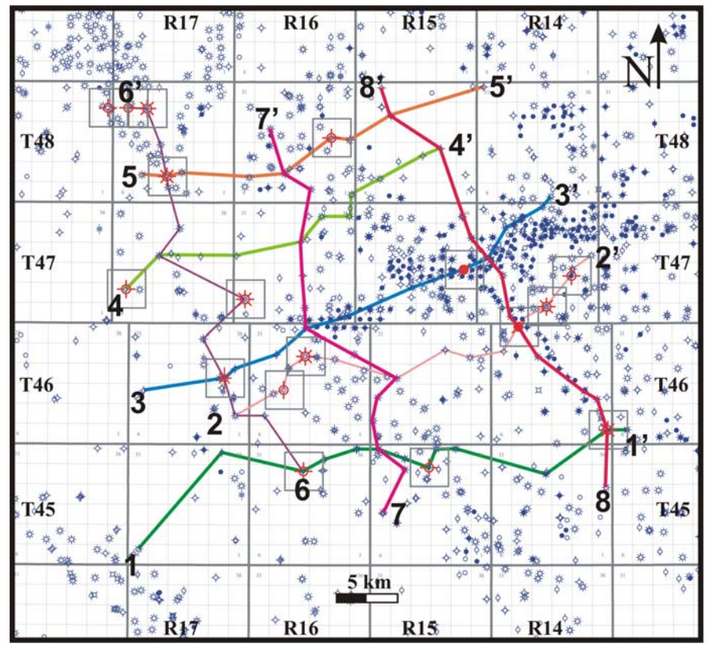

Figure 2-14: Southwest-northeast stratigraphic cross section 2-2'. Section is based on the gamma ray and induction log signatures. This section is oriented approximately in an orthogonal direction to the paleo shoreline trend and generally shows a decrease in thickness in the Cardium Formation toward the northeast. Blue UWI locations in cross section indicate logs that tie to other cross sections. Township and Range map shows the location of cross sections. Red wells with surrounding grey rectangle on the Township and Range index map indicate cored wells from the study area that were examined.

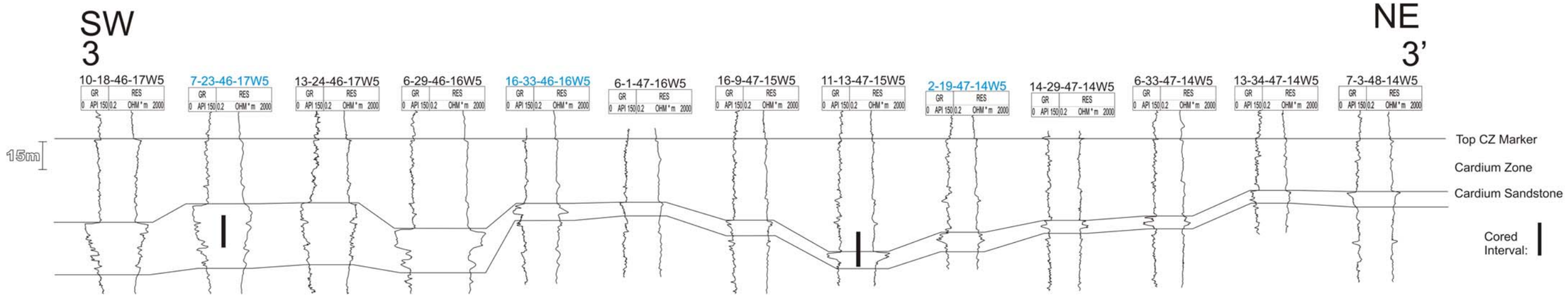

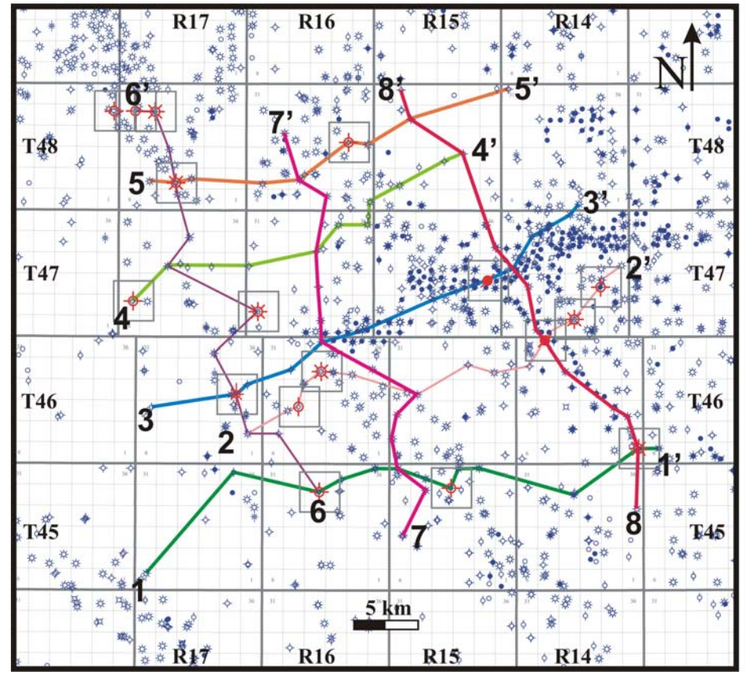

Figure 2-15: Southwest-northeast stratigraphic cross section 3-3'. Section is based on the gamma ray and induction log signatures. This section is oriented approximately in an orthogonal direction to the paleo shoreline trend and generally shows a decrease in thickness in the Cardium Formation toward the northeast. Blue UWI locations in cross section indicate logs that tie to other cross sections. Township and Range map shows the location of cross sections. Red wells with surrounding grey rectangle on the Township and Range index map indicate cored wells from the study area that were examined.

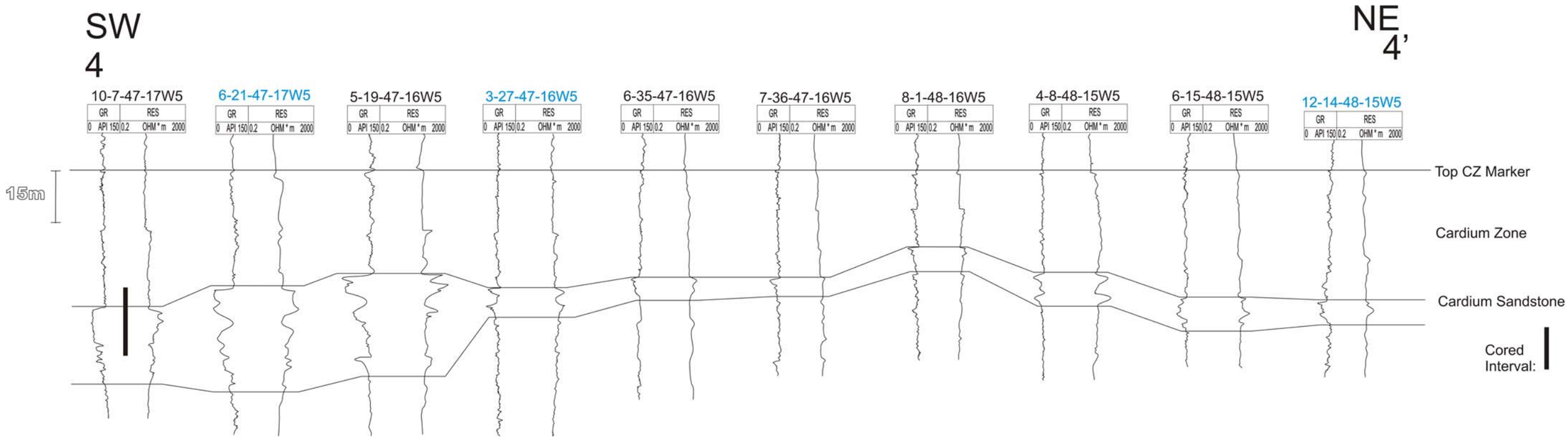

Figure 2-16: Southwest-northeast stratigraphic cross section 4-4'. Section is based on the gamma ray and induction log signatures. This section is oriented approximately in an orthogonal direction to the paleo shoreline trend and generally shows a decrease in thickness in the Cardium Formation toward the northeast. Blue UWI locations in cross section indicate logs that tie to other cross sections. Township and Range map shows the location of cross sections. Red wells with surrounding grey rectangle on the Township and Range index map indicate cored wells from the study area that were examined.

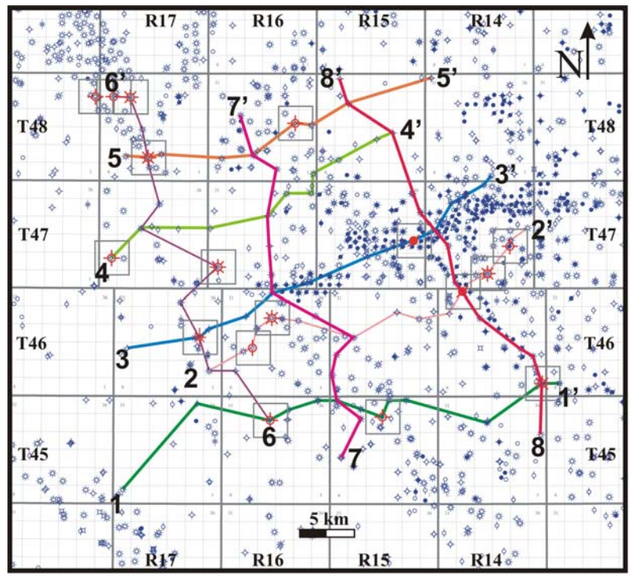

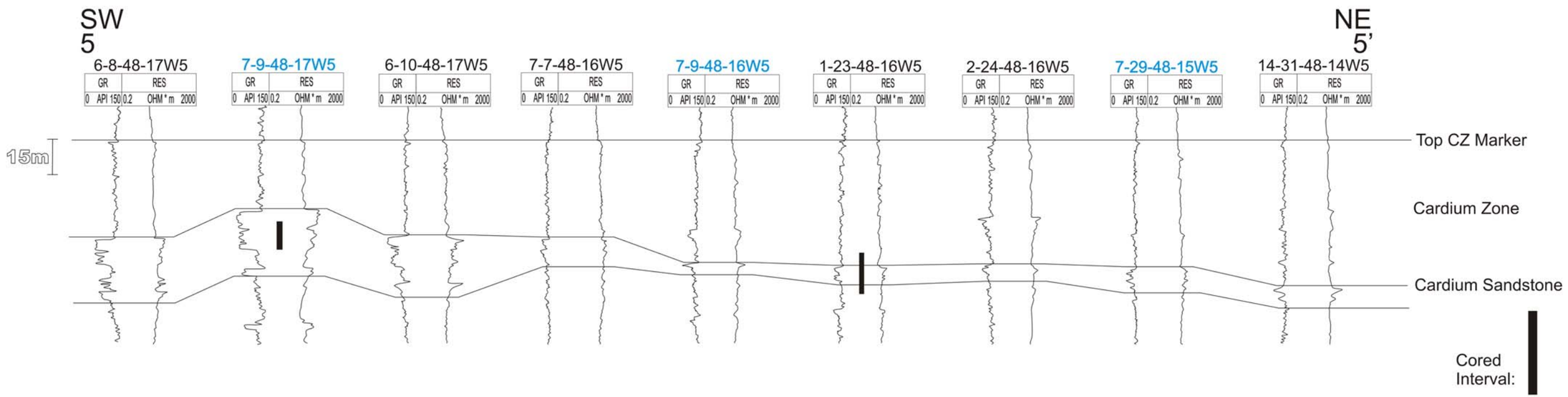

Figure 2-17: Southwest-northeast stratigraphic cross section 5-5’. Section is based on the gamma ray and induction log signatures. This section is oriented approximately in an orthogonal direction to the paleo shoreline trend and generally shows a decrease in thickness in the Cardium Formation toward the northeast. Blue UWI locations in cross section indicate logs that tie to other cross sections. Township and Range map shows the location of cross sections. Red wells with surrounding grey rectangle on the Township and Range index map indicate cored wells from the study area that were examined.

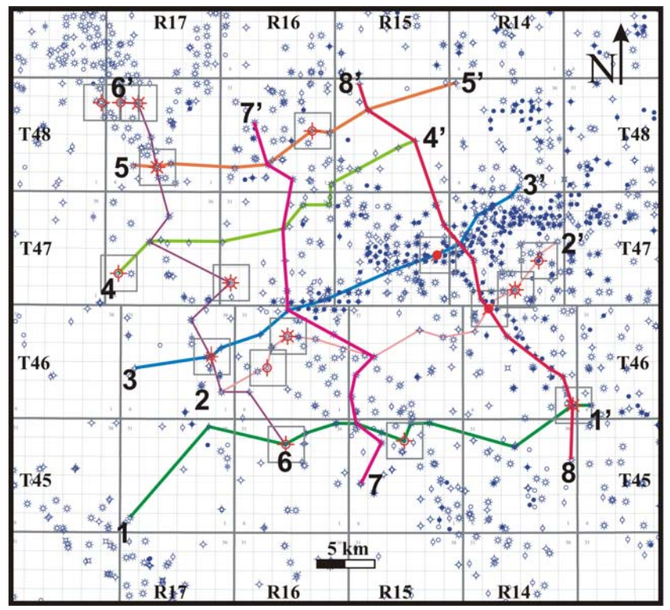

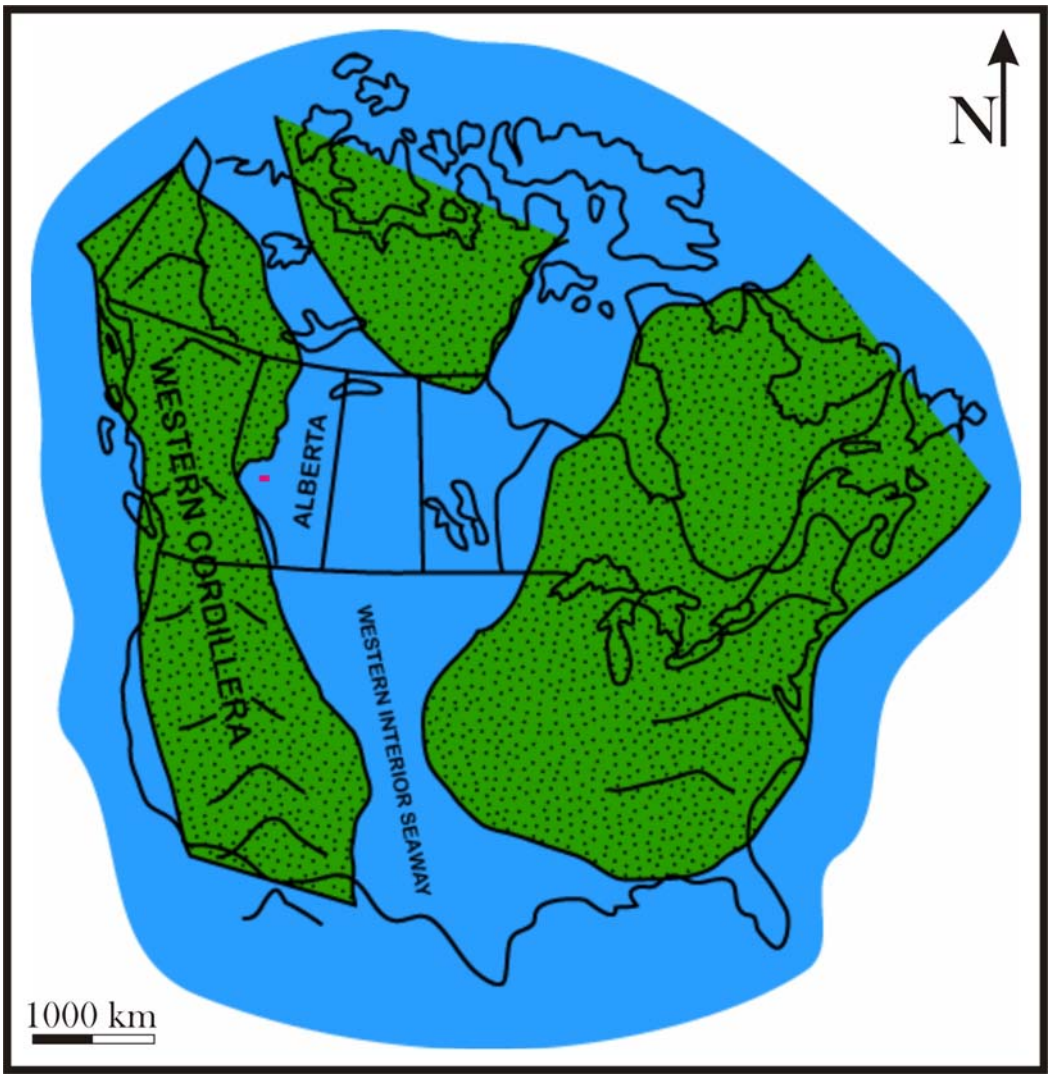

Figure 2-18: Approximate reconstruction of North America in Cretaceous-Turonian time. The approximate location of the study area is indicated by the pink rectangle. Modified from Williams and Stelck (1975).

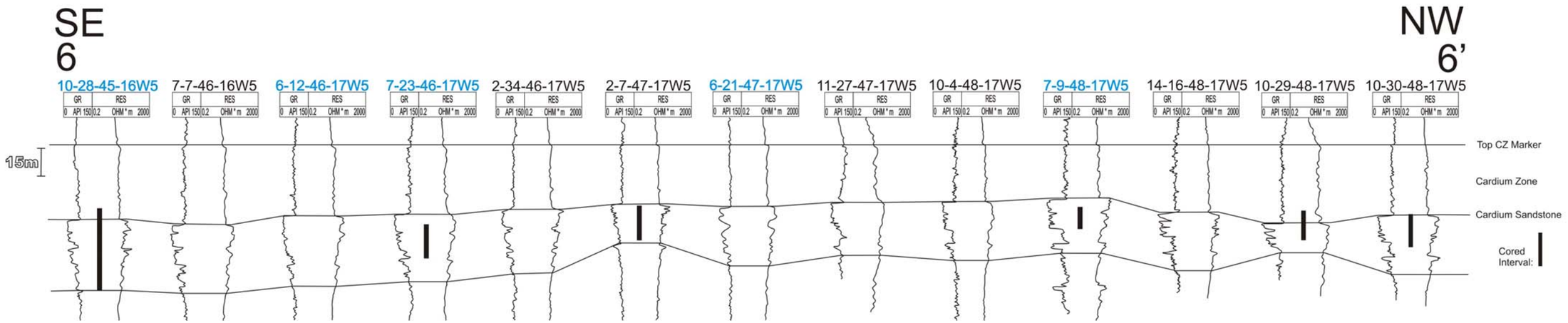

Figure 2-19: Southeast-Northwest stratigraphic cross section 6-6’. Section is based on the gamma ray and induction log signatures. This section is oriented approximately in a parallel direction to the paleo shoreline trend and generally shows a consistent thickness trend in the Cardium Formation. Blue UWI locations in cross section indicate logs that tie to other cross sections. Township and Range map shows the location of cross sections. Red wells with surrounding grey rectangle on the Township and Range index map indicate cored wells from the study area that were examined.

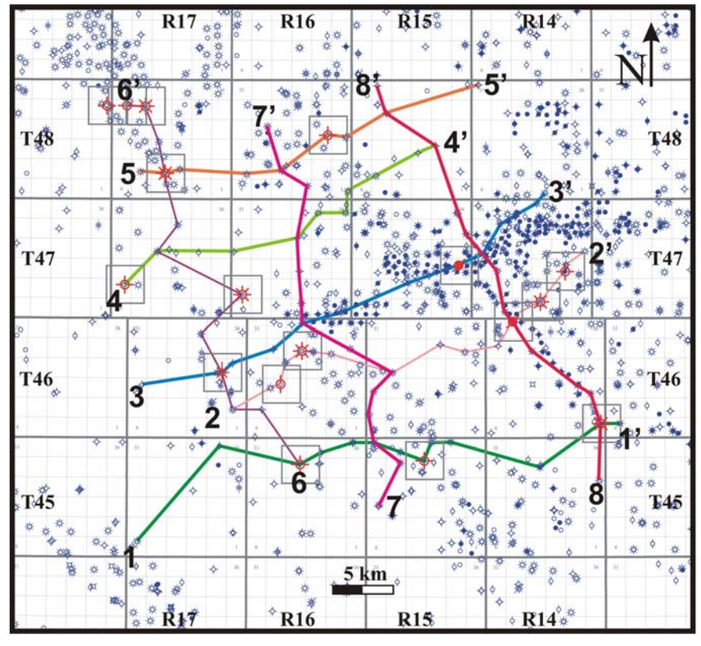

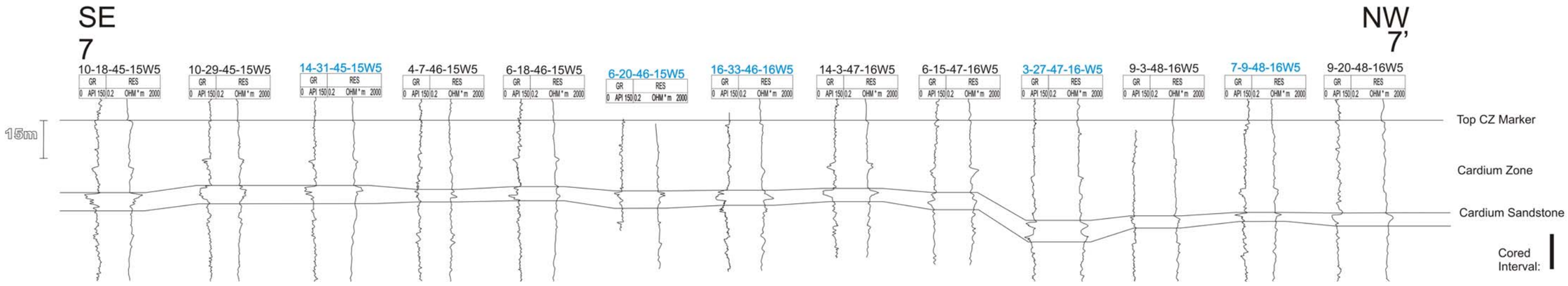

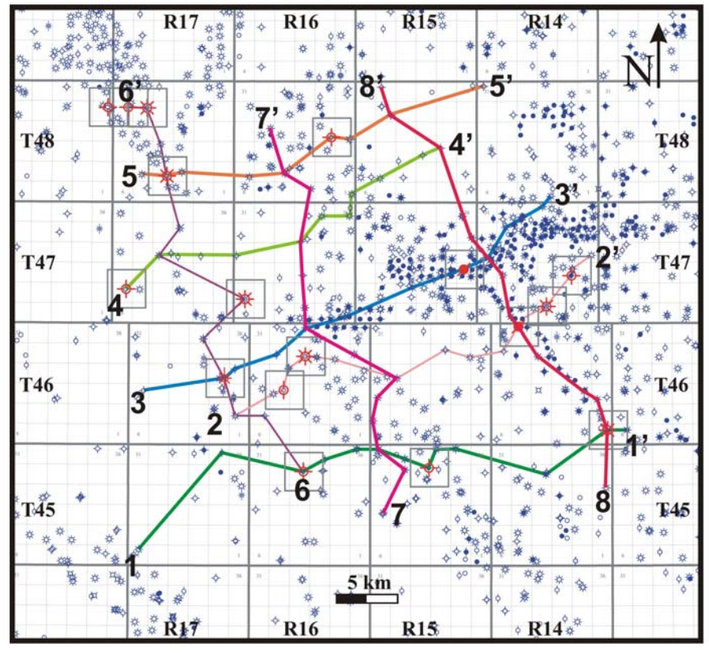

Figure 2-20: Southeast-Northwest stratigraphic cross section 7-7'. Section is based on the gamma ray and induction log signatures. This section is oriented approximately in a parallel direction to the paleo shoreline trend and generally shows a consistent thickness trend in the Cardium Formation. Blue UWI locations in cross section indicate logs that tie to other cross sections. Township and Range map shows the location of cross sections. Red wells with surrounding grey rectangle on the Township and Range index map indicate cored wells from the study area that were examined.

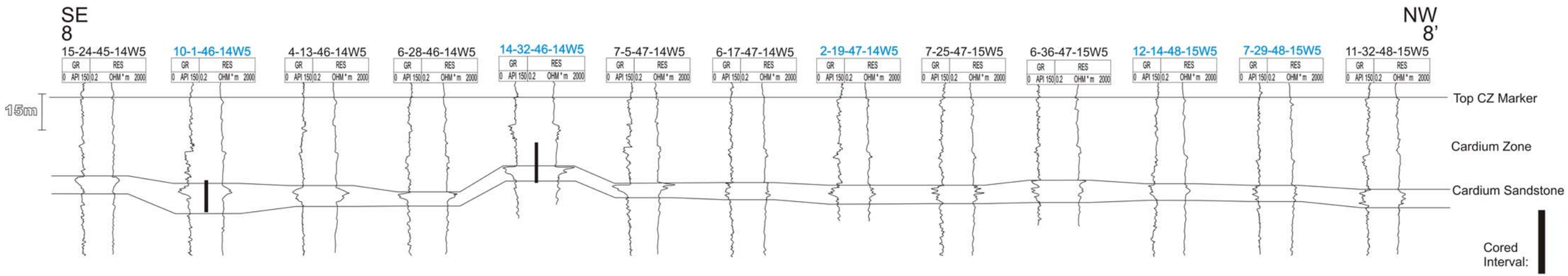

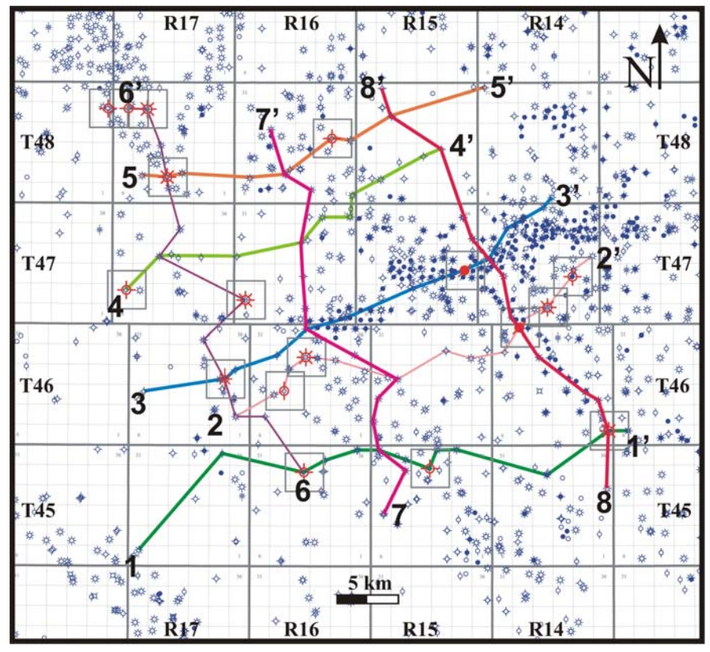

Figure 2-21: Southeast-Northwest stratigraphic cross section 8-8'. Section is based on the gamma ray and induction log signatures. This section is oriented approximately in a parallel direction to the paleo shoreline trend and generally shows a consistent thickness trend in the Cardium Formation. Blue UWI locations in cross section indicate logs that tie to other cross sections. Township and Range map shows the location of cross sections. Red wells with surrounding grey rectangle on the Township and Range index map indicate cored wells from the study area that were examined.

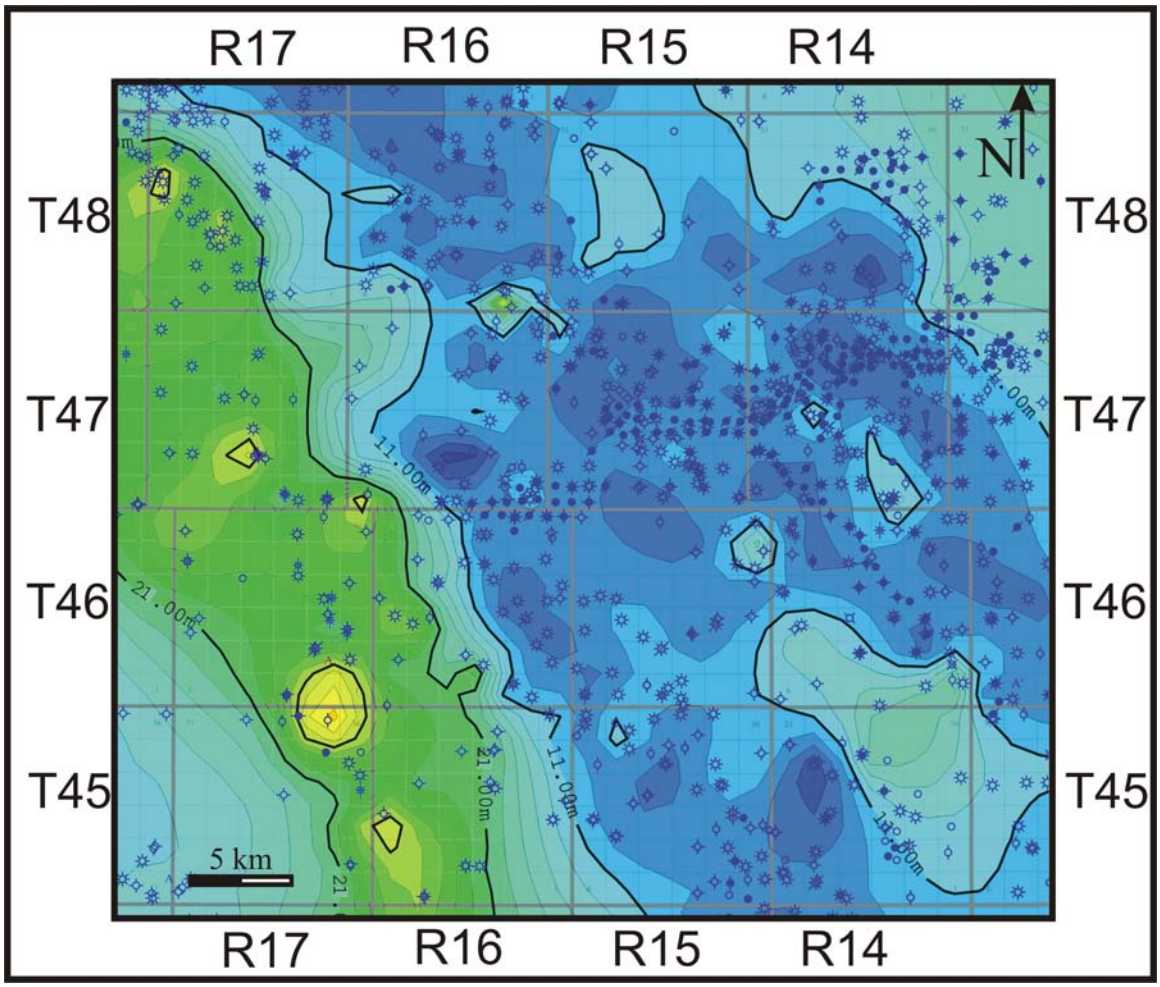

Figure 2-22: Isopach map of the Cardium Formation sandstone generated from depth picks made from the gamma ray and induction wireline log signatures. This isopach map represents only the first occurrence of a Cardium Formation sandstone intersection in wellbore, as wells typically do not penetrate deeply enough to intersect a structural repeat. This isopach map does not account for structurally repeated areas and exists in a non-palinspastically restored state. See section 2-8 for a detailed discussion. A prominent thick sandstone package is noted in the western part of the study area with a northwest-southeast trend. The map shows that development of thicker sandstones in the rest of the study area is limited. There is a slight thickening in the south-central part of the map (approximately Township 45/46-14W5) but it is non-continuous. Contour interval is 2 m.

the strike of the regional structural dip. Development of other thick sandstone packages parallel to the trend of the thickest package in the western part of the study area is not very evident from the isopach map and dip sections 7-7' and 8-8' (Figures 2-20 and 2-21) generated. A small, thick area is noted in the south-central section of Figure 2-22 (approximately Township 45/46-14W5) and slightly north of that point, but remains patchy and non-continuous, as identified from cross sections 1-1' and 8-8' (Figures 2-13 and 2-21) and evident from the isopach map.

Comparing the isopach map (Figure 2-22) to the structure contour map (Figure 2-11) reveals a geometric relationship between the two. The isopach map shows the thickest sandstone of the Cardium Formation has developed in the westernmost portion of the study area. The location of the thick sandstone coincides with the structurally lowest area on the subsea structure map (Figure 2-11) when the two images are superimposed on one another. As the top of the Cardium Formation sandstone surface becomes structurally higher up-dip to the east, the isopach thickness of the formation becomes noticeably thinner. A more detailed discussion of the creation of this geometry will be addressed later in the chapter. An isopach map of the Cardium Zone Member (Figure 2-23) was constructed to show the variation in thickness of the shale overlying the Cardium Formation sandstone. The top of the Cardium Zone Member has been identified as a horizontal depositional surface, so the isopach map can effectively show variations in thickness of the shale based on the thickness of the underlying Cardium Formation sandstones. Figure 2-23 displays that the thinnest deposits

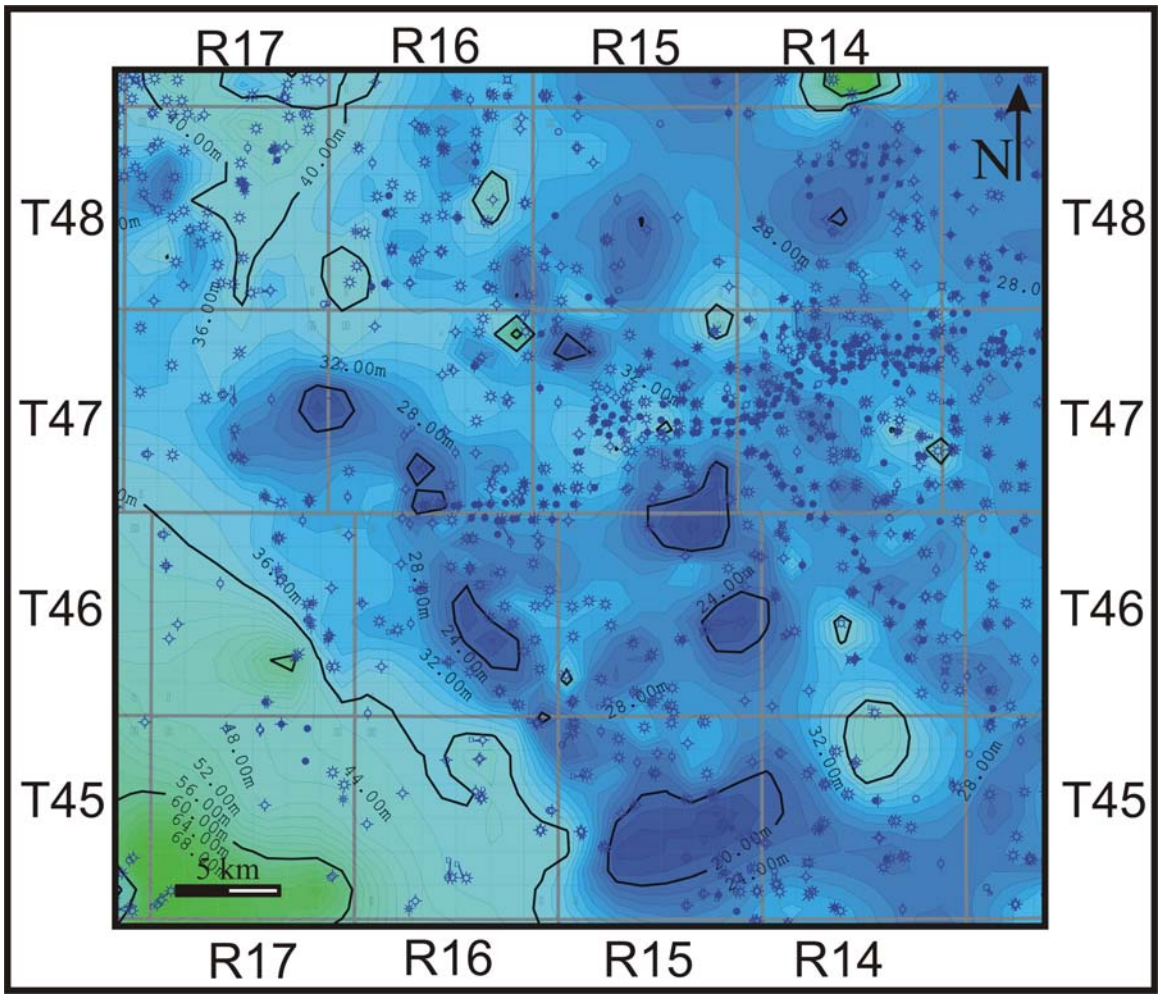

Figure 2-23: Isopach map of the Cardium Zone Member generated from depth picks made from the gamma ray and induction wireline log signatures. Contour interval is 2 m.

of Cardium Zone Member shale are present in the western and east-central parts of the map and they are coincident with where the thickest linear or patchy deposits within the Cardium Formation sandstone are developed as noted on the isopach map (Figure 2-22).

Accurate conglomerate depositional trends were difficult to establish due to the limited number of cores available for investigation, so establishing the trends has not been attempted. High concentrations of authigenic siderite distributed within the conglomerate often causes high resistivities in the wireline log signature, possibly indicating the presence of a conglomerate (F. Krause, Pers. Comm.); however sideritic matrix material within conglomerates was not always noted in the cores investigated and correlatable to noticeable increases in resistivity character in the associated wireline log, and therefore was not deemed to be a reliable indicator of the presence of F5 from wireline signatures when cores were not available. Nielsen (1957) and Krause et al. (1987) have noted that the conglomerates in the Pembina field are oriented in NW-SE trending pods and deposited in topographic lows at the upper surface of the Cardium Formation sandstone sequence. To the north and south of this thesis area, in the Carrot Creek (Swagor, 1975), Ferrier (Griffith, 1981), Willesden Green (Keith, 1985, 1991) and Crossfield fields (Krause and Nelson, 1991), similar trending, elongate bar geometries of the Cardium Formation conglomerate have also been noted.

2.8 Discussion of Development of Regional Thickness Trends

The Cardium Formation sandstone within the study area displays a general thinning trend toward the northeast, as noted in the isopach map (Figure 2-22). The general thinning trend of the Cardium Formation sandstone in the study area is consistent with the overall regional trend established by Krause *et al.* (1994). Occurrences of structural repeats from wireline log signatures within the Cardium Formation have been commonly documented at the western margin of this study area. The structural repeats observed in electric wireline logs are often complete (Figure 2-24), but partial repeats are also commonly noted. For the purpose of developing the isopach map, only the first, uppermost occurrence of the Cardium Formation sandstone top was picked from the wireline logs. This was done since the “total depth” of wells drilled in the study area typically target the Cardium Formation. If wells terminate in the Cardium Formation it is unknown whether there is potential for the presence of the Cardium Formation deeper down, and whether the first intersection represents a repeated section, or the only stratigraphic occurrence. High resolution seismic data has the potential to indicate where structural repeats occur where wells do not penetrate deeply enough. The seismic data received that cover the western margin of this study area are of lower resolution and do not clearly display any Cardium Formation repeats. When repeated sections are present in a log, the deeper repeat is subtracted from the total thickness and not represented on the isopach map (Figure 2-22). Since most of the repeats observed in electric wireline logs are

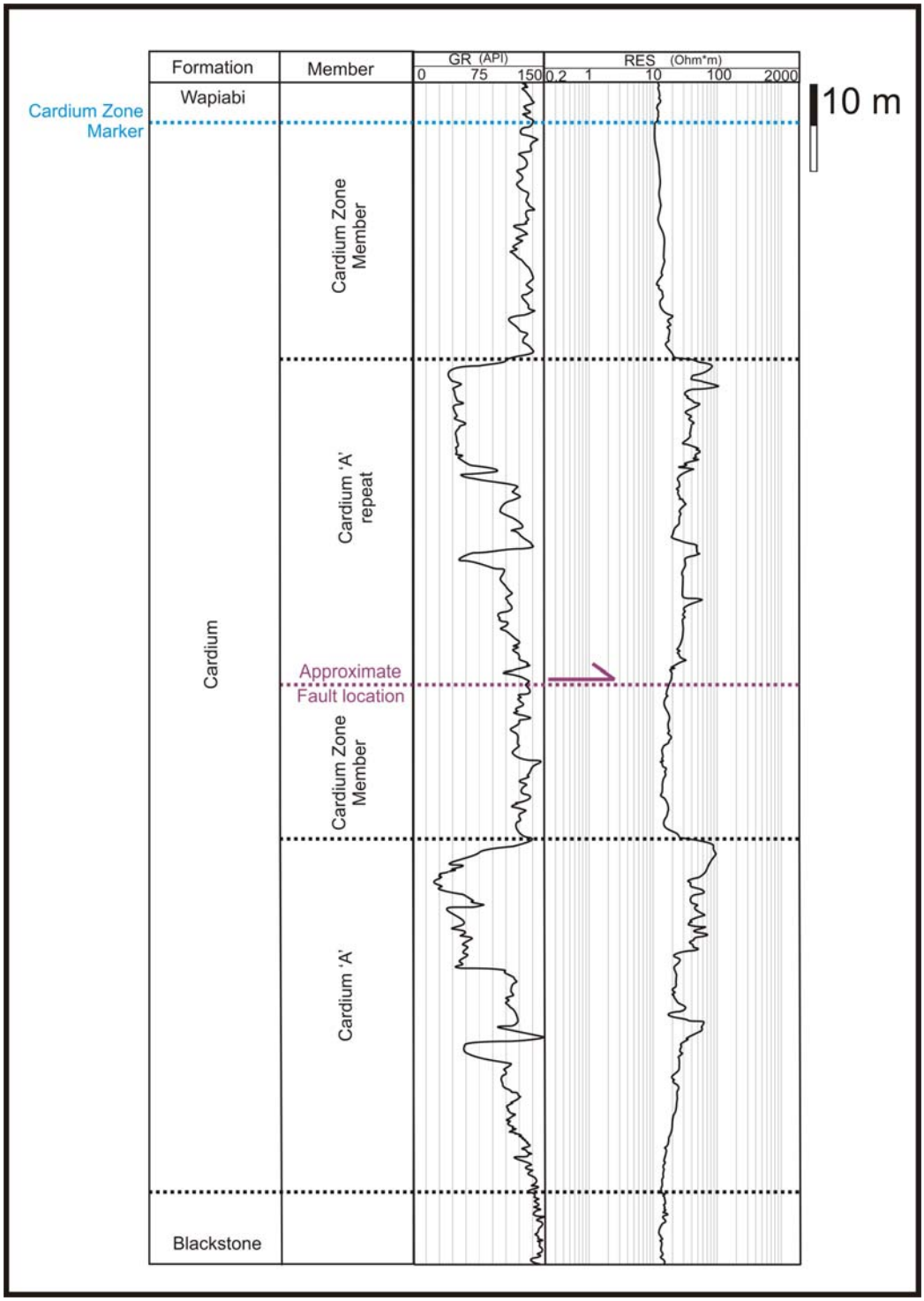

Figure 2-24: Log 15-17-048-17W5 showing a near complete structural repeat observed in electric wireline log from the northwest corner of the regional study area.

complete repeats, the isopach map is still considered to be representative of the true variation in stratigraphic thickness of the Cardium Formation sandstone across the entire study area, as though no structural deformation had occurred. Figure 2-25 shows the locations of structural repeats identified from log examination highlighted on the structure contour map of the top of the uppermost Cardium Formation sandstone.

Once the locations of the structural repeats are identified, Figure 2-25 helps to explain the topographical variation noted in the structure contour map (Figure 2-11) near the western margin of the study area, specifically in Townships 46-16W5, 46-17W5 and 48-17W5. The topographical variation at these locations is coincident with the locations of the structural repeats identified from the electric wireline logs. Since the uppermost occurrence of the Cardium Formation sandstone is chosen to represent the stratigraphic top, the wells with identified structural repeats place the Cardium Formation sandstone repeat at a structurally higher elevation that is not consistent with the regional dip of undeformed strata in the area, and causes the localised variation that is noted on the structure contour map. Some variation within the Cardium Formation sandstone isopach map (Figure 2-22) is noted along strike of the three townships that have common structural repeats and may represent zones of structural thickening of varying amounts. This hypothesis is inconclusive since no repeats are obvious in the wireline logs, the wells do not penetrate deeply enough in these areas, and the seismic data do not resolve any structural repeats. A palinspastically restored map would represent the Cardium Formation sandstone

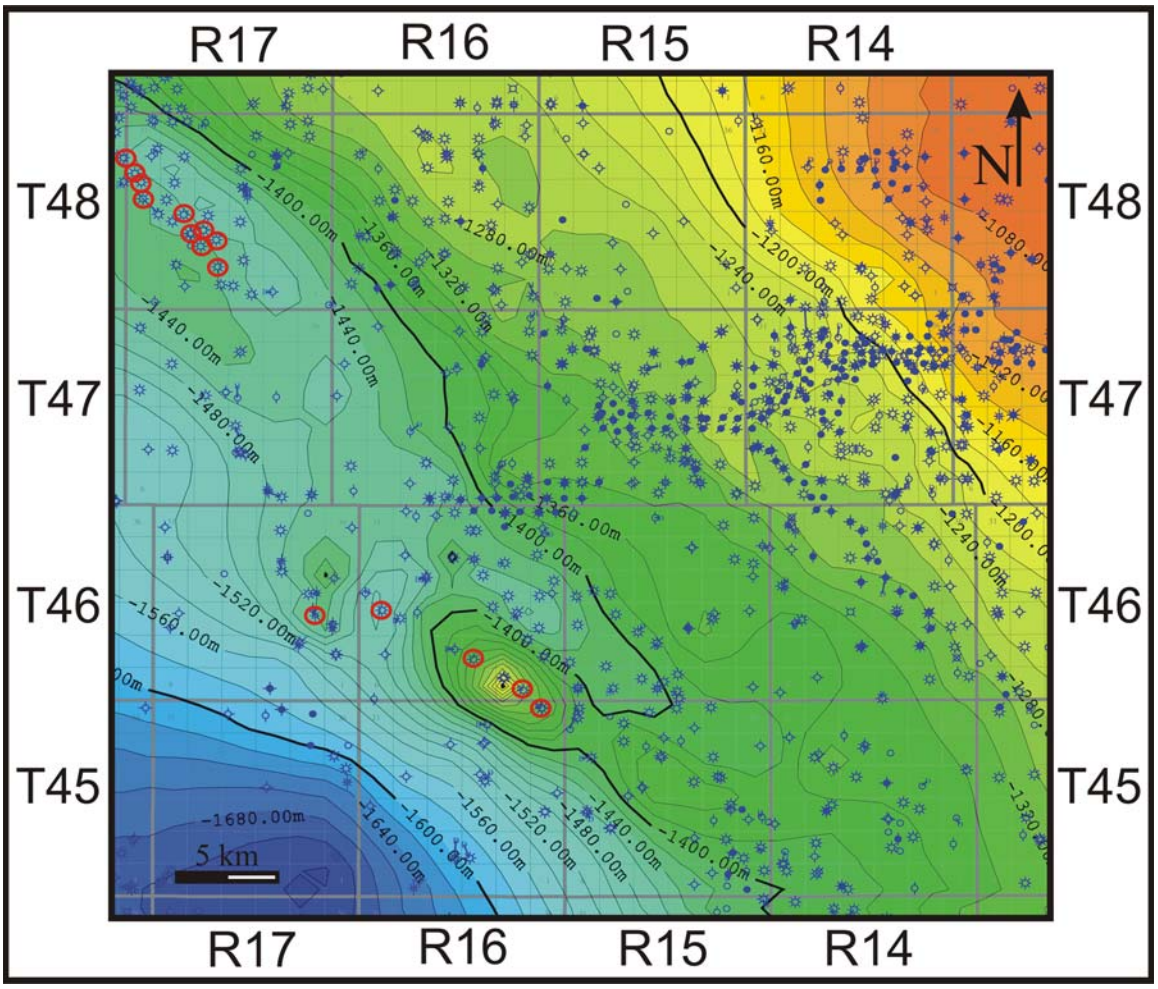

Figure 2-25: Regional structure contour map of the top of the uppermost Cardium Formation sandstone. Well locations containing structural repeats of the Cardium Formation that have been identified from log examination are highlighted with red circles on the structure contour map. The datum used in the construction of the structural map is sea level. Contour interval is 20 m.

at the time of deposition. Figure 2-26 displays the isopach map with superimposed positions of approximate thrust fault traces based on the locations of the identified structural repeats from the wireline logs.

The fault traces are noted to closely align with the locations where the Cardium Formation is over-thickened.

Swagor (1976), Griffith (1981), Plint (1988), Krause and Nelson (1991), Keith (1991) and others have noted that the Cardium Formation sandstone often develops on a zone of pre-existing topography, where sandstone is deposited as a ridge-like body. Topographical variation can also develop due to pre-existing structural deformation based on the reactivation of basement fault blocks. Hart and Plint (1993) suggest that the distribution of incised shoreface remnants in the Cardium Formation are linked to basement fault blocks. This study has not identified the presence of any pre-existing topographical surface caused by either changes in slope or structural deformation upon which the Cardium Formation sandstone would have been deposited based on the interpretation of cross sections, seismic data or isopach and structure contour maps generated for this study.

2.9 Current Interpretation and Discussion

The lithofacies identified in this study indicate that the Cardium Formation was deposited in a marine setting. The abundant presence of such traces as *Zoophycos sp.*, *Chondrites sp.*, *Rosselia sp.*, *Palaeophycus sp.*, *Terebellina sp.*,

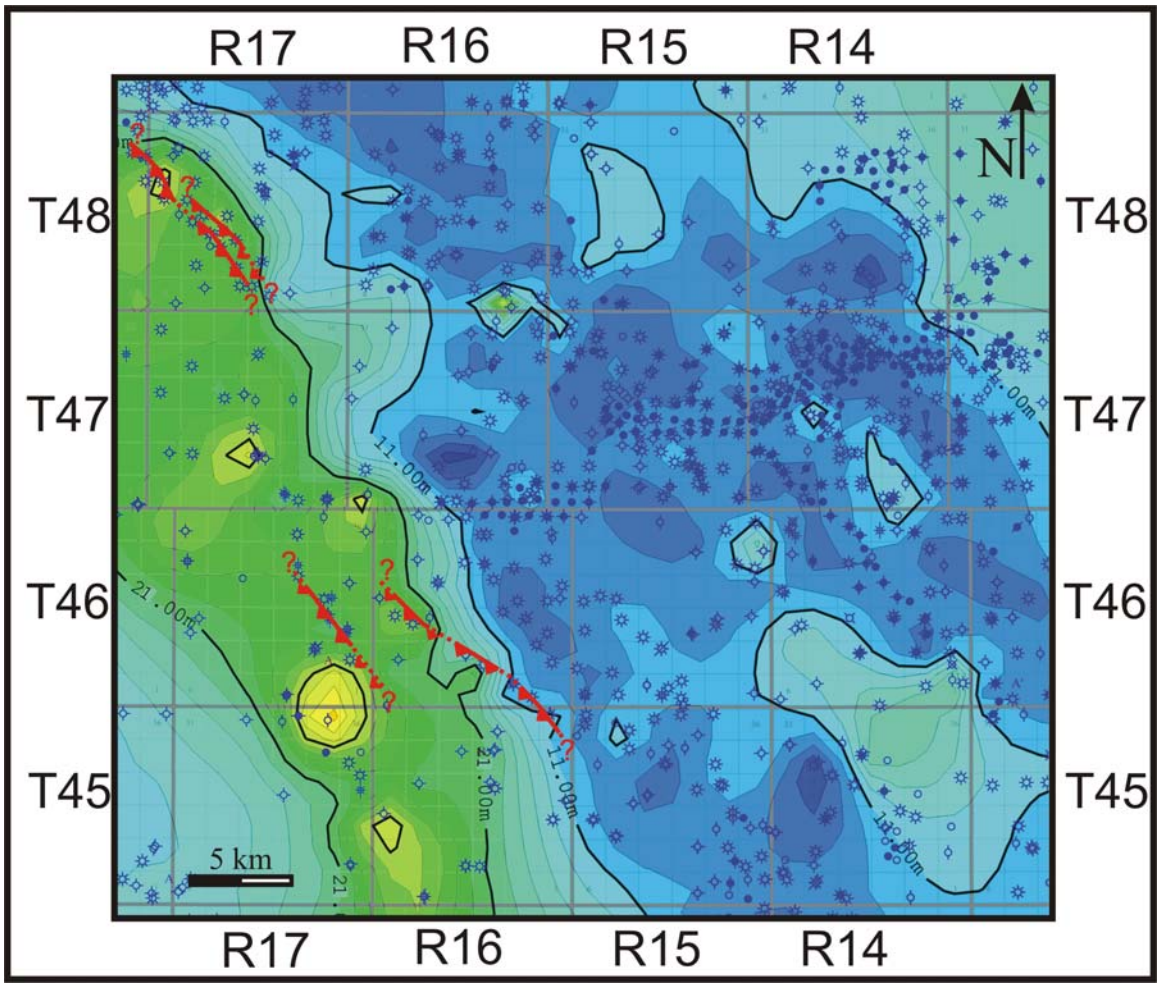

Figure 2-26: Isopach map of the Cardium Formation sandstone generated from depth picks made from the gamma ray and induction wireline log signatures. Isopach map has superimposed positions of Cardium Formation fault trace locations based on identified structural repeats from the wireline logs. The fault traces are noted to closely align with the locations where the Cardium Formation is over-thickened. Contour interval is 2 m.

and *Rhyzocorallium sp.* within the five lithofacies confirms the marine classification. Pemberton and Frey (1984) and Crimes (1975) state that such an ichnofacies assemblage suggests a sub-littoral to bathyal marine environment. There is no direct lithological/paleontological evidence in this thesis area suggesting and supporting a beach shore or coastal plain as being the depositional environment. No sedimentary structures indicative of these environments such as coaly beds, rootlets/paleosol horizons and well-sorted conglomerates excluding mud matrices have been documented during core investigation.

The lower sections of the cores examined are predominantly bioturbated shales and siltstones of F2 and Three that grade into siltstones and sandstones of F3 and F4 higher in each section. The intensity of bioturbation is commonly noted to decrease upward as the shale transitions to the sandstone. The sandstone commonly shows low-angle inclined parallel lamination (LIS), parallel laminations, ‘rip-up’ shale clasts, and wave ripple structures, all indicative of higher energy environments. The intensity of bioturbation decreases upward from the shale through to the sandstones because the higher energy environments prevent pervasive biogenic activity from occurring within the sediment. Typically overlying the sandstone is poorly sorted chert conglomerate. These conglomerates are overlain by a massive to very finely laminated shale with rare interbedded siltstones of F1, suggesting a change to a lower energy environment. Where the conglomerates of F5 are not present, the thicker sandstones of F4 are directly overlain by the shales of F1. The stratigraphy

observed in the study area is suggestive of a depositional history that has included a number of processes involving varying levels of energy for emplacement. The lowermost shales of the stratigraphic sequence indicate deposition below storm-weather wave-base, transitioning above this into a higher energy environment within storm-weather wave-base that deposited the sandstones and conglomerates. The shales that cap the sandstone and conglomerate indicate a rapid shift back into deeper water deposition, below storm-weather wave-base.

Krause and Nelson (1984) state that the distribution of physically reworked beds versus biologically disturbed beds are isolated into discrete packages and are indicative of contrasting energy regimes within the Cardium Formation in the Pembina area of west-central Alberta. This discrete segregation between the physically and biologically reworked sediments is also noted in this study area. Gani *et al*. (2004) examined deposits of deltaic complexes from the Cretaceous Western Interior Seaway in Wyoming and Utah and indicate that storm and river-flood deposits tend to show low levels of bioturbation because of high sedimentation rates and energy levels. They note that the top surfaces of individual storm and flood beds may show an increase in bioturbation and be indicative of transition back into fair-weather conditions. Similarly, Carey *et al.* (2003) record segregation between intervals of storm reworked sediments and extensively bioturbated intervals of shelf sediments of the Holocene and Pleistocene in cores taken from the Northern California margin. Again, the authors attribute the isolated zones of bioturbation to indicate periods of reduced

sedimentation or smaller, less destructive storm depositional events. During periods of intense storm activity, biogenic disruption is halted due to the increase in energy levels. The physically reworked sediments of the Cardium Formation sandstone within the study area of this thesis would have occurred over periods of higher energy wave activity, such as during storm-dominated deposition. Intervals showing intense biological reworking would have been deposited during times of lower energy conditions, when the substrate was stable and exhibited low agitation under fair-weather conditions.

Studies of modern, storm-dominated shelves indicate that significant volumes of sediment can be transported large distances in a relatively short period of time. Drake *et al.* (1972) recorded sediment distribution on the Santa Barbara/Oxnard shelf following a storm. They showed that a large volume of terrigenous sediment was delivered to the shelf during a seasonal river flood. The fine grained sediments were distributed across a wide area over the shelf within several months, while the coarser grained sediments were deposited on the inner shelf. The coarser sands initially deposited on the inner shelf were subsequently transported to the middle and outer shelf by wave currents and storm activity, interpreted in a separate paper by Howard and Reineck (1981). Cleary *et al*. (1999) discusses the impact of Hurricanes Bertha and Fran on the North Carolina coast in 1996. They state that these hurricanes were responsible for the removal of approximately 60 m of shoreline dune coverage, transporting several million cubic meters of sediment offshore toward the shelf. Morton (1981) studied sediment distribution patterns of the storm layer from Hurricane Carla

(1967) and suggests that bottom current velocities reached values as high as 2 m/s. This velocity would be capable of transporting pebble- and potentially even cobble-sized clasts. It is evident from studies of modern day storm dominated shelves that intense storms such as hurricanes have the ability to transport and distribute large volumes of sediment faster than combinations of other transport processes combined.

Lithologically, modern storm shelves typically become finer grained in more distal locations (Johnson and Baldwin, 1996). Howard and Reineck (1981) note that from the shoreline seaward, physically created sedimentary structures become less abundant and biogenic disruption becomes more common. Johnson and Baldwin (1996) state that box cores taken from modern storm layer deposits have a number of common characteristics: 1) erosive bases; 2) basal lags of mud clasts, shells, plant debris or rock fragments; 3) horizontal to low angle cross lamination which may represent hummocky cross stratification; 4) wave ripple cross lamination; and 5) burrowed intervals. The cores examined in this study area have identified sedimentological and lithological features that are consistent with Johnson and Baldwin's (1996) study. The lithofacies identified from core examination within this study area are comparable to the cores examined from the high energy California coastline by Howard and Reineck (1981), interpreted to represent modern storm related deposition and also to what has been noted by Krause and Nelson (1984) of the Cardium Formation deposits with the Pembina field.

Based on the ichnological and sedimentological work of others, including Krause and Nelson (1984), Pemberton and Frey (1984) and Joiner (1991), the Cardium Formation has been interpreted to be shelfal in origin. The evidence from core examined within this study area reveals ichnofacies (*Cruziana, Zoophycos* and *Nereites)* and sedimentary structures (low angled inclined stratification, wave ripples and parallel laminations) that are consistent with the results of these authors. The interpretation within this study area is one that represents deposition on a muddy marine shelf that was frequently influenced by storms. Deposition, based on the range of ichnofossil assemblages from the individual lithofacies identified and bedding structures preserved within the lithofacies is suggestive of an environment that existed predominantly between fair- and storm-weather wave-base. The core study reveals that an offshore zone is defined by commonly bioturbated mudstones and siltstones. Stratigraphically overlying the mudstones and siltstones is finer sandstone and siltstone showing hydrodynamic overprinting of low angle inclined stratification and wave ripples, representative of a transition zone where the majority of storm activity would have been occurring. Only rare instances of conglomerate are noted to unconformably overlie the deposits of the transition zone.

Transport of the fine sands, silts and muds to the shelf may have been strongly influenced by riverine inflow, which is a common transport mechanism of fine grained material noted at the mouths of modern drainage systems in the world, such as the Amazon shelf in Brazil and the Yellow Sea in China (Johnson and Baldwin, 1996). Subsequent redistribution and reworking of fine sediment

plumes can occur by waves, tides and nearshore currents, creating a trend parallel to the shore, often extending for many tens of kilometres as noted by McCave (1984), Gibbs (1976) and others. Storms may have largely contributed to the movement of the sands to more distal locations on the shelf after being initially delivered to the shore and may have also caused the low angle inclined stratification hydrodynamic overprinting noted in core. The interpretation of low angle inclined stratification in core as being equivalent to hummocky cross stratification in outcrop has been noted by Krause and Nelson (1991) and is indicative that the sandstone has become reworked in a storm dominated environment (Harms *et al.,* 1975).

The emplacement of the coarse siliciclastic material and its stratigraphic position is probably the most difficult part of the Cardium Formation to explain. The actual provenance of the conglomerates is debatable, but may partially be a function of a renewed period of tectonic uplift to the west. From core examination, thin pebble veneers and conglomeratic layers have been noted to be interspersed within the F4 sandstones and indicate the beginning of a clear change in grain size and bed load transport capabilities.

Initial delivery of the conglomerates to the shoreline would have been through normal riverine flow and at time perhaps assisted by denser hyperpycnal flows. Krause and Nelson (1991) note that coarse conglomeratic material may have been provided to the shelf by transgressive ‘breaching’ of nearshore coarse grained deposits. Strong oscillatory wave patterns near shore have been noted to preferentially trap sediment (Swift and Thorne, 1991). This boundary is known as

the littoral energy fence and could act as a temporary coastal storage mechanism and barrier to the outer shelf for the conglomerates that would have been dumped there by the rivers. During a transgressive event, water depths would have become sufficient for storm currents to pick up the coarser conglomerates and distribute them farther out onto the shelf to become emplaced on the sandstones. The emplacement of the conglomerate is interpreted to have occurring synchronously with the final stages of deposition of F4. Synchronous development of the unconformity underlying the conglomerate is evidenced by the occurrence of isolated, biogenically emplaced pebbles present in the underlying sandstone of F4. If an extended period of time had existed before the emplacement of the conglomerates, a more pervasive biogenic imprint would likely be noted at the Lithofacies contact. Additionally, fair-weather depositional processes would likely be present, capping the sandstones of F4 in the cores.

The lack of wave-associated sedimentary structures, imbrication of conglomeratic clasts and the poorly sorted nature of the conglomerate noted in core suggests that the delivery to the shelf was not by fluvial methods and also indicates that following deposition, little wave activity was present to alter the conglomerate. More so, if the conglomeratic deposits were severely reworked during and following their deposition, it is likely that any sand or shale matrix constituent deposited within it would have been winnowed out and transported away. The lack of these features suggests that transgression was continuing, deepening sea level and gradationally depositing marine shales of F1 over the

conglomerates. Deeper water marine shales (F1 equivalents) have been noted to overlie the conglomerate and sandstones in all of the Cardium Formation fields surrounding this study area by various authors.

2.10 Conclusions

This chapter investigated the Cardium Formation lithofacies, lithofacies associations, distribution, depositional environment and approximate geometry across the study area based on examination of wireline logs and available cores. From the analysis of the data available, a number of conclusions are presented, and are as follows:

1) Deposition of the Cardium Formation across the study area occurred in a fully marine setting on a marine shelf/shelf edge, below fair-weather wave-base but typically within storm-weather wave-base. From core investigation, the storm dominated marine depositional environment is evidenced by the sedimentary structures and ichnofossils. The sedimentary structures include low angled inclined stratification, wave ripples, parallel laminations and the ichnofossil assemblages preserved belong to the *Cruziana, Zoophycos* and *Nereites* ichnofacies.

2) Five primary lithofacies are identified in the study area. They are: F1. *Bioturbated dark shales*; F2*. Bioturbated, thinly interbedded shales and siltstones with very fine sandstone stringers*; F3. *Bioturbated, thinly bedded sandstone and siltstone with minor to common interbedded shale stringers*; F4. *Thickly bedded, very fine to medium grained sandstone*, and F5. *Chert Conglomerates*.

3) Discrete intervals of bioturbation are interspersed within layers with strong signatures of physical reworking. This represents a difference in energy levels and signifies alternation between fair-weather and storm-weather depositional events. The occurrence and identification of low angled inclined stratification and wave ripples in the Cardium Formation sandstone suggests storm dominated processes assisted the emplacement of the siliciclastic units and the subsequent hydrodynamic overprinting within the study area. High-energy storm events can prevent pervasive bioturbation of these lithofacies, whereas fair-weather depositional events within the range of fair-weather wave-base were conducive to environments that allowed the development of prolific bioturbation.

4) Modern shallow sea environments show that sediment is commonly introduced to the coastline by seasonal floods, hyperpycnal riverine inflow, storms and shifts in the shoreline during changes in sea level. These processes may have also been responsible for the delivery of sediment to the shore and shelf within this study area. The primary processes responsible for the redistribution of the sands and silts to the shelf would have occurred during major storm events, assisted by their associated longshore and geostrophic currents.

5) The cores and wireline logs display a depositional interval in the upper Blackstone Formation and lower Cardium Formation sandstone that records an offshore zone with deposition that occurred below storm-weather wave-base. Here, deeper water marine shales with little biogenic disruption grade upward into interbedded shales and siltstones with abundant bioturbation and only rare

wave and current related bedforms. Overlying this, in the upper Cardium Formation sandstone, interbedded siltstones and sandstones record a transitional environment where the environment becomes depositionally dominated by storm-weather wave processes. The Cardium Zone Member shales overlie the Cardium Formation sandstones and represent a shift into deeper water sedimentation, caused by a transgressional event.

6) The conglomeratic unit that is present in patches throughout the study area unconformably overlies the sandstones and siltstones of the Cardium Formation sandstone. The conglomerate distribution is not well delineated due to limited core availability and difficult identification from wireline logs alone.

7) The isopach map of the Cardium Formation sandstone in the study area displays the thickest sandstone developed in a northwest-southeast trend in the western part of the study area and regionally thins to the northeast. This is consistent with the basin-wide depositional trend of the Cardium Formation that is noted from current research. No significant development of any isolated, depositional sandstone pods parallel to this regional trend suggestive of the existence of pre-exisiting topographical variation are noted within the Cardium Formation sandstone in the study area. However, pods or zones of localized structural thickening within the Cardium Formation, particularly in the westernmost parts of the study area, have been observed in wireline logs and cause variation of the top of the Cardium Formation structural surface.

Chapter Three: Structural Geology

3.1 Introduction

The structural geology in the Foothills west of Pembina has not been extensively documented in the literature. Presently, no detailed geological map is available in the area. It has been previously thought that the frontal Foothills show little to no subsurface structural deformation and that the triangle zone represented the most foreland expression of deformation. Poor seismic imaging, interpretation and general understanding of the geometries of the frontal part of the triangle zone led to early interpretations showing triangle zones terminating abruptly at the leading edge, with the upper detachment/backthrust joining the lower detachment at a “tip” (Jones, 1982, 1987; Charlesworth and Gagnon, 1985).

More recently, Skuce *et al*. (1992) and Skuce (1996) noted that subsurface frontal Foothills deformation is quite apparent, involving ‘passive-roof’ duplexes and is often well resolved with modern seismic imaging. Detailed seismic images have shown that the upper and lower detachments of a triangle zone commonly do not terminate at a tip, but rather extend parallel to each other far into the foreland, advantageously using shales as the detachment horizons (Skuce *et al.,* 1992; Skuce, 1996). Duplex structures may develop between two foreland detachments as far as 50 km from the outcropping foreland edge of deformation (Figure 3-1). Most notable are the sections shown in Skuce (1996)

located near Edson, Robb and Brazeau River, Alberta, and which are northwest of this thesis study area.

Significant variations along strike within the triangle zone have been noted by Spratt and Lawton (1996) and this study attempts to show that blind leading edge-frontal triangle zone structures also vary along strike.

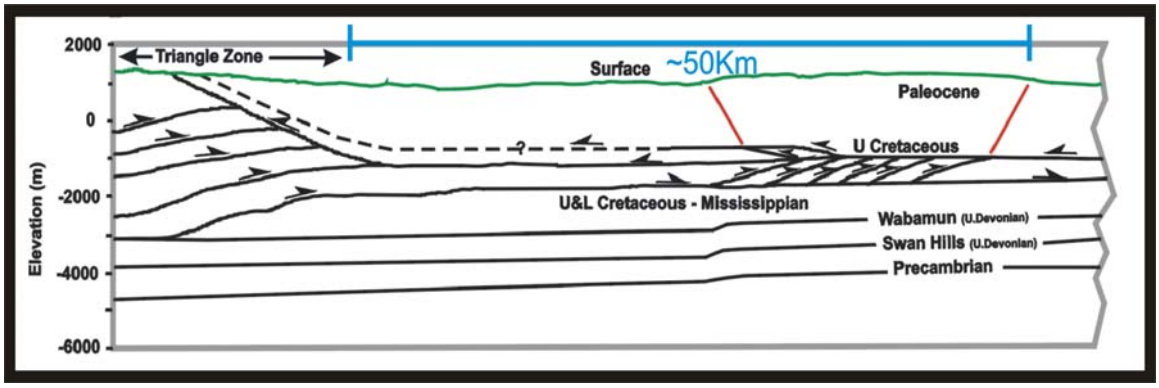

Figure 3-1: Model depicting parallel upper and lower detachments of a triangle zone extending into the foreland for a distance of 50 km. Duplexes are often noted to form between the detachment horizons visible in seismic sections. Modified from Skuce, 1996.

3.2 Study Area

The study area outlined on a township and range map (Figure 3-2) extends from Township 45 to 48 between Ranges 14 and 17, west of the Fifth Meridian, Alberta, Canada. 2D seismic data covering the entire region were made available by ConocoPhillips and have vintages ranging from the 1970's through to the early 1990's. The seismic data with the greatest resolution and structural deformation are located in a township in the southeastern quadrant of

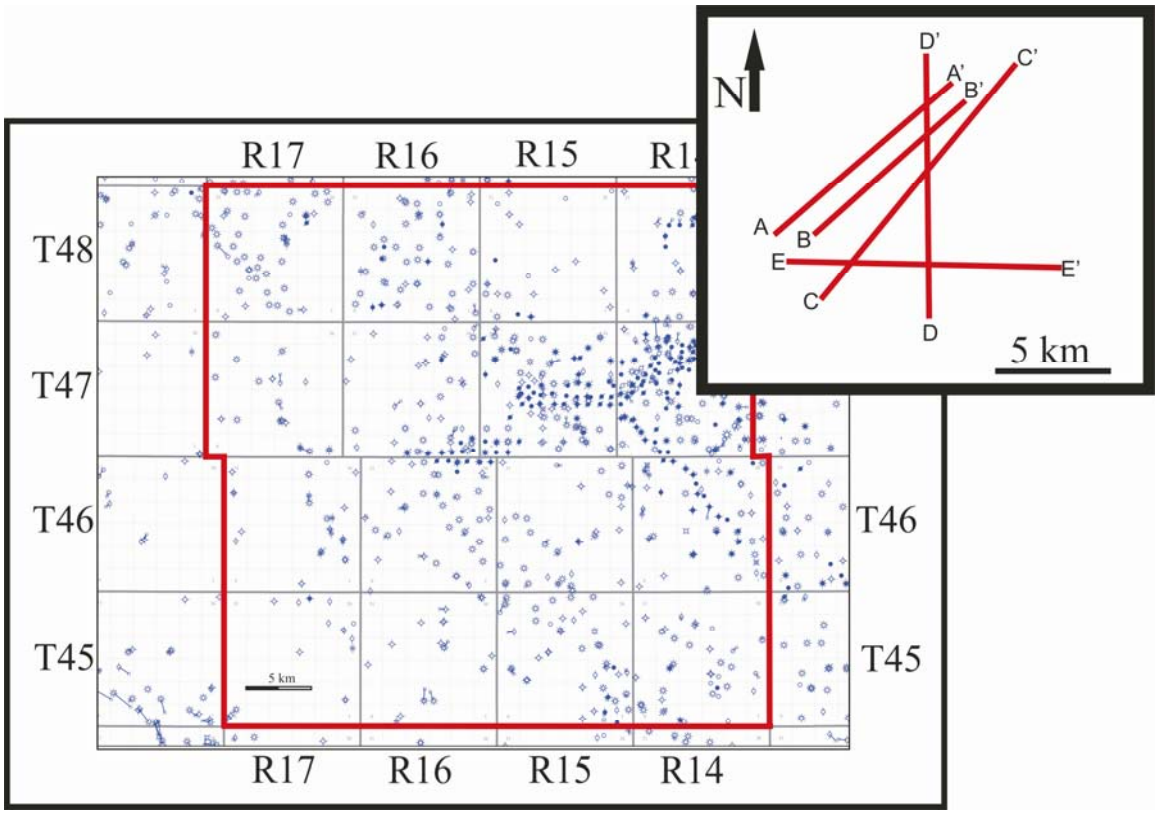

Figure 3-2: Township and range map of the regional study area. Available seismic data lie within the area outlined by the red box, which extends from Township 45 to 48 and between Ranges 14 and 17, west of the Fifth Meridian. The red lines shown in the inset box give the orientations of the five seismic lines used for the structural analysis in this study and are labelled accordingly. The seismic lines are located in a southeastern township of the regional study area.

the study area and are, therefore, the focus of this structural study. While subsurface structural deformation is present in the northwest corner of the study area, the seismic images did not strongly display this, a condition that will be discussed later in the chapter.

3.3 Methods

The proprietary time seismic data received from ConocoPhillips had a standard processing stream (Figure 3-3) performed on them prior to being depth converted in this study. Dr. Helen Isaac at the University of Calgary generated a synthetic seismogram from the sonic log of well 10-28-45-16W5 in *GeoSyn*®. The synthetic seismogram was used to correlate some key seismic reflection events. Polygons were created between the primary reflection horizons and were each assigned an average velocity based on gross lithology changes. Once the seismic processing was completed, a velocity model was created in *Promax*® based on the synthetic seismogram to convert the time sections to depth (Figure 3-4). The time to depth conversion uses a function that accomplishes depth stretching by repositioning the cross section along its vertical ray traces. Once the sections were converted to depth, the formation tops in seven wells in the study area were picked from *AccuMap*®. These wells are located on or directly adjacent to the seismic lines and were placed or projected into the seismic sections. Seismic interpretations were guided and constrained by correlating the known stratigraphic tops from the seven wells to the seismic lines.

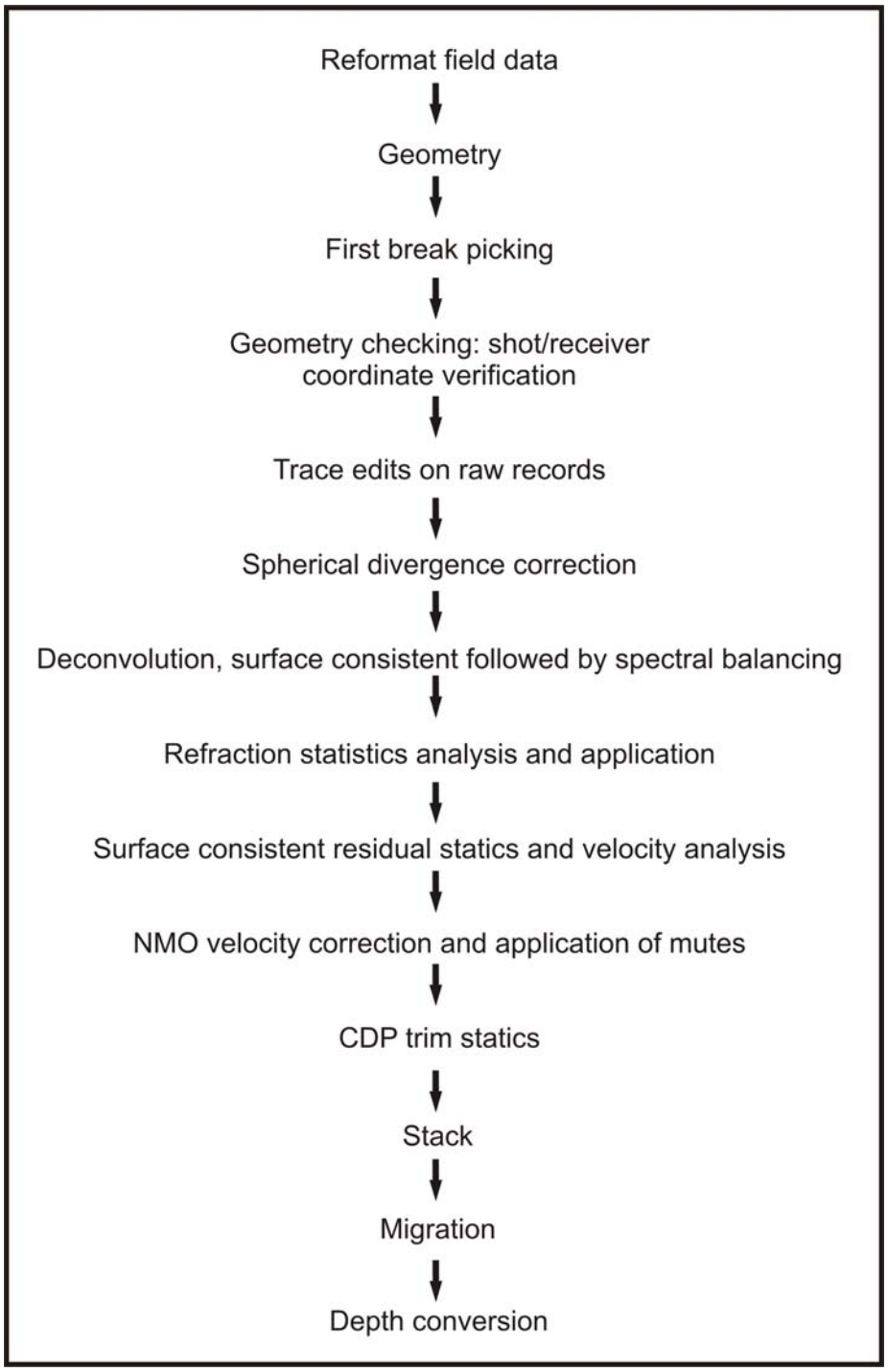

Figure 3-3: Seismic processing flow performed by ConocoPhillips.

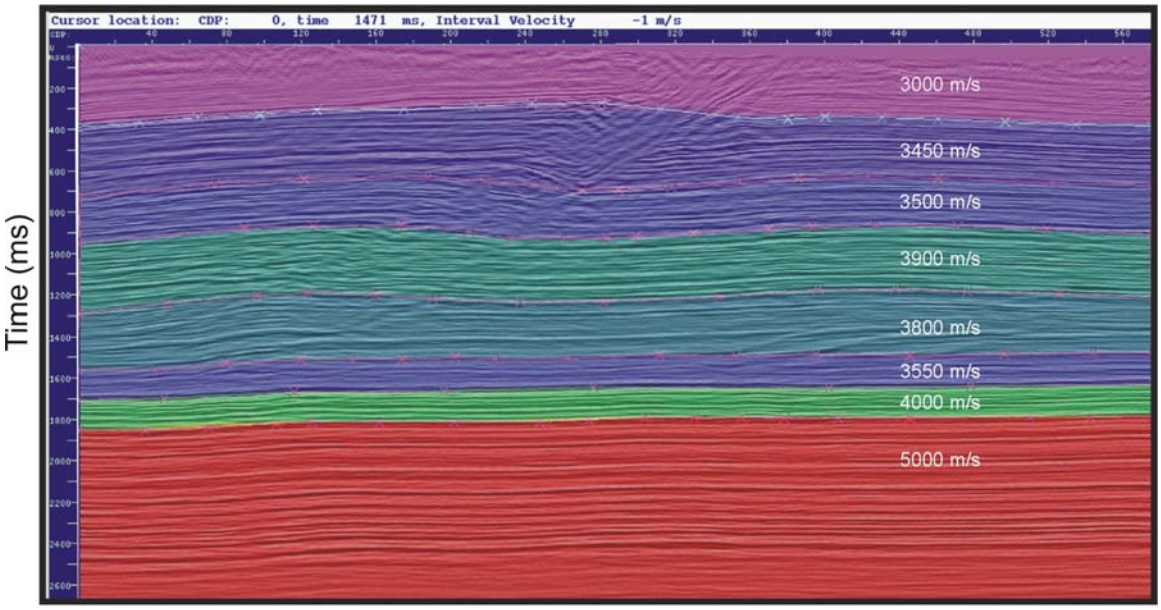

Figure 3-4: Velocity model used in this study to convert the five seismic sections from time to depth. Velocities were averaged based on the coloured polygon sections. The contacts of the polygons are based on lithological formation boundaries. Vertical axis is time in milliseconds and horizontal axis is CDP (Common Depth Point). Average velocities for each subdivision are annotated on the figure.

3.3.1 Seismic Data Interpretation

The seismic interpretation was completed using Midland Valley's *2DMove*® software. Subsequent image and seismic palinspastic restoration of the dip sections was completed in *2DMove*® to confirm the viability of the structural interpretation. Marshak and Mitra (1988) and Woodward *et al.* (1989) note that cross section restoration should be performed at the same time as the deformed state section is interpreted to confirm that the interpretation is viable and admissible. More so, the authors note that "balance" occurs when the deformed and restored states preserve both line length and sectional area. Dahlstrom (1969) mentions that line-length balancing suggests that the length of

any bed is the same as the beds above and below it. This is based on the assumption that there is no interbed slip and plane strain occurs (all motion is contained within the plane of the section). The palinspastic restoration algorithm utilized in *2DMove*® is Fault Parallel Flow. This algorithm was developed in collaboration with the University of Keele (Kane *et al*., 1997, and Egan *et al*., 1997) and designed to kinematically model geological structures in the hangingwall where deformation is assumed to occur by particle flow that is parallel to the fault surface and parallel to the plane of cross section (plane strain assumption) (Midland Valley, 2005). The Fault Parallel Flow algorithm works well for restoring this model because of the flat-ramp-flat (fault-bend fold) geometry characteristic of the deformation in the frontal Foothills section of the triangle zone.

3.3.2 3D Interpretation

After completion of the 2D models, Midland Valley's *4DVista*® software was used to confirm that the individual interpretations from *2DMove*® were viable based on the formation intersections at the seismic tie points. *4DVista*® was also used as a visual aid enabling construction of the 3D model in Midland Valley's *3DMove*®. *4DVista*® serves as an intermediate, iterative tool, between *2DMove*® and *3DMove*® assisting in model visualization. To construct a 3D model, the individual 2D sections are loaded into *3DMove*® and then surfaces are created by linking individual formation tops and faults across the model area. A number of intermediate cross sections needed to be developed and placed in

3DMove® in order to extrapolate and construct the surfaces to appropriately represent what the 2D sections and *4DVista*® model displayed.

3.3.3 Aeromagnetic Data

High Resolution Aeromagnetic (HRAM) Total Field, Total Magnetic Intensity (TMI) Band Pass, Matched Filter and calculated Horizontal Gradient data were used in this study to compare the subsurface seismic interpretations to the magnetic signatures recorded over the study area (see section 3.10). The data were acquired at 600 m x 1800 m line spacing and gridded with a 200 m cell size. The data were made available and processed by GEDCO.

3.3.4 Core Analysis

Seventeen cores (see Appendix) across the regional study area were logged and investigated for any sort of structural disturbances such as: fractures (filled and non-filled), slickensides, fault brecciation, gouging and associated deformation. Although no cores in the entire study area are noted to penetrate through a Cardium Formation fault repeated zone, some are in close proximity based on repeats observed in wireline log signatures available from *AccuMap*®. It was thought that the best chance of recording structurally associated features in core was to closely examine the cores that are located in the closest proximity to wireline logs showing repeated sections of the Cardium Formation.

3.3.5 Surface Geology

There is essentially no outcrop visible in the study area and because of this only one day of reconnaissance observation was necessary in the summer of 2006. Locales investigated in the field were chosen based on access roads, aerial photographs that showed potentially promising locations and areas identified from the seismic lines that showed potential for outcropping structures. The purpose of the field work was primarily to observe if any outcrops in the study area contained surficial expressions of faulting or bed thickening as a result of deformation.

3.4 Interpreted 2D Structural Sections

Five seismic sections A-A', B-B', C-C', D-D', E-E' were interpreted (Figures 3-5, 3-6, 3-7, 3-8, 3-9) to delineate the 2D and 3D structural geometry in the study area. The primary constraint for the structural interpretation is based on the identification and correlation to the seismic sections of stratigraphic formation tops from seven wells drilled in the study area (Figures 3-5a to 3-9a). The corresponding uninterpreted seismic images are Figures 3-5b to 3-9b.

During the study's interpretational phase, seismic reflection data, pre-existing conceptual models about structural styles associated with frontal Foothills deformation, and proper cross section balancing techniques were also taken into account. The sections include three dip sections (A-A' to C-C') and two oblique sections (D-D' and E-E'). The dip sections are parallel to one another and oriented northeast-southwest. The three dip sections are parallel to the

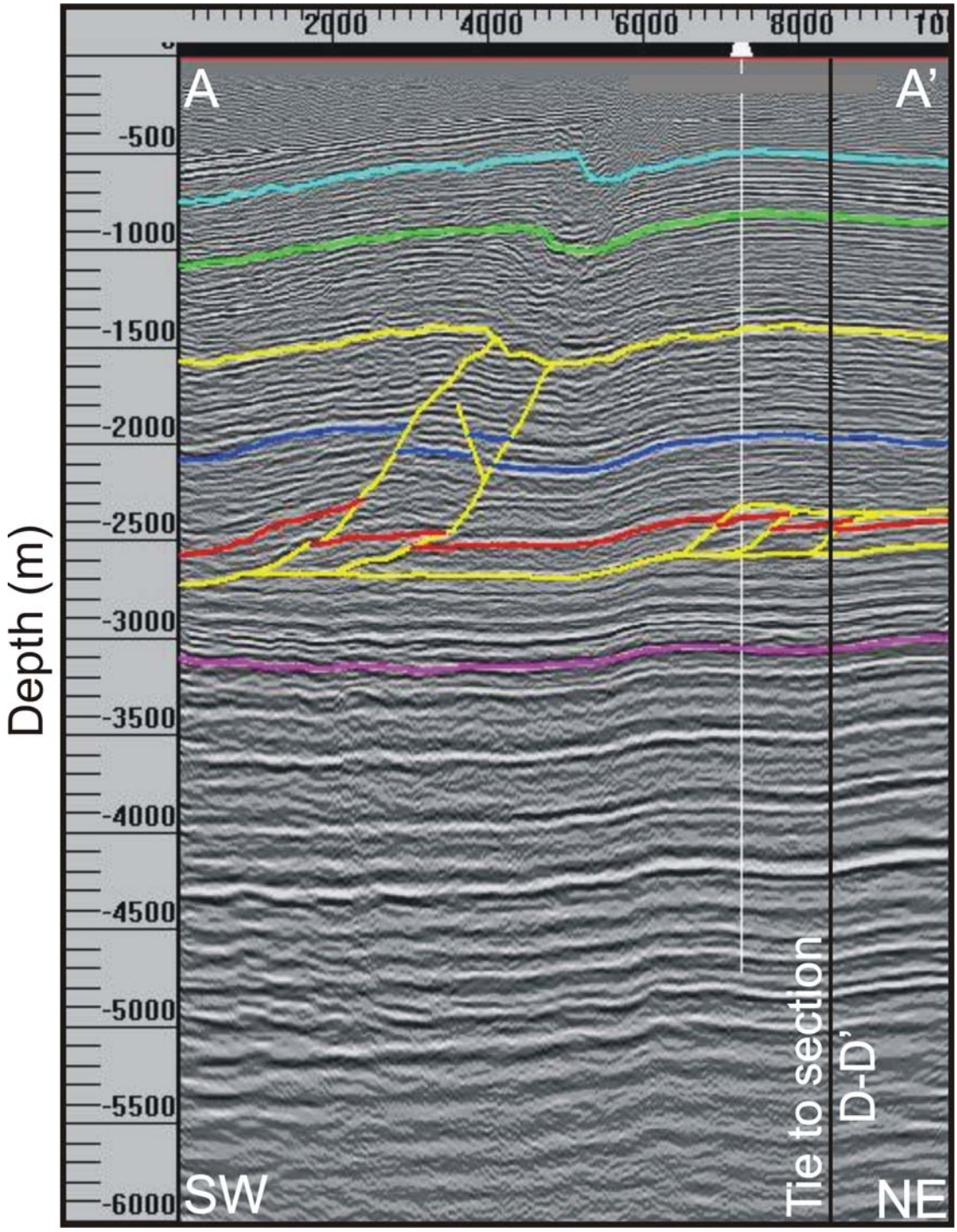

Figure 3-5a: Interpreted seismic line A – A'. Light blue and light green: Upper Cretaceous; Dark blue: Lea Park Formation; Red: Cardium Formation; Pink: Paleozoic top; Yellow: Faults. Scale in meters (see Figure 3-2 inset for location, see Figure 2-2 for stratigraphic column). Vertical exaggeration approximately 2.5X.

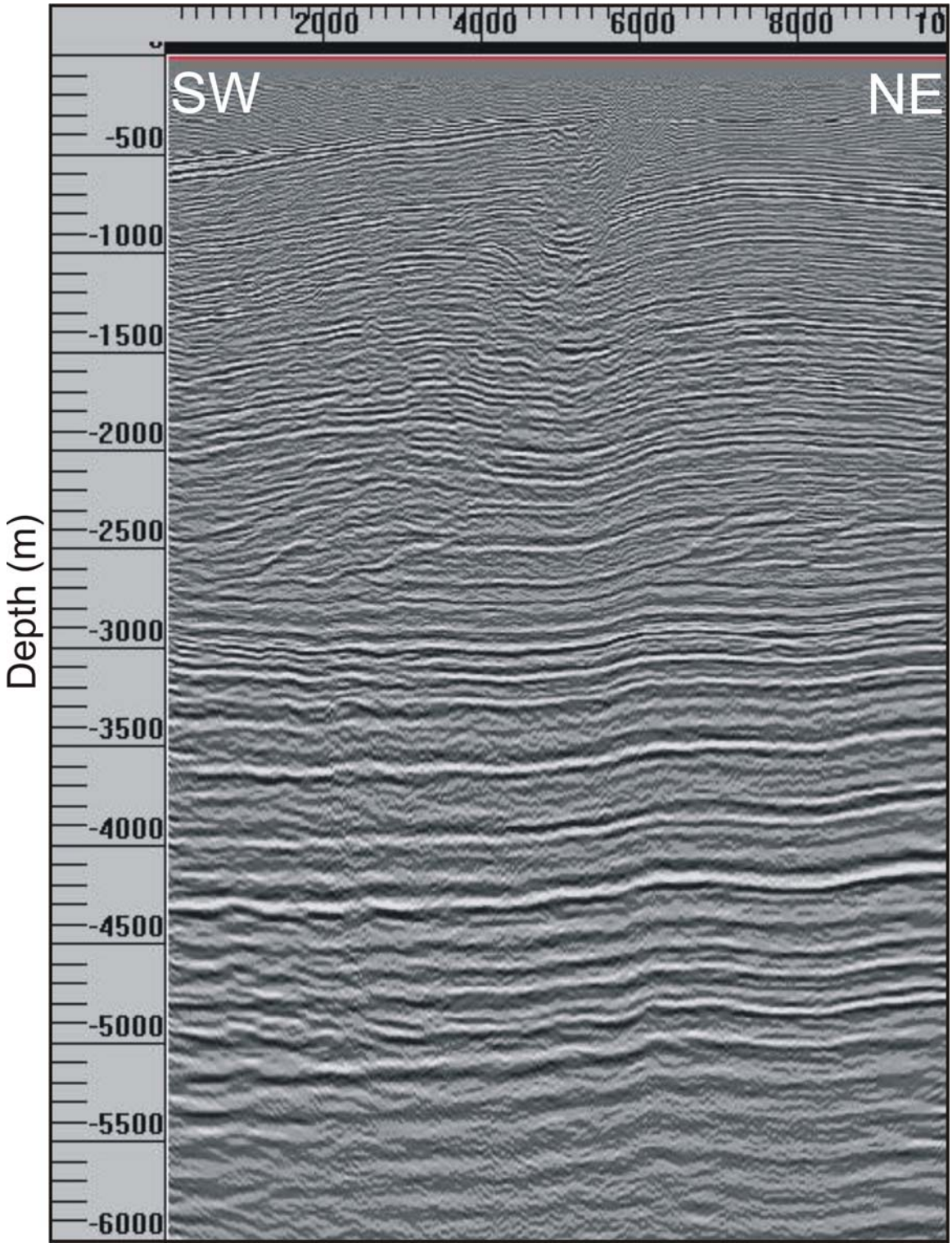

Figure 3-5b: Uninterpreted seismic line A – A'. Scale in meters (see Figure 3-2 inset for location). Vertical exaggeration approximately 2.5X.

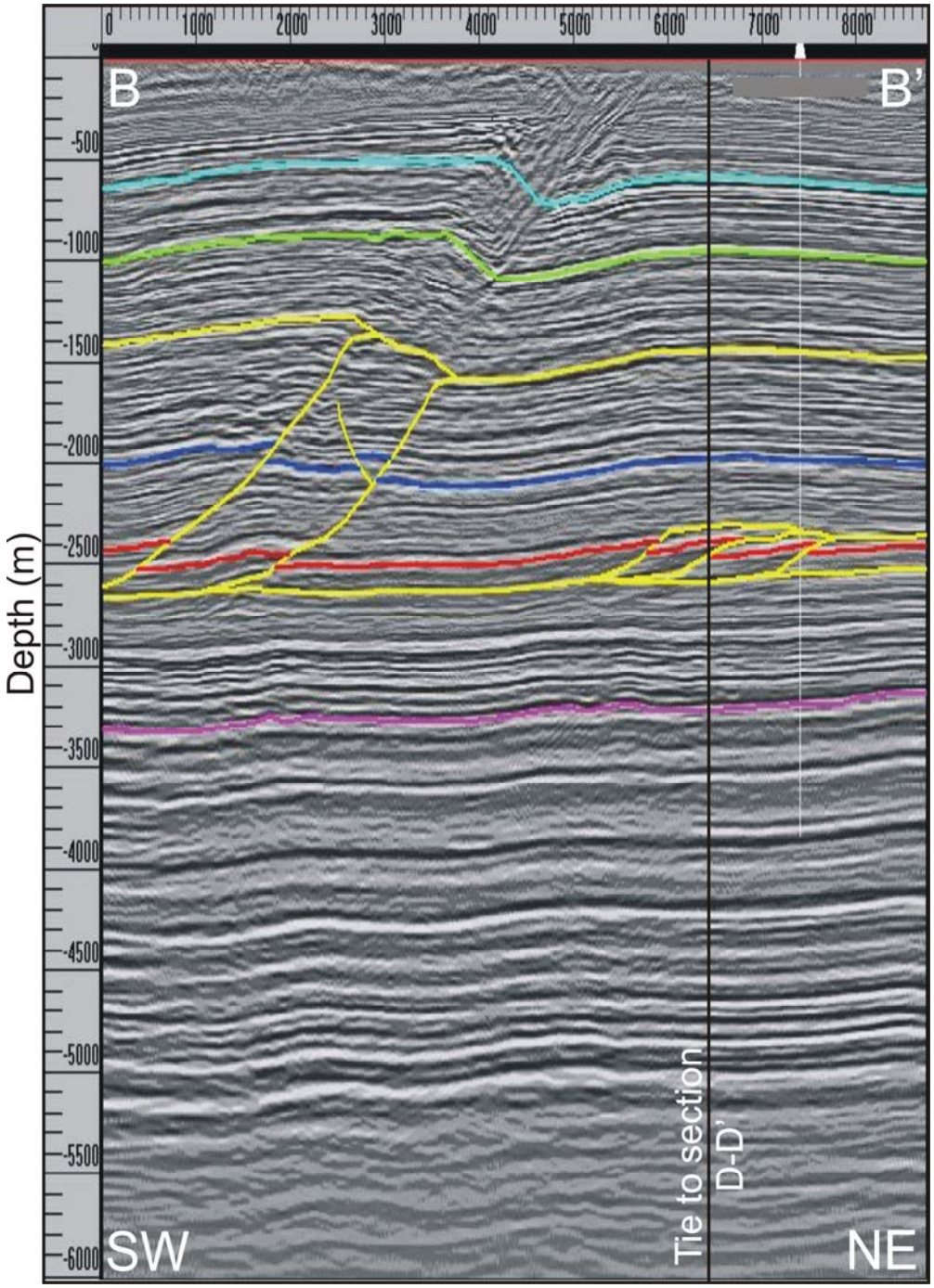

Figure 3-6a: Interpreted seismic line B - B'. Light blue and light green: Upper Cretaceous; Dark blue: Lea Park Formation; Red: Cardium Formation; Pink: Paleozoic top; Yellow: Faults. Scale in meters (see Figure 3-2 inset for location, see Figure 2-2 for stratigraphic column). Vertical exaggeration approximately 2.0X.

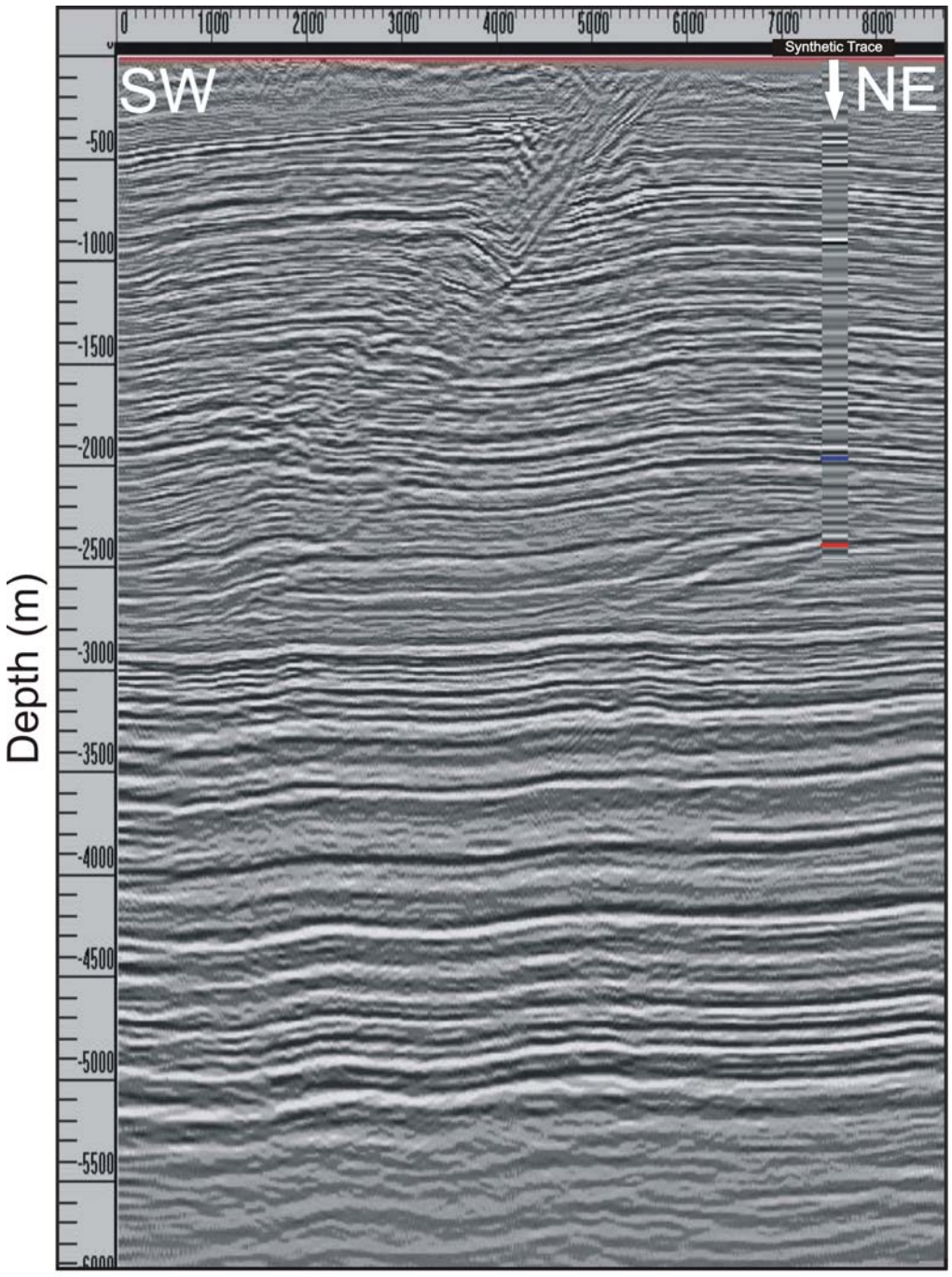

Figure 3-6b: Uninterpreted seismic line B - B'. Scale in meters (see Figure 3-2 inset for location). The synthetic seismogram created from the sonic log of well 10-28-45-16W5 is placed over the well location. The synthetic was used to tie the key horizons of the Cardium and Lea Park formations (noted as red and blue lines respectively on the synthetic image) to the seismic data in the study area. Vertical exaggeration approximately 2.0X.

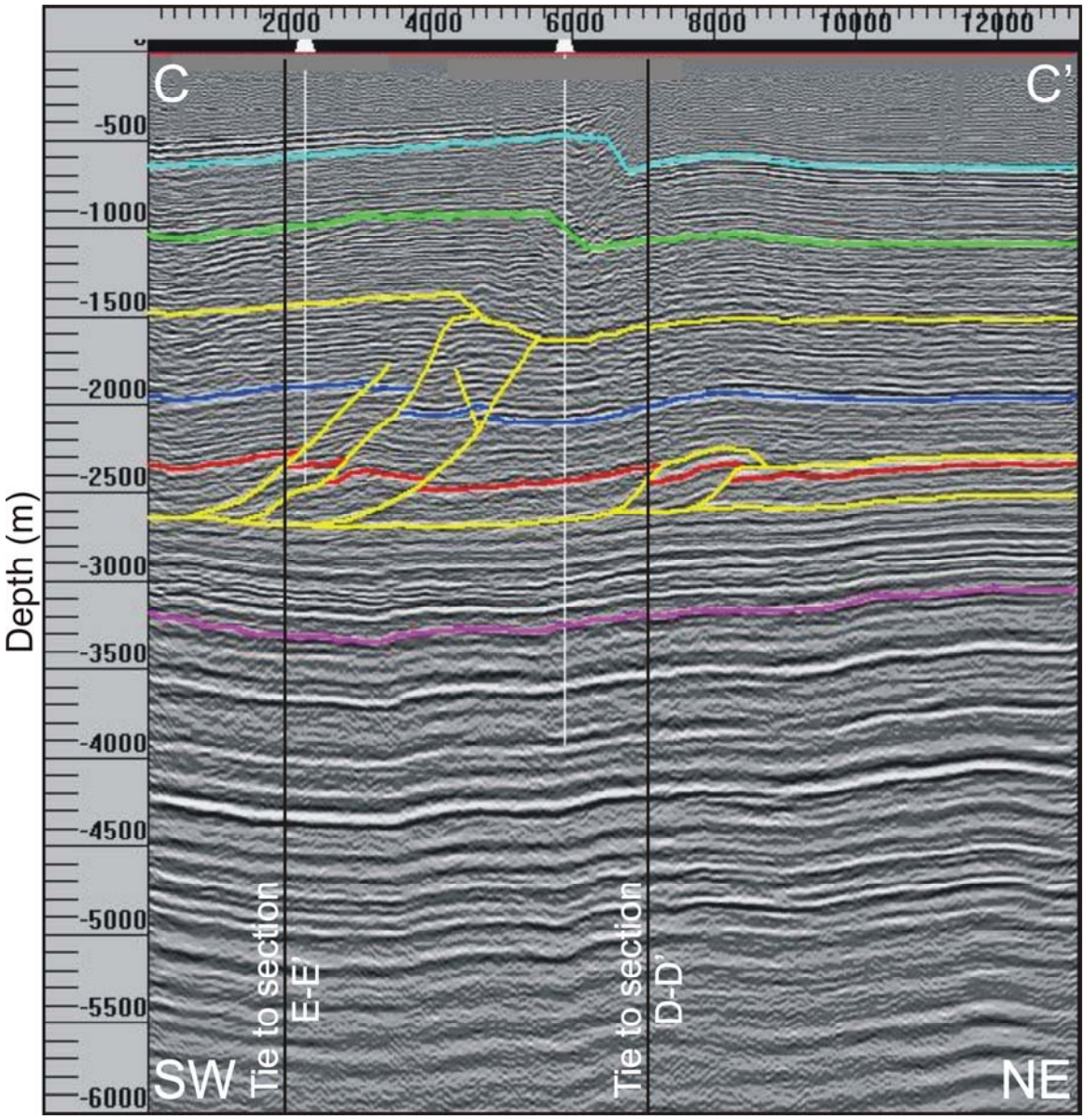

Figure 3-7a: Interpreted seismic line C - C'. Light blue and light green: Upper Cretaceous; Dark blue: Lea Park Formation; Red: Cardium Formation; Pink: Paleozoic top; Yellow: Faults. Scale in meters (see Figure 3-2 inset for location, see Figure 2-2 for stratigraphic column). Vertical exaggeration approximately 2.5X.

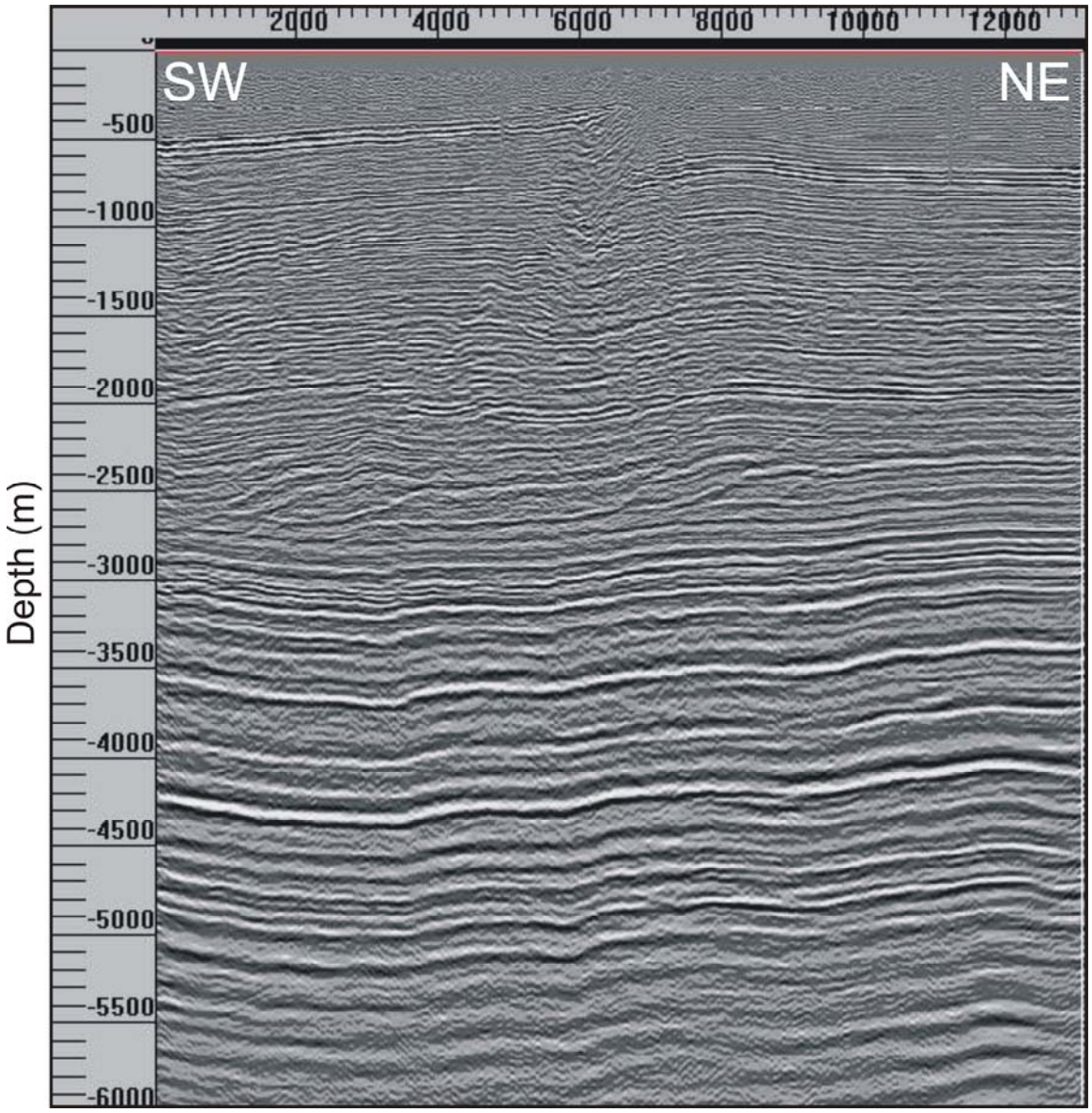

Figure 3-7b: Uninterpreted seismic line C - C'. Scale in meters (see Figure 3-2 inset for location). Vertical exaggeration approximately 2.5X.

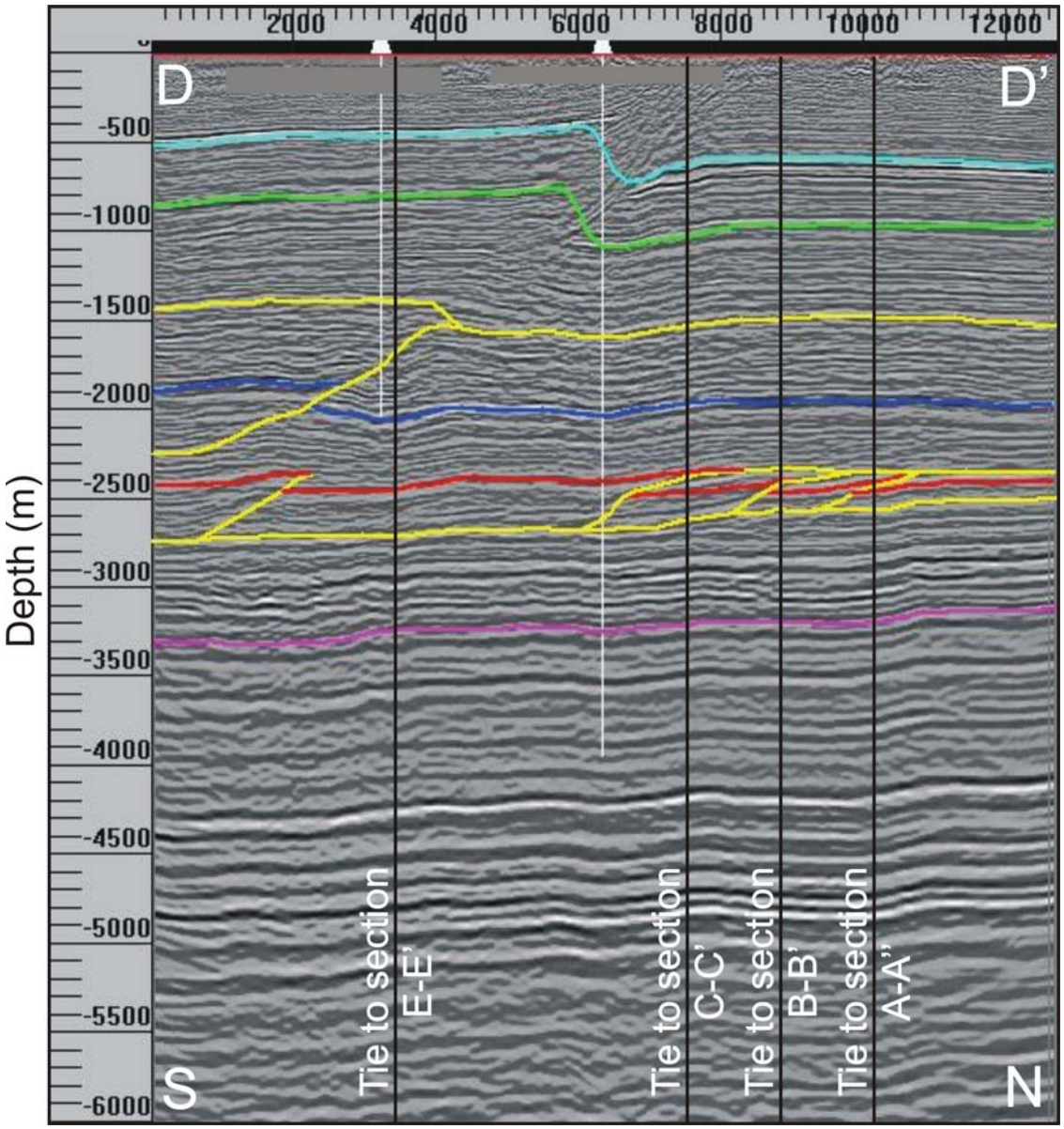

Figure 3-8a: Interpreted seismic line D - D'. Light blue and light green: Upper Cretaceous; Dark blue: Lea Park Formation; Red: Cardium Formation; Pink: Paleozoic top; Yellow: Faults. Scale in meters (see Figure 3-2 inset for location, see Figure 2-2 for stratigraphic column). Vertical exaggeration approximately 2.5X.

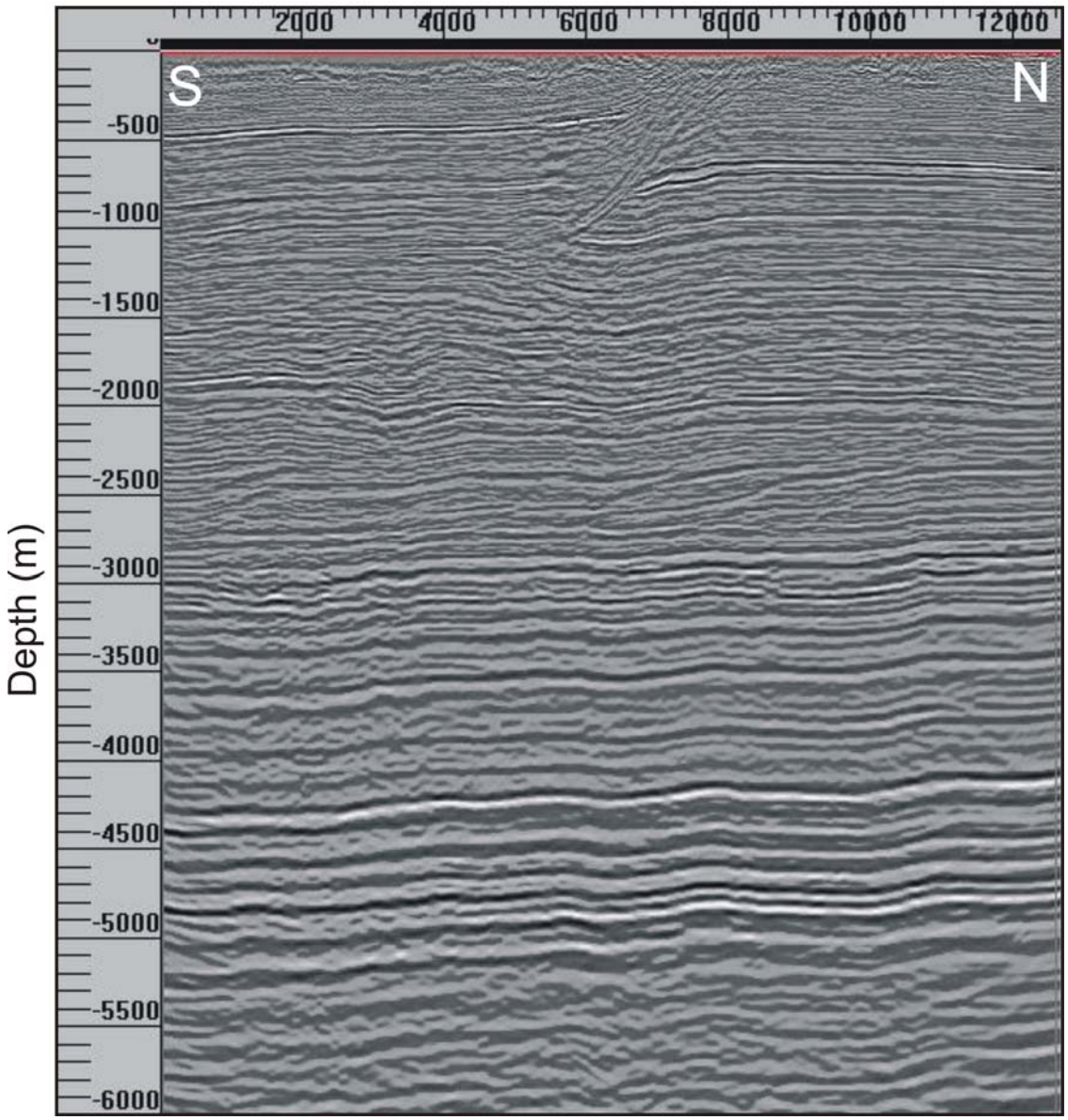

Figure 3-8b: Uninterpreted seismic line D - D'. Scale in meters (see Figure 3-2 inset for location). Vertical exaggeration approximately 2.5X.

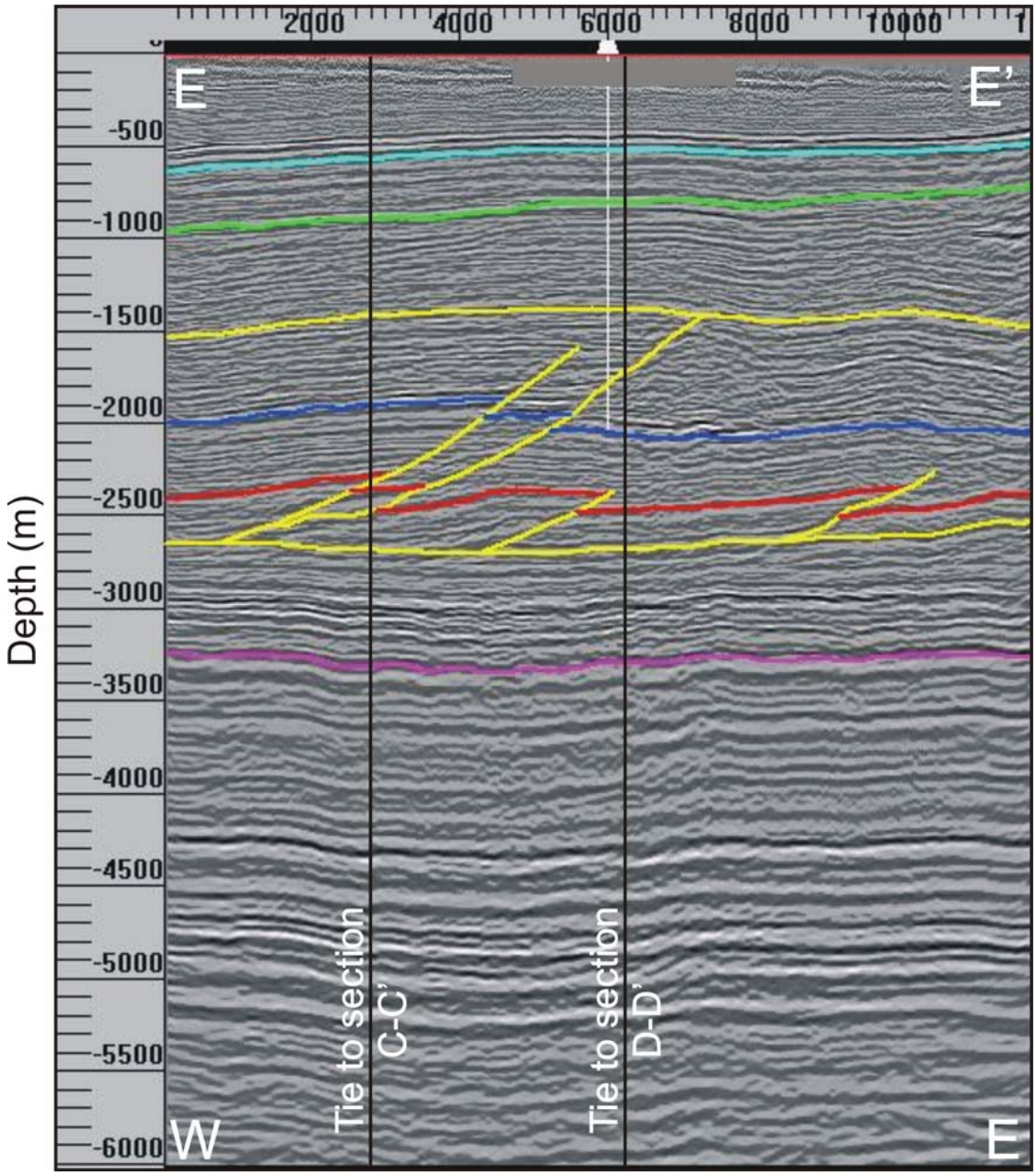

Figure 3-9a: Interpreted seismic line E - E'. Light blue and light green: Upper Cretaceous; Blue: Lea Park Formation; Red: Cardium Formation; Pink: Paleozoic top; Yellow: Faults. Scale in meters (see Figure 3-2 inset for location, see Figure 2-2 for stratigraphic column). Vertical exaggeration approximately 2.5X.

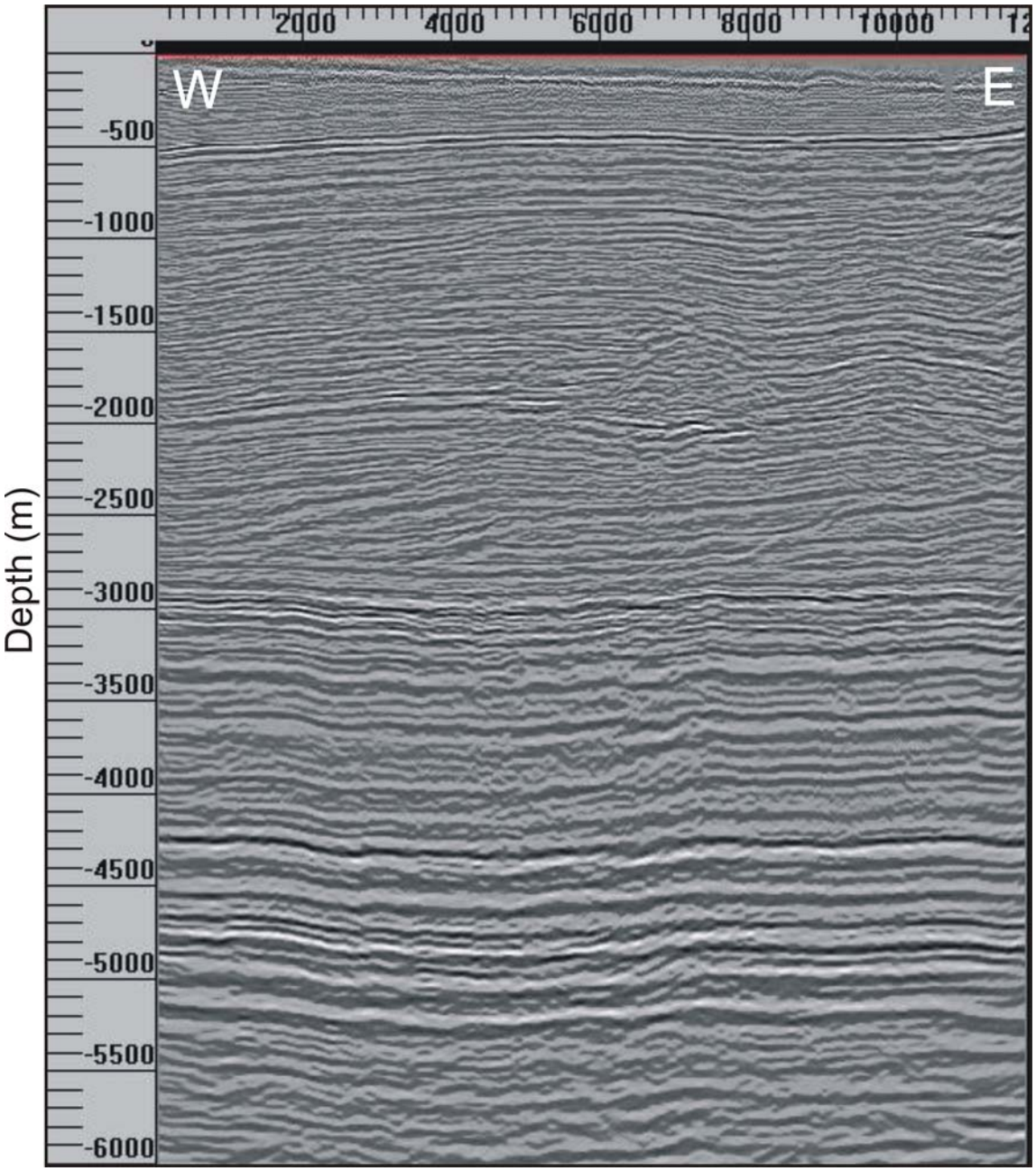

Figure 3-9b: Uninterpreted seismic line E - E'. Scale in meters (see Figure 3-2 inset for location). Vertical exaggeration approximately 2.5X.

presumed principal direction of the displacement vector or maximum compressive stress (σ_1) direction during the Laramide Orogeny in the Canadian Cordillera as interpreted by Gabrielse (1991). The north-south oblique section D-D' lies at an acute angle to the dip sections, and offers along-strike verification of a valid interpretation between dip sections. Section line E-E' is oriented east-west, obliquely to the dip sections, and allows the variation along strike to be interpreted into the southern limit of the study area.

3.4.1 Sequence of Thrusting

The sequence of thrusting is an important issue to address when attempting to palinspastically restore deformed sections. Bally *et al*. (1966) and Dahlstrom (1969) state that generally deformation in the central and southern Alberta Foothills occurred sequentially from west to east or, from the hinterland to the foreland. This conclusion is based on the fact that we see stratigraphically older thrusts being folded above lower level detachments in such structures as antiformal stacks (Bally *et al.*, 1966; Jones, 1971). For this study, based on the geometries observed in this part of the frontal Foothills, all structures are assumed to have formed in a west to east sequence, as there is no evidence to the contrary.

3.4.2 Conventions of the Structural Sections

The structures and faults in this study area have not been formally named, but for the purpose of describing the structural style, informal names have been applied

to them. Most of the structures are common across the entire study area. Figure 3-10 shows section A-A’ and highlights the names given to the structural features in this section that are then referenced in all of the other sections. These structural features include: the upper detachment (UD); the lower detachment (L De); the hinterland duplex (HD); the duplex-pop-up (DP); the foreland duplex-culmination (FDC), where the two duplexes contained within the culmination have been designated as the leading horse (LH) and trailing horse (TH) and represent the foreland and hinterland side of the structure respectively. All of the formational tops are noted in Figures 3-5 to 3-9.

3.4.3 Section A-A’

Section A-A’ (Figure 3-5) is the northwestern-most dip line and shows the foreland duplex-culmination with two internal horses. The foreland duplex-culmination is carried by the lower detachment, its roof thrust is the upper detachment, and the entire structure is blind. The trailing and the leading horses within the culmination show only slight (~60 m) vertical separation of the Cardium Formation. The hinterland duplex connects the upper detachment and the lower detachment. Again, the vertical separation (throw) of the Cardium Formation across the foreland thrust of the hinterland duplex is approximately 60 m. There is a pop-up structure that has developed in the hinterland duplex and displaces the Lea Park Formation approximately 100 m on the foreland side and 70 m on the hinterland side of the structure. The pop-up has slightly folded the hinterland fault in the hinterland duplex as it developed. In the hangingwall of the hinterland

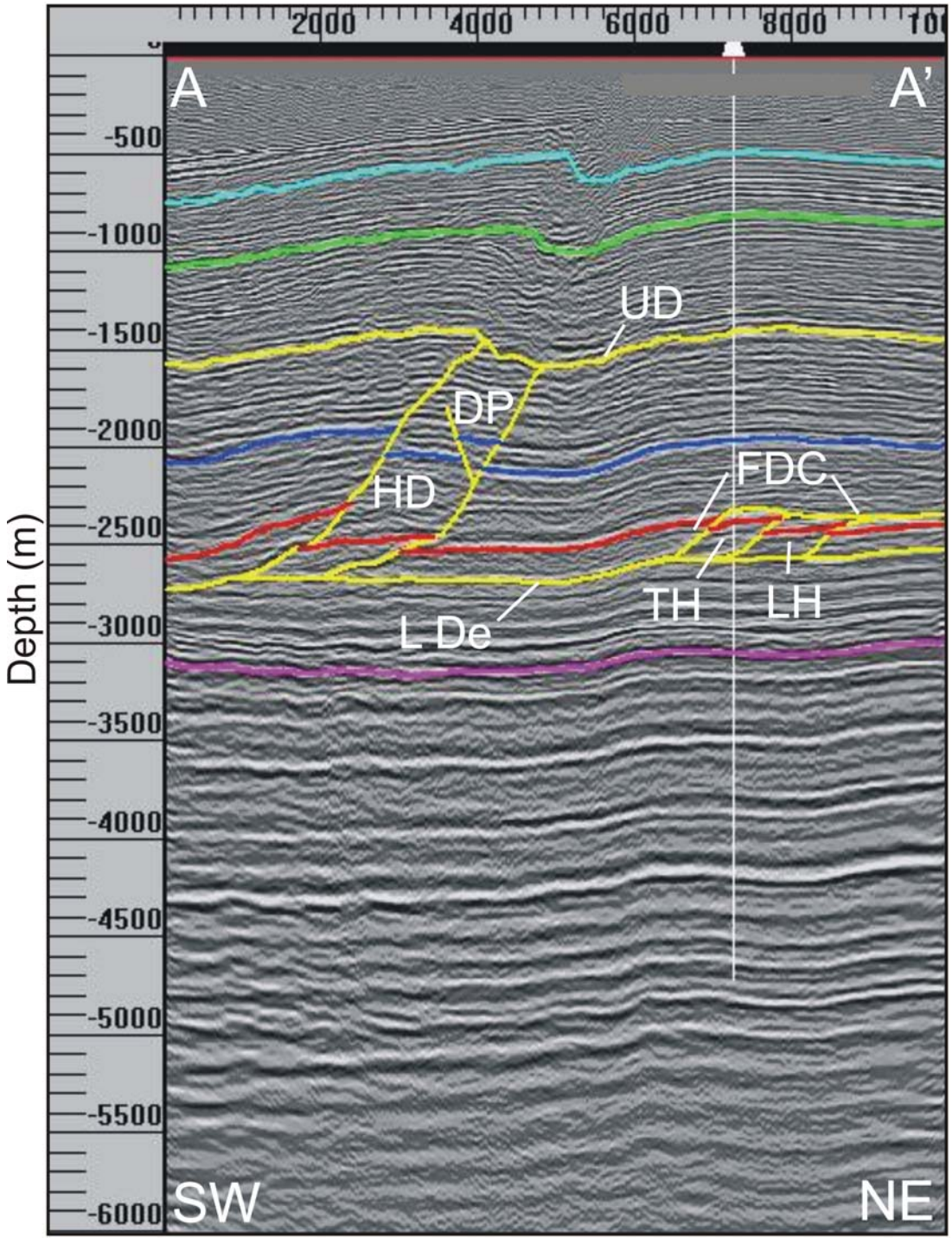

Figure 3-10: Section A – A' with the abbreviated names for specific structures highlighted on the image. upper detachment: UD; lower detachment: L De; hinterland duplex: HD; duplex-pop-up: DP; foreland duplex-culmination: FDC; leading horse: LH and; trailing horse: TH. Scale in meters.

thrust of the hinterland duplex there is approximately 120 m of vertical separation. The upper detachment is slightly folded directly above the hinterland fault in the hinterland duplex. The Upper Cretaceous strata overlying the upper detachment are also folded. The geometry observed in the overlying strata is controlled by the geometry of the upper detachment.

3.4.4 Section B-B'

Section B-B' (Figure 3-6) is located approximately 1.0 km southeast of section A-A'. The section shows almost the identical geometry to that of section A-A'. The foreland duplex-culmination is noted again to ride on the lower detachment and has the upper detachment as its roof thrust. The hinterland thrust of the hinterland duplex is not folded by the pop-up structure as it is in section A-A'. On the other hand, the upper detachment is slightly more folded. The vertical separations across the faults are equal to those noted in section A-A'. All of the overlying Upper Cretaceous strata above the upper detachment are folded in the same manner as in section A-A', parallel to the upper detachment.

3.4.5 Section C-C'

Section C-C' (Figure 3-7) is located approximately 1.5 km southeast of section B-B'. The section is slightly oblique to the two northern dip sections, but still is considered to be a dip section. Section C-C' shows significant variation compared to the two other dip lines. The foreland duplex-culmination only contains the trailing horse in this section. The hinterland duplex pop-up structure

has less displacement and the Lea Park Formation shows almost no offset compared to the two northerly dip sections. The vertical separation of the Cardium Formation is lessened in this section to approximately 50 m in the trailing duplex as well as in the hinterland duplex. Westward of the hinterland thrust of the hinterland duplex, a blind imbricate branches from the lower detachment. Shortening between the two detachment horizons has been taken up equally by the additional thrust and the hinterland thrust of the hinterland duplex such that they each show a vertical separation of approximately 60 m, versus the two northern sections where this extra fault does not exist. Because of the development of the blind imbricate to the hinterland of the hinterland duplex, the upper detachment is noted to be slightly more folded (steeper dip toward the foreland) in section C-C' than in sections A-A' and B-B'. As in both of the northern lines, the overlying Upper Cretaceous strata in section C-C' are folded conformably along with the upper detachment.

3.4.6 Section D-D'

Section D-D' (Figure 3-8) is oriented north-south and is used to verify the three dip line interpretations and is also useful to interpret the along-strike variation. The hinterland duplex structure, seen in the three dip sections, is no longer present. The foreland fault of the hinterland duplex loses displacement in the southern part of the study area and terminates slightly above where it cuts the Cardium Formation. The tip of the hinterland thrust of the hinterland duplex is shallower than in the other sections and it is not seen to sole into the (sub-

Cardium Formation) lower detachment in this section; instead it soles into a detachment above the Cardium Formation. The upper detachment is still folded above the hinterland ramp of the hinterland duplex as in the dip sections. The overlying Upper Cretaceous strata appear to be folded more steeply in this section compared to the dip sections.

3.4.7 Section E-E’

Section E-E’ (Figure 3-9) is oriented east-west and is used to determine the variation along strike to the southern limit of the study area. In this section the foreland duplex-culmination is not present. The foreland duplex-culmination is replaced by a single imbricate thrust that splays from the lower detachment and terminates slightly above the hanging wall cut-off of the Cardium Formation. Similarly, the hinterland duplex is noted to not be fully developed in this section. The foreland thrust of the hinterland duplex terminates directly at the hanging wall cut-off of the Cardium Formation. The hinterland thrust of the hinterland duplex soles into a thrust that lies directly west of it. The imbricate thrust west of the hinterland thrust of the hinterland duplex is also present in section C-C’. Because section E-E’ is not a true dip section, only apparent dips are displayed, so the upper detachment appears to be barely folded above the hinterland thrust of the hinterland duplex and Cretaceous strata overlying the upper detachment appear to be only broadly folded. All of the faults between the upper and lower detachments in this section appear to dip at shallower angles than in the true dip and less oblique sections.

3.5 Detachment Horizons

There are two dominant detachment horizons in the study area that are observable in all five sections. These detachment horizons run parallel to one another and are separated by an average vertical distance of 1100 m in the sections. The upper detachment occurs in the Bearpaw Formation whereas the lower detachment occurs in the Blackstone Formation. These two formations are favourable detachment horizons because of the shale lithology. Detachment horizons are necessary kinematically to explain situations where shortening is significantly greater above or below a horizon (Dahlstrom, 1969; Drover, 2000).

The detachment zones in the study area are difficult to detect from drilling data alone, but with the aid of modern seismic data, the parallel detachments are easier to discern. The lower detachment horizon is located by noting the stratigraphic horizon from which all of the thrusts in the study area branch. The thrust ramps between the two detachments flatten into the upper detachment horizon. The upper detachment is detected by noting the upper limit of deformation, above which the seismic reflectors are coherent and parallel.

3.6 2D Palinspastic Seismic Restorations

For the interpretations of the seismic sections to be considered viable, palinspastic restorations were carried out for the three dip sections (Figures 3-5 to 3-7; A-A’ to C-C’). The two oblique sections were not restored because only sections that are parallel to the transport direction can be properly restored.

Oblique strain encountered in the oblique sections would not allow for proper restorations to be carried out.

The palinspastic restorations were applied to the line interpretations of the seismic data as well as to the seismic images using *2DMove's*® Seismic Restoration algorithm combined with the Fault Parallel Flow algorithm. *2DMove's*® seismic restoration tool requires that polygons be created to outline every body of rock bound by either formational tops or faults (Figure 3-11). Once the polygons are created, the algorithm applies a two dimensional restoration to all of the hanging wall lines and polygons selected for each iterative restoration phase, restoring the structures from foreland to hinterland, opposite to the presumed order of formation of the structures. The polygon restoration is based on the restoration input parameters to the Fault Parallel Flow algorithm as specified by the user. The intricacies of the Fault Parallel Flow algorithm have been described in section 3.3.1. Once applied, the lines and polygons are restored at the same time. The foreland edge of the seismic sections was chosen to be the pin line from which the restoration was performed. The strata that lie above the upper detachment were not pinned and because of this the restoration is incorrectly applied to it. The restored image incorrectly makes the strata above the upper detachment appear as though the deformation to it were caused by foreland-vergent thrusting. Figures 3-12, 3-13 and 3-14 show the palinspastically restored dip sections A-A', B-B' and C-C' respectively.

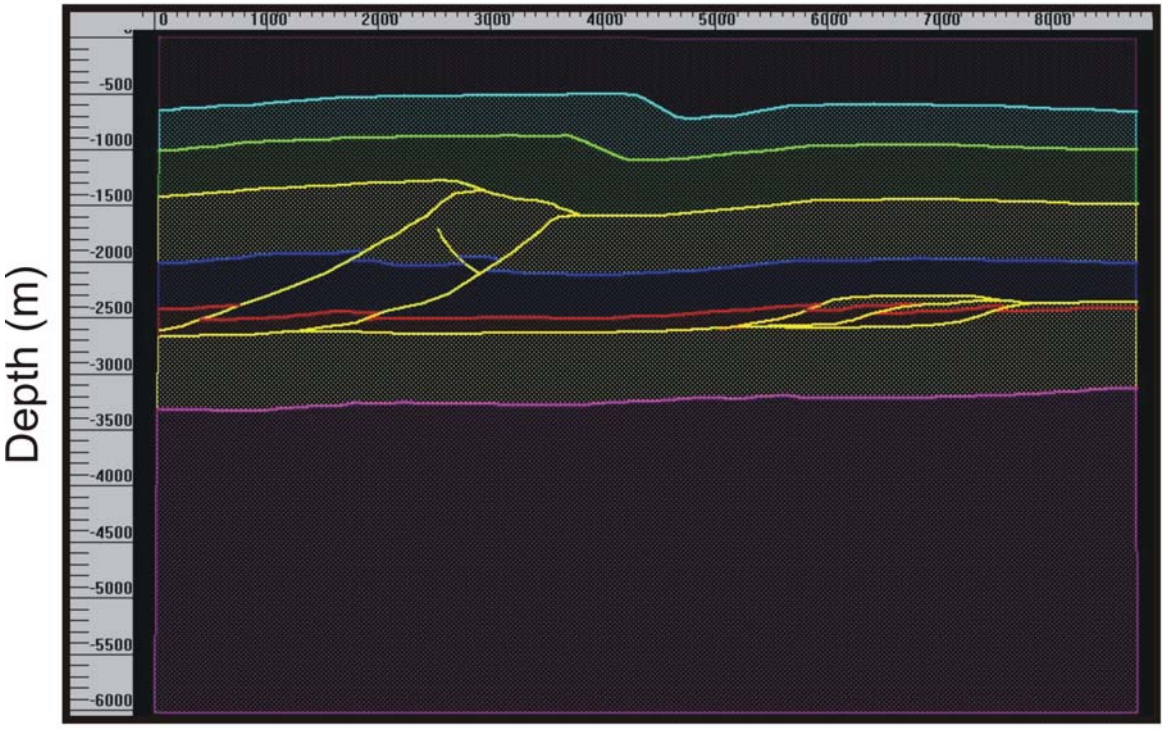

Figure 3-11: Polygon image outlining isolated structural “segments” of a seismic image that are used to restore the seismic image and line geometries that underlie it. Polygon boundaries are either faults or formational tops. Scale in meters.

3.6.1 Restored Section A-A’

The restored section A-A’, Figure 3-12, shows that the stratigraphic horizons between the parallel detachments restore to a near horizontal state – specifically the Cardium Formation top. The Lea Park Formation shows slightly more variation after restoration, focused near the pop-up area within the hinterland duplex and in the hanging wall of the hinterland thrust of the hinterland duplex. The upper detachment is somewhat crenulated in nature and has caused the overlying stratigraphic horizons and seismic image to be crenulated in a similar geometrical fashion during the restoration process. In the restored section, the strata lying above the upper detachment directly over the hinterland duplex, show a slight increase in thickness. This thickness variation is not noted to the areas east and west of the hinterland duplex. In this part of the Foreland no deformation associated with the Laramide Orogeny has taken place below the lower detachment. For this reason all restoration was performed above the lower detachment horizon.

3.6.2 Restored Section B-B’

Section B-B’, Figure 3-13, displays a restored stratigraphic geometry that is slightly more planar in nature than section A-A’. The stratigraphic tops in this section line up almost perfectly between all faulted sections. The Lea Park Formation only shows slight offset present after restoration of the pop-up in the hinterland duplex and in the hangingwall of the hinterland thrust of the hinterland duplex, but not as much as is noted in section A-A’. The upper detachment in this

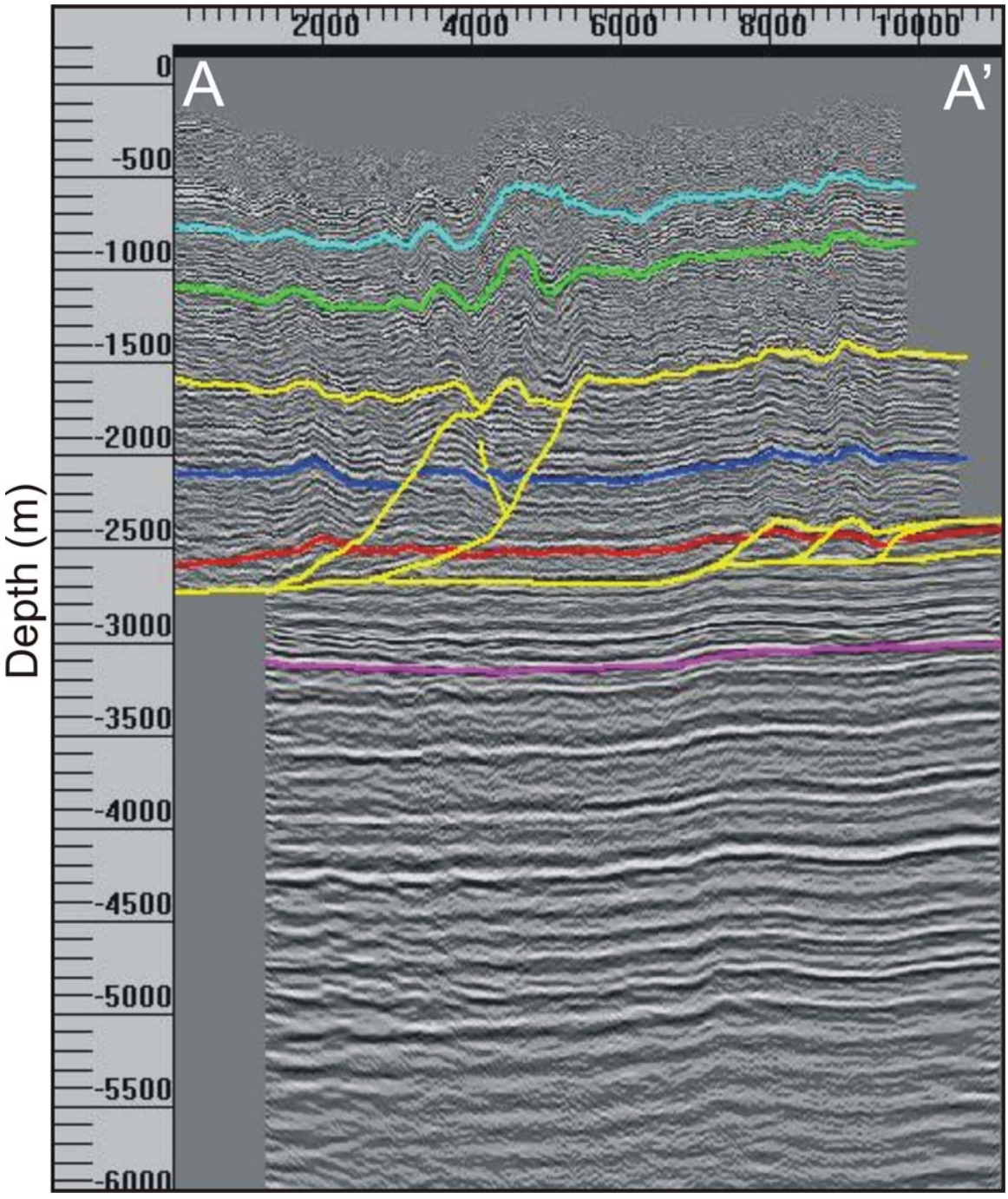

Figure 3-12: Cardium restored in section A – A'. Light blue and light green: Upper Cretaceous; Dark blue: Lea Park Formation; Red: Cardium Formation; Pink: Paleozoic top; Yellow: Faults. Scale in meters.

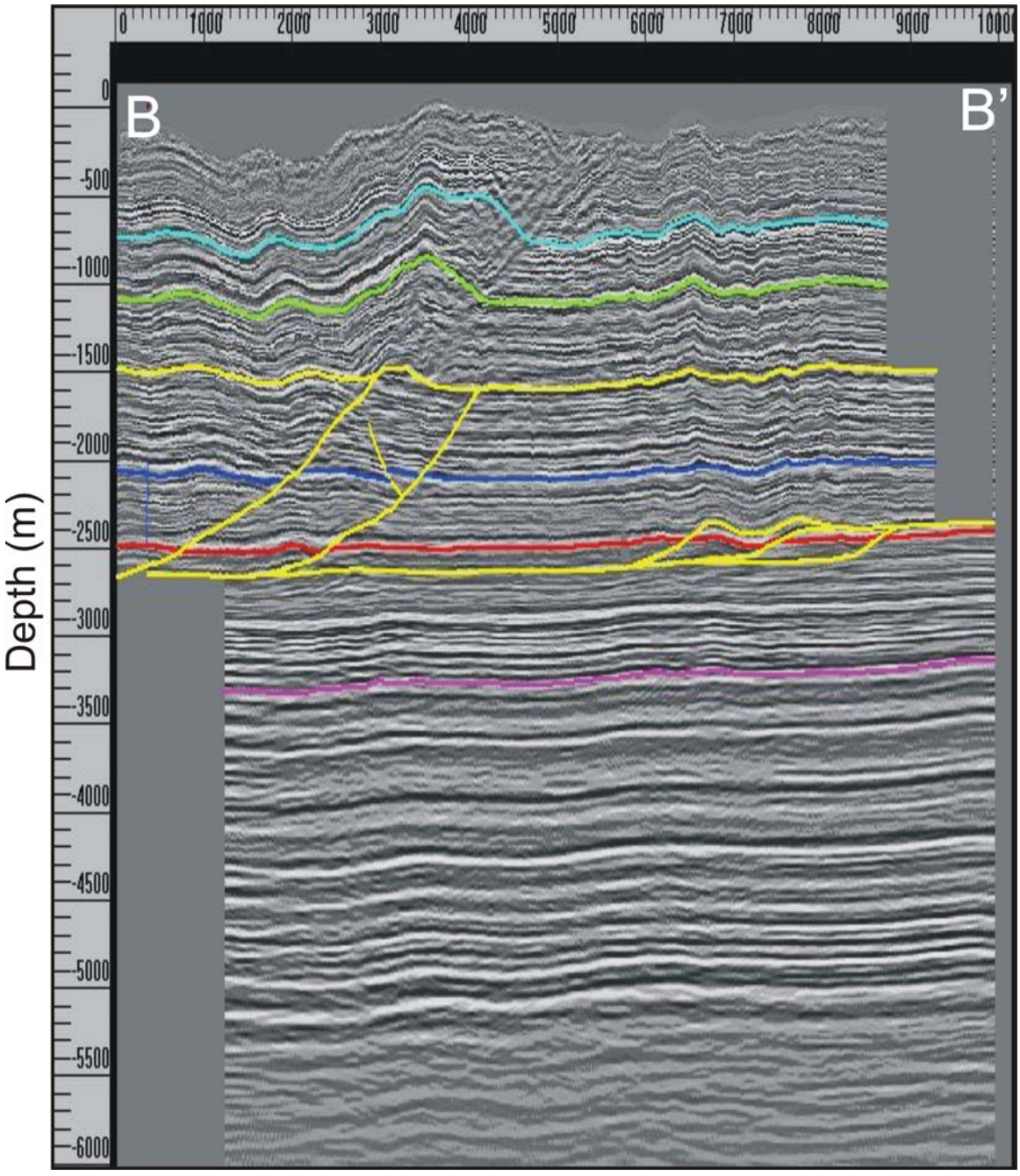

Figure 3-13: Cardium restored section B – B'. Light blue and light green: Upper Cretaceous; Dark blue: Lea Park Formation; Red: Cardium Formation; Pink: Paleozoic top; Yellow: Faults. Scale in meters.

section is almost horizontal, showing only a slight perturbation from horizontality above the pop-up structure. The strata overlying the upper detachment mimic the geometry of the upper detachment. There is a slight thickening of the strata above the upper detachment directly overlying the hinterland duplex. As in section A-A', all deformation in this section has taken place above the lower detachment and below the upper detachment.

3.6.3 Restored Section C-C'

Restored section C-C', Figure 3-14, closely resembles restored section A-A'. The section shows all of the stratigraphic horizons lining up quite well across the faults, although they are sub-parallel compared to sections A-A' and B-B'. The upper detachment in this section shows moderate to heavy crenulation, whereas the overlying strata again mimic the detachment surface. There is also an over-thickening in the strata noted above the upper detachment overlying the hinterland duplex, as noted in the two other restored sections. As in the other two restored sections, all of the deformation in this section has occurred above the lower detachment.

3.7 Seismic Image versus Line Length Palinspastic Restorations

Conventionally, when deformed sections are palinspastically restored, the reader only sees the line interpretation of the undeformed state (and often an edited, tidied-up interpretation). When readers see this they are led to believe that the beds were unfolded and restored to perfect horizontality with no

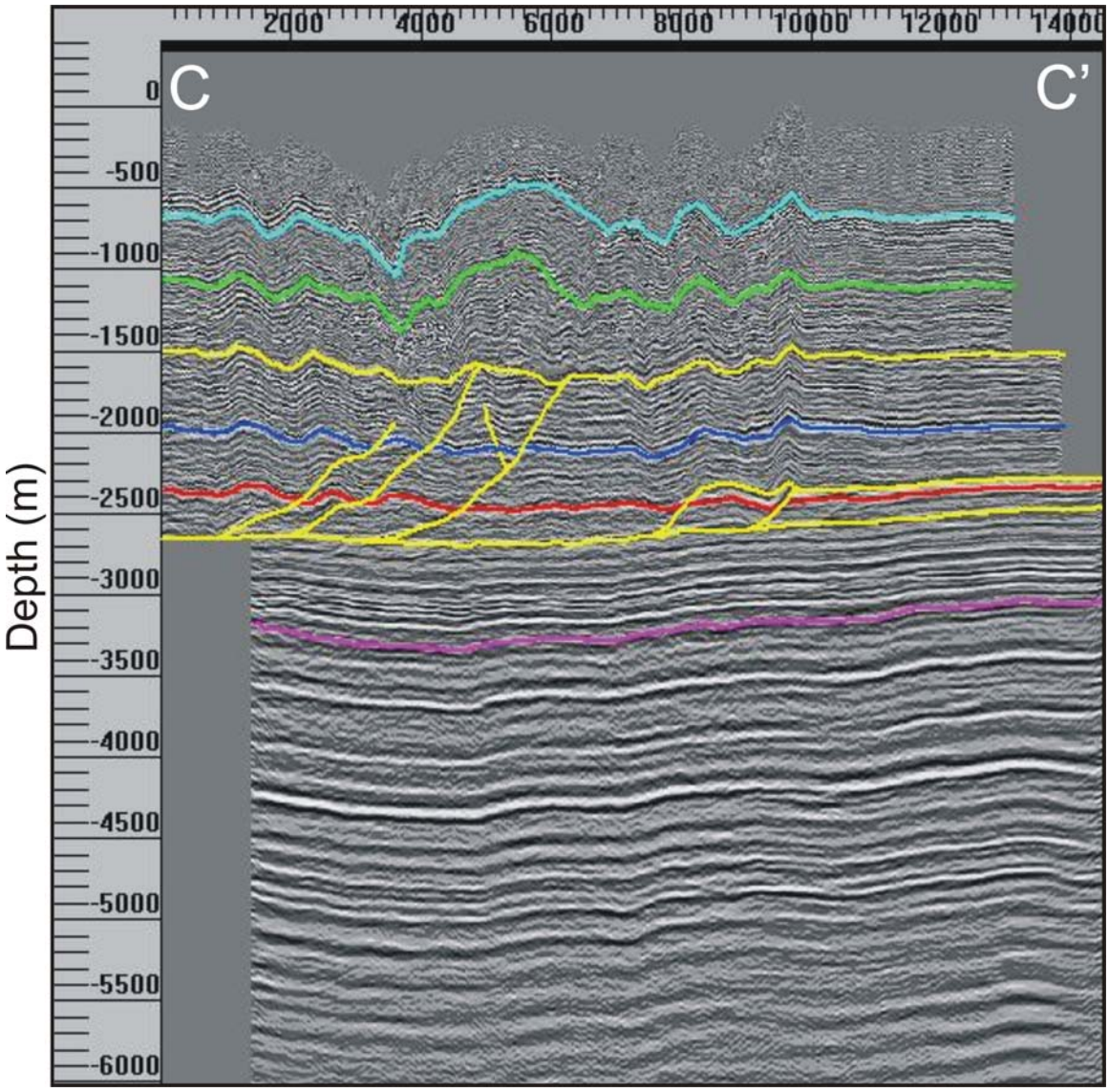

Figure 3-14: Cardium restored section C – C'. Light blue and light green: Upper Cretaceous; Dark blue: Lea Park Formation; Red: Cardium Formation; Pink: Paleozoic top; Yellow: Faults. Scale in meters.

discontinuity. If this were the case in this thesis, the undeformed section B-B' would appear as it does in Figure 3-15A. Minor variations will always be noticeable when the restored seismic image is displayed with the restored line image. The properly restored line image for section B-B', appearing without the seismic background (Figure 3-15B), may lead the reader to think that the restoration is not completely balanced, when in fact the restoration is a very close approximation to nature itself.

The primary causes for minor variations in the restored image can be attributed to a number of reasons that include: 1) The simplicity of the Fault Parallel Flow algorithm attempting to approximate the complexity of nature. 2) The fault-bend fold line geometry that outlines the structures interpreted from the seismic image has many nodes from which dip bisector lines are projected during restoration. This causes 'kinking' of the lines and seismic image as a sequential restoration is performed. The fault-bend fold geometry in the study area is not as simple as the model presented in Suppe, 1983, where dip bisectors project only from the bends in the fold (Figure 3-16 A and B) and thus cause 'kinking' of lines and image from occurring during restoration. 3) Not all thrusting may have occurred exactly in-sequence. And; 4) Angular shear is difficult to account for accurately when attempting to restore sections.

3.8 Shortening

The thicknesses, areas and line lengths remain within 4% of each other from the deformed to restored states. The restoration of the sections to a

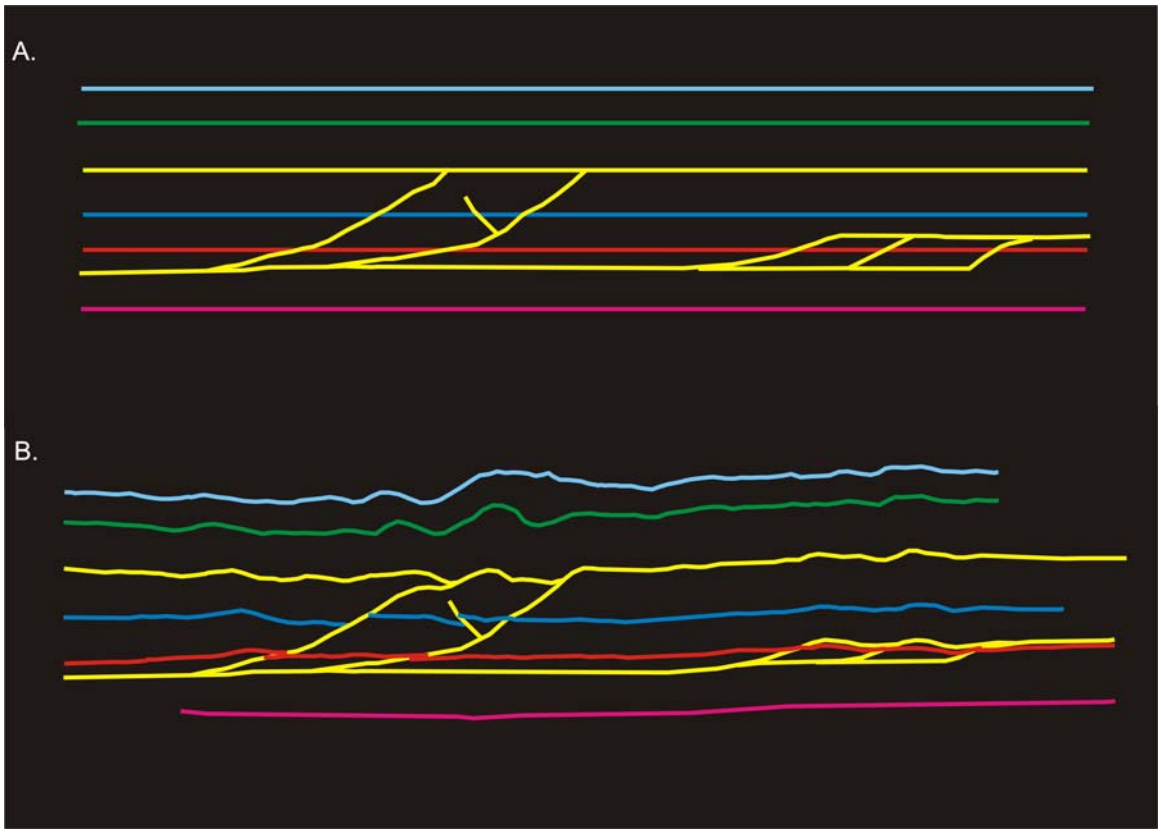

Figure 3-15: **A)** Line diagram of what a typical palinspastic restoration in the study area would look like if no seismic restoration is performed. Lines are horizontal because uncontrollable variables such as seismic processing have not been addressed; **B)** The palinspastically restored line image as it appears when the seismic image is also restored.

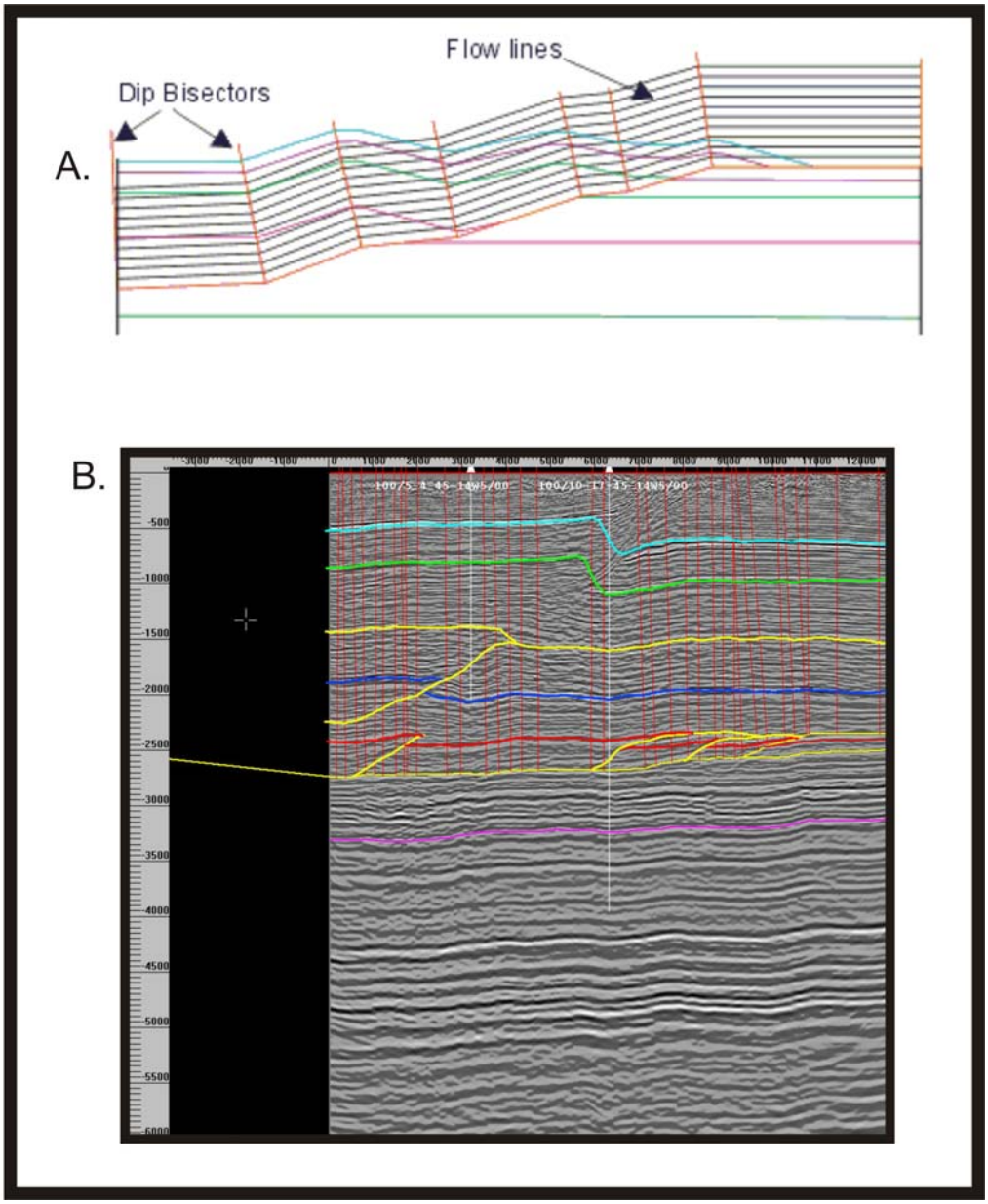

Figure 3-16: **A)** Simple model of a fault-bend fold, outlining the geometry of flow lines along which restoration occurs in each dip domain. Dip domain-dip bisector angles are determined by dividing the angle between a ramp and a flat in half. There are a limited number of bisectors due to the simple, stepped nature of the model. Model modified from Suppe (1983a) and *2DMove*®; **B)** Image of a seismic section from the study area taken during restoration. Dip bisectors are seen as red projection lines above the basal detachment. The seismic interpretation has created many "nodes" from which the restoration algorithm generates bisectors. During stages of sequential restoration, changes in flow line angle across nodes causes a cumulative "kinking" of the overlying seismic image (seismic section is not fully restored).

horizontal state suggests that the interpretation of the deformed sections is a viable one. A calculation of shortening describes the amount of contraction that rock strata have undergone while being deformed. Shortening can be explained by the following formula:

Shortening (S) = $[(L_o - L_f)/ L_o]$

Where:

L_o = The horizontal bed length that is measured in the undeformed, restored section.

L_f = The length of the same bed in the deformed section.

This equation is then rewritten to express the shortening as a percentage, such that:

Percentage Shortening = $(\{(L_o - L_f) / L_o\} * 100\%)$.

Percentage line length shortening can be viewed in Table 3-1**.** The percentage of shortening is greatest in section B-B', where it reaches 14% and least in section C-C' where it reaches only 9.5%. There is a general decreasing trend in shortening southward in the sections studied. The southern extent of the study area has no section in a suitable orientation from which a restoration could be performed to calculate the amount of shortening that has occurred there. A discussion of the structural change southward along strike in the study area will be addressed later in section 3.14.

Table 3-1: Percentage line length shortening of the Cardium Formation from the three primary dip sections, A-A', B-B' and C-C'.

Section	Deformed Length	Restored Length	Length Shortening	Percentage Shortening
A-A'	9.94 km	11.17 km	1.23 km	11%
B-B'	8.73 km	10.15 km	1.42 km	14%
C-C'	13.07 km	14.46 km	1.39 km	9.5%

3.9 3D Modelling

After completion of the 2D interpretation and section balancing, an appropriate 3D model could be constructed. This led to a better understanding of the structural style and changes along strike in the study area. 3D modelling was accomplished using Midland Valley's *3DMove*® software.

Figure 3-17 illustrates the complete 3D model geometry with views of the deformed state to the southeast and southwest. The model shows that the overlying Upper Cretaceous strata are folded in the same geometric fashion as the upper detachment, which was noted in each 2D section. The primary deformational features are evident within the Cardium Formation in the foreland duplex-culmination and the hinterland duplex between the primary detachment horizons. The Lea Park Formation remains relatively undeformed, apart from the area located in the pop up structure within the hinterland duplex. The Paleozoic strata in the model are undeformed as all deformation in the study area occurs above the lower detachment. Figure 3-18 displays the model with the Upper Cretaceous strata, upper detachment and Lea Park Formation removed, so that the thrust faults, the lower detachment and the Cardium Formation deformation can be seen clearly. Figure 3-19A displays the model in plan view and Figure 3-

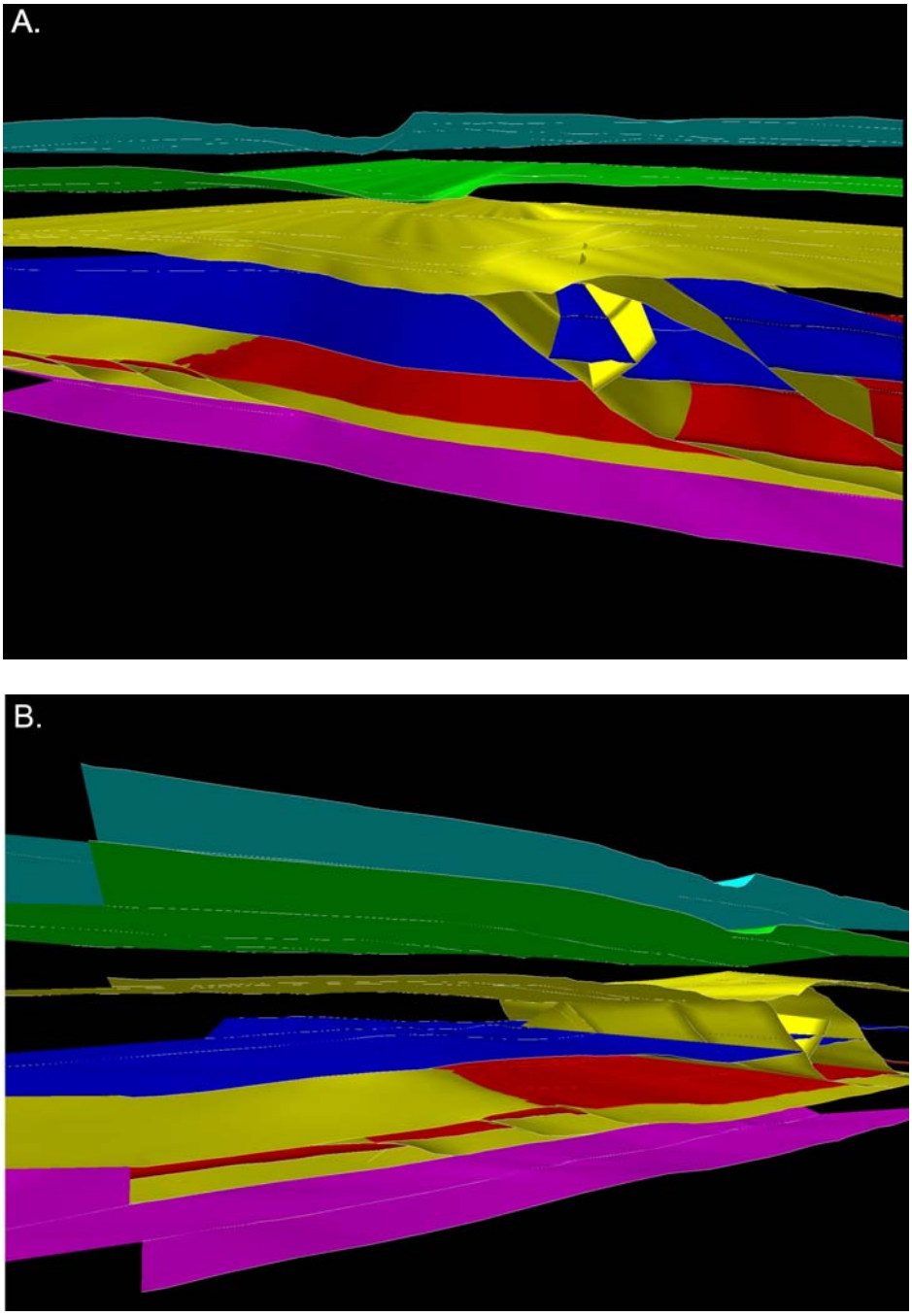

Figure 3-17: **A)** 3D block model with view to the southeast; **B)** 3D block model with view to the southwest. Light blue and light green: Upper Cretaceous; Dark blue: Lea Park Formation; Red: Cardium Formation; Pink: Paleozoic top; Yellow: Faults.

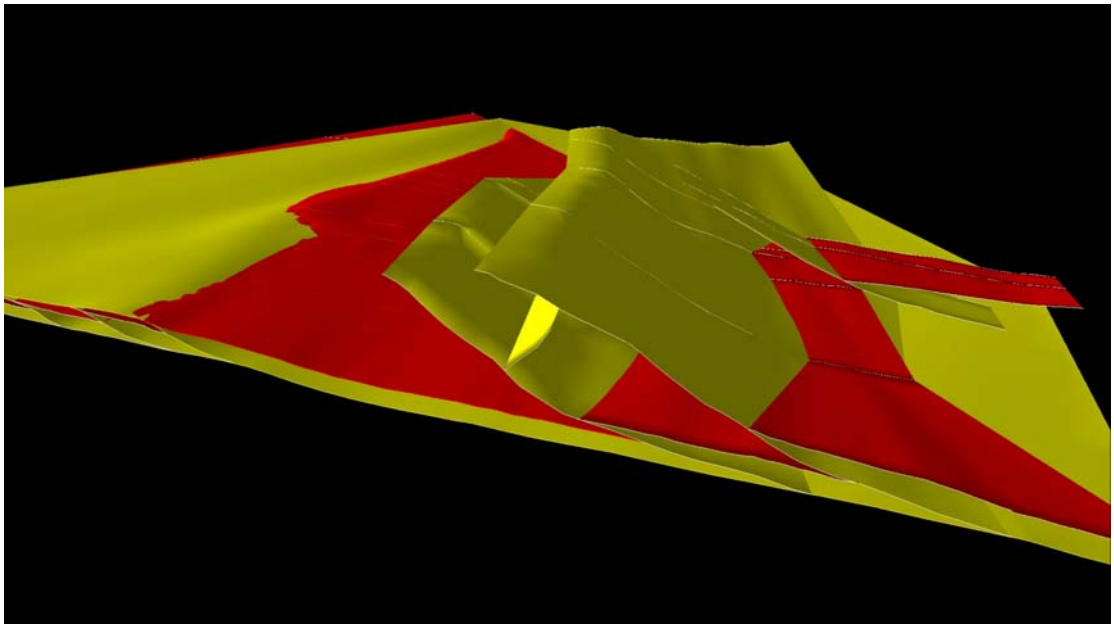

Figure 3-18: 3D block model with upper detachment, upper Cretaceous and Paleozoic strata removed. View to the southeast. Red: Cardium Formation; Yellow: Faults. Upper detachment and overlying formations removed.

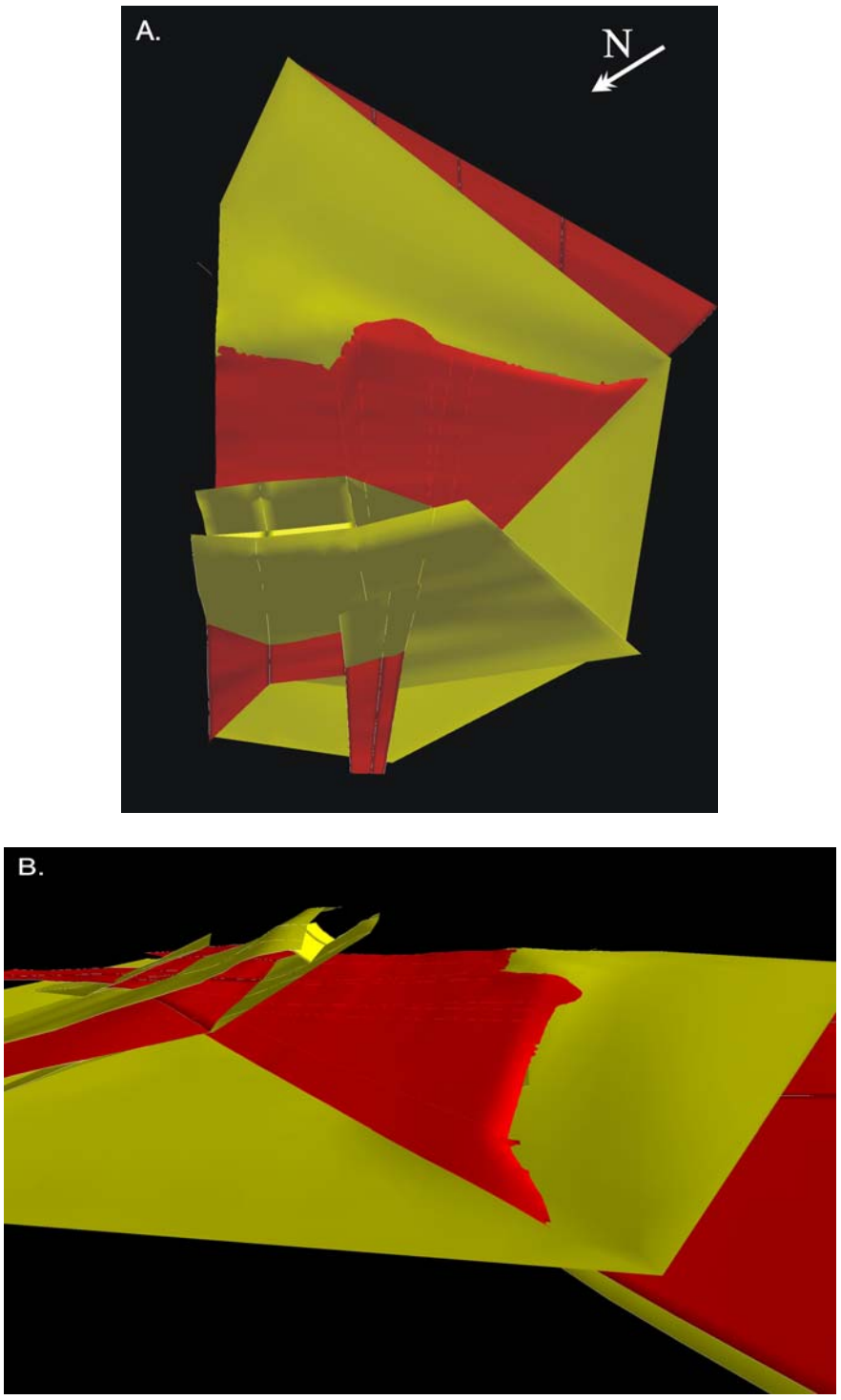

Figure 3-19: **A)** 3D block model in plan view; **B)** 3D block model with view to the north. Red: Cardium Formation; Yellow: Faults. Upper detachment and overlying formations removed.

19B is a view to the north. The plan view in Figure 3-19A clearly illustrates that the Cardium Formation in the hanging wall of the foreland duplex-culmination shows less shortening southward in the model. This is caused by the loss of displacement in the foreland duplex-culmination's duplexes. At the northern edge of the study area two duplexes are contained within the foreland duplex-culmination, whereas in the mid-northern part of the study area only one duplex in the foreland duplex-culmination structure is present and by the southern edge of the study area, there are no longer any duplex structures remaining in the foreland duplex-culmination. The only remaining expression of the foreland duplex-culmination at the southern end of the study area is an imbricate that dies out between the lower and upper detachment horizons.

Figure 3-19B offers another perspective of the Cardium Formation looking northward and similarly shows the increase in stratigraphic shortening in the hanging wall of the foreland duplex-culmination towards the northern end of the study area. From this perspective it is easily seen that, in all of the thrust sheets west of the hinterland duplex's leading thrust, the Cardium Formation maintains a constant shortening along strike.

3.10 Correlation of Magnetic Data to Subsurface Structure

High Resolution Aeromagnetic (HRAM) data were acquired across the study area and have been processed to provide images that offer additional confidence in the interpretations from the 2D seismic data. HRAM total magnetic field intensity data (Figure 3-20) show 'highs' and 'lows' that are caused by a

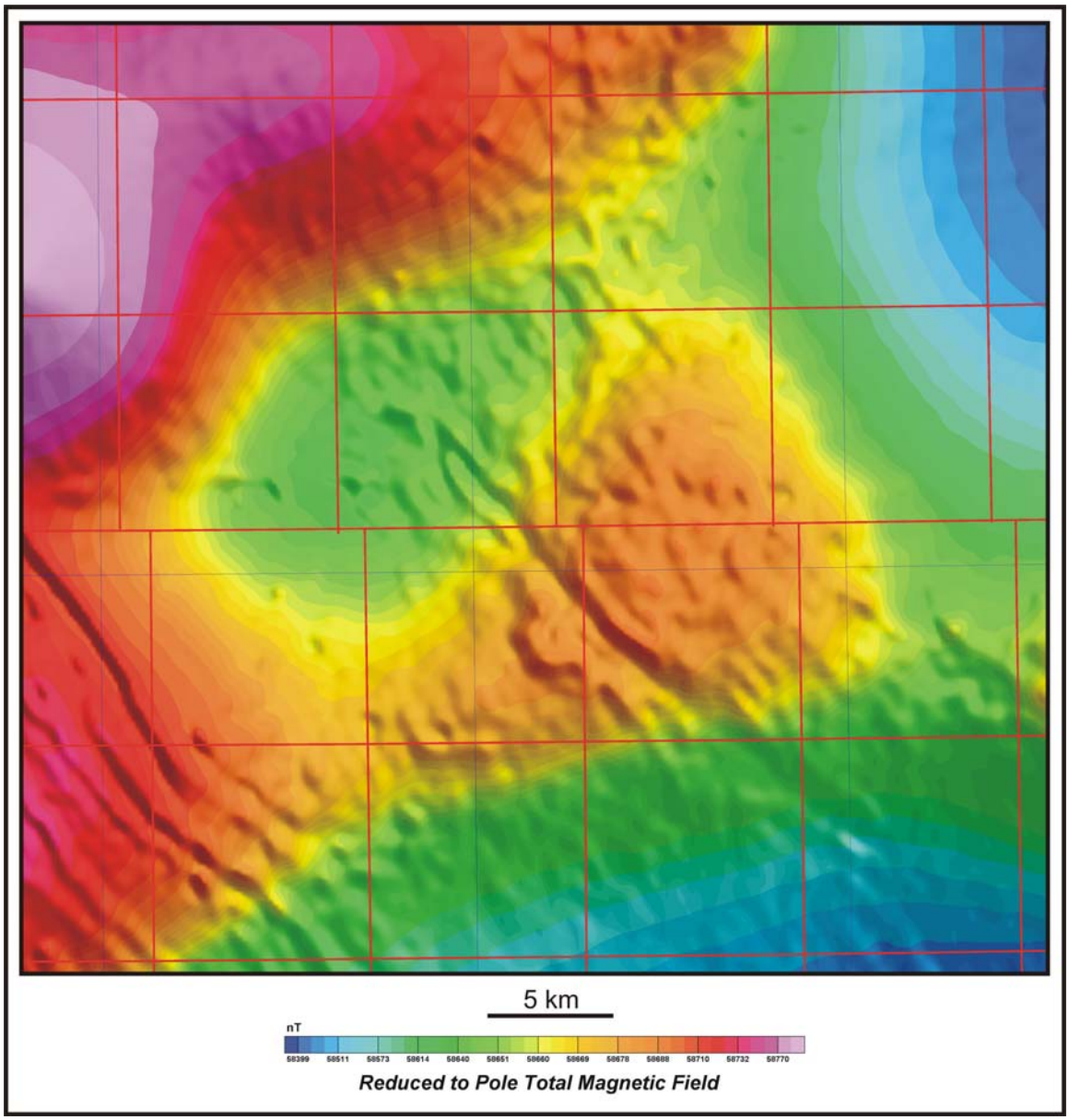

Figure 3-20: Total magnetic field intensity map of the study area.

contrast in the magnetic character of adjacent rocks. Differences in magnetic susceptibility are caused by varying amounts of magnetic minerals in the strata, and these differences can be caused by depositional variations, erosion, structure, or some combination of all three. The most common magnetic minerals that cause a magnetic response include: magnetite, illmenite, siderite and less commonly chromite.

The Horizontal Gradient (HG) map, (Figure 3-21) is calculated from the Total Field magnetic grid with the algorithm:

$$HG = [(\delta F/\delta x)^2 + (\delta F/\delta y)^2]^{1/2}$$

Where:

F = Total magnetic field.

x = East-West direction.

y = North-South direction.

Calculation of the Horizontal Gradient is an ideal tool to provide indications of faults and infer lineaments associated with structures as it enhances the lateral rate of change of the magnetic field in any direction. The power spectrum of the Total Field shows the power of the magnetic signal as a function of wavelength. The magnetic source depth can be related to the slope of the power spectrum (Figure 3-22).

The Horizontal Gradient map (Figure 3-21) was rotated into a perspective map view and combined with the three dip sections (Figures 3-5 to 3-9; A-A', B-

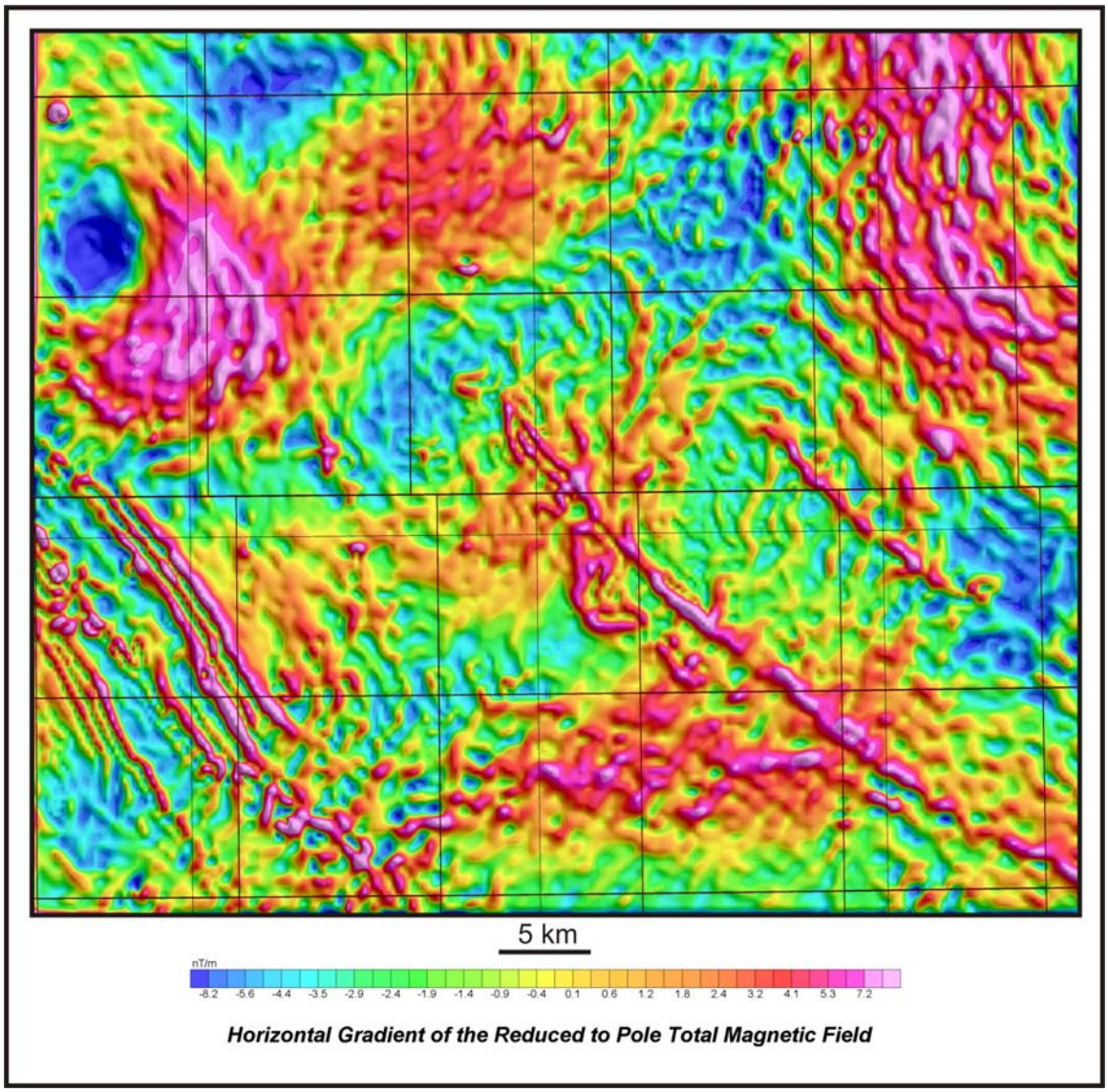

Figure 3-21: Horizontal Gradient map derived from the absolute value of the horizontal derivative calculated from the total magnetic field intensity. Scale in nano Tesla/metre.

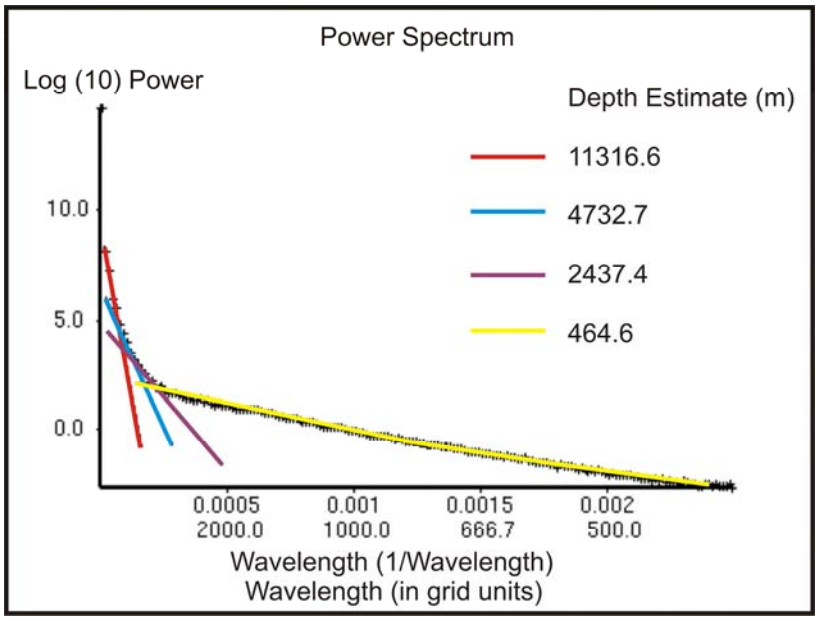

Figure 3-22: Power spectrum showing the power of the magnetic field as a function of wavelength. The magnetic source depth (signal) is related to the slope of the power spectrum in a certain interval.

B’ and C-C’) to yield a composite cross-sectional view of magnetic changes along strike with reference to the seismic sections (Figures 3-23, 3-24 and 3-25). The seismic interpretation matches up quite well with the two distinct Horizontal Gradient maxima, oriented along a northwest-southeast trend. There are two possible explanations for the Horizontal Gradient maxima noted in the magnetic image.

The magnetic anomalies may be caused by the tilted Upper Cretaceous strata overlying the upper detachment. The shallow band pass map (Figure 3-26) appears to corroborate this interpretation perspective. The tilting of the strata can cause a lateral variation in the magnetic signature because of the orientation of the rocks. Abaco (2003) has noted a similar near-surface magnetic anomaly response in Upper Cretaceous rocks of south-central Alberta. Since all of the magnetization (remanent and induced) of these rocks occurred before lithification, the post lithification deformation rotates any remanently magnetized areas into a new orientation. The change in orientation of the remanent magnetization combined with the induced magnetization could create a stronger magnetic signature that is represented by the two magnetic lineaments on the anomaly map.

An alternate explanation for the magnetic anomalies is that they represent small faults along which magnetic-rich solutions traveled and precipitated. These small faults may branch from the upper detachment or be associated with the folded strata lying above the upper detachment, and their near-surface expression is what the horizontal gradient map is displaying.

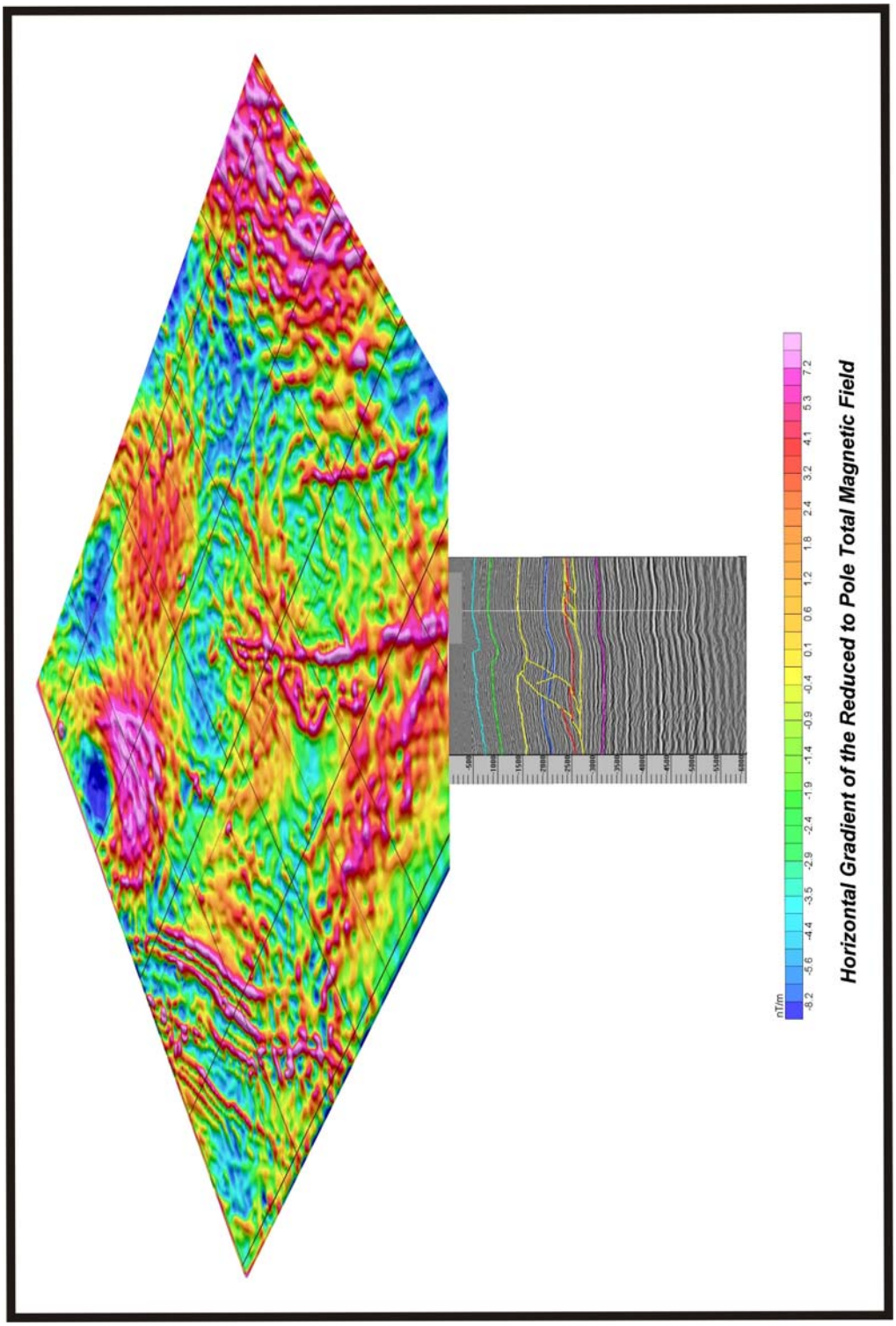

Figure 3-23: Horizontal Gradient magnetic map rotated and aligned with seismic section A-A'. Scale in nano Tesla/metre.

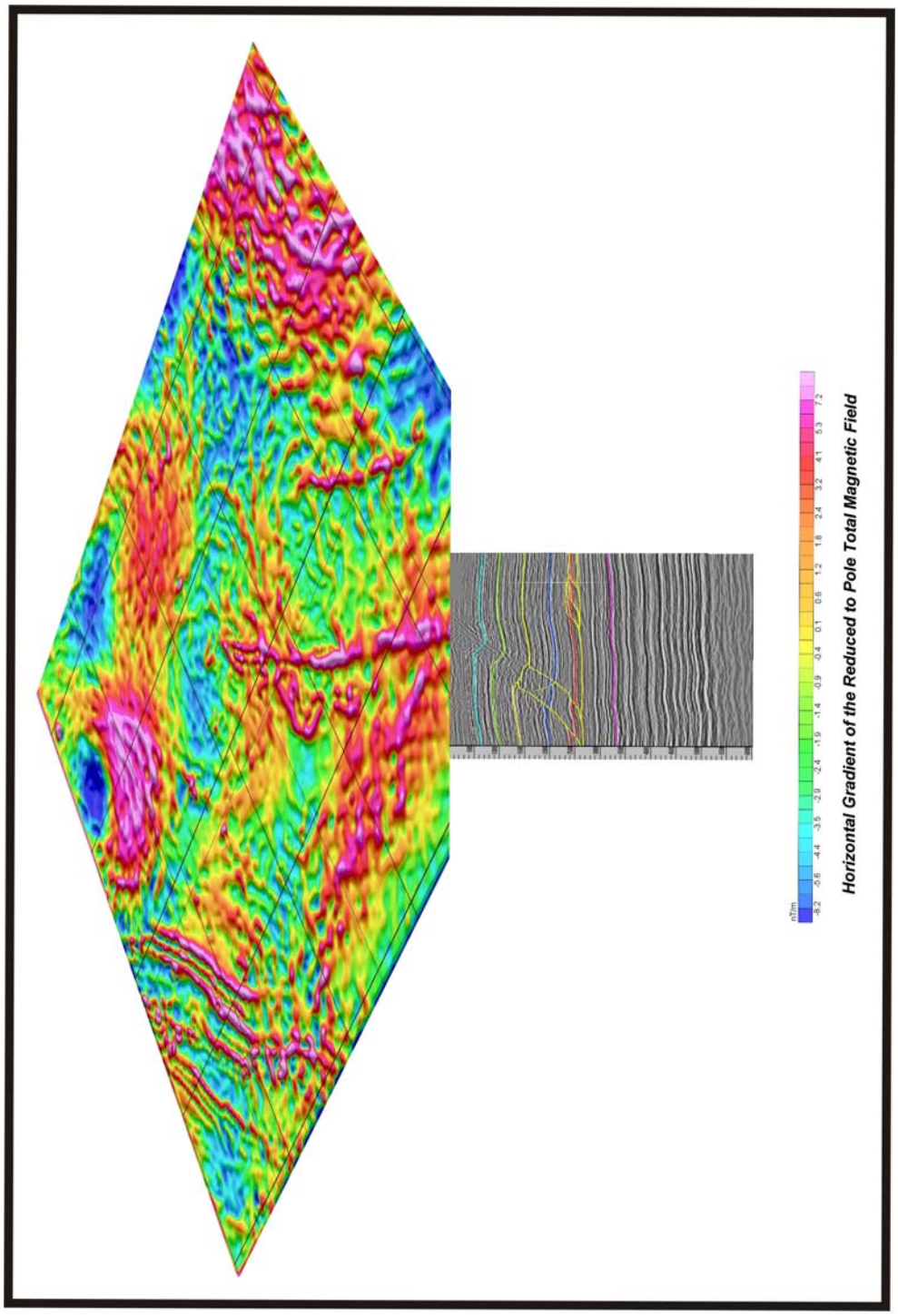

Figure 3-24: Horizontal Gradient magnetic map rotated and aligned with seismic section B-B'. Scale in nano Tesla/metre.

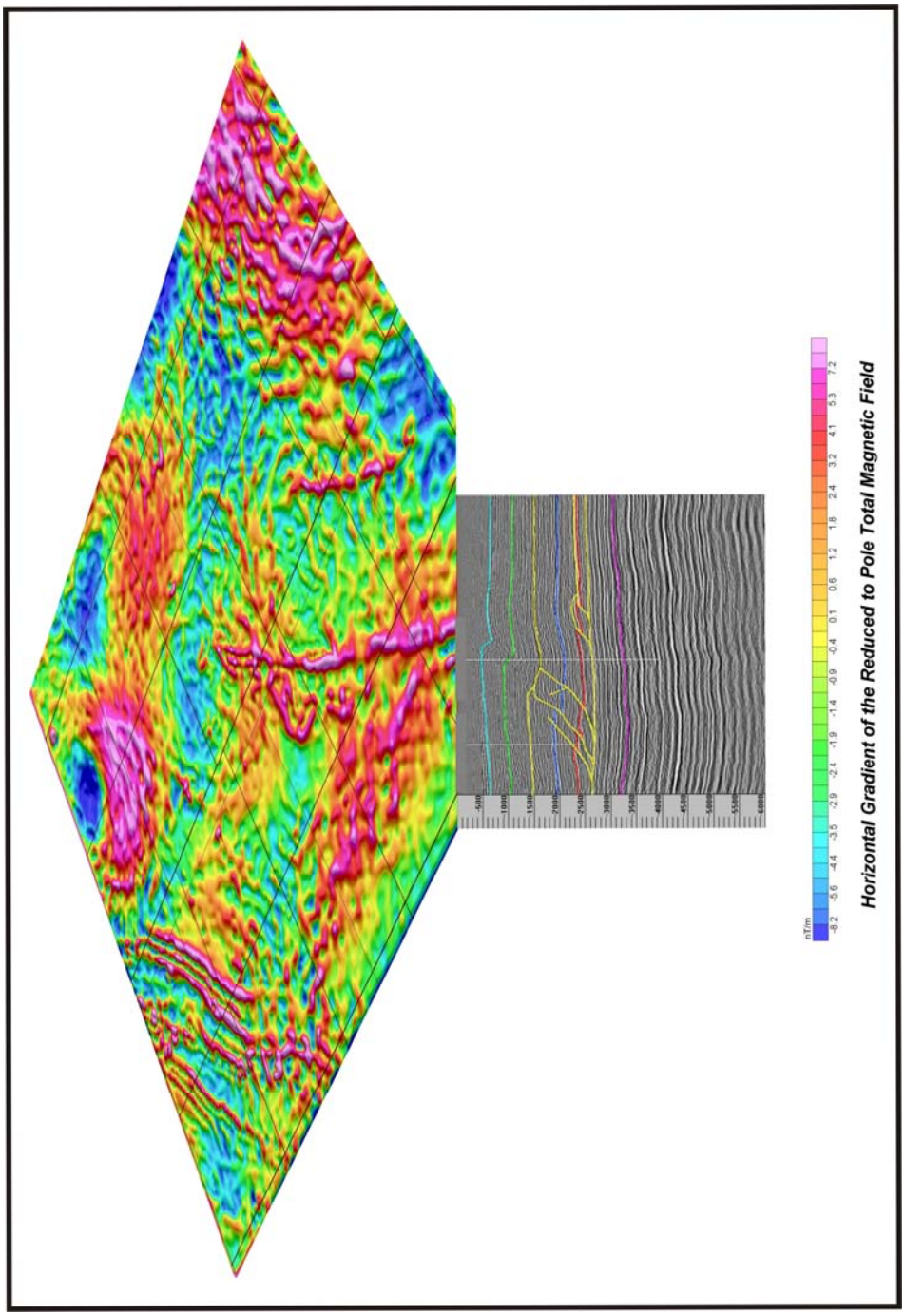

Figure 3-25: Horizontal Gradient magnetic map rotated and aligned with seismic section C-C'. Scale in nano Tesla/metre.

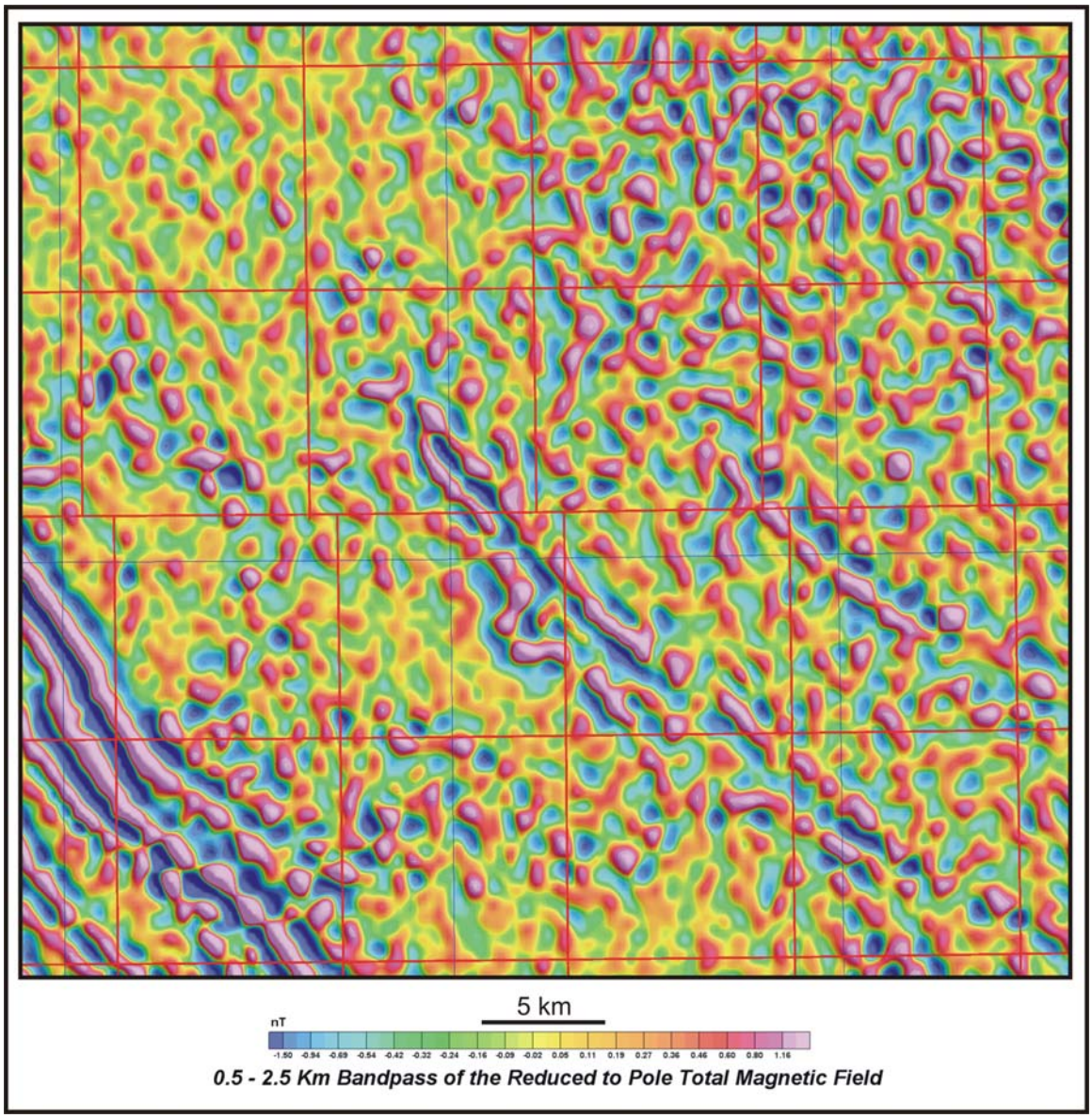

Figure 3-26: Shallow band pass filter of the total magnetic field intensity (500 – 2500m wavelength cut-off).

3.11 Structural Fieldwork

An outcrop study was undertaken in the summer of 2006 to determine if there was any surface expression that could be mapped and correlated to the interpreted seismic or magnetic data. The field work was constrained to the southeastern township from which the seismic data were interpreted. Based on the limited size of the field area, only one day of investigation was required to examine the predetermined areas for potential outcrop. If suitable outcrops could be located, it would offer additional confirmation and correlation for the subsurface interpretations. A combination of aerial photographs, township and range maps and *Google*® *Earth* maps were used to identify the locations to be investigated. The field area has little topographical relief, is densely forested and has limited road access. Due to the combination of these factors, only a limited area could be traversed by foot. In the primary township where the seismic interpretation was made, no outcrops were found.

3.12 Core Correlation to Seismic Interpretation

A principal reason for core investigation in this study, aside from the determination of the depositional environment, was to draw any possible associations between the lithology/lithofacies of the Cardium Formation and the zones of structural deformation. One goal during examination of the cores was to locate any structural disturbances such as slickensides, fault surfaces and mineral coatings as well as fault gouges/breccias and open and filled fractures. If such structures were located it could be possible to associate the lithological

variations within the Cardium Formation on a micro to meso scale to the deformational events.

A total of 17 cores were examined and documented over the regional study area (see Appendix). There is limited core coverage across the study area that intersects the Cardium Formation. Cores containing the Cardium Formation within the thesis study area were examined for significant structural disturbances if a well developed sandstone signature was noted on the electric wireline log and the interval was noted to be more than two meters in length. No cores within the study area were noted to intersect a Cardium Formation repeat.

The limited coverage of the cores drilled, as well as the locations of the cores, has made correlation of the sedimentology to the structural deformation difficult. Only a small sample of structural disruption was noted in the cores examined. In core, slickensided surfaces are commonly noted in shale detachment horizons that directly overlie and underlie the Cardium Formation, while also being observed in thinner, interlaminated shales within the sandstone (Figure 3-27). These slickensided surfaces indicate that movement has taken place, although the direction and magnitude of movement cannot be quantified. As well, a small number of calcite filled, natural fractures have been noted in core (Figure 3-28).

3.13 Interpretations in the Northwest Corner of the Study Area

The northwest corner of the regional study area (Figure 3-2), specifically townships 47-17W5 and 48-17W5, presented a particularly difficult problem

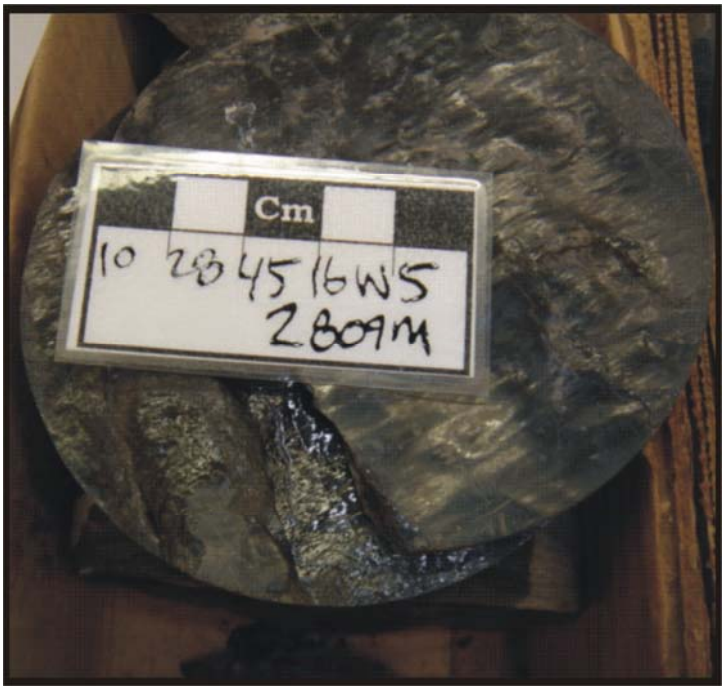

Figure 3-27: Slickensided shales within the Cardium Formation.

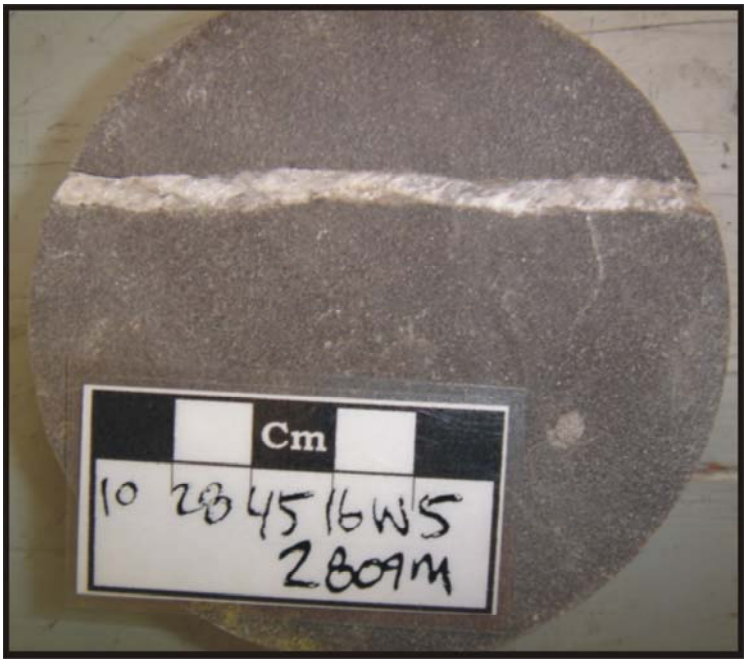

Figure 3-28: Calcite filled fracture in the Cardium Formation sandstone.

during the interpretational phase of the project. The wireline logs that were examined across this area highlighted several locations where partial or complete structural repeats of the Cardium Formation were present (Figure 2-24). The indication of repeats within the Cardium Formation at these locations prompted the starting point for seismic investigation in the region.

Initial ideas regarding the deformational style of the study area, based on examination of the work of Skuce *et al.* (1992) and Skuce (1996), suggested that areas closer to the frontal position of the triangle zone have a higher probability for development of passive-roof duplexes than locations that are more distal. In contrast to this, the seismic data from the study area show the greatest development of passive-roof duplexes in the southeastern corner. Passive-roof duplex structures probably exist in many Foreland positions but may become more difficult to recognize to the west as they become more proximal to the triangle zone.

Figure 3-29 shows a dip-section seismic line close to a well where Cardium Formation repeats were identified. The well with a complete structural repeat was projected into the seismic section and analysed to determine if the wireline data could be linked to the seismic data. Investigation of the seismic data reveals that the structural repeats are almost unresolvable based on the thickness of the repeated stratigraphic section and the seismic image quality.

Typically, the frontal parts of the Foothills were thought to be relatively unstructured. Consequently, some seismic interpreters and processors may have eliminated any sort of small scale structures that would now be interpreted as a

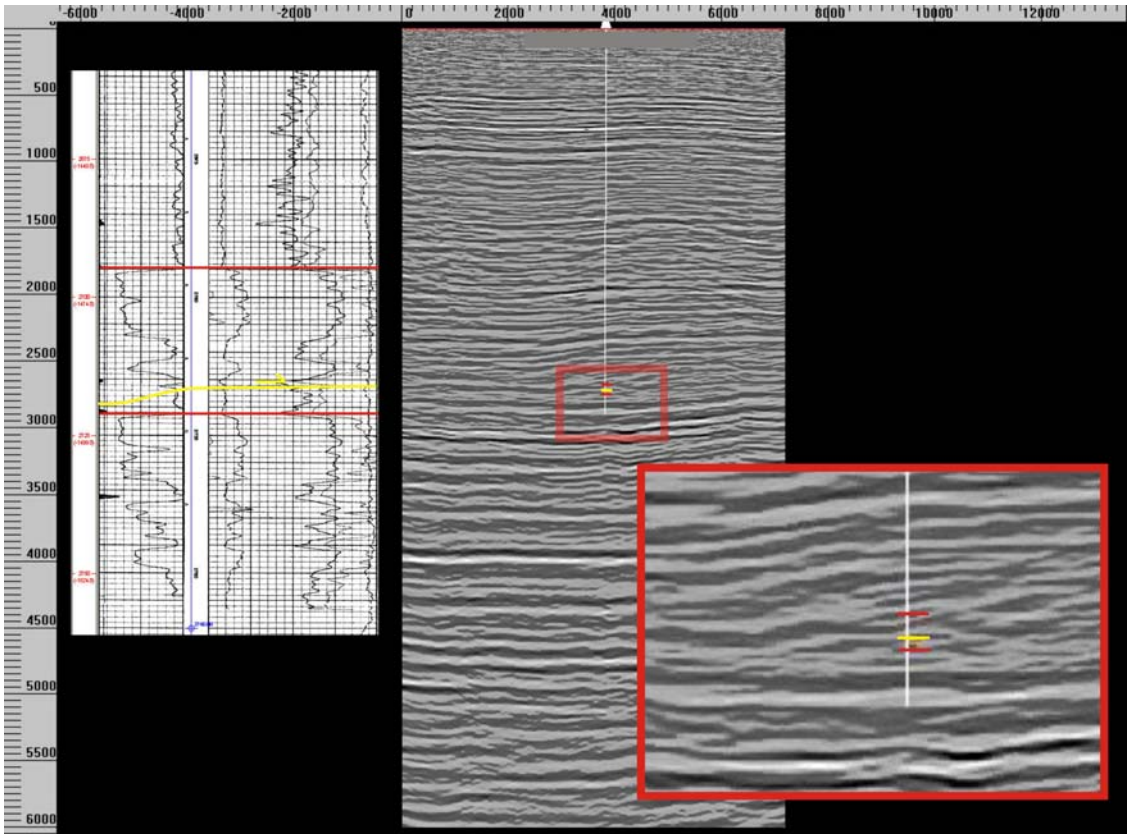

Figure 3-29: Seismic dip section from the northwest corner of the regional study area. Left inset shows the electric log of the Cardium Formation repeated in the well located in the center of the seismic line. Little to no structural deformation is noted in the seismic section. The red outlined box inset on the right shows a magnified view of the bottom of the hole from the main seismic section highlighting the Cardium Formation's repeated signature. Red: Cardium Formation top; Yellow: Fault plane. Scale bar in meters.

passive-roof duplex (W. Rydman, Pers. Comm.).

The seismic data from the southeastern corner of the regional study area show clear evidence of deformation. The interpreted seismic data clearly show the structural repeats of the Cardium Formation, although the wireline data from the wells within this township do not show any partial or complete Cardium Formation repeats. The simple explanation for this is that none of the wells in this township intersect the foreland duplex-complex or hinterland duplex structures (Figures 3-5 to 3-9), which are very localized, and only intersect the Cardium Formation where it is not repeated.

3.14 Along-Strike Variation

Developing the 2D and 3D model utilizing *2DMove*® and *3DMove*® has offered viable and restorable geometries while also showing the variation along strike. Along-strike variation is a common characteristic noted in triangle zone sections of the Foothills (Soule, 1993; Spratt and Lawton, 1996; LeDrew, 1997 and Drover, 2000). The rapidly changing geometries in the triangle zone are commonly attributable to the variation in the involvement of deeper Paleozoic strata during deformation, detachment levels and ramp angles. Only a small percentage of frontal foreland passive-roof duplex structures have been studied, yielding a limited amount of data for comparative purposes on a regional scale.

Most of the structural variation within the study area exists between the upper and lower detachment horizons. There is only slight deformation or contraction in the overlying uppermost Cretaceous and Tertiary rocks. There is

no deformation noted in the autochthonous rocks of the Mesozoic and Paleozoic rocks underlying the lower detachment. All of the deformation in the region is ‘thin-skinned’, having no basement involved in any stage of the deformation. Skuce *et al.* (1992) and Skuce (1996) have noted similar results from areas northwest of the study area.

The primary variation along strike noted in the study area is the loss of displacement within the foreland duplex-culmination structure towards the southern end of the model. In the northern part of the model, the foreland duplex-culmination contains two horses. The leading horse in the foreland duplex-culmination loses displacement near the central part of the study area, leaving only the trailing horse contained within the foreland duplex-culmination at that point. In the southern part of the study area, the trailing fault of the duplex has progressively lost displacement within the foreland duplex-culmination such that the structure is manifested as a blind imbricate that dies out upward between the two primary detachments. Figures 3-30, 3-31 and 3-32 show three multi-cross sectional views in varying orientations to demonstrate the variation in the foreland duplex-culmination structure along strike. The primary cause of loss of displacement along strike to the south in the study area is a lateral ramp.

A lateral ramp is a geological structure defined as a portion of a fault surface where the fault transects bedding in an orientation where bedding cut-off lines are sub-parallel to the fault movement or tectonic transport direction (Deline, 2003). Deline (2003) also states that lateral ramps locally accommodate displacement transfer between neighbouring portions of a thrust sheet at varying

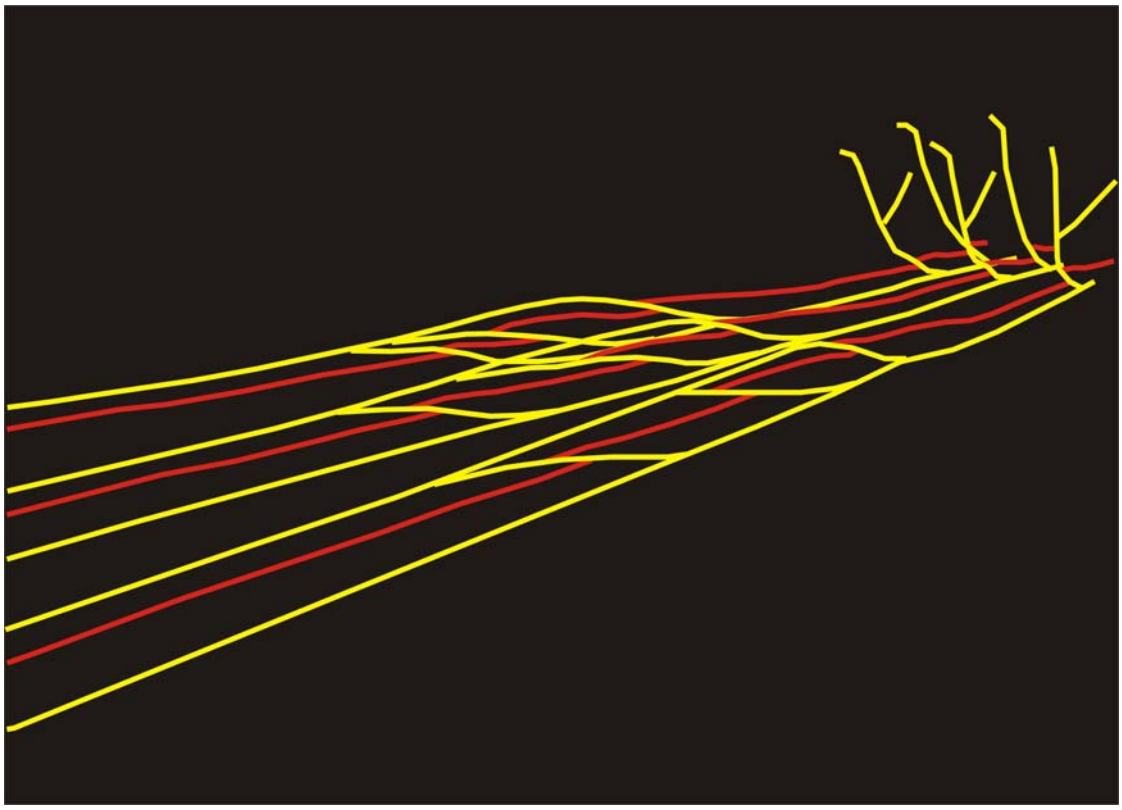

Figure 3-30: Multi-cross sectional view of the 3D block model showing the loss of displacement on the lower detachment of the foreland duplex-culmination toward the south. View to south/southwest. Red: Cardium Formation; Yellow: Faults.

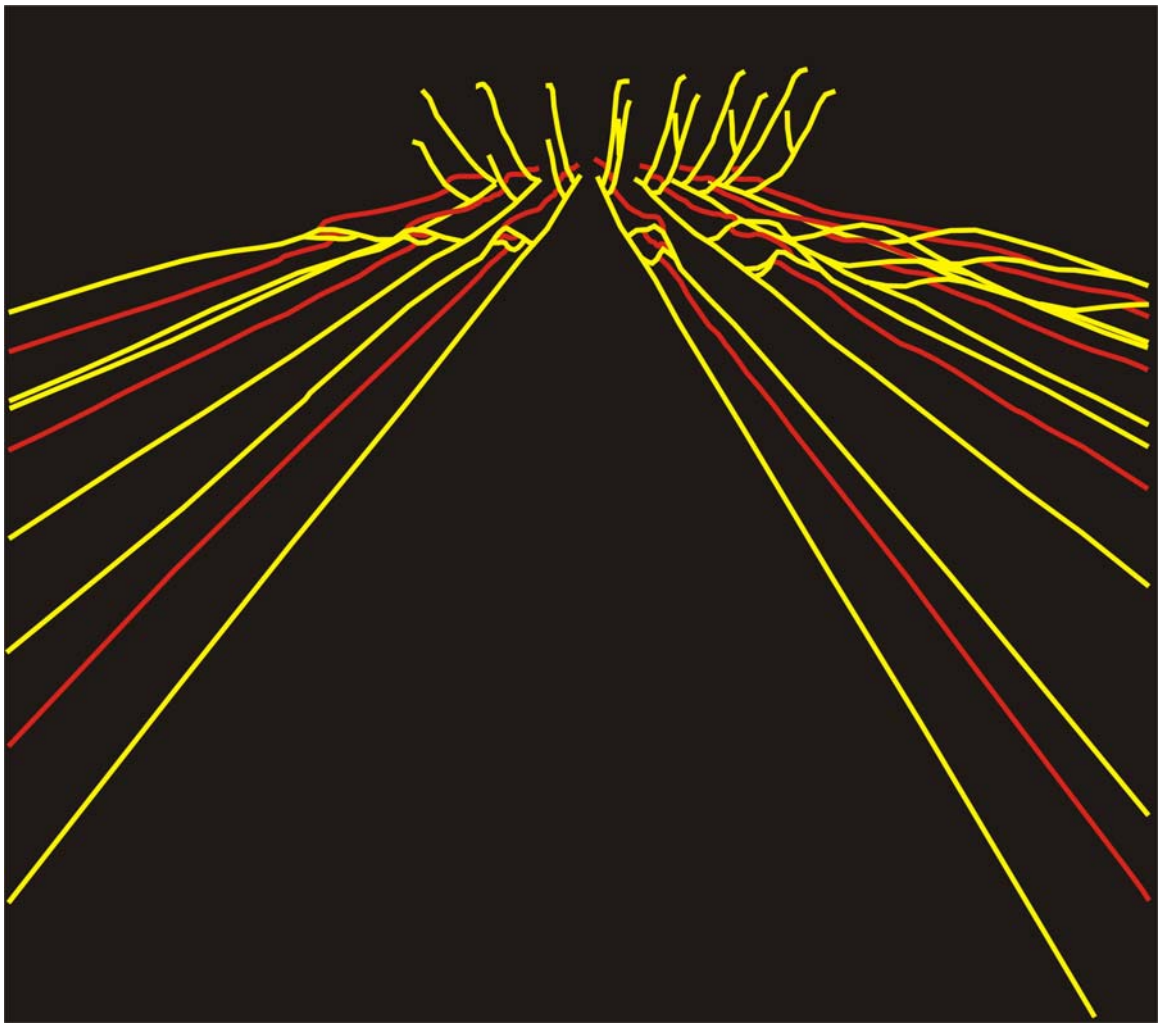

Figure 3-31: Multi-cross sectional view of the 3D block model showing the complete loss of displacement on and disappearance of the lower detachment in the foreland duplex-culmination in the central part of the model. The trailing horse begins to lose displacement from the central part of the model toward the south. View to southwest. Red: Cardium Formation; Yellow: Faults.

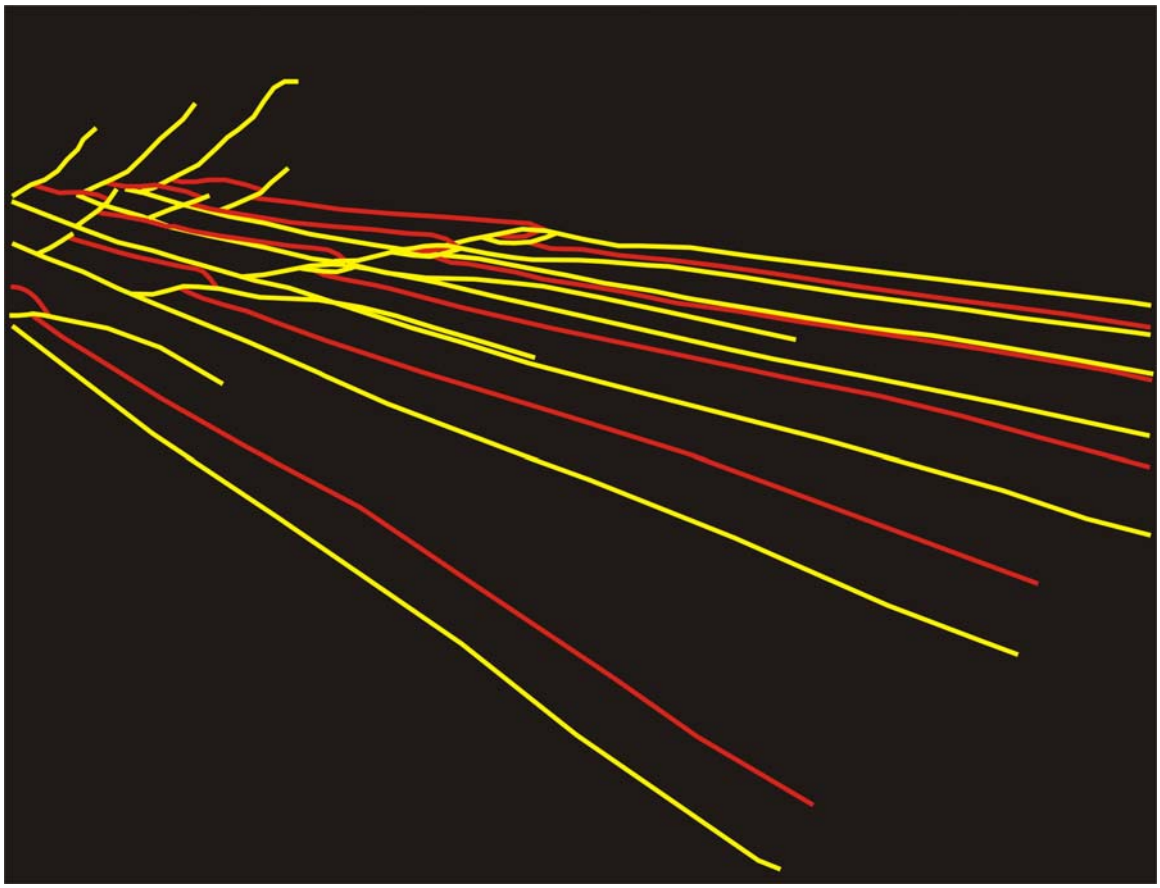

Figure 3-32: Multi-cross sectional view of the 3D block model showing total loss of displacement in the trailing horse of the foreland duplex-culmination at the southern edge. There is no expression of the foreland duplex-culmination structure at the southern edge of the model. A total loss of displacement within the foreland duplex-culmination places the Cardium Formation directly on the Cardium Formation, separated by a blind thrust between the two primary detachments horizons. View to northwest. Red: Cardium Formation; Yellow: Faults.

stratigraphic and/or structural levels. The formation of lateral ramps in the frontal part of the triangle zone in Alberta has been noted to be a partial cause for variation along strike by Soule (1993), Sukaramongkol (1993), and Soule and Spratt (1996). The lateral ramp at the leading edge of the foreland duplex-culmination in the study area is associated with a progressive loss of displacement along strike on the leading thrust. As displacement is lost in the foreland duplex-culmination structure, the Cardium Formation shortening within the individual horses is transferred to the hanging wall of the foreland duplex-culmination. Toward the south of the foreland duplex-culmination, the formation of the lateral ramp structure results in the Cardium Formation only being repeated once, as noted in the 3D plan view of Figure 3-19A.

The hinterland duplex structure shows relatively little variation along strike. The southern edge of the study area lacks significant data for a complete analysis the variation within the structure. The most notable change in the hinterland duplex structure is the loss of displacement in the pop-up structure within the duplex. The pop-up is noted in the three dip lines A-A’ to C-C’ (Figures 3-5 to 3-7) but is absent in the east-west oriented section E-E’ (Figure 3-9). Between section C-C’ and E-E’ there is a total loss of displacement such that the pop-up structure is no longer present at the southern limit of the study area. Shortening west of the hinterland duplex structure is accounted for by the development of an additional imbricate between the two detachment horizons. This fault develops at some point between sections B-B’ and C-C’ and extends through section E-E’.

The parallel detachments in the study area are thought to have formed at the same time along their respective detachment horizons directed towards the foreland. During the structural formation of the hinterland duplex structure, the upper detachment became folded. The formation of the folded structure is caused by the development of an upper “sticking point” at the top of the two thrust sheets that compose the hinterland duplex. A sticking point is a point at which the thrust (or fold) propagation ‘overshoots’ the upper detachment horizon and causes piggybacking of the hangingwall units, such that the upper detachment appears as a folded surface. The sticking point can be caused by slight lithological variation where the two faults meet. The deformation of the upper detachment has caused all of the Upper Cretaceous and Tertiary strata overlying it to become deformed harmonically. The suggestion of a sticking point has also been noted by Skuce (1992) to be the cause for the origin of the duplex structures along the flats of the passive-roof duplex structures far into the Foreland.

3.15 Discussion

The structures in the study area were formed during the final stages of the Laramide Orogeny as the rocks that overlie the upper detachment are passively uplifted by the development of the underlying duplexes. Skuce *et al.* (1992) notes the same result from their sections near Edson, Alberta. The two detachment horizons are likely to have formed at, or near the same time. Skuce *et al.* (1992) and Skuce (1996) suggest that the development of the upper and lower

detachment resulted from over-pressuring of the shales in which they occur. The over-pressuring is thought to have resulted from the rapid burial of the shales with about 3000 m of overburden deposited in a period of approximately 25 m.y.

From the cores examined, no direct correlation could be determined between the lithofacies across the study area and the structural seismic interpretations. The problem is that although deformation-associated events such as slickensides and minor fractures are noted to have limited distribution, they are not abundant enough for quantitative statistical averages to be determined or definitively linked to the lithofacies. Additionally, not enough cores have been drilled in appropriate locations proximal to structurally disturbed areas within the study area for correlations of this type to be drawn. Ideally, attempting to associate the structural deformation to variations in lithology would require a larger study area with a larger number of cores that are closely spaced to properly establish any potential relationships of this kind. Slickensides identified from core in the overlying Cardium Zone Member shale, Wapiabi Formation shale and underlying Blackstone Formation shale suggest that some deformation occurred outside of the Cardium Formation sandstone and confirms the detachment horizons that were identified from seismic interpretation.

The structural shortening in the seismic study area is greatest in the northern and central parts, decreasing toward the south. The decrease in shortening southward is shown by the quantitative results in Table 3-1 and is well supported by the interpretation of the 3D model, showing the disappearance of the foreland duplex-culmination and pop-up structures toward the southern edge

of the study area. The decrease in shortening southward in the study area is primarily associated with the lateral ramp under the foreland duplex-culmination.

The seismic and line image palinspastic restorations remain within 4% of the deformed state measurements. The close range between the deformed and restored states suggests that the interpretations presented are viable and admissible. The upper detachment horizon is slightly crenulated and some slight thickening of stratigraphic units is observed above the restored state hinterland duplex. The thickening is primarily attributed to small blind imbricates that may have developed from the upper detachment horizon but that cannot be resolved in the seismic sections. During restoration the blind thrusts that have not been accounted for cause the stratigraphy above the hinterland duplex to be slightly thicker than is noted in the adjacent parts of the restored section.

The magnetic data have provided secondary verification of the seismic interpretation. The data support the interpretation that the Upper Cretaceous strata above the upper detachment have become folded harmonically and highlight a magnetic contrast based on the changes in the attitude of the bedding. No outcrop exposure was located that could provide an alternative interpretation of the seismic data presented in this study.

3.16 Summary and Exploration Significance

The study area provides insight into the geometry of a frontal Foothills triangle zone blind duplex structure. Parallel detachment thrust faults linked by duplexes continue toward the foreland for a distance of over 50 km from the

surface exposure of the triangle zone. The average thickness between the confining detachment horizons is approximately 1000 m, whereas the foreland duplex-culmination sheet riding on the lower detachment horizon has a thickness of approximately 300 m.

This structural investigation has confirmed that duplexes are present at other points along strike at the frontal part of the triangle zone as Skuce *et al*. (1992) originally suggested. The variation within the structure in the study area differs slightly from other locations in Alberta that have been identified to contain duplexes, much like the changes that are noted along strike within the triangle zone itself.

Hydrocarbons discovered within the Cardium Formation across the regional study area are quite significant. To date, no hydrocarbons have been produced from the Cardium Formation from the area in which the seismic interpretation was made. The chance of trapping and extracting significant reserves is possible if a structural repeat is properly targeted and encountered while drilling. Deline (2003) states that lateral ramps may cause hanging wall structures such as lateral ramp folds and lateral hanging wall monoclines to develop. The development of such structures may provide critical structural closure and can also affect the compartmentalization and/or connectivity of a reservoir. Lateral ramps may also increase the fracture potential of the clastic reservoir due to the stress concentration associated with their formation. The fractures would aid in the creation of permeability within the Deep Basin, making tight rock viable for production. The presence of anticlines or folded strata above

the upper detachment horizon may be useful for identifying the location of a duplex structure beneath it, even if the duplex cannot be resolved well seismically (Skuce *et al*., 1992). These passive anticlinal folds may also be suitable economic targets if reservoir and seal rocks are well positioned and deformed properly. If a passive anticline contains a reservoir quality lithology and is capped by an impermeable lithology such as shale, then a hydrocarbon play may be possible.

The economic implication of this research directly impacts the oil and gas industry. If suitable blind duplex structures are imaged appropriately with seismic methods and targeted along strike, access to Deep Basin tight gas accumulations in a proven clastic reservoir may continue to be achieved.

Chapter Four: Conclusions

4.1 Summary

This study investigated the significance of the structural deformation, stratigraphy and depositional systems of the subsurface Cardium Formation west of the Pembina oilfield. The results of this study have yielded a number of conclusions.

1) Five lithofacies characterize the Cardium Formation within the study and are: F1, *Bioturbated dark shales*; F2, *Bioturbated, thinly interbedded shales and siltstones with very fine sandstone stringers*; F3, *Bioturbated, thinly bedded sandstone and siltstone with minor to common interbedded shale stringers*; F4, *Thickly bedded, very fine to medium grained sandstone*, and F5, *Chert Conglomerates*. These lithofacies represent a slight modification from the lithofacies identified by Krause and Nelson (1984) in the Pembina Field, located directly east of the study area.

2) The Cardium ‘A’ sandstone within the study area represents a coarsening upward sequence deposited in a completely marine setting. The occurrence of low angled inclined stratification, wave ripples, parallel lamination sedimentary structures and the ichnofacies of *Cruziana, Zoophycos* and *Nereites* support that the Cardium Formation was deposited on a marine shelf to shelf edge position,

generally between fair-weather and storm-weather wave-base. This interpretation is based on the observations made in 17 cores examined across the study area.

3) Large flooding events, hyperpycnal riverine flow and high energy storms are the primary processes that would have delivered the sediments to the shoreline. The identification of low angle inclined stratification from core examination in the Cardium ‘A’ sandstones, and its correlation to hummocky cross stratification in outcrop based on previous scientific studies, confirms storm dominated processes were active across the study area. Storms and the associated geostrophic flows were the principal methods by which the sandstones and siltstones were transported to the shelf, which also created the hydrodynamic overprinting.

4) An isopach map of the Cardium ‘A’ sandstone outlines a decreasing trend in thickness of the sandstone from the southwest to northeast across the study area. This trend is consistent with the regional distribution of the Cardium Formation noted in the basin. There is no evidence within the study area that suggests the development of a pre-existing topographical surface by either a slope change or a structural discontinuity where isolated sandstone ‘pods’ could have accumulated. Localised variations in the structural top surface of the Cardium Formation, predominantly focussed at the western side of the study area, are attributed to zones of partial or complete structural repetition, as noted from wireline log investigation.

5) A chert conglomeratic unit (F5) is observed in some cores across the study area and is noted to overlie the sandstones and siltstones of the Cardium Formation unconformably and in some wells. The distribution of the conglomerate is not well established because of the limited core coverage and difficulty interpreting individual lithofacies from wireline logs.

6) Following the deposition of the Cardium ‘A’ sandstone, a contemporaneous progressive rising of sea level occurred with the emplacement of the conglomerate and overlying marine shales. The conglomerate was contained by coastal storage and unable to be effectively transported to deeper water on the shelf. As sea level rose and shifted landward, the conglomerate could escape the littoral energy fence and receive enough wave energy to be emplaced on top of the sandstone sequence. The general unsorted nature of the conglomerate intermixed with mudstones and sandstones, with no apparent stratified bedding structure, supports that the conglomerate was emplaced quite rapidly and chaotically. The overlying marine shales of the Cardium Zone Member represent continued transgression, evidenced by rare bioturbation and rare instances of interbedded very fine siltstone lenses.

7) A link between sedimentary lithofacies analysis and zones of structural deformation (locations of faulting) was investigated in an attempt to establish a relationship between the two. Due to the limited core coverage and distance (> 5.5 km) of cores with respect to interpreted zones of deformation, no positive

correlation could be established that linked specific lithofacies to zones of preferential weakness. However, abundant slickensides were noted in the shale intervals over- and underlying the Cardium ‘A’ sandstone, at approximately the same levels as the detachments identified in the seismic data. Exact horizon correlations between the seismic interpretations (in depth) and the core and well logs were not possible due to the very small interval investigated.

8) The presence of a blind duplex structure is confirmed in the study area determined from the 2D seismic interpretation. The duplex structures are confined between upper and lower detachment horizons in the Bearpaw and Blackstone formation shales respectively.

9) The detachment horizons continue for a distance of over 50 km from the surface exposure of the triangle zone into the Foreland. The vertical distance between the primary detachment horizons averages 1000 m within the seismic study area, and up to 70 m of structural thickening is modelled.

10) The development of two horses in the Foreland Duplex Complex (FDC) carried on the lower detachment is noted to lose displacement from north to south in the 3D model. The complete loss of displacement within the structure is attributed to a lateral ramp under the Foreland Duplex Complex such that the duplex is no longer present at the southern edge of the 3D interpretation area.

11) By identifying passive anticlines or folded strata above an upper detachment surface, one may be able to locate passive-roof duplex structures even if they are not well resolved seismically.

12) The blind duplex structure identified in this study varies from similar structures identified in other studies, particularly Skuce *et al.* (1992) and Skuce (1996). There are two horses contained within the duplex in this study area, whereas Skuce *et al.* (1992) and Skuce (1996) show variations of up to three horses per duplex and multiple duplexes existing above a single detachment horizon. This confirms that just as the exposed triangle zone varies in geometry along strike, so does the blind frontal continuation of the structure.

4.2 Exploration Significance and Economic Implications

This study details the geometry of the Cardium ‘A’ sandstone and how frontal Foothills deformation can place the formation in an ideal configuration for potential hydrocarbon trapping. Although no hydrocarbons have been discovered to date within the Cardium Formation in the area where the 3D model exists, a large potential for future discoveries remains. Because of previous issues, such as over-processing of seismic data, blind duplex structures have been commonly overlooked as potentially economic hydrocarbon traps. With increased imaging potential in seismic processing methods, blind duplex structures should be resolvable in many places in front of the triangle zone along strike. The development of lateral ramp structures may control structural closure along strike

and compartmentalisation of a targeted reservoir. Additionally, lateral ramps and associated thrust faulting may increase fracture intensity in any given reservoir and provide the necessary permeability required for viable production. Secondary economic objectives of passive anticlines above passive-roof duplex structures may be targeted as potentially promising conventional stratigraphic or low amplitude structural traps.

Within the study area, in the zones where the Cardium Formation is faulted and repeated, structural thickening may be up to 70 m. This presents significant opportunities for increasing the formational thickness and number of zones that may hold production potential. Ideal zones to target for production are where the Cardium Formation is structurally repeated. This zone of structural thickening would increase the potential pay zone and additionally may have fracture development associated with the faulting, which would enhance the permeability of this tight Deep Basin reservoir. Development of fracture permeability is a critical component in the economic feasibility of drilling Deep Basin targets. All of the wells drilled in the study area that penetrate the Cardium Formation missed the localised repeated structures interpreted within the duplex from the seismic data analysis.

The discovery and recognition of blind duplex structures carrying the Cardium Formation opens the door for economic avenues of exploration in a basin where it is becoming increasingly more difficult to find significant hydrocarbon reserves.

4.3 Recommendations for Future Work

Although a positive link between the stratigraphy and structural deformation in this study area could not be ascertained, a relationship may be present. Establishing a positive correlation between the two may involve developing a larger, regional 3D structural model and attempting to use more cores to tie to the model where deformation has been identified. Because of the limited amount of core coverage in the regional study area, development of a 3D model may be ideally suited to a location along strike where a more abundant supply of core exists in the appropriate stratigraphic intervals. Additionally, the use of 3D seismic data versus 2D data would be beneficial to negate any potential affects such as ‘side-swipe’ that may cause a misinterpretation of structure and relative positioning with respect to core locations. With further investigation into the variations that exist along strike of such structures and associations linking zones of deformation to lithofacies types, precise models can be generated to predict zones of further academic study and potential economic interest.

REFERENCES

Abaco, C. 2003. Integrated Magnetic and Seismic Geophysical Study in the South-Central Alberta Foothills. M.Sc. Thesis, The University of Calgary, 238 p.

Arnott, R.W.C., 2003. The role of fluid- and sediment-gravity flow processes during deposition of deltaic conglomerates (Cardium Formation, Upper Cretaceous), west-central Alberta. *In:* T.F. Moslow, and J.P. Zonneveld, eds., Marine conglomerate reservoirs; Cretaceous of Western Canada and modern analogues; Part 1.

Beach, F.K., 1955. Cardium, a turbidity current deposit. Journal of the Alberta Society of Petroleum Geologists, v. 3, p. 123-125.

Bergman, K. and R.G. Walker, 1987. The importance of sea level fluctuations in the formation of linear conglomerate bodies, Carrot Creek Member, Cardium Fm., Alberta. Journal of Sedimentary Petrology, v. 57, p. 651-665.

Berven, R.J. 1966. Cardium sandstone bodies, Crossfield-Garrington area, Alberta. Bulletin of Canadian Petroleum Geology, v. 14, p. 208-240.

Carey, J.S., C. Reed, A. Niedoroda, D.J.P. Swift and M.S. Steckler, 2003. Modeling event-bed successions and long-term sediment flux on a storm-dominated continental shelf, Northern California margin. Congress of the International Union for Quaternary Research. v. 16, p.159.

Cleary, W.J., C.D. Johnsen, M.K. Johnston and M. Sault, 1999. Storm impacts and shoreline recovery in SE NC; role of the geologic framework. In: Coastal sediments '99, N.C. Kraus and W.G. McDougal, Eds., Coastal Sediments: Proceedings of the 4th International Symposium on Coastal Engineering and Science of Coastal Sediment Processes, v. 4, p. 1798-1813.

Charlesworth, H.A.K., and L.G. Gagnon, 1985, Intercutaneous wedges, the triangle zone and structural thickening of the Mynheer Coal seam at Coal Valley in the Rocky Mountain foothills of central Alberta: Bulletin of Canadian Petroleum Geology, v. 33, p. 22-30.

Crimes, T.P., 1975. The stratigraphical significance of trace fossils. *In:* R.W. Frey, Ed., The study of trace fossils; a synthesis of principles, problems, and procedures in ichnology. New York, N.Y., United States, Springer-Verlag, p. 109-130.

Dahlstrom, C.D.A., 1969, Balanced cross sections: Canadian Journal of Earth Sciences, v. 6, p. 743-757.

Deline, D.W. 2003. Investigation of a Sub-Surface Lateral Ramp in the Southern Canadian Rocky Mountains (Crowsnest Pass Area, S.W. Alberta) Using 3-D Seismic Interpretation and Physical Analog Modelling. M.Sc. Thesis, Queens University, 189 p.

DeWeil, J.E.F., 1956. Viking and Cardium not turbidity current deposits. Journal of the Alberta Society of Petroleum Geologists, v. 4, p. 173-174.

Deutsch, K.B. and F.F. Krause, 1991. A comparison between sand- and mud-dominated shelf to shoreline sequences deposited in the Cretaceous Western Interior Seaway: Examples from the Cardium Formation, Kakwa region, west-central Alberta. Bulletin of Canadian Petroleum Geology, Technical Program Abstracts, v. 39, p. 210.

Drake, D.E., R.L. Kolpack and J. Fischer, 1972. Sediment transport on the Santa Barbera-Oxnard Shelf, Santa Barbera Channel, California. *In*: Shelf Sediment Transport: process and pattern. D.J.P. Swift, D.B. Duane and O.H. Pilkey, Eds., Dowden, Hutchinson and Ross, Inc. p. 307-331.

Drover, D.H. 2000, Regional and Detailed Structural Geology of the Quirk Creek Structure, S.W. Alberta. M.Sc. Thesis, The University of Calgary, 103 p.

Dumas, S. and R.W.C. Arnott, 2006. Origin of hummocky and swaley cross-stratification; the controlling influence of unidirectional current strength and aggradation rate. Geology, v. 34, p.1073-1076.

Ekdale, A.A., R.G. Bromley and S.G. Pemberton, 1984. Ichnology; the use of trace fossils in sedimentology and stratigraphy. SEPM Short Course, Society of Sedimentary Geology, v. 15, p. 315.

Frey, R.W., and S.G. Pemberton, 1985. Biogenic structures in outcrops and cores; I, Approaches to ichnology. Bulletin of Canadian Petroleum Geology, v. 33, no. 1, p. 72-115.

Gabrielse, H., J.W.H. Monger, J.O. Wheeler, and C.J. Yorath, 1991, Tectonic framework, Chapter 2. *In*: Gabrielse, H. & Yorath, C. J. Ed. Geology of the Cordilleran orogen in Canada. Geological Survey of Canada, Geology of Canada 4, p. 13-59.

Gani, M.R., J.P. Bhattacharya and J.A. MacEachern, 2004. Using ichnology to determine relative influence of waves, storms, tides, and rivers in deltaic deposits; examples from Cretaceous delta complexes in the Western

Interior Seaway, Wyoming-Utah, U.S.A. Annual Meeting Expanded Abstracts - American Association of Petroleum Geologists, v. 13, p. 49-50.

Gibbs, R.J. 1976. Amazon River sediment transport in the Atlantic Ocean. Geology, v. 4, p. 45-48.

Griffith, L.A., 1981. Depositional environment and conglomerate diagenesis of the Cardium Formation, Ferrier Field, Alberta. M.Sc. Thesis, The University of Calgary, Calgary, Alberta, 132 p.

Hall, R.L., F.F. Krause, S.D. Joiner, K.B. Deutsch. 1994. Biostratigraphic evaluation of a sequence stratigraphic bounding surface: The Cardinal/Leyland unconformity ("E5/T5 surface") in the Cardium Formation (Upper Cretaceous; upper Turonian-lower Coniacian) at Seebe, Alberta. Bulletin of Canadian Petroleum Geology. v. 42, n. 3, p. 296-311.

Hart, B.S. and G.A. Plint, 1989. Gravelly shoreface deposits: a comparison of modern and ancient facies sequences. Sedimentology, v. 36, p. 551-557.

Hart, B.S. and G.A. Plint, 1993. Tectonic influence on deposition and erosion in a ramp setting; Upper Cretaceous Cardium Formation, Alberta foreland basin. American Association of Petroleum Geology Bulletin, v. 77, n. 12, p. 2092-2107.

Hayes, M.O., 1967. Hurricanes as geological agents: case studies of Hurricanes Carla, 1961 and Cindy, 1963. Report on Investigations No. 61, Bureau of Economic Geology, University of Texas.

Howard, J.D. and H.E. Reineck, 1981. Depositional facies of high-energy beach to offshore sequence: Comparison with low-energy sequence. American Association of Petroleum Geologists Bulletin, v. 65, p. 07-830.

http://www.stratigraphy.org/cheu.pdf [accessed August 25, 2007].

Ingram, R.L., 1954. Terminology for the thickness of stratification and parting units in sedimentary rocks. Geological Society of America Bulletin, v. 65. p. 937-938.

Joiner, S.D., 1991. Stratigraphic architecture of a parasequence set and the genetic implications for the Cardium Fm. at Pembina. M.Sc. Thesis, The University of Calgary, Calgary, Canada, 384 p.

Johnson, H.D. and C.T. Baldwin, 1996. Shallow Clastic Seas. *In*: Sedimentary Environments: Processes, Facies and Stratigraphy. Chapter 7. H.G. Reading, Ed., Blackwell Scientific, Oxford, p. 232-280.

Jones, P.B., 1982, Oil and gas beneath east-dipping underthrust faults in the Alberta Foothills, Canada, *In*: Geologic Studies in the Cordilleran Thrust Belt: Volume 1. R. B. Powers, Ed. Rocky Mountain Association of Geologists, Denver, p. 61-74.

Jones, P.B., 1987. Quantitative Geometry of thrust and fold belt structures. Methods in Exploration Series No. 6 American Association of Petroleum Geologists, 26 p.

Kane, S.J., G.D. Williams, T.S. Buddin, S.S. Egan, D. Hodgetts, and Anonymous, 1997, Flexural-slip based restoration in 3-D; a new approach, Annual Meeting Abstracts - American Association of Petroleum Geologists and Society of Economic Paleontologists and Mineralogists, v. 6, p. 58.

Keith, D.A.W., 1985. Sedimentology of the Cardium Formation (Upper Cretaceous), Willesden Green Field, Alberta. M.Sc. Thesis, McMaster University, Hamilton, Canada, 241 p.

Keith, D.A.W. 1991. Sedimentology and geometry of the Cardium (Turonian) sandstone and conglomerate at Willesden Green Field, Alberta: Offshore sand body or incised prograding strand plain deposit? *In*: Shelf Sand and Sandstone Bodies: Geometry, Facies and Sequence Stratigraphy. D.J.P. Swift, G.F. Oertel, R.W. Tillman, and J.A. Thorne, Ed. International Association of Sedimentologists, Special Publication 14, p. 457-486.

Krause, F.F. 1982. Geology of the Pembina Cardium Pool. *In*: Depositional Environments and Reservoir Facies in Some Western Canadian Oil and Gas Fields. J.C. Hopkins, Ed., University of Calgary Core Conference, Department of Geology and Geophysics, p. 15-27.

Krause, F.F. 1983. Sedimentology of a tempestite: episodic deposition in the Cardium Formation in the Pembina oilfield area, west central Alberta, Canada. *In*: Sedimentology of selected Mesozoic clastic sequences. J.R. McLean, and G.E. Reinson, eds., Canadian Society of Petroleum Geologists, Special Publication 5 - 12, 140 p.

Krause, F.F., H.N. Collins, D.A. Nelson, S.D. Machemer, and P.R. French, 1987. Multiscale anatomy of a reservoir; geological characterization of Pembina-Cardium Pool, west-central Alberta, Canada: AAPG Bulletin, v. 71, p. 1233-1260.

Krause, F.F., H.N. Collins, P.R. French and J.D. Warner. 1987a. Bibliography of geological and engineering studies of the Cardium Formation and its hydrocarbon reservoirs. Petroleum Recovery Institute, Report 1987-3, 61 p.

Krause, F.F., N.N. Collins, D.A. Nelson, S.D. Machemer, and P.R. French. 1987b. Multiscale anatomy of a reservoir: Geological characterization of Pembina-Cardium pool, west-central Alberta, Canada. American Association of Petroleum Geologists Bulletin, v. 71, p. 1233-1260.

Krause, F.F., K.B. Deutsch, S.D. Joiner, J.E. Barclay, R.L. Hall, and L.V. Hills, 1994. Cretaceous Cardium Formation of the Western Canada Sedimentary Basin. Geological Atlas of the Western Canada Sedimentary Basin, *In: G.*D. Mossop, and I. Shetsen, Ed. p. 374-385.

Krause, F.F. and D.A. Nelson, 1984. Storm event sedimentation: Lithofacies association in the Cardium Formation, Pembina area, west-central Alberta, Canada. *In*: The Mesozoic of Middle North America. D.F. Stott and D.J. Glass, Ed. Canadian Society of Petroleum Geologists, Memoir 9, p. 485-511.

Krause, F.F. and D.A. Nelson, 1991. Evolution of an Upper Cretaceous (Turonian) shelf sandstone ridge: Analysis of the Crossfield - Cardium pool, Alberta, Canada. *In*: Shelf Sand and Sandstone Bodies: Geometry, Facies and Sequence Stratigraphy. D.J.P. Swift, G.F. Oertel, R.W. Tillman, and J.A. Thorne, Ed. International Association of Sedimentologists, Special Publication 14, p. 427-456.

LeDrew, J. 1997. Three-dimensional Geometry and Evolution of the Lovett River Triangle Zone, central Alberta Foothills. M.Sc. Thesis, The University of Calgary, 113 p.

Leggitt, S.M., R.G. Walker, and C.H. Eyles, 1990. Control of reservoir geometry and stratigraphic trapping by erosion surface E5 in the Pembina-Carrot Creek area, Upper Cretaceous Cardium Formation, Alberta, Canada. AAPG Bulletin, v. 74, p. 1165-1182.

Marshak, S. and G. Mitra, 1988. Basic Methods in Structural Geology, Part I Elementary Techniques. Prentice-Hall Inc., Englewood Cliffs, N.J., 446 p.

McCave, I.N., 1984. Erosion, transport and deposition of fine-grained marine sediments. *In*: Fine-grained sediments; deep-water processes and facies. D.A.V. Stow, D.J.W. Piper, Eds., Geological Society Special Publications, v. 15, p. 35-69.

Michaelis, E.R., 1957. Cardium sedimentation in the Pembina River area. Journal of the Alberta Society of Petroleum Geologists, v. 5, p. 73-77.

Michaelis, E.R. and G. Dixon, 1969. Interpretation of depositional processes from sedimentary structures in the Cardium sand. Bulletin of Canadian Petroleum Geology, v. 17, p. 410-443.

Midland Valley Ltd. 2005. User Manual: Unpublished reference help manual for © 2DMove.

Morton, R.A. 1981. Formation of storm deposits by wind-forced currents in the Gulf of Mexico and the North Sea. *In*: Holocene Marine Sedimentation in the North Sea Basin. S.D. Nio, R.T.E. Shutterhum and Tj.C.E. van Weering, Ed. University Press, Cambridge, p. 385-396.

Mossop, G.D. and Shetsen, L. 1994. Geological atlas of the Western Canada Sedimentary Basin; Canadian Society of Petroleum Geologists and Alberta Research Council, Calgary, Alberta, URL <http://www.ags.gov.ab.ca/publications/ATLAS_WWW/ATLAS.shtml>, [accessed August 20, 2007].

Nielsen, A.R., 1957. Cardium stratigraphy of the Pembina field [summary]. Journal of the Alberta Society of Petroleum Geologists, v. 5, p. 64-72.

Off, T. 1963. Rhythmic linear sand bodies caused by tidal currents. American Association of Petroleum Geologists Bulletin, v. 47, p. 324-341.

Parsons, H.E., 1955a. Pembina's now Canada's second biggest producer. Reserves are largest. Oil and Gas Journal, v. 54, no.15, p. 120-125.

Parsons, H. E., 1955b. Pembina -- Local geology. Canadian Oil and gas Industries, v. 8, p. 57-63.

Pemberton, S.G. and R.W. Frey, 1984. Ichnology of storm-influenced shallow marine sequence: Cardium Formation (Upper Cretaceous) at Seebe, Alberta. *In*: The Mesozoic of Middle North America. D.F. Stott and D.J. Glass, eds., Canadian Society of Petroleum Geologists, Memoir 9, p. 281-304.

Plint, G.A., 1988. Sharp-based shoreface sequences and "offshore bars" in the Cardium Formation of Alberta; their relationship to relative changes in sea level. *In*: Sea-level changes; an integrated approach. C.K. Wilgus, B.S. Hastings, C.A. Ross, H. Posamentier, J. Van Wagoner, C.G. Kendall, Eds., Society of Economic Paleontologists and Mineralogists, Special Publication, v. 42, p. 357-370.

Plint, A.G., R.G. Walker, and K.M. Bergman, 1986. Cardium Formation 6. Stratigraphic framework of the Cardium in subsurface. Bulletin of Canadian Petroleum Geology, v. 34, p. 213-225.

Plint, A.G. and R.G. Walker, 1987. Cardium Formation 8: Facies and environments of the Cardium shoreline and coastal plain in the Kakwa Field and adjacent areas, northwestern Alberta. Bulletin of Canadian Petroleum Geology, v. 35, p. 48-64.

Seilacher, A., 1967. Bathymetry of trace fossils. Marine Geology, v. 5, p. 413-429.

Skuce, A.G., 1996, Frontal foothills structures in central Alberta; the thin end of the intercutaneous wedge?: Bulletin of Canadian Petroleum Geology, v. 44, p. 153-164.

Skuce, A.G., N.P. Goody, and J. Maloney, 1992, Passive-roof duplexes under the Rocky Mountain foreland basin, Alberta: AAPG Bulletin, v. 76, p. 67-80.

Soule, G.S. 1993. The Triangle Zone and Foothills structures in the Grease Creek syncline area, Alberta. M.Sc. Thesis, The University of Calgary, 88 p.

Soule, G.S., and D.A. Spratt, 1996, En échelon geometry and two-dimensional model of the triangle zone, Grease Creek Syncline area, Alberta: Bulletin of Canadian Petroleum Geology, v. 44, p. 244-257.

Spratt, D.A., and D.C. Lawton, 1996, Variations in detachment levels, ramp angles and wedge geometries along the Alberta thrust front: Bulletin of Canadian Petroleum Geology, v. 44, p. 313-323.

Stelck, C.R. 1955. Cardium Formation of the foothills of northeast British Columbia. Canadian Institute of Mining and Metallurgy Bulletin, v. 48, p. 266-273.

Stott, D.F., 1963. The Cretaceous Alberta Group and equivalent rocks, Rocky Mountain Foothills, Alberta. Geological Survey of Canada, Memoir 317, 306 p.

Sukaramongkol, C. 1993. Seismic imaging of a non-emergent thrust front in the fallen Timber Creek area, southern Alberta Foothills. M.Sc. Thesis, The University of Calgary, 140 p.

Suppe, J., 1983, Geometry and kinematics of fault-bend folding: American Journal of Science, v. 283, p. 684-721.

Swagor, N.S., 1975. The Cardium conglomerate at Carrot Creek Field, central Alberta. M.Sc. Thesis, The University of Calgary, Calgary, Alberta, 151 p.

Swagor, N.S., T.A. Oliver, and B.A. Johnson, 1976. Carrot Creek Field, central Alberta. *In*: Sedimentology of Selected Clastic Oil and Gas Reservoirs in Alberta. M.M. Lerand, Ed., Canadian Society of Petroleum Geologists, 4th Core Conference, p. 78-95.

Swift, D.J.P., A.G. Figueiredo, Jr., G.L. Freeland, and G.F. Oertel, 1983. Hummocky cross-stratification and megaripples; a geological double standard? Journal of Sedimentary Petrology, v. 53, p. 1295-1317.

Swift, D.J.P. and J.A. Thorne, 1991. Sedimentation on continental margins; I, A general model for shelf sedimentation. *In*: Shelf sand and sandstone bodies; geometry, facies and sequence stratigraphy. D.J.P. Swift, G.F. Oertel, R.W. Tillman, and J.A. Thorne, Ed. International Association of Sedimentologists, Special Publication 14, p. 3-31.

Vosselar, S. and S.G. Pemberton, 1989. Skolithos in the Upper Cretaceous Cardium Formation: an ichnofossil example of opportunistic ecology. Lethania, v. 21, p. 351-362.

Walker, R.G. 1983a. Cardium Formation 1. "Cardium a turbidity current deposit" (Beach, 1955): A brief history of ideas. Bulletin of Canadian Petroleum Geology, v. 31, p. 205-212.

Walker, R.G. 1983b. Cardium Formation 2. Sand-body geometry and stratigraphy in the Garrington-Caroline-Ricinus area, Alberta - the "ragged blanket" model. Bulletin of Canadian Petroleum Geology, v. 31, p. 14-26.

Walker, R.G. 1983c. Cardium Formation 3. Sedimentology and stratigraphy in the Garrington-Caroline area, Alberta. Bulletin of Canadian Petroleum Geology, v. 31, p. 213-230.

Walker, R.G. and C.H. Eyles, 1988. Geometry and facies of stacked shallow-sandier upward sequences dissected by erosion surface, Cardium Formation, Willesden Green, Alberta. American Association of Petroleum Geologists, v. 72, p. 1469-1494.

Williams, G.D. and C.R. Stelck, 1975. Speculations on the Cretaceous paleogeography of North America. *In*: The Cretaceous System in the Western Interior of North America. W.G.E. Caldwell, Ed. Geological Association of Canada, Special Paper 13, p. 1-20.

Woodward, N. B., Boyer, S. E. and Suppe, S. 1989. Balanced Geological Cross-Sections: An Essential Technique in Geological Research and Exploration. American Geophysical Union, Short Course in Geology, Volume 6, 132 p.

Wright, M.E., and R.G. Walker, 1981. Cardium Formation (U. Cretaceous) at Seebe, Alberta; storm-transported sandstones and conglomerates in shallow marine depositional environments below fair-weather wave base. Canadian Journal of Earth Sciences, v. 18, p. 795-809.

APPENDIX

CORED WELL LOCATION	Log curves displayed	Digital log curves not available
100/7-9-48-17W5/0	Gamma Ray, Caliper, SP, Density Porosity, Neutron Porosity, PEF, Induction	
100/7-28-46-16W5/0	Gamma Ray, Caliper, SP, Density Porosity, Neutron Porosity, PEF, Induction	
100/7-23-46-17W5/0	Gamma Ray, Caliper, SP, Density Porosity, Neutron Porosity, Induction	PEF
100/7-14-47-14W5/0	Gamma Ray, Caliper, Density Porosity, Neutron Porosity, Induction	PEF, SP
100/2-7-47-16W5/0	Gamma Ray, Caliper, SP, Density Porosity, Neutron Porosity, Induction	PEF
100/16-28-45-15W5/0	Gamma Ray, Caliper, SP, Neutron Porosity	Induction, PEF, Density Porosity
100/14-3-47-14W5/0	Gamma Ray, Caliper, SP, Density Porosity, Neutron Porosity, PEF, Induction	
100/14-32-46-14W5/0	Gamma Ray, Caliper, SP, Neutron Porosity, Induction	Density Porosity, PEF
100/1-23-48-16W5/0	Gamma Ray, Caliper, SP, Density Porosity, Neutron Porosity, PEF, Induction	
100/11-13-47-15W5/2	Gamma Ray, Density Porosity, Neutron Porosity, Induction	PEF, SP, Caliper
100/10-7-47-17W5/0	Gamma Ray, Caliper, SP, Density Porosity, Neutron Porosity, Induction	PEF
100/10-30-48-17W5/0	Gamma Ray, Caliper, SP, Neutron Porosity, Induction	PEF, Density Porosity
100/10-29-48-17W5/0	Gamma Ray, Caliper, SP, Induction	Neutron Porosity, Density Porosity, PEF
100/10-28-45-16W5/0	Gamma Ray, Caliper, SP, Density Porosity, Neutron Porosity, Induction	PEF
100/10-25-48-18W5/0	Gamma Ray, Caliper, SP, Induction	Neutron Porosity, Density Porosity, PEF
100/10-17-46-16W5/0	Gamma Ray, Caliper, SP, Density Porosity, Neutron Porosity, PEF, Induction	
100/10-1-46-14W5/0	Gamma Ray, Caliper, SP, Density Porosity, Neutron Porosity, Induction	PEF

Core location map

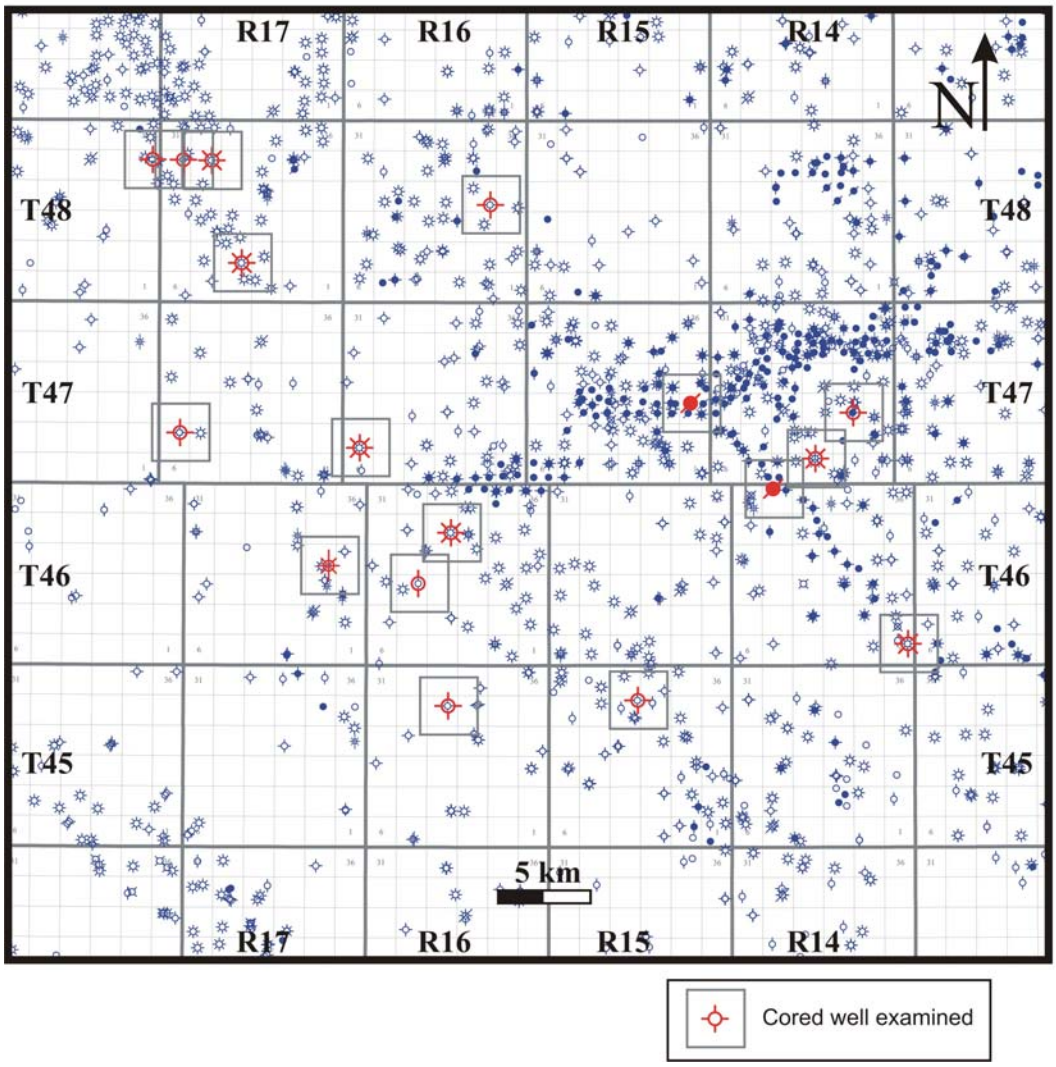

Core Log Legend

Lithologies


Sandstone


Siltstone


Conglomerate


Light gray shale


Dark gray shale


Claystone

Stringers


Sandstone


Siltstone


Conglomerate


Shale


Siderite


Coal

Contacts


Gradational


Scoured/Irregular

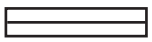
Sharp

Bioturbation


Chondrites sp.


Helminthopsis sp.


Palaeophycus sp.


Phycosiphon sp.


Planolites sp.


Skolithos sp.


Teichichnus sp.


Terebellina sp.


Unidentified trace


Zoophycos sp.

Frequency

0 - 30%

30 - 60%

60 - 100%

Bedforms


Low Angled-Inclined


Parallel horizontal


Wave rippled


Soft sediment deformation/faulted


Fractured


Slickensided surface

Unidentified/massive

Accessory Minerals/ Textures


Argillaceous grain


Calcareous


Carbonaceous


Dark chert

Fossil

Light chert

Siderite

Sandy

Silty

Pyrite

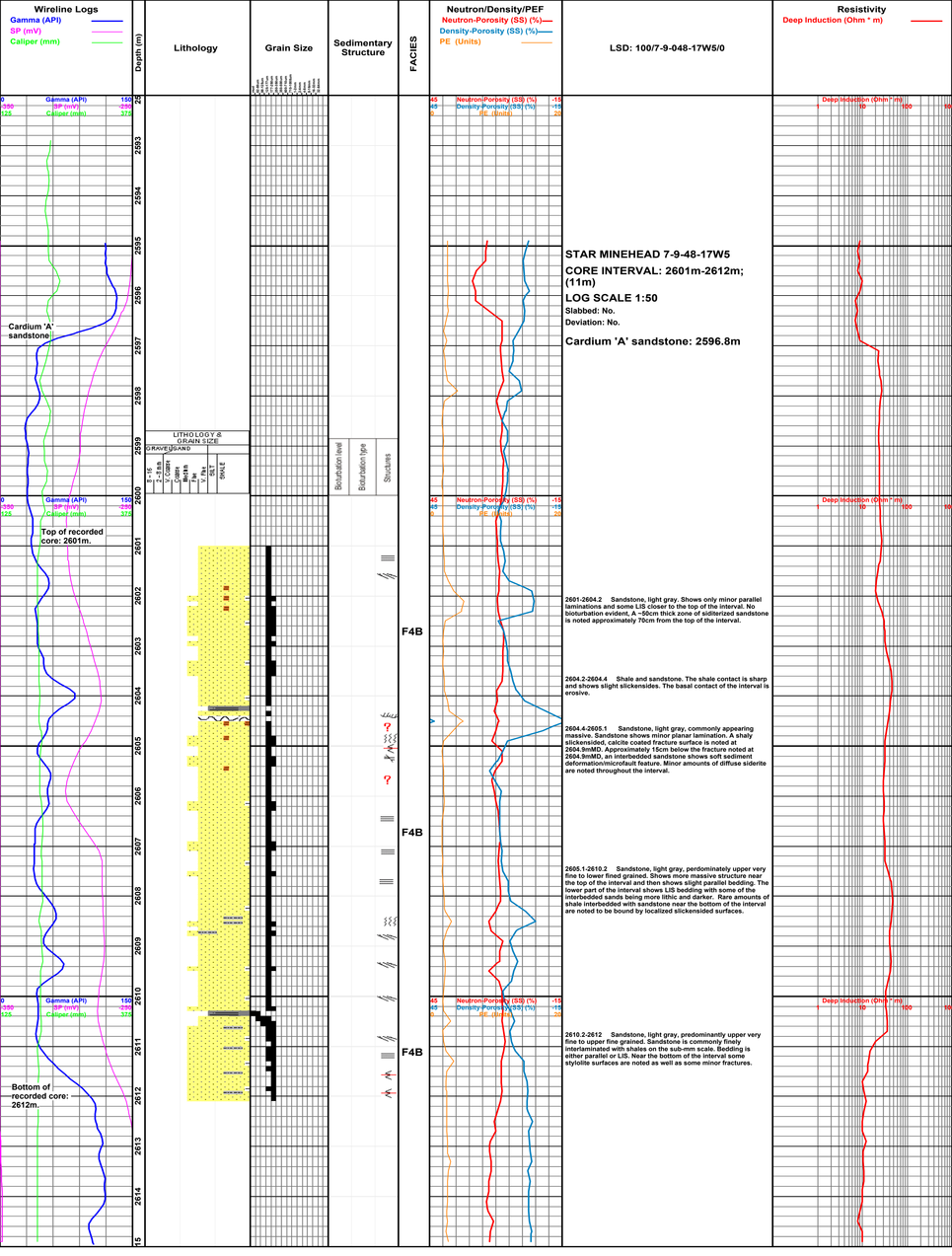
Wireline Logs
Gamma (API)
SP (mV)
Caliper (mm)
Depth (m)
Lithology
Grain Size
Sedimentary Structure
FACIES
Neutron/Density/PEF
Neutron-Porosity (SS) (%)
Density-Porosity (SS) (%)
PE (Units)
LSD: 100/7-9-048-17W5/0
Resistivity
Deep Induction (Ohm * m)
Gamma (API) 0 150
SP (mV) -200 200
Caliper (mm) 125 375
Neutron/Porosity (SS) (%) 45 -15
Density-Porosity(SS) (%) 45 -15
PE (Units) 0 30
Deep Induction (Ohm*m) 0.2 2000
2592
2593
2594
2595
2596
2597
2598
2599
2600
2601
2602
2603
2604
2605
2606
2607
2608
2609
2610
2611
2612
2613
2614
2615
Cardium 'A' sandstone
Top of recorded core: 2601m.
Bottom of recorded core: 2612m.
LITHOLOGY & GRAIN SIZE
GRAVEL/SAND
CLAY/SILT
SHALE
Bioturbation level
Bioturbation type
Structures
F4B
F4B
F4B
STAR MINEHEAD 7-9-48-17W5
CORE INTERVAL: 2601m-2612m; (11m)
LOG SCALE 1:50
Slabbed: No.
Deviation: No.
Cardium 'A' sandstone: 2596.8m
2601-2604.2 Sandstone, light gray, Shows only minor parallel laminations and some LIS closer to the top of the interval. No bioturbation evident, A ~50cm thick zone of siditerized sandstone is noted approximately 70cm from the top of the interval.
2604.2-2604.4 Shale and sandstone. The shale contact is sharp and shows slight slickensides. The basal contact of the interval is erosive.
2604.4-2605.1 Sandstone, light gray, commonly appearing massive. Sandstone shows minor planar lamination. A shaly slickensided, calcite coated fracture surface is noted at 2604.9mMD. Approximately 15cm below the fracture noted at 2604.9mMD, an interbedded sandstone shows soft sediment deformation/microfault feature. Minor amounts of diffuse siderite are noted throughout the interval.
2605.1-2610.2 Sandstone, light gray, perdominately upper very fine to lower fined grained. Shows more massive structure near the top of the interval and then shows slight parallel bedding. The lower part of the interval shows LIS bedding with some of the interbedded sands being more lithic and darker. Rare amounts of shale interbedded with sandstone near the bottom of the interval are noted to be bound by localized slickensided surfaces.
2610.2-2612 Sandstone, light gray, predominantly upper very fine to upper fine grained. Sandstone is commonly finely interlaminated with shales on the sub-cm scale. Bedding is either parallel or LIS. Near the bottom of the interval some stylolite surfaces are noted as well as some minor fractures.

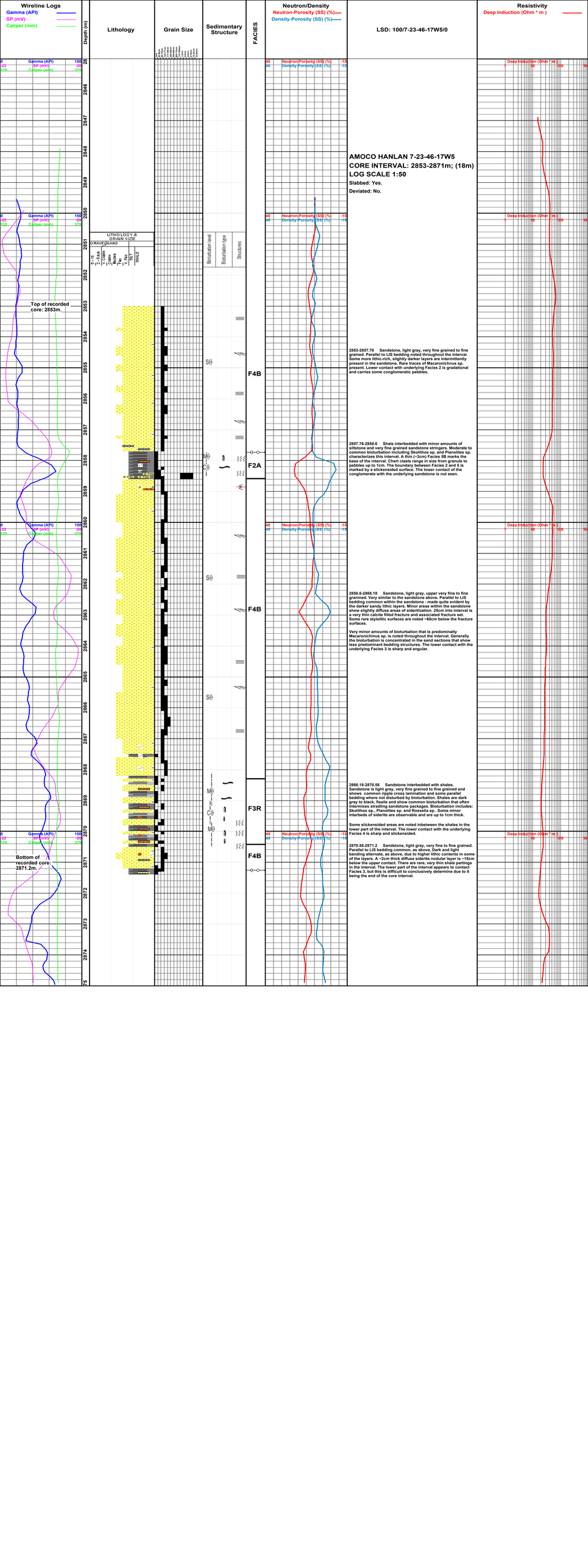
Wireline Logs
Gamma (API)
SP (mV)
Caliper (mm)
Depth (m)
Lithology
Grain Size
Sedimentary Structure
FACIES
Neutron/Density
Neutron-Porosity (SS) (%)
Density-Porosity (SS) (%)
LSD: 100/7-23-46-17W5/0
Resistivity
Deep Induction (Ohm * m)
AMOCO HANLAN 7-23-46-17W5
CORE INTERVAL: 2853-2871m; (18m)
LOG SCALE 1:50
Slabbed: Yes.
Deviated: No.
LITHOLOGY & GRAIN SIZE
GRAVEL/SAND
Bioturbation level
Bioturbation type
Structures
Top of recorded core: 2853m.
Bottom of recorded core: 2871.2m.
F4B
F2A
F4B
F3R
F4B
2853-2857.76 Sandstone, light gray, very fine grained to fine grained. Parallel to LIS bedding noted throughout the interval. Some more lithic-rich, slightly darker layers are intermittently present in the sandstone. Rare traces of Macaronichnus sp. present. Lower contact with underlying Facies 2 is gradational and carries some conglomeratic pebbles.
2857.76-2858.6 Shale interbedded with minor amounts of siltstone and very fine grained sandstone stringers. Moderate to common bioturbation including Skolithos sp. and Planolites sp. characterizes this interval. A thin (~3cm) Facies 5B marks the base of the interval. Chert clasts range in size from granule to pebbles up to 1cm. The boundary between Facies 2 and 5 is marked by a slickensided surface. The lower contact of the conglomerate with the underlying sandstone is not seen.
2858.6-2868.18 Sandstone, light gray, upper very fine to fine grained. Very similar to the sandstone above. Parallel to LIS bedding common within the sandstone - made quite evident by the darker sandy lithic layers. Minor areas within the sandstone show slightly diffuse areas of sideritization. 25cm into interval is a very thin calcite filled fracture and associated fracture set. Some rare stylolitic surfaces are noted ~60cm below the fracture surfaces.
Very minor amounts of bioturbation that is predominatly Macaronichnus sp. is noted throughout the interval. Generally the bioturbation is concentrated in the sand sections that show less predominant bedding structures. The lower contact with the underlying Facies 3 is sharp and angular.
2868.18-2870.58 Sandstone interbedded with shales. Sandstone is light gray, very fine grained to fine grained and shows common ripple cross lamination and some parallel bedding where not disturbed by bioturbation. Shales are dark gray to black, fissile and show common bioturbation that often intermixes straddling sandstone packages. Bioturbation includes: Skolithos sp., Planolites sp. and Rosselia sp.. Some minor interbeds of siderite are observable and are up to 1cm thick.
Some slickensided areas are noted inbetween the shales in the lower part of the interval. The lower contact with the underlying Facies 4 is sharp and slickensided.
2870.58-2871.2 Sandstone, light gray, very fine to fine grained. Parallel to LIS bedding common, as above. Dark and light banding alternate, as above, due to higher lithic contents in some of the layers. A ~2cm thick diffuse siderite nodular layer is ~15cm below the upper contact. There are rare, very thin shale partings in the interval. The lower part of the interval appears to contact Facies 3, but this is difficult to conclusively determine due to it being the end of the core interval.

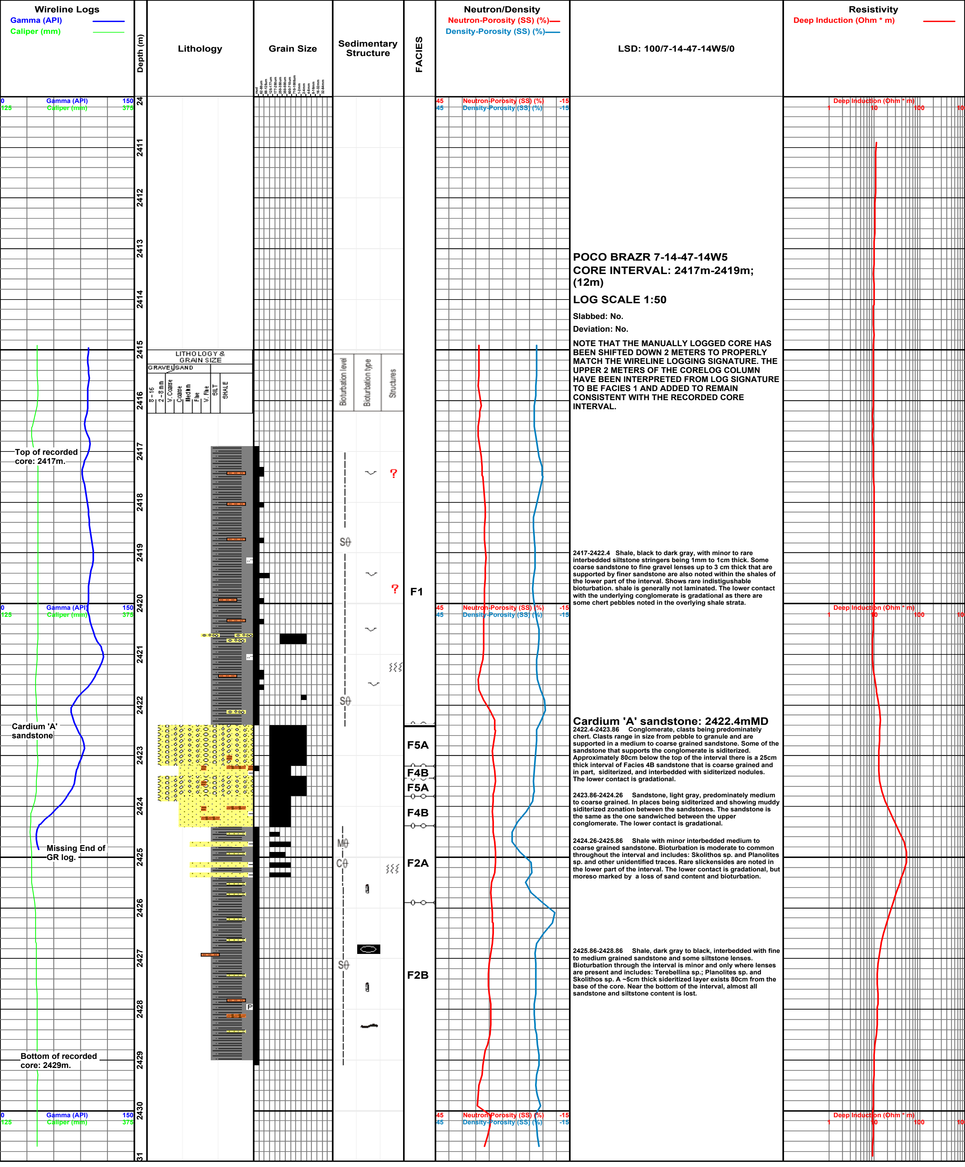

POCO BRAZR 7-14-47-14W5
CORE INTERVAL: 2417m-2419m; (12m)

LOG SCALE 1:50

Slabbed: No.

Deviation: No.

NOTE THAT THE MANUALLY LOGGED CORE HAS BEEN SHIFTED DOWN 2 METERS TO PROPERLY MATCH THE WIRELINE LOGGING SIGNATURE. THE UPPER 2 METERS OF THE CORELOG COLUMN HAVE BEEN INTERPRETED FROM LOG SIGNATURE TO BE FACIES 1 AND ADDED TO REMAIN CONSISTENT WITH THE RECORDED CORE INTERVAL.

2417-2422.4 Shale, black to dark gray, with minor to rare interbedded siltstone stringers being 1mm to 1cm thick. Some coarse sandstone to fine gravel lenses up to 3 cm thick that are supported by finer sandstone are also noted within the shales of the lower part of the interval. Shows rare indistiguishable bioturbation. shale is generally not laminated. The lower contact with the underlying conglomerate is gradational as there are some chert pebbles noted in the overlying shale strata.

Cardium 'A' sandstone: 2422.4mMD

2422.4-2423.86 Conglomerate, clasts being predominately chert. Clasts range in size from pebble to granule and are supported in a medium to coarse grained sandstone. Some of the sandstone that supports the conglomerate is siditerized. Approximately 80cm below the top of the interval there is a 25cm thick interval of Facies 4B sandstone that is coarse grained and in part, siditerized, and interbedded with siditerized nodules. The lower contact is gradational.

2423.86-2424.26 Sandstone, light gray, predominately medium to coarse grained. In places being siditerized and showing muddy siditerized zonation between the sandstones. The sandstone is the same as the one sandwiched between the upper conglomerate. The lower contact is gradational.

2424.26-2425.86 Shale with minor interbedded medium to coarse grained sandstone. Bioturbation is moderate to common throughout the interval and includes: Skolithos sp. and Planolites sp. and other unidentified traces. Rare slickensides are noted in the lower part of the interval. The lower contact is gradational, but moreso marked by a loss of sand content and bioturbation.

2425.86-2428.86 Shale, dark gray to black, interbedded with fine to medium grained sandstone and some siltstone lenses. Bioturbation through the interval is minor and only where lenses are present and includes: Terebellina sp.; Planolites sp. and Skolithos sp. A ~5cm thick sidiritized layer exists 80cm from the base of the core. Near the bottom of the interval, almost all sandstone and siltstone content is lost.

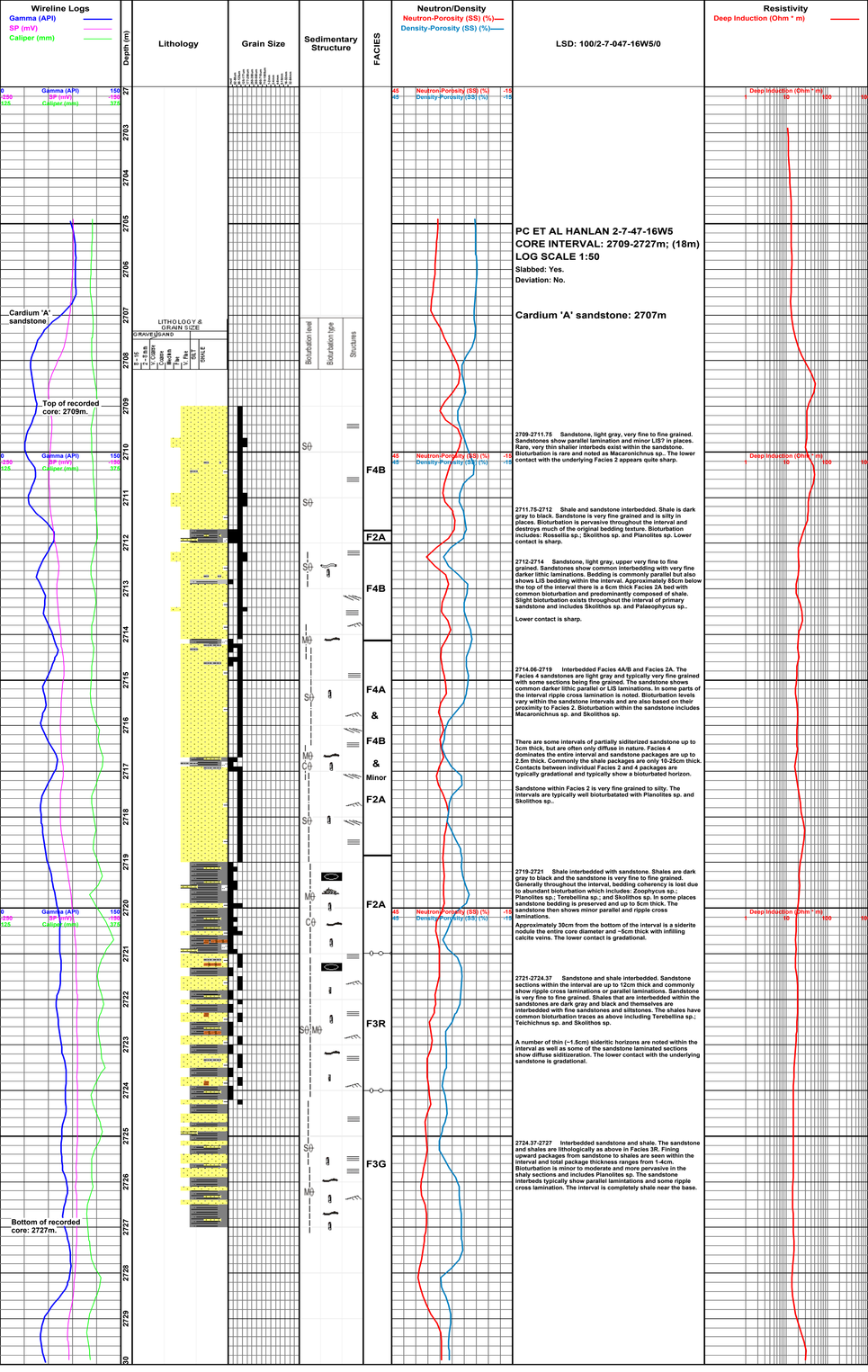

PC ET AL HANLAN 2-7-47-16W5
CORE INTERVAL: 2709-2727m; (18m)
LOG SCALE 1:50
Slabbed: Yes.
Deviation: No.

Cardium 'A' sandstone: 2707m

2709-2711.75 Sandstone, light gray, very fine to fine grained. Sandstones show parallel lamination and minor LS? in places. Rare, very thin shaler interbeds exist within the sandstone. Bioturbation is rare and noted as Macaronichnus sp.. The lower contact with the underlying Facies 2 appears quite sharp.

2711.75-2712 Shale and sandstone interbedded. Shale is dark gray to black. Sandstone is very fine grained and is silty in places. Bioturbation is pervasive throughout the interval and destroys much of the original bedding texture. Bioturbation includes: Rosselia sp.; Skolithos sp. and Planolites sp. Lower contact is sharp.

2712-2714 Sandstone, light gray, upper very fine to fine grained. Sandstones show common interbedding with very fine darker lithic laminations. Bedding is commonly parallel but also shows LIS bedding within the interval. Approximately 85cm below the top of the interval there is a 6cm thick Facies 2A bed with common bioturbation and predominantly composed of shale. Slight bioturbation exists throughout the interval of primary sandstone and includes Skolithos sp. and Palaeophycus sp..

Lower contact is sharp.

2714.06-2719 Interbedded Facies 4A/B and Facies 2A. The Facies 4 sandstones are light gray and typically very fine grained with some sections being fine grained. The sandstone shows common darker lithic parallel or LIS laminations. In some parts of the interval ripple cross lamination is noted. Bioturbation levels vary within the sandstone intervals and are also based on their proximity to Facies 2. Bioturbation within the sandstone includes Macaronichnus sp. and Skolithos sp.

There are some intervals of partially siderized sandstone up to 3cm thick, but are often only diffuse in nature. Facies 4 dominates the entire interval and sandstone packages are up to 2.5m thick. Commonly the shale packages are only 10-25cm thick. Contacts between individual Facies 2 and 4 packages are typically gradational and typically show a bioturbated horizon.

Sandstone within Facies 2 is very fine grained to silty. The intervals are typically well bioturbatated with Planolites sp. and Skolithos sp..

2719-2721 Shale interbedded with sandstone. Shales are dark gray to black and the sandstone is very fine to fine grained. Generally throughout the interval, bedding coherency is lost due to abundant bioturbation which includes: Zoophycus sp.; Planolites sp.; Terebellina sp.; and Skolithos sp. In some places sandstone bedding is preserved and up to 5cm thick. The sandstone then shows minor parallel and ripple cross laminations.

Approximately 30cm from the bottom of the interval is a siderite nodule the entire core diameter and ~5cm thick with infilling calcite veins. The lower contact is gradational.

2721-2724.37 Sandstone and shale interbedded. Sandstone sections within the interval are up to 12cm thick and commonly show ripple cross laminations or parallel laminations. Sandstone is very fine to fine grained. Shales that are interbedded within the sandstones are dark gray and black and themselves are interbedded with fine sandstones and siltstones. The shales have common bioturbation traces as above including Terebellina sp.; Teichichnus sp. and Skolithos sp.

A number of thin (~1.5cm) sideritic horizons are noted within the interval as well as some of the sandstone laminated sections show diffuse sideritization. The lower contact with the underlying sandstone is gradational.

2724.37-2727 Interbedded sandstone and shale. The sandstone and shales are lithologically as above in Facies 3R. Fining upward packages from sandstone to shales are seen within the interval and total package thickness ranges from 1-4cm. Bioturbation is minor to moderate and more pervasive in the shaly sections and includes Planolites sp. The sandstone interbeds typically show parallel laminations and some ripple cross lamination. The interval is completely shale near the base.

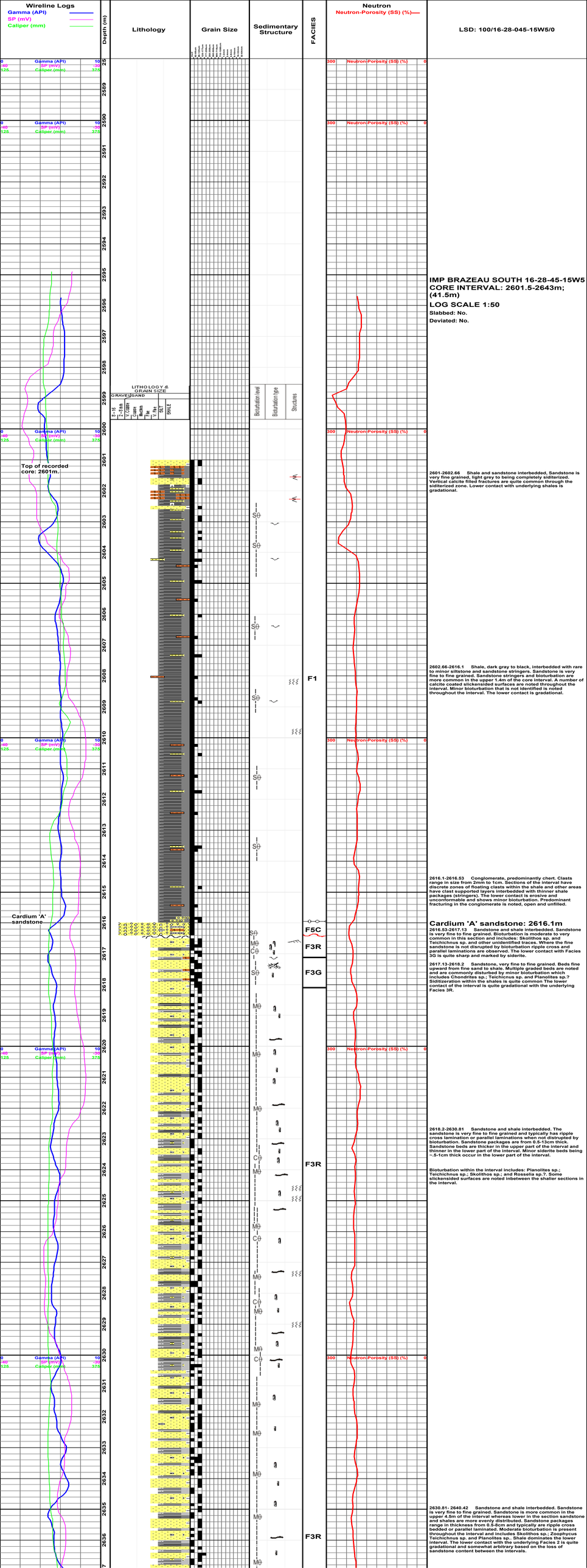

IMP BRAZEAU SOUTH 16-28-45-15W5
CORE INTERVAL: 2601.5-2643m; (41.5m)
LOG SCALE 1:50
Slabbed: No.
Deviated: No.

2601-2602.66 Shale and sandstone interbedded, Sandstone is very fine grained, light grey to being completely sideritized. Vertical calcite filled fractures are quite common through the sideritized zone. Lower contact with underlying shales is gradational.

2602.66-2616.1 Shale, dark gray to black, interbedded with rare to minor siltstone and sandstone stringers. Sandstone is very fine to fine grained. Sandstone stringers and bioturbation are more common in the upper 1.4m of the core interval. A number of calcite coated slickensided surfaces are noted throughout the interval. Minor bioturbation that is not identified is noted throughout the interval. The lower contact is gradational.

2616.1-2616.53 Conglomerate, predominantly chert. Clasts range in size from 2mm to 1cm. Sections of the interval have discrete zones of floating clasts within the shale and other areas have clast supported layers interbedded with thinner shale packages (stringers). The lower contact is erosive and unconformable and shows minor bioturbation. Predominant fracturing in the conglomerate is noted, open and unfilled.

Cardium 'A' sandstone: 2616.1m

2616.53-2617.13 Sandstone and shale interbedded, Sandstone is very fine to fine grained. Bioturbation is moderate to very common in this section and includes: Skolithos sp. and Teichichnus sp. and other unidentified traces. Where the fine sandstone is not disrupted by bioturbation ripple cross and parallel laminations are observed. The lower contact with Facies 3G is quite sharp and marked by siderite.

2617.13-2618.2 Sandstone, very fine to fine grained. Beds fine upward from fine sand to shale. Multiple graded beds are noted and are commonly disturbed by minor bioturbation which includes Chondrites sp.; Teichicnus sp. and Planolites sp.? Sidilizeration within the shales is quite common The lower contact of the interval is quite gradational with the underlying Facies 3R.

2618.2-2630.81 Sandstone and shale interbedded. The sandstone is very fine to fine grained and typically has ripple cross lamination or parallel laminations when not distrupted by bioturbation. Sandstone packages are from 0.5-13cm thick. Sandstone beds are thicker in the upper part of the interval and thinner in the lower part of the interval. Minor siderite beds being ~.5-1cm thick occur in the lower part of the interval.

Bioturbation within the interval includes: Planolites sp.; Teichichnus sp.; Skolithos sp.; and Rossella sp.?. Some slickensided surfaces are noted inbetween the shalier sections in the interval.

2630.81- 2640.42 Sandstone and shale interbedded. Sandstone is very fine to fine grained. Sandstone is more common in the upper 4.5m of the interval whereas lower in the section sandstone and shales are more evenly distributed. Sandstone packages range in thickness from 0.5-8cm and typically are ripple cross bedded or parallel laminated. Moderate bioturbation is present throughout the interval and includes Skolithos sp.; Zoophycus Teichichnus sp. and Planolites sp.. Shale dominates the lower interval. The lower contact with the underlying Facies 2 is quite gradational and somewhat arbitrary based on the loss of sandstone content between the intervals.

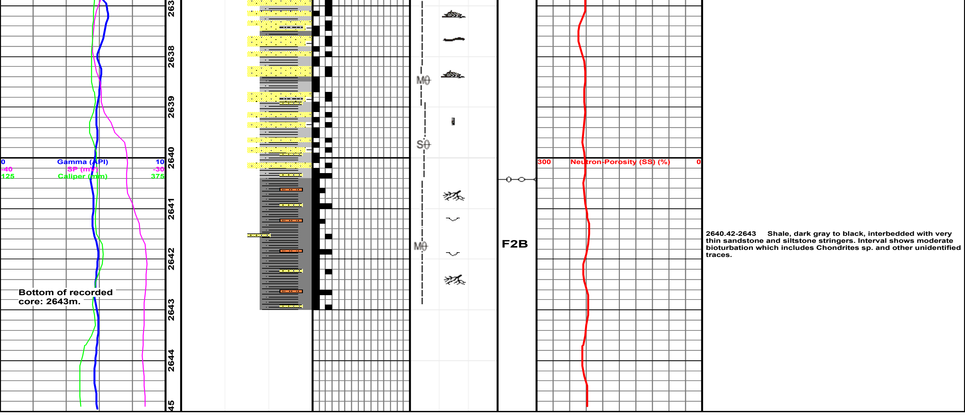
0
Gamma (API)
150
SP (mV)
Caliper (mm)
125
375
2637
2638
2639
2640
2641
2642
2643
2644
45
MD
SD
MD
F2B
300
Neutron Porosity (SS) (%)
0
Bottom of recorded core: 2643m.
2640.42-2643 Shale, dark gray to black, interbedded with very thin sandstone and siltstone stringers. Interval shows moderate bioturbation which includes Chondrites sp. and other unidentified traces.

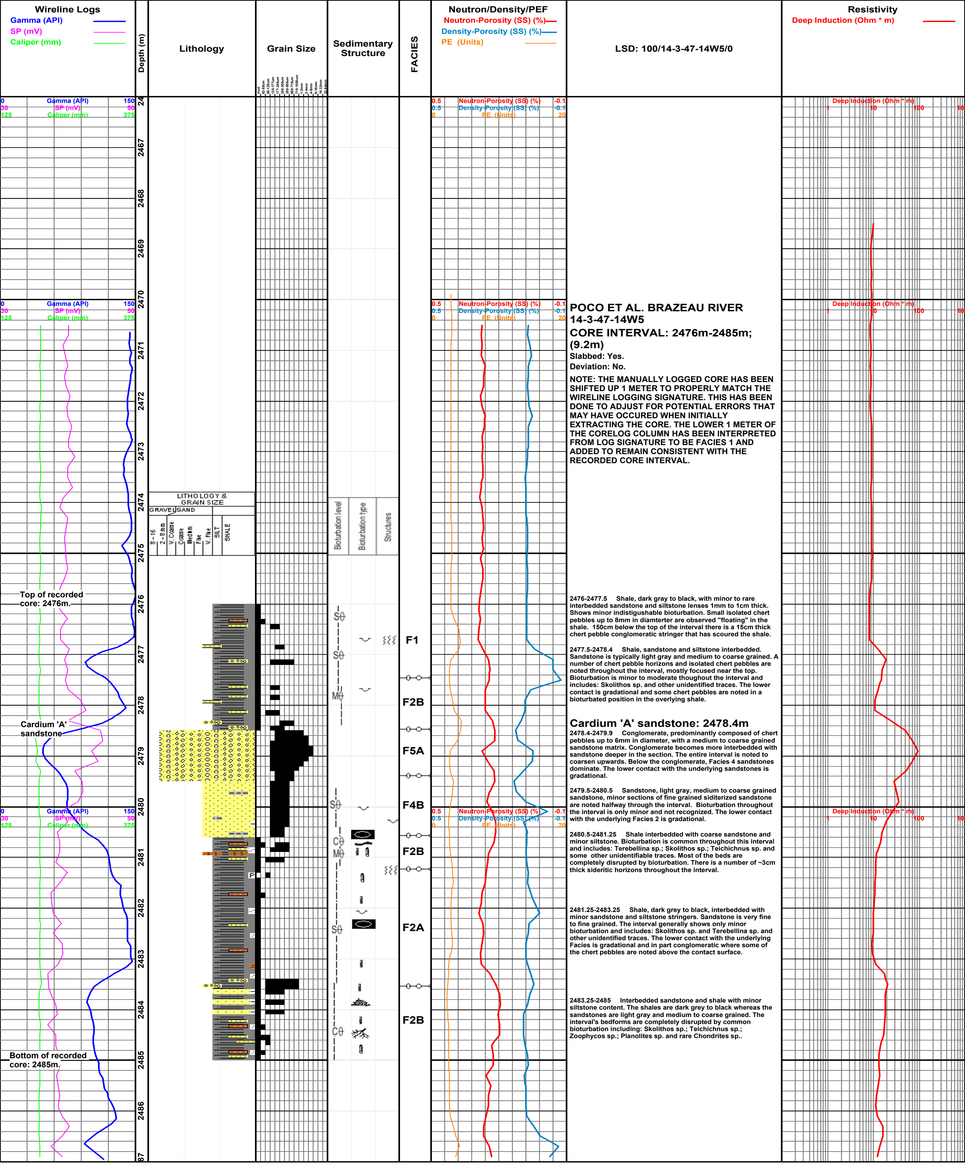

POCO ET AL. BRAZEAU RIVER 14-3-47-14W5

CORE INTERVAL: 2476m-2485m; (9.2m)

Slabbed: Yes.

Deviation: No.

NOTE: THE MANUALLY LOGGED CORE HAS BEEN SHIFTED UP 1 METER TO PROPERLY MATCH THE WIRELINE LOGGING SIGNATURE. THIS HAS BEEN DONE TO ADJUST FOR POTENTIAL ERRORS THAT MAY HAVE OCCURED WHEN INITIALLY EXTRACTING THE CORE. THE LOWER 1 METER OF THE CORELOG COLUMN HAS BEEN INTERPRETED FROM LOG SIGNATURE TO BE FACIES 1 AND ADDED TO REMAIN CONSISTENT WITH THE RECORDED CORE INTERVAL.

2476-2477.5 Shale, dark gray to black, with minor to rare interbedded sandstone and siltstone lenses 1mm to 1cm thick. Shows minor indistiguishable bioturbation. Small isolated chert pebbles up to 8mm in diamterter are observed "floating" in the shale. 150cm below the top of the interval there is a 15cm thick chert pebble conglomeratic stringer that has scoured the shale.

2477.5-2478.4 Shale, sandstone and siltstone interbedded. Sandstone is typically light gray and medium to coarse grained. A number of chert pebble horizons and isolated chert pebbles are noted throughout the interval, mostly focused near the top. Bioturbation is minor to moderate throughout the interval and includes: Skolithos sp. and other unidentified traces. The lower contact is gradational and some chert pebbles are noted in a bioturbated position in the overlying shale.

Cardium 'A' sandstone: 2478.4m

2478.4-2479.9 Conglomerate, predominantly composed of chert pebbles up to 6mm in diameter, with a medium to coarse grained sandstone matrix. Conglomerate becomes more interbedded with sandstone deeper in the section. The entire interval is noted to coarsen upwards. Below the conglomerate, Facies 4 sandstones dominate. The lower contact with the underlying sandstones is gradational.

2479.5-2480.5 Sandstone, light gray, medium to coarse grained sandstone, minor sections of fine grained siditerized sandstone are noted halfway through the interval. Bioturbation throughout the interval is only minor and not recognized. The lower contact with the underlying Facies 2 is gradational.

2480.5-2481.25 Shale interbedded with coarse sandstone and minor siltstone. Bioturbation is common throughout this interval and includes: Terebellina sp.; Skolithos sp.; Teichichnus sp. and some other unidentifiable traces. Most of the beds are completely disrupted by bioturbation. There is a number of ~3cm thick sideritic horizons throughout the interval.

2481.25-2483.25 Shale, dark grey to black, interbedded with minor sandstone and siltstone stringers. Sandstone is very fine to fine grained. The interval generally shows only minor bioturbation and includes: Skolithos sp. and Terebellina sp. and other unidentified traces. The lower contact with the underlying Facies is gradational and in part conglomeratic where some of the chert pebbles are noted above the contact surface.

2483.25-2485 Interbedded sandstone and shale with minor siltstone content. The shales are dark grey to black whereas the sandstones are light gray and medium to coarse grained. The interval's bedforms are completely disrupted by common bioturbation including: Skolithos sp.; Teichichnus sp.; Zoophycos sp.; Planolites sp. and rare Chondrites sp..

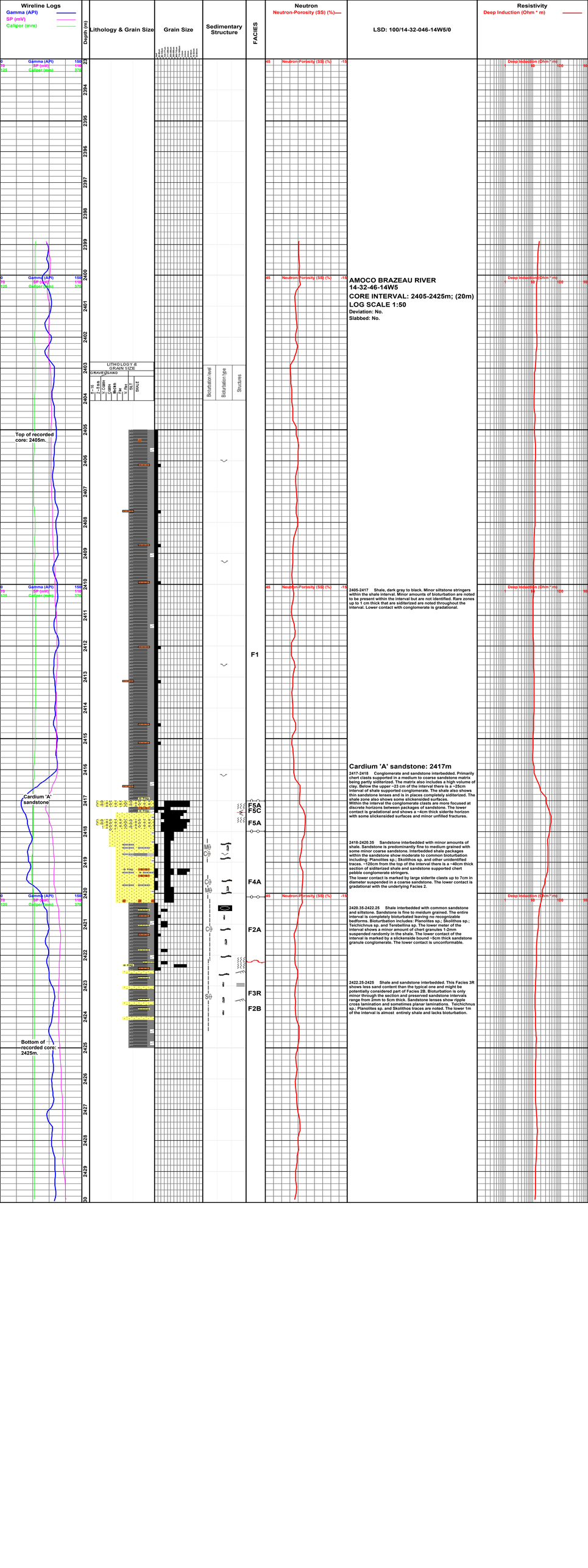
Wireline Logs
Gamma (API)
SP (mV)
Caliper (mm)
Depth (m)
Lithology & Grain Size
Grain Size
Sedimentary Structure
FACIES
Neutron
Neutron-Porosity (SS) (%)
LSD: 100/14-32-046-14W5/0
Resistivity
Deep Induction (Ohm * m)
LITHOLOGY & GRAIN SIZE
GRAVEL
SAND
Bioturbation level
Bioturbation type
Structures
Top of recorded core: 2405m.
Cardium 'A' sandstone
Bottom of recorded core: 2425m.
F1
F5A
F5C
F5A
F4A
F2A
F3R
F2B
AMOCO BRAZEAU RIVER
14-32-46-14W5
CORE INTERVAL: 2405-2425m; (20m)
LOG SCALE 1:50
Deviation: No.
Slabbed: No.
2405-2417 Shale, dark gray to black. Minor siltstone stringers within the shale interval. Minor amounts of bioturbation are noted to be present within the interval but are not identified. Rare zones up to 1 cm thick that are siditerized are noted throughout the interval. Lower contact with conglomerate is gradational.
Cardium 'A' sandstone: 2417m
2417-2418 Conglomerate and sandstone interbedded. Primarily chert clasts supported in a medium to coarse sandstone matrix being partly siditerized. The matrix also includes a high volume of clay. Below the upper ~23 cm of the interval there is a ~25cm interval of shale supported conglomerate. The shale also shows thin sandstone lenses and is in places completely siditerized. The shale zone also shows some slickensided surfaces.
Within the interval the conglomerate clasts are more focused at discrete horizons between packages of sandstone. The lower contact is gradational and shows a ~4cm thick siderite horizon with some slickensided surfaces and minor unfilled fractures.
2418-2420.35 Sandstone interbedded with minor amounts of shale. Sandstone is predominantly fine to medium grained with some minor coarse sandstone. Interbedded shale packages within the sandstone show moderate to common bioturbation including: Planolites sp.; Skolithos sp. and other unidentified traces. ~120cm from the top of the interval there is a ~40cm thick section of siditerized shale and sandstone supported chert pebble conglomerate stringers.
The lower contact is marked by large siderite clasts up to 7cm in diameter suspended in a coarse sandstone. The lower contact is gradational with the underlying Facies 2.
2420.35-2422.25 Shale interbedded with common sandstone and siltstone. Sandstone is fine to meidum grained. The entire interval is completely bioturbated leaving no recognizable bedforms. Bioturbation includes: Planolites sp.; Skolithos sp.; Teichichnus sp. and Terebellina sp. The lower meter of the interval shows a minor amount of chert granules 1-2mm suspended randomly in the shale. The lower contact of the interval is marked by a slickenside bound ~5cm thick sandstone granule conglomerate. The lower contact is unconformable.
2422.25-2425 Shale and sandstone interbedded. This Facies 3R shows less sand content than the typical one and might be potentially considered part of Facies 2B. Bioturbation is only minor through the section and preserved sandstone intervals range from 2mm to 5cm thick. Sandstone lenses show ripple cross lamination and sometimes planar laminations. Teichichnus sp.; Planolites sp. and Skolithos traces are noted. The lower 1m of the interval is almost entirely shale and lacks bioturbation.

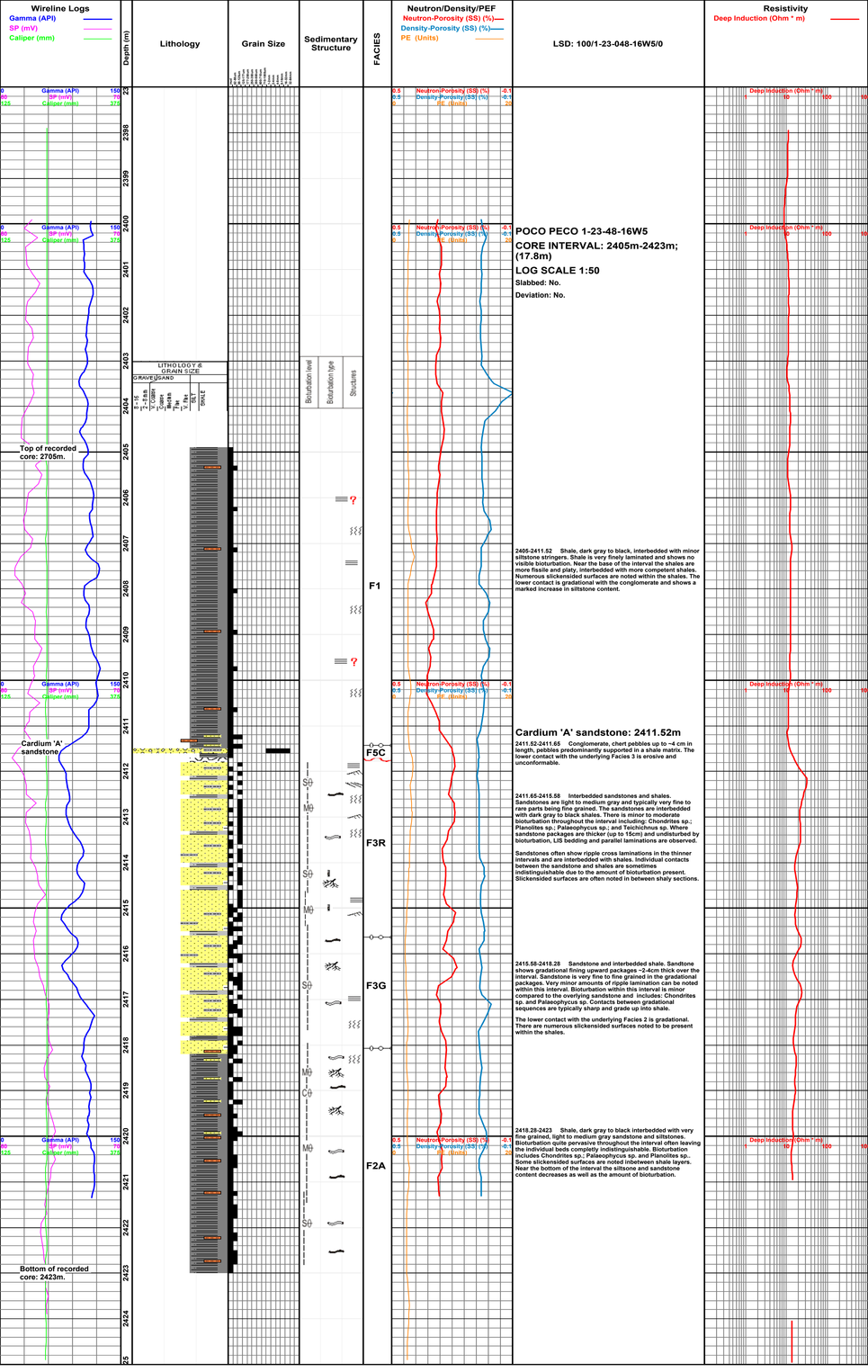
Wireline Logs
Gamma (API)
SP (mV)
Caliper (mm)
Depth (m)
Lithology
Grain Size
Sedimentary Structure
FACIES
Neutron/Density/PEF
Neutron-Porosity (SS) (%)
Density-Porosity (SS) (%)
PE (Units)
LSD: 100/1-23-048-16W5/0
Resistivity
Deep Induction (Ohm * m)
Gamma (API) 0 150
SP (mV) 100 -100
Caliper (mm) 125 375
Neutron/Porosity (SS) (%) 0.5 -0.1
Density-Porosity (SS) (%) 0.5 -0.1
PE (Units) 0 20
Deep Induction (Ohm*m) 1 10 100 1000
2398
2399
2400
2401
2402
2403
2404
2405
2406
2407
2408
2409
2410
2411
2412
2413
2414
2415
2416
2417
2418
2419
2420
2421
2422
2423
2424
2425
LITHOLOGY & GRAIN SIZE
GRAVEL SAND
Clay
Silt
Very Fine
Fine
Medium
Coarse
Very Coarse
Granules
Pebbles
Cobbles
Boulders
CLAY
SILT
SAND
GRAVEL
Bioturbation level
Bioturbation type
Structures
Top of recorded core: 2705m.
Cardium 'A' sandstone
Bottom of recorded core: 2423m.
F1
F5C
F3R
F3G
F2A
POCO PECO 1-23-48-16W5
CORE INTERVAL: 2405m-2423m; (17.8m)
LOG SCALE 1:50
Slabbed: No.
Deviation: No.
2405-2411.52 Shale, dark gray to black, interbedded with minor siltstone stringers. Shale is very finely laminated and shows no visible bioturbation. Near the base of the interval the shales are more fissile and platy, interbedded with more competent shales. Numerous slickensided surfaces are noted within the shales. The lower contact is gradational with the conglomerate and shows a marked increase in siltstone content.
Cardium 'A' sandstone: 2411.52m
2411.52-2411.65 Conglomerate, chert pebbles up to ~4 cm in length, pebbles predominantly supported in a shale matrix. The lower contact with the underlying Facies 3 is erosive and unconformable.
2411.65-2415.58 Interbedded sandstones and shales. Sandstones are light to medium gray and typically very fine to rare parts being fine grained. The sandstones are interbedded with dark gray to black shales. There is minor to moderate bioturbation throughout the interval including: Chondrites sp.; Planolites sp.; Palaeophycus sp.; and Teichichnus sp. Where sandstone packages are thicker (up to 15cm) and undisturbed by bioturbation, LS bedding and parallel laminations are observed.
Sandstones often show ripple cross laminations in the thinner intervals and are interbedded with shales. Individual contacts between the sandstone and shales are sometimes indistinguishable due to the amount of bioturbation present. Slickensided surfaces are often noted in between shaly sections.
2415.58-2418.28 Sandstone and interbedded shale. Sandtone shows gradational fining upward packages ~2-4cm thick over the interval. Sandstone is very fine to fine grained in the gradational packages. Very minor amounts of ripple lamination can be noted within this interval. Bioturbation within this interval is minor compared to the overlying sandstone and includes: Chondrites sp. and Palaeophycus sp. Contacts between gradational sequences are typically sharp and grade up into shale.
The lower contact with the underlying Facies 2 is gradational. There are numerous slickensided surfaces noted to be present within the shales.
2418.28-2423 Shale, dark gray to black interbedded with very fine grained, light to medium gray sandstone and siltstones. Bioturbation quite pervasive throughout the interval often leaving the individual beds completly indistinguishable. Bioturbation includes Chondrites sp.; Palaeophycus sp. and Planolites sp.. Some slickensided surfaces are noted inbetween shale layers. Near the bottom of the interval the siltsone and sandstone content decreases as well as the amount of bioturbation.

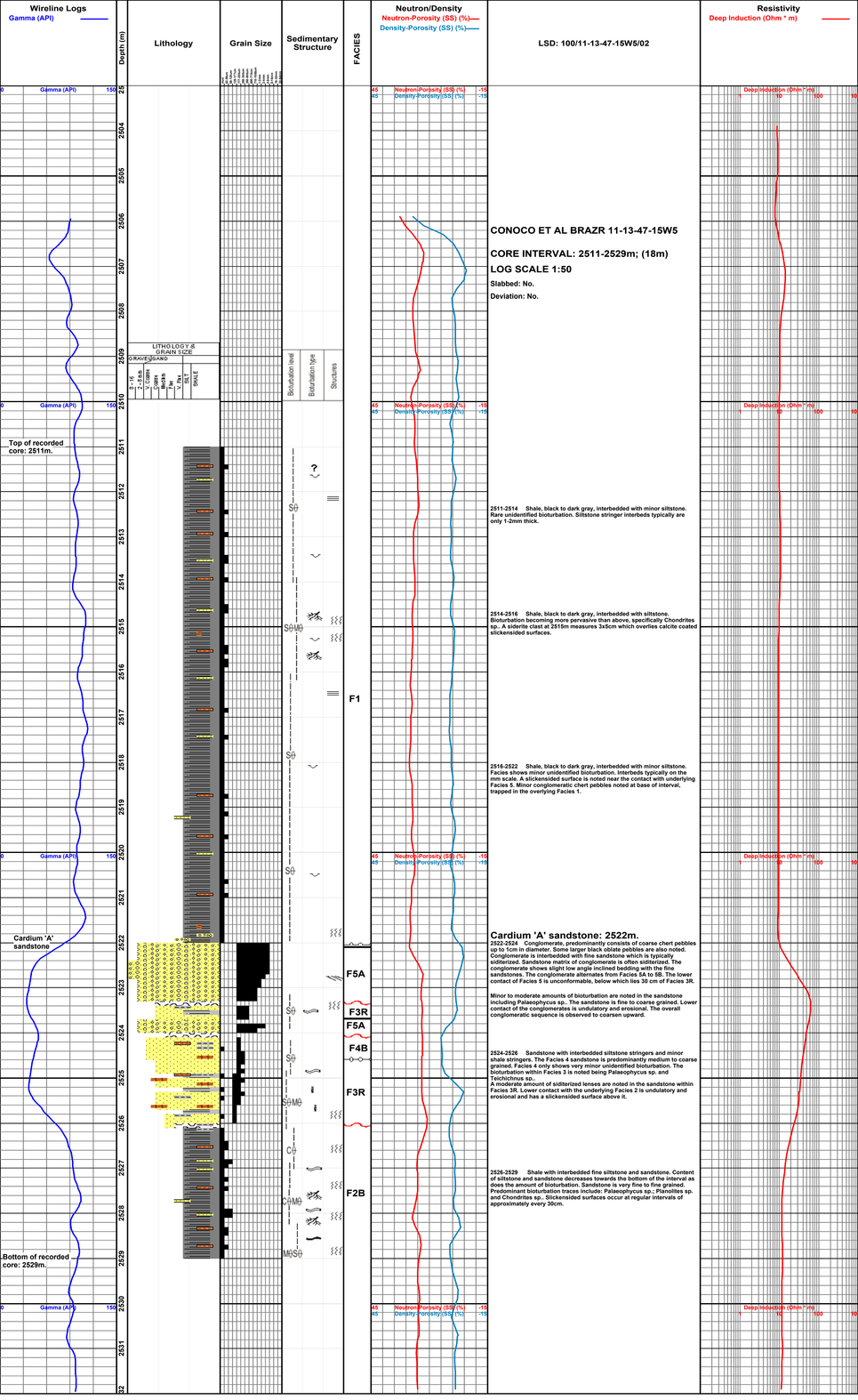
Wireline Logs
Gamma (API)
Depth (m)
Lithology
Grain Size
Sedimentary Structure
FACIES
Neutron/Density
Neutron-Porosity (SS) (%)
Density-Porosity (SS) (%)
LSD: 100/11-13-47-15W5/02
Resistivity
Deep Induction (Ohm * m)
CONOCO ET AL BRAZR 11-13-47-15W5
CORE INTERVAL: 2511-2529m; (18m)
LOG SCALE 1:50
Slabbed: No.
Deviation: No.
Top of recorded core: 2511m.
Cardium 'A' sandstone
Bottom of recorded core: 2529m.
Cardium 'A' sandstone: 2522m.
2511-2514 Shale, black to dark gray, interbedded with minor siltstone. Rare unidentified bioturbation. Siltstone stringer interbeds typically are only 1-2mm thick.
2514-2516 Shale, black to dark gray, interbedded with siltstone. Bioturbation becoming more pervasive than above, specifically Chondrites sp.. A siderite clast at 2515m measures 3x5cm which overlies calcite coated slickensided surfaces.
2516-2522 Shale, black to dark gray, interbedded with minor siltstone. Facies shows minor unidentified bioturbation. Interbeds typically on the mm scale. A slickensided surface is noted near the contact with underlying Facies 5. Minor conglomeratic chert pebbles noted at base of interval, trapped in the overlying Facies 1.
2522-2524 Conglomerate, predominantly consists of coarse chert pebbles up to 1cm in diameter. Some larger black oblate pebbles are also noted. Conglomerate is interbedded with fine sandstone which is typically sideritized. Sandstone matrix of conglomerate is often sideritized. The conglomerate shows slight low angle inclined bedding with the fine sandstones. The conglomerate alternates from Facies 5A to 5B. The lower contact of Facies 5 is unconformable, below which lies 30 cm of Facies 3R.
Minor to moderate amounts of bioturbation are noted in the sandstone including Palaeophycus sp.. The sandstone is fine to coarse grained. Lower contact of the conglomerates is undulatory and erosional. The overall conglomeratic sequence is observed to coarsen upward.
2524-2526 Sandstone with interbedded siltstone stringers and minor shale stringers. The Facies 4 sandstone is predominantly medium to coarse grained. Facies 4 only shows very minor unidentified bioturbation. The bioturbation within Facies 3 is noted being Palaeophycus sp. and Teichichnus sp..
A moderate amount of sideritized lenses are noted in the sandstone within Facies 3R. Lower contact with the underlying Facies 2 is undulatory and erosional and has a slickensided surface above it.
2526-2529 Shale with interbedded fine siltstone and sandstone. Content of siltstone and sandstone decreases towards the bottom of the interval as does the amount of bioturbation. Sandstone is very fine to fine grained. Predominant bioturbation traces include: Palaeophycus sp.; Planolites sp. and Chondrites sp.. Slickensided surfaces occur at regular intervals of approximately every 30cm.
F1
F5A
F3R
F5A
F4B
F3R
F2B

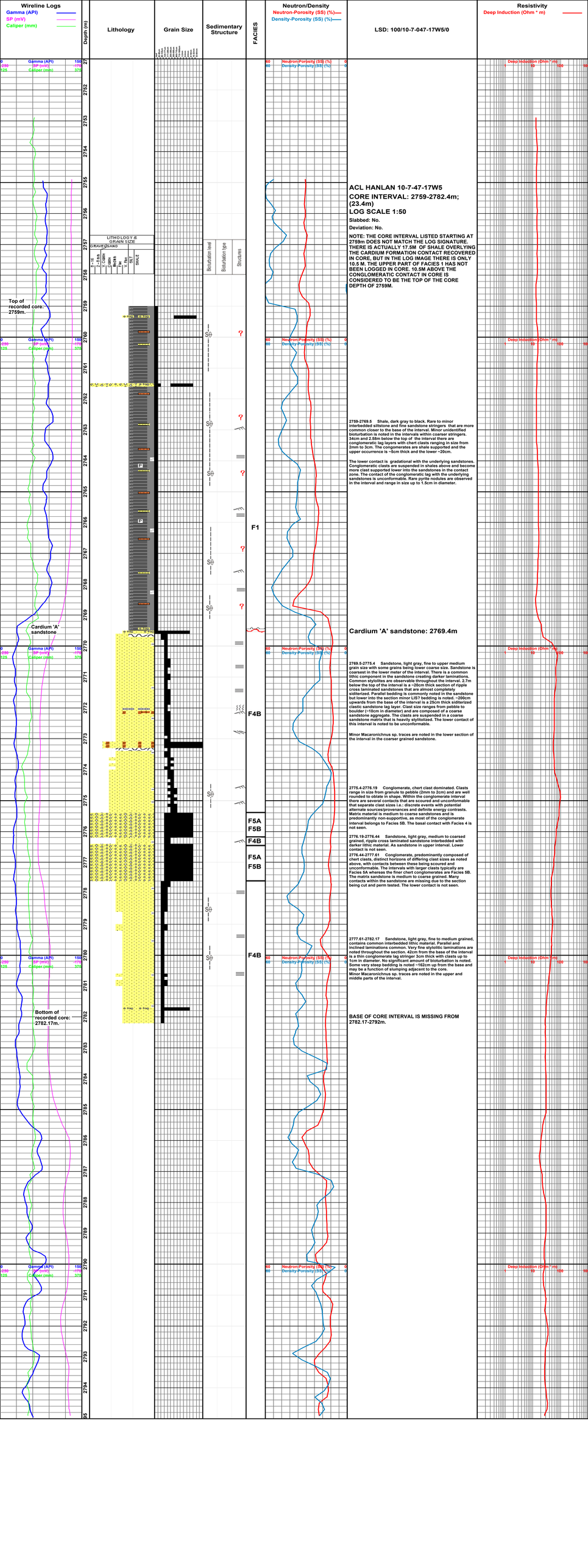

ACL HANLAN 10-7-47-17W5

CORE INTERVAL: 2759-2782.4m; (23.4m)

LOG SCALE 1:50

Slabbed: No.

Deviation: No.

NOTE: THE CORE INTERVAL LISTED STARTING AT 2759m DOES NOT MATCH THE LOG SIGNATURE. THERE IS ACTUALLY 17.5M OF SHALE OVERLYING THE CARDIUM FORMATION CONTACT RECOVERED IN CORE, BUT IN THE LOG IMAGE THERE IS ONLY 10.5 M. THE UPPER PART OF FACIES 1 HAS NOT BEEN LOGGED IN CORE. 10.5M ABOVE THE CONGLOMERATIC CONTACT IN CORE IS CONSIDERED TO BE THE TOP OF THE CORE DEPTH OF 2759M.

2759-2769.5 Shale, dark gray to black. Rare to minor interbedded siltstone and fine sandstone stringers that are more common closer to the base of the interval. Minor unidentified bioturbation is noted in the intervals within coarser stringers. 34cm and 2.58m below the top of the interval there are conglomeratic lag layers with chert clasts ranging in size from 2mm to 3cm. The congomerates are shale supported and the upper occurrence is ~5cm thick and the lower ~20cm.

The lower contact is gradational with the underlying sandstones. Conglomeratic clasts are suspended in shales above and become more clast supported lower into the sandstones in the contact zone. The contact of the conglomeratic lag with the underlying sandstones is unconformable. Rare pyrite nodules are observed in the interval and range in size up to 1.5cm in diameter.

2769.5-2775.4 Sandstone, light gray, fine to upper medium grain size with some grains being lower coarse size. Sandstone is coarsest in the lower meter of the interval. There is a common lithic component in the sandstone creating darker laminations. Common stylolites are observable throughout the interval. 2.7m below the top of the interval is a ~20cm thick section of ripple cross laminated sandstones that are almost completely siditerized. Parallel bedding is commonly noted in the sandstone but lower into the section minor LIS? bedding is noted. ~200cm upwards from the base of the interval is a 25cm thick siditerized clastic sandstone lag layer. Clast size ranges from pebble to boulder (~10cm in diameter) and are composed of a coarse sandstone aggregate. The clasts are suspended in a coarse sandstone matrix that is heavily stylitolized. The lower contact of this interval is noted to be unconformable.

Minor Macaronichnus sp. traces are noted in the lower section of the interval in the coarser grained sandstone.

2775.4-2776.19 Conglomerate, chert clast dominated. Clasts range in size from granule to pebble (2mm to 2cm) and are well rounded to oblate in shape. Within the conglomerate interval there are several contacts that are scoured and unconformable that separate clast sizes i.e.: discrete events with potential alternate sources/provenances and definite energy contrasts. Matrix material is medium to coarse sandstones and is predominantly non-supportive, as most of the conglomerate interval belongs to Facies 5B. The basal contact with Facies 4 is not seen.

2776.19-2776.44 Sandstone, light gray, medium to coarsed grained, ripple cross laminated sandstone interbedded with darker lithic material. As sandstone in upper interval. Lower contact is not seen.

2776.44-2777.61 Conglomerate, predominantly composed of chert clasts, distinct horizons of differing clast sizes as noted above, with contacts between these being scoured and unconformable. The intervals with larger clasts typically are Facies 5A whereas the finer chert conglomerates are Facies 5B. The matrix sandstone is medium to coarse grained. Many contacts within the sandstone are missing due to the section being cut and perm tested. The lower contact is not seen.

2777.61-2782.17 Sandstone, light gray, fine to medium grained, contains common interbedded lithic material. Parallel and inclined laminations common. Very fine stylolitic laminations are noted throughout the section. 42cm from the base of the interval is a thin conglomerate lag stringer 3cm thick with clasts up to 1cm in diameter. No significant amount of bioturbation is noted. Some very steep bedding is noted ~162cm up from the base and may be a function of slumping adjacent to the core. Minor Macaronichnus sp. traces are noted in the upper and middle parts of the interval.

BASE OF CORE INTERVAL IS MISSING FROM 2782.17-2792m.

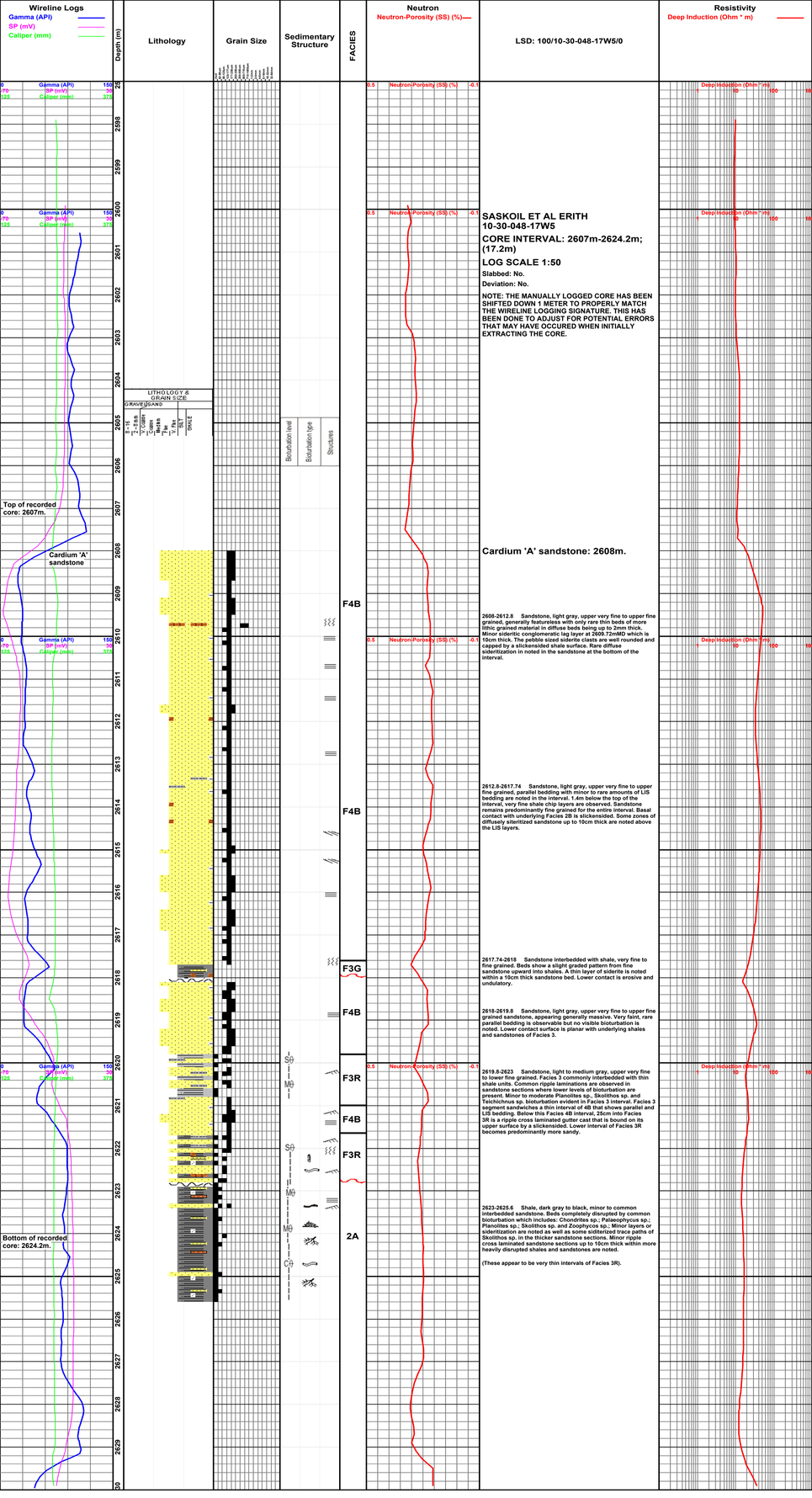
Wireline Logs
Gamma (API)
SP (mV)
Caliper (mm)
Depth (m)
Lithology
Grain Size
Sedimentary Structure
FACIES
Neutron
Neutron-Porosity (SS) (%)
LSD: 100/10-30-048-17W5/0
Resistivity
Deep Induction (Ohm * m)
Gamma (API) 0 150
SP (mV) -70 30
Caliper (mm) 125 375
0.5 Neutron-Porosity (SS) (%) -0.1
Deep Induction (Ohm * m) 1 10 100 1K
SASKOIL ET AL ERITH
10-30-048-17W5
CORE INTERVAL: 2607m-2624.2m; (17.2m)
LOG SCALE 1:50
Slabbed: No.
Deviation: No.
NOTE: THE MANUALLY LOGGED CORE HAS BEEN SHIFTED DOWN 1 METER TO PROPERLY MATCH THE WIRELINE LOGGING SIGNATURE. THIS HAS BEEN DONE TO ADJUST FOR POTENTIAL ERRORS THAT MAY HAVE OCCURED WHEN INITIALLY EXTRACTING THE CORE.
LITHOLOGY & GRAIN SIZE
GRAVEL SAND
Top of recorded core: 2607m.
Cardium 'A' sandstone
Cardium 'A' sandstone: 2608m.
Bioturbation level
Bioturbation type
Structures
F4B
F3G
F3R
2A
2608-2612.8 Sandstone, light gray, upper very fine to upper fine grained, generally featureless with only rare thin beds of more lithic grained material in diffuse beds being up to 2mm thick. Minor sideritic conglomeratic lag layer at 2609.72mMD which is 10cm thick. The pebble sized siderite clasts are well rounded and capped by a silickensided shale surface. Rare diffuse sideritization in noted in the sandstone at the bottom of the interval.
2612.8-2617.74 Sandstone, light gray, upper very fine to upper fine grained, parallel bedding with minor to rare amounts of LIS bedding are noted in the interval. 1.4m below the top of the interval, very fine shale chip layers are observed. Sandstone remains predominantly fine grained for the entire interval. Basal contact with underlying Facies 2B is silckensided. Some zones of diffusely siterlized sandstone up to 10cm thick are noted above the LIS layers.
2617.74-2618 Sandstone interbedded with shale, very fine to fine grained. Beds show a slight graded pattern from fine sandstone upward into shales. A thin layer of siderite is noted within a 10cm thick sandstone bed. Lower contact is erosive and undulatory.
2618-2619.8 Sandstone, light gray, upper very fine to upper fine grained sandstone, appearing generally massive. Very faint, rare parallel bedding is observable but no visible bioturbation is noted. Lower contact surface is planar with underlying shales and sandstones of Facies 3.
2619.8-2623 Sandstone, light to medium gray, upper very fine to lower fine grained. Facies 3 commonly interbedded with thin shale units. Common ripple laminations are observed in sandstone sections where lower levels of bioturbation are present. Minor to moderate Planolites sp., Skolithos sp. and Teichichnus sp. bioturbation evident in Facies 3 interval. Facies 3 segment sandwiches a thin interval of 4B that shows parallel and LSB bedding. Below this Facies 4B interval, 25cm into Facies 3R is a ripple cross laminated gutter cast that is bound on its upper surface by a silckensided. Lower interval of Facies 3R becomes predominantly more sandy.
2623-2625.6 Shale, dark gray to black, minor to common interbedded sandstone. Beds completely disrupted by common bioturbation which includes: Chondrites sp.; Palaeophycus sp.; Planolites sp.; Skolithos sp. and Zoophycos sp.; Minor layers or sideritization are noted as well as some sideritized trace paths of Skolithos sp. in the thicker sandstone sections. Minor ripple cross laminated sandstone sections up to 10cm thick within more heavily disrupted shales and sandstones are noted.
(These appear to be very thin intervals of Facies 3R).
Bottom of recorded core: 2624.2m.

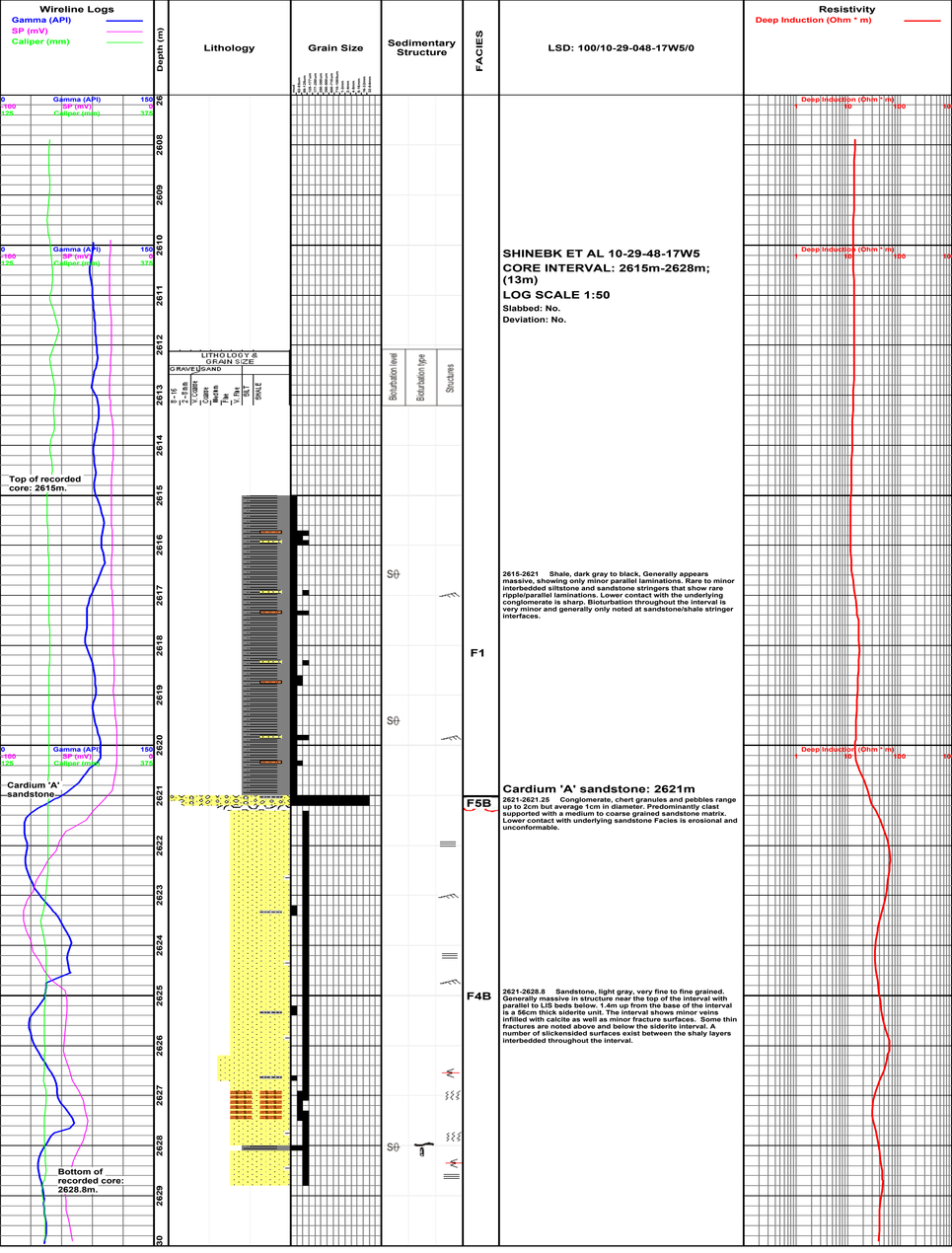
Wireline Logs
Gamma (API)
SP (mV)
Caliper (mm)
Depth (m)
Lithology
Grain Size
Sedimentary Structure
FACIES
LSD: 100/10-29-048-17W5/0
Resistivity
Deep Induction (Ohm * m)
SHINEBK ET AL 10-29-48-17W5
CORE INTERVAL: 2615m-2628m; (13m)
LOG SCALE 1:50
Slabbed: No.
Deviation: No.
Top of recorded core: 2615m.
Cardium 'A' sandstone
Bottom of recorded core: 2628.8m.
Cardium 'A' sandstone: 2621m
2615-2621 Shale, dark gray to black, Generally appears massive, showing only minor parallel laminations. Rare to minor interbedded siltstone and sandstone stringers that show rare ripple/parallel laminations. Lower contact with the underlying conglomerate is sharp. Bioturbation throughout the interval is very minor and generally only noted at sandstone/shale stringer interfaces.
2621-2621.25 Conglomerate, chert granules and pebbles range up to 2cm but average 1cm in diameter. Predominantly clast supported with a medium to coarse grained sandstone matrix. Lower contact with underlying sandstone Facies is erosional and unconformable.
2621-2628.8 Sandstone, light gray, very fine to fine grained. Generally massive in structure near the top of the interval with parallel to LIS beds below. 1.4m up from the base of the interval is a 56cm thick siderite unit. The interval shows minor veins infilled with calcite as well as minor fracture surfaces. Some thin fractures are noted above and below the siderite interval. A number of slickensided surfaces exist between the shaly layers interbedded throughout the interval.
F1
F5B
F4B

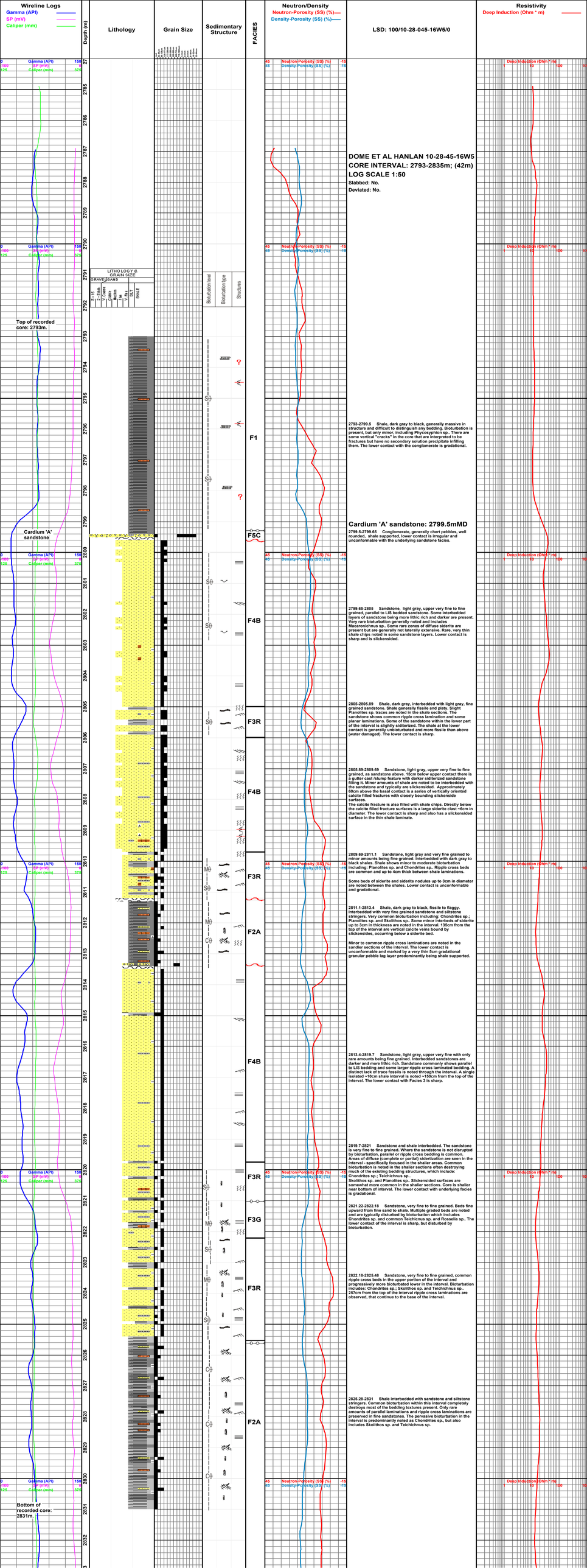
Wireline Logs
Gamma (API)
SP (mV)
Caliper (mm)
Depth (m)
Lithology
Grain Size
Sedimentary Structure
FACIES
Neutron/Density
Neutron-Porosity (SS) (%)
Density-Porosity (SS) (%)
LSD: 100/10-28-045-16W5/0
Resistivity
Deep Induction (Ohm * m)
DOME ET AL HANLAN 10-28-45-16W5
CORE INTERVAL: 2793-2835m; (42m)
LOG SCALE 1:50
Slabbed: No.
Deviated: No.
LITHOLOGY & GRAIN SIZE
GRAVEL/SAND
SILT
SHALE
Bioturbation level
Bioturbation type
Structures
Top of recorded core: 2793m.
Cardium 'A' sandstone
Bottom of recorded core: 2831m.
Cardium 'A' sandstone: 2799.5mMD
2793-2799.5 Shale, dark gray to black, generally massive in structure and difficult to distinguish any bedding. Bioturbation is present, but only minor, including Phycosyphion sp.. There are some vertical "cracks" in the core that are interpreted to be fractures but have no secondary solution precipitate infilling them. The lower contact with the conglomerate is gradational.
2799.5-2799.65 Conglomerate, generally chert pebbles, well rounded, shale supported, lower contact is irregular and unconformable with the underlying sandstone facies.
2799.65-2805 Sandstone, light gray, upper very fine to fine grained, parallel to LIS bedded sandstone. Some interbedded layers of sandstone being more lithic rich and darker are present. Very rare bioturbation generally noted and includes Macaronichnus sp.. Some rare zones of diffuse siderite are present but are generally not laterally extensive. Rare, very thin shale chips noted in some sandstone layers. Lower contact is sharp and is slickensided.
2805-2805.89 Shale, dark gray, interbedded with light gray, fine grained sandstone. Shale generally fissile and platy. Slight Planolites sp. traces are noted in the shale sections. The sandstone shows common ripple cross lamination and some planar laminations. Some of the sandstone within the lower part of the interval is slightly sideritized. The shale at the lower contact is generally unbioturbated and more fissile than above (water damaged). The lower contact is sharp.
2805.89-2809.69 Sandstone, light gray, upper very fine to fine grained, as sandstone above. 15cm below upper contact there is a gutter cast /slump feature with darker sideritized sandstone filling it. Minor amounts of shale are noted to be interbedded with the sandstone and typically are slickensided. Approximately 60cm above the basal contact is a series of vertically oriented calcite filled fractures with closely bounding slickenside surfaces.
The calcite fracture is also filled with shale chips. Directly below the calcite filled fracture surfaces is a large siderite clast ~6cm in diameter. The lower contact is sharp and also has a slickensided surface in the thin shale laminate.
2809.69-2811.1 Sandstone, light gray and very fine grained to minor amounts being fine grained. Interbedded with dark gray to black shales. Shale shows minor to moderate bioturbation including: Planolites sp. and Chondrites sp.. Ripple cross beds are common and up to 4cm thick between shale laminations.
Some beds of siderite and siderite nodules up to 3cm in diameter are noted between the shales. Lower contact is unconformable and gradational.
2811.1-2813.4 Shale, dark gray to black, fissile to flaggy. Interbedded with very fine grained sandstone and siltstone stringers. Very common bioturbation including: Chondrites sp.; Planolites sp. and Skolithos sp.. Some minor interbeds of siderite up to 3cm in thickness are noted in the interval. 135cm from the top of the interval are vertical calcite veins bound by slickensides, occurring below a siderite bed.
Minor to common ripple cross laminations are noted in the sandier sections of the interval. The lower contact is unconformable and marked by a very thin 5cm gradational granular pebble lag layer predominantly being shale supported.
2813.4-2819.7 Sandstone, light gray, upper very fine with only rare amounts being fine grained. Interbedded sandstones are darker and more lithic rich. Sandstone commonly shows parallel to LIS bedding and some larger ripple cross laminated bedding. A distinct lack of trace fossils is noted through the interval. A single isolated ~10cm shale interval is noted ~150cm from the top of the interval. The lower contact with Facies 3 is sharp.
2819.7-2821 Sandstone and shale interbedded. The sandstone is very fine to fine grained. Where the sandstone is not disrupted by bioturbation, parallel or ripple cross bedding is common. Areas of diffuse (complete or partial) sidertization are seen in the interval - specifically focused in the shalier areas. Common bioturbation is noted in the shalier sections often destroying much of the existing bedding structures, which include: Chondrites sp.; Teichichnus sp.; Skolithos sp. and Planolites sp.. Slickensided surfaces are somewhat more common in the shalier sections. Core is shalier near bottom of interval. The lower contact with underlying facies is gradational.
2821.22-2822.18 Sandstone, very fine to fine grained. Beds fine upward from fine sand to shale. Multiple graded beds are noted and are typically disturbed by bioturbation which includes Chondrites sp. and common Teichichnus sp. and Rosselia sp.. The lower contact of the interval is sharp, but disturbed by bioturbation.
2822.18-2825.48 Sandstone, very fine to fine grained, common ripple cross beds in the upper portion of the interval and progressively more bioturbated lower in the interval. Bioturbation includes: Chondrites sp.; Skolithos sp. and Teichichnus sp.. 257cm from the top of the interval ripple cross laminations are observed, that continue to the base of the interval.
2825.28-2831 Shale interbedded with sandstone and siltstone stringers. Common bioturbation within this interval completely destroys most of the bedding textures present. Only rare amounts of parallel laminations and ripple cross laminations are preserved in fine sandstones. The pervasive bioturbation in the interval is predominantly noted as Chondrites sp., but also includes Skolithos sp. and Teichichnus sp.
F1
F5C
F4B
F3R
F4B
F3R
F2A
F4B
F3R
F3G
F3R
F2A

2635
2634
25

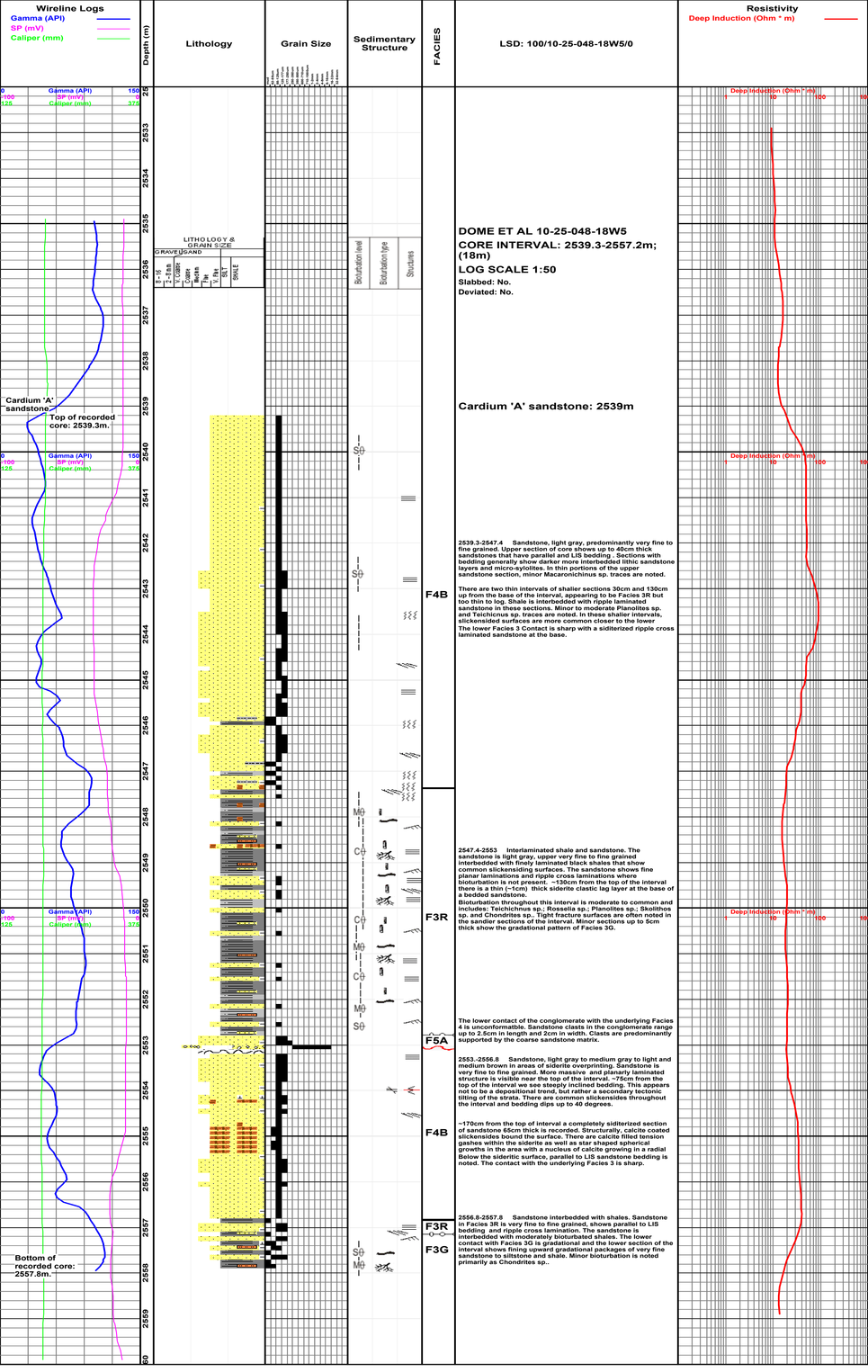
Wireline Logs
Gamma (API)
SP (mV)
Caliper (mm)
Depth (m)
Lithology
Grain Size
Sedimentary Structure
FACIES
LSD: 100/10-25-48-18W5/0
Resistivity
Deep Induction (Ohm * m)
Gamma (API)
SP (mV)
Caliper (mm)
LITHOLOGY & GRAIN SIZE
GRAVEL SAND
Bioturbation level
Bioturbation type
Structures
DOME ET AL 10-25-048-18W5
CORE INTERVAL: 2539.3-2557.2m; (18m)
LOG SCALE 1:50
Slabbed: No.
Deviated: No.
Cardium 'A' sandstone: 2539m
Cardium 'A' sandstone
Top of recorded core: 2539.3m.
Bottom of recorded core: 2557.8m.
2539.3-2547.4 Sandstone, light gray, predominantly very fine to fine grained. Upper section of core shows up to 40cm thick sandstones that have parallel and LIS bedding . Sections with bedding generally show darker more interbedded lithic sandstone layers and micro-xylolites. In thin portions of the upper sandstone section, minor Macaronichinus sp. traces are noted.
There are two thin intervals of shalier sections 30cm and 130cm up from the base of the interval, appearing to be Facies 3R but too thin to log. Shale is interbedded with ripple laminated sandstone in these sections. Minor to moderate Planolites sp. and Teichichnus sp. traces are noted. In these shalier intervals, slickensided surfaces are more common closer to the lower
The lower Facies 3 Contact is sharp with a siditerized ripple cross laminated sandstone at the base.
F4B
2547.4-2553 Interlaminated shale and sandstone. The sandstone is light gray, upper very fine to fine grained interbedded with finely laminated black shales that show common slickensiding surfaces. The sandstone shows fine planar laminations and ripple cross laminations where bioturbation is not present. ~130cm from the top of the interval there is a thin (~1cm) thick siderite clastic lag layer at the base of a bedded sandstone.
Bioturbation throughout this interval is moderate to common and includes: Teichichnus sp.; Rosselia sp.; Planolites sp.; Skolithos sp. and Chondrites sp.. Tight fracture surfaces are often noted in the sandier sections of the interval. Minor sections up to 5cm thick show the gradational pattern of Facies 3G.
F3R
The lower contact of the conglomerate with the underlying Facies 4 is unconformable. Sandstone clasts in the conglomerate range up to 2.5cm in length and 2cm in width. Clasts are predominantly supported by the coarse sandstone matrix.
F5A
2553.-2556.8 Sandstone, light gray to medium gray to light and medium brown in areas of siderite overprinting. Sandstone is very fine to fine grained. More massive and planarly laminated structure is visible near the top of the interval. ~75cm from the top of the interval we see steeply inclined bedding. This appears not to be a depositional trend, but rather a secondary tectonic tilting of the strata. There are common slickensides throughout the interval and bedding dips up to 40 degrees.
~170cm from the top of interval a completely siditerized section of sandstone 65cm thick is recorded. Structurally, calcite coated slickensides bound the surface. There are calcite filled tension gashes within the siderite as well as star shaped spherical growths in the area with a nucleus of calcite growing in a radial
Below the siderritic surface, parallel to LIS sandstone bedding is noted. The contact with the underlying Facies 3 is sharp.
F4B
2556.8-2557.8 Sandstone interbedded with shales. Sandstone in Facies 3R is very fine to fine grained, shows parallel to LIS bedding and ripple cross lamination. The sandstone is interbedded with moderately bioturbated shales. The lower contact with Facies 3G is gradational and the lower section of the interval shows fining upward gradational packages of very fine sandstone to siltstone and shale. Minor bioturbation is noted primarily as Chondrites sp..
F3R
F3G

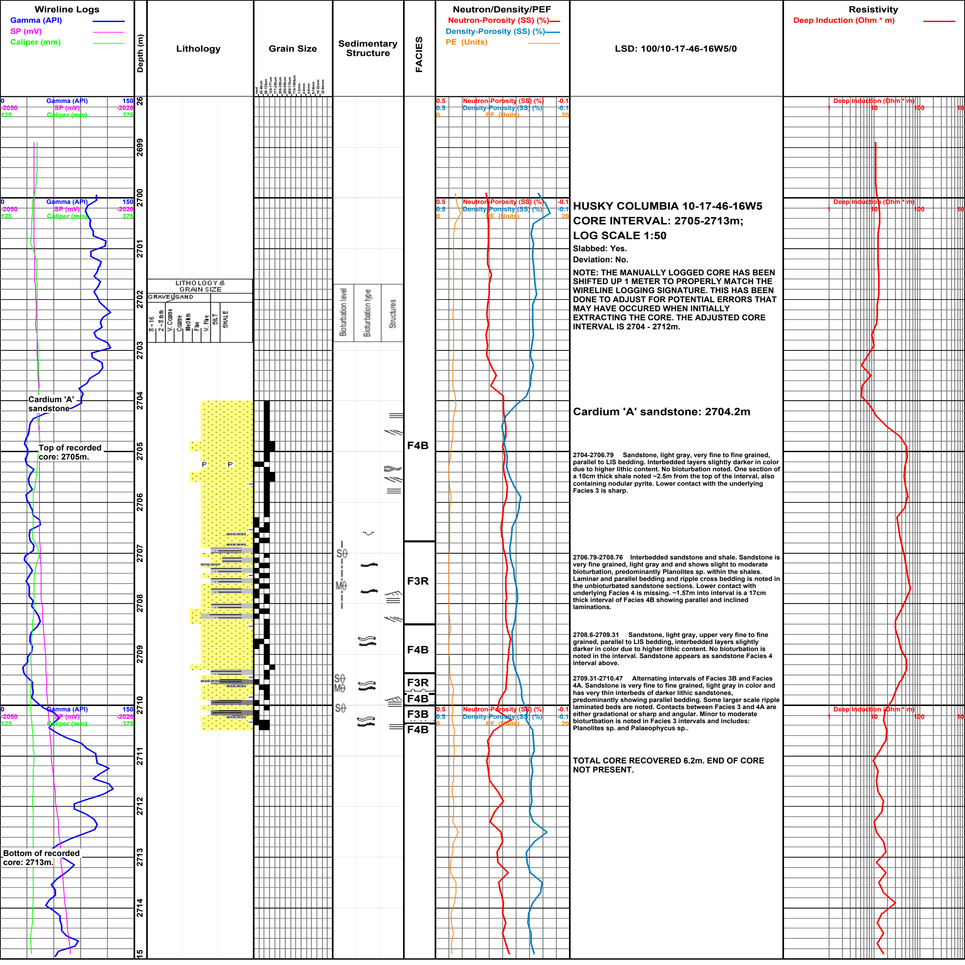
Wireline Logs
Gamma (API)
SP (mV)
Caliper (mm)
Depth (m)
Lithology
Grain Size
Sedimentary Structure
FACIES
Neutron/Porosity (SS) (%)
Density-Porosity (SS) (%)
PE (Units)
LSD: 100/10-17-46-16W5/0
Resistivity
Deep Induction (Ohm * m)
Gamma (API) 0 150
SP (mV) -2050 -2025
Caliper (mm) 125 375
Cardium 'A' sandstone
Top of recorded core: 2705m.
Bottom of recorded core: 2713m.
LITHOLOGY & GRAIN SIZE
GRAVEL SAND
CLAY SILT
Bioturbation level
Bioturbation type
Structures
F4B
F3R
F4B
F3R
F4B
F3B
F4B
HUSKY COLUMBIA 10-17-46-16W5
CORE INTERVAL: 2705-2713m;
LOG SCALE 1:50
Slabbed: Yes.
Deviation: No.
NOTE: THE MANUALLY LOGGED CORE HAS BEEN SHIFTED UP 1 METER TO PROPERLY MATCH THE WIRELINE LOGGING SIGNATURE. THIS HAS BEEN DONE TO ADJUST FOR POTENTIAL ERRORS THAT MAY HAVE OCCURED WHEN INITIALLY EXTRACTING THE CORE. THE ADJUSTED CORE INTERVAL IS 2704 - 2712m.
Cardium 'A' sandstone: 2704.2m
2704-2706.79 Sandstone, light gray, very fine to fine grained, parallel to LIS bedding. Interbedded layers slightly darker in color due to higher lithic content. No bioturbation noted. One section of a 10cm thick shale noted ~2.5m from the top of the interval, also containing nodular pyrite. Lower contact with the underlying Facies 3 is sharp.
2706.79-2708.76 Interbedded sandstone and shale. Sandstone is very fine grained, light gray and and shows slight to moderate bioturbation, predominantly Planolites sp. within the shales. Laminar and parallel bedding and ripple cross bedding is noted in the unbioturbated sandstone sections. Lower contact with underlying Facies 4 is missing. ~1.57m into interval is a 17cm thick interval of Facies 4B showing parallel and inclined laminations.
2708.6-2709.31 Sandstone, light gray, upper very fine to fine grained, parallel to LIS bedding, interbedded layers slightly darker in color due to higher lithic content. No bioturbation is noted in the interval. Sandstone appears as sandstone Facies 4 interval above.
2709.31-2710.47 Alternating intervals of Facies 3B and Facies 4A. Sandstone is very fine to fine grained, light gray in color and has very thin interbeds of darker lithic sandstones, predominantly showing parallel bedding. Some larger scale ripple laminated beds are noted. Contacts between Facies 3 and 4A are either gradational or sharp and angular. Minor to moderate bioturbation is noted in Facies 3 intervals and includes: Planolites sp. and Palaeophycus sp..
TOTAL CORE RECOVERED 6.2m. END OF CORE NOT PRESENT.

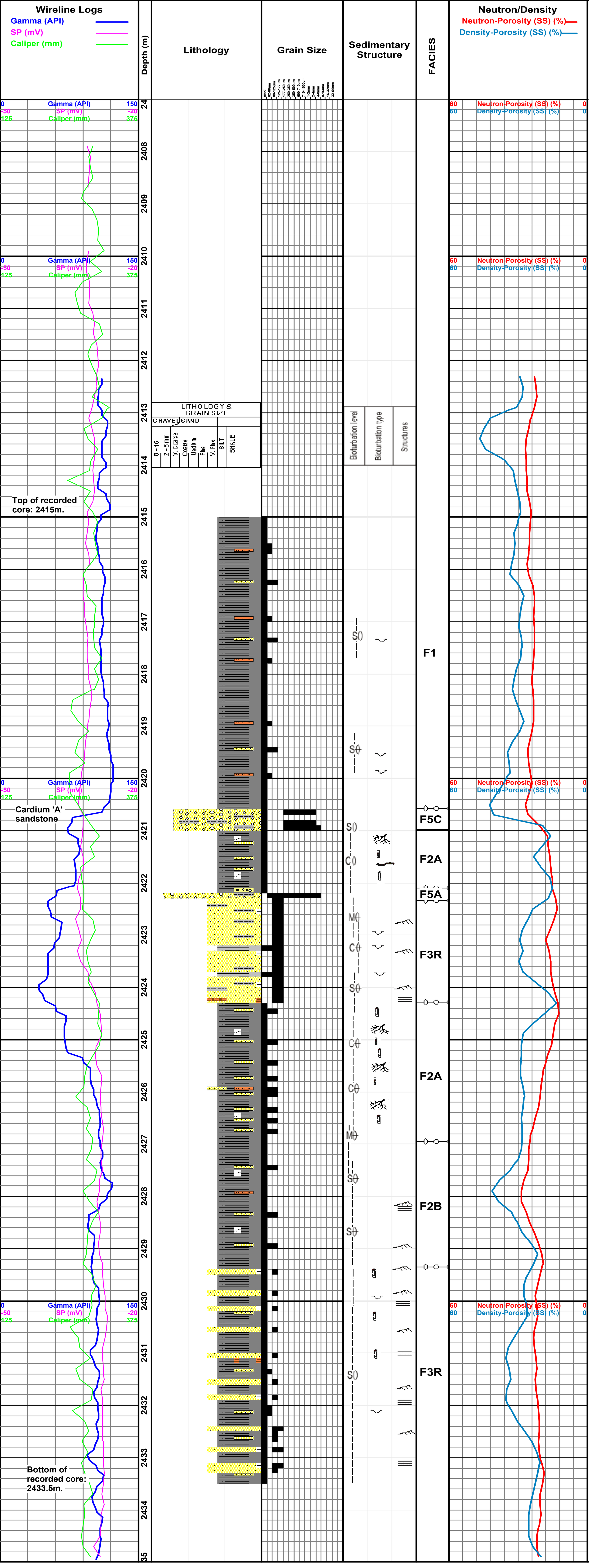

LSD: 100/10-1-046-14W5/0

AMOCO BRAZR 10-1-46-14W5
CORE INTERVAL: 2415-2433.2m; (18.2m)
LOG SCALE 1:50

Deviation: No.

Slabbed: No.

2415-2720.7 Shale, dark gray to black, interbedded with rare, very fine sandstone and siltstone stringers. Only minor unidentified bioturbation is noted in the interval where the siltstone/sandstone are present. The lower contact with the underlying conglomerate is gradational.

Cardium 'A' sandstone: 2420.7m

2720.7-2720.97 Conglomerate, predominantly chert. The chert clasts are suppported in shale matrix and have discrete layers of concentrated pebble lags between interbedded shales. Chert clasts range up to 5mm in diameter. Shale matrix partially siditerized near the bottom of the interval and shows minor unidentified bioturbation. The lower contact is gradational.

2720.97-2722.22 Interbedded shale and very fine to fine grained light gray sandstone. Common to pervasive bioturbation completely disrupts bedding. Identifiable bioturbation includes Chondrites sp.; Planolites sp.; Teichichnus sp. and Skolithos sp.. Lower contact with the underlying conglomerate is gradational.

2722.22-2722.47 Conglomerate and sandstone. Chert clasts generally range up to 3mm in diameter. Conglomerate is clast supported. Lower contact with sandstone is a scour below which the sandstone becomes interbedded with shales.

2722.47-2724.29 Shale interbedded with very fine to fine grained light gray sandstone. Moderate to common bioturbation present, but not generally identified. Interbedded sandstones show ripple cross lamintations where not completely disrupted by bioturbation. One meter from the base of the interval, thicker packages of sandstone up to 9cm are interbedded with thinner sections of shales and siltstones. The thicker sandstones display parallel and ripple cross laminations and Skolithos sp.

The lower contact is gradational with the underlying facies.

2724.29-2726.95 Shale interbedded with fine grained sandstones and minor siltstones. Interval is completely bioturbated. The pervasiveness of the bioturbation causes a complete intermixing of the bedding. Bioturbation includes Skolithos sp.; Chondrites sp. and Teichichnus sp. The contact is gradational between the facies.

2726.95-2729.35 Shale interbedded with minor amounts of very fine sandstone stringers. Sandstone content is significantly decreased from above, as well as the level of evident bioturbation. Where the sandstone stringers are not bioturbated, they show ripple or parallel laminations. Lower contact is gradational.

2729.35-2733.5 Interbedded shale and sandstone. This Facies 3R has less sand content than the interval noted above. Minor bioturbation is noted through the section and preserved sandstone intervals range from 2mm to 5cm. Sandstone lenses show common ripple cross lamination and sometimes planar laminations.